DOCTORAL THESIS

Progressive Landslides in Long Natural Slopes

Formation, Potential Extension and Configuration of Finished Slides in Strain-Softening Soils

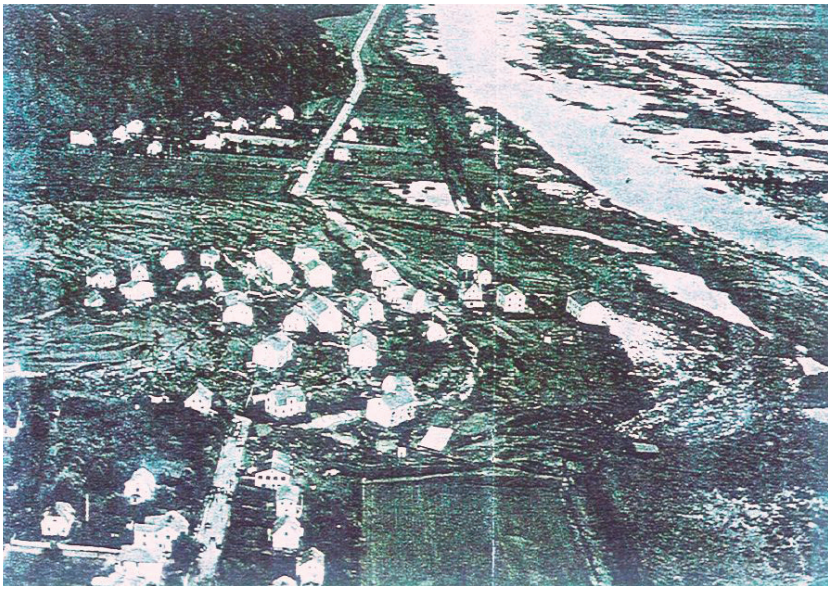

Stig Bernander

LULEÅ UNIVERSITY OF TECHNOLOGY

LULEÅ
UNIVERSITY
OF TECHNOLOGY

Doctoral Thesis

Progressive Landslides in Long Natural Slopes

Formation, Potential Extension and Configuration of Finished Slides in Strain-Softening Soils

Stig Bernander

Division of Soil Mechanics and Foundation Engineering
Division of Structural Engineering
Department of Civil, Environmental and Natural Resources Engineering
Luleå University of Technology
SE-971 87 Luleå
Sweden

Progressive Landslides in Long Natural Slopes
Formation, Potential Extension and Configuration of Finished Slides in Strain-Softening Soils
STIG BERNANDER
Avdelningen för geoteknik i samverkan med Avdelningen för konstruktionsteknik
Institutionen för samhällsbyggnad och naturresurser
Luleå Tekniska universitet

Akademisk avhandling

som med tillstånd av Dekanus för Tekniska fakulteten vid Luleå tekniska universitet
för avläggande av teknologie doktorsexamen kommer att offentligt försvaras:

Tisdagen den 16 augusti 2011, kl 10.00
i Sal F1031, Luleå tekniska universiteet

Opponent: Professor Steinar Nordal, Institutt for Bygg, anlegg og transport, NTNU, Trondheim, Norge

Betygsnämnd: Dr Hans-Petter Jostad, Norges Geotekniske Institutt (NGI), Oslo, Norge

Professor Stefan Larsson, Inst. för byggvetenskap, Avd. för jord- och bergmekanik, KTH, Stockholm

Professor Claes Alén, Inst. för bygg- och miljöteknik, Avd för geologi och geoteknik, Chalmers tekniska högskola, Göteborg

Professor Ola Dahlblom, Inst. för byggnadsmekanik, Lunds tekniska högskola, Lund

Professor Thomas Olofsson, Inst. för samhällsbyggnad och naturresurser, Avd. för byggkonstruktion och byggproduktion, LTU

Docent Lars Bernspång, Inst. för samhällsbyggnad och naturresurser, Avd. för byggkonstruktion och byggproduktion, LTU (Ersättare)

Tryck: Universitetstryckeriet, Luleå 2011, 2nd version 2011.
ISBN: 978-91-7439-283-8
ISSN: 1402-1544
www.ltu.se

The photo on the cover illustrates the Surte Landslide on September 29, 1950, in the valley of Göta River some 10 km north of Gothenburg, Sweden

Preface

In May 2000, I presented a licentiate thesis “Progressive Landslides in Long Natural Slopes”, LTU 2000:16.

Already at this time it was my intention to up-date this edition in various ways – primarily in respect of addressing also up-hill progressive (or retrogressive) slides. Yet, other commitments delayed the work on up-hill slides until mid 2005.

During the years 1978 to 1989 the author conducted a research program focused on the possible effects of brittle failure mechanisms in natural slopes of highly strain-softening clay.

The analytical approach, on which the LTU 2000:16 licentiate thesis was essentially based, had been briefly published on various international conferences among other Xth ICSMFE, Stockholm, (1981), NGM, Linköping, (1984), IVth ISL Toronto, (1984), XIth ICSMFE, San Fransisco, (1985), NGM, Oslo, (1988), XIIth ICSMFE, Rio de Janeiro, (1989).

A relatively simple computer program addressing these issues was developed already in 1981. However, a more sophisticated 2-dimensional Finite Difference version, developed in the years 1984-1985, was first published in Oslo 1988.
However, the engineering department of Skanska Väst AB – then a subsidiary of Skanska Ltd, (a leading Swedish contracting company) applied this computer software to a number of practical cases in the mid-eighties both on behalf of Skanska as well as of the Swedish Geotechnical Institute (SGI).

Yet, although the principles of brittle failure in soft sensitive clays have neither been rejected nor considered inconceivable by most soil mechanics engineers, little R & D on the subject was conducted before the turn of the century.
However, since about 2003, intensified R & D on the topic of progressive failure in landslide formation is ongoing in several countries, particularly in Norway, Canada, Italy, and Switzerland.

Geotechnical analysis of brittle slope failure has of course many traits in common with various types of progressive or brittle failures in other disciplines of structural mechanics. Yet, the analysis of stability of long natural slopes harbours some rather specific additional complications. The strength parameters required are for instance strongly dependant on conditions that, for a number of reasons, are often not easy to define with sufficient accuracy in natural soil deposits. Such conditions are for instance:

- The crucial – but often difficult – task of establishing the in-situ state of stress in accordance with past geological history, erosion, hydrology and other contributing agents.

- Time dependent strain-/ and deformation-softening that is strongly dependent on the rate of load application, as well as on drainage conditions in the potential failure zone.

- Loss of available shear resistance in over-consolidated clay on account of past and ongoing deformations and due deformation-softening closely related to the degree of over-consolidation (OCR).

- Progressive failure, being time-dependent, tends to develop in distinctly different phases, in which the conditions governing landslide development may vary widely. This implies in effect that the risk related to progressive landslide failure cannot be clearly defined on the basis of just a singular static condition or event.

The safety criteria and basic State-of-the-Art research related to slope stability has in practical soil mechanics engineering long been adapted to the principle of the perfectly plastic equilibrium failure condition.
In the opinion of the author the complications listed above demand *new definitions* for safety criteria, *modified procedures* for soil investigations and laboratory testing as well as radically *different appraisal* of the possible impact of local additional load effects.

Hence, even for the engineer who recognizes the phenomenon of brittle slope failure its implications for practical engineering is hardly a straight forward procedure, as the entire philosophy related to landslide hazard is significantly changed.
The objective of the present document is to highlight the complexity of progressive slope failure development, hopefully leading to improved understanding of the issues involved and to recognized investigation procedures.

So although the Finite Difference method (FDM) applied is basically the same as the one developed in the mid-eighties, the present document largely focuses on various phenomena, conditions and failure criteria that are closely related to landslide formation in soft sensitive or in highly deformation-softening over-consolidated clays.
For instance, importantly, the FDM-approach not only *expressively* predicts the high vulnerability of some slopes to local additional loading, but also *compellingly* explains the massive spread of downhill progressive landslides over large areas of level ground to great depth - and that already in terms of static loading.

Analysis of case records and theoretical exemplifications over the years have rendered experience of brittle slope failure that believably may be of interest to practicing engineers and to those responsible for on-going and future R & D.

MSc and PhD courses in Soil Mechanics and Fracture Mechanics have been conducted at LTU. These courses have proved to be valuable for the understanding among students of the principles and the complexity of these issues. Analyses have been performed with easy-to-use spread sheets.
.

****

As mentioned above, work on up-hill progressive slides was performed in mid 2005.
In October 2005, I was invited by professor Serge Leroueil (at 'Faculté des sciences et de génie', Laval University, Québec) to hold a few lectures on the topic of progressive failure formation.
On this occasion there was also time for personal communication on this subject and existing computer software on both downhill and uphill progressive failure analysis was made available to the faculty for the intended study of the Saint-Barnabè-Nord landslide (December, 2005).

The results of the investigation of Saint-Barnabè-Nord slide were presented in 2007 as a master thesis by Ariane Locat (Etude d´un Étalement Latéral dans les Argiles de l´Ést du Canada et de la Rupture Progressive), where the slide was explained in terms of an uphill

progressive (or retrogressive) landslide. For the part of this comprehensive study dealing retrogressive failure analysis, the Finite Difference approach presented in the current document was applied.

In view of the good progress in this field of geotechnical engineering being made by young researchers, I personally decided not to focus my further studies on retrogressive failure formation thus leaving them in the state they had reached in mid 2005.

Acknowledgements

First of all, I am greatly indebted to emeritus professor Lennart Elfgren, Division of Structural Engineering, LTU, not only for having initiated the inception of this project but also for his constant and inspiring support. Without his dedicated commitment, this document would not have come into being.

Furthermore, I want to thank professor Sven Knutsson, Division of Soil Mechanics and Foundation Engineering, LTU, for making it possible to present this thesis at his division, for undertaking the task as main supervisor and for his positive commitment and support.

I also want to thank emeritus professor Roland Pusch for his many appropriate comments on various aspects of the contents of the document.

I wish to express my gratitude to the other the members of the reference group, docent Leif Jendeby, Trafikverket, and chief eng. Jan Olofsson, Skanska, for having read the manuscript of the thesis (or parts thereof) and for the advice and comments made.
In particular, I must thank Per-Evert Bengtsson (SGI) for his detailed, constructive and knowledgeable criticism.

Further, I want to acknowledge the financial support given by the Development Fund of the Swedish Construction Industry (SBUF). Many figures have been up-dated by Niklas Bagge and Anders Bennitz.

Moreover, I am aware of being indebted to many a colleague, who in discussion or even by opposing the novelty in some of my reasoning, have contributed to what I believe to be a further step in the development of concepts of brittle failures in natural slopes.

Finally, I want to express thanks to my friend Mrs Laila Berglund for having endured tedious explanations on the subject of the thesis.

Luleå in May 2011

Stig Bernander

In this second version some clarifications have been made conforming to the discussion during the Ph D Defence on August 16, 2011. Some printing errors have also been corrected.

Luleå in August 2011.

Stig Bernander

Preface to Licentiate Thesis LTU 2000:16

In the late 1960's and the early 1970's, a number of large planar landslides took place in southwestern Sweden. On inspecting the sites of some of these slides, I observed that the topography of the finished slides seemed to be inconsistent with the failure mechanism based on ideal-plastic limit equilibrium, by which practicing engineers generally predict potential slide hazards.

Therefore, in my capacity of heading the Engineering Department of Skanska Väst AB during 1970 - 91 (then a subsidiary of a leading contracting company in Sweden), I conducted a research program focused on the possible effects of brittle failure mechanisms in landslides, which had occurred in deformation-softening clays. A computer software for incorporating the effects of deformation-softening into the analysis of slope stability was developed. The progress of this work was presented to a larger audience in a number of separate publications in Swedish and English during the period 1978 to 1989. However, the various reports reflected different aspects of the problem of brittle failures in soils as well as different stages in the development of an engineering approach.

The purpose of the present report is to synthesize the essential principles, ideas and findings that resulted from this research and motivated the above mentioned publications.

In 1997 the bodies mentioned below granted funding for a research project with the following three objectives:

1) Establishing a report giving a coherent account of the various issues involved in brittle slope failures i.e.
- Limitations as to the applicability of the ideal-plastic failure type of analysis;
- Defining the different phases of a progressive failure event;
- Detailing and exemplifying the basic equations of the applied analytical model;
- Identification of factors and circumstances conducive to brittle slope failures;
- Practical recommendations regarding procedures for investigating slope stability in deformation softening soils.

2) Updating existing computer software in Basic to a Windows environment.

3) Applying the analytical model on a few well documented landslides, and examining the viability of the method of analysis by checking if the computational results match or explain the actual slide events.

The organizations supporting this research program are:

- **the Swedish Council for Building Research (BFR 970330-6)**
- **the Development Fund of the Swedish Construction Industry (SBUF)**
- **the Division of Structural Engineering, Luleå University of Technology**
- **Skanska AB**
- **Congeo AB, Mölndal**

An advisory reference group was appointed for the project consisting of the following members:

Elvin Ottosson	Chief engineer,	SGI (the Swedish Geotechnical Institute)
Per-Evert Bengtsson	Research engineer	SGI
Göran Sällfors	Professor	Chalmers University of Technology
Jan Hartlén	Doctor of technology	JH Geo Consulting HB
Ingmar Svensk	Civil engineer	Skanska Teknik AB
Ulf Ericsson	Civil engineer	NCC Teknik AB

I wish to express my gratitude to the members of the reference group for having read the manuscript of the report (or parts thereof) and for the advising and critical comments made. In particular I must thank Per-Evert Bengtsson (SGI) for his detailed, constructive and knowledgeable criticism. Also, his rapid implementation of the proposed differential equations in Chapter 4 into Excel facilitated checking of numbers in the numerical examples in the report. Editorial comments by Jan Lindgren (SGI) have been of considerable value.

I am indebted to professor Lennart Elfgren (Head of the Department of Civil and Mining Engineering, Luleå University of Technology) for not only initiating the current project but also for his constant and inspiring support. Working with him and with professor Krister Cederwall, coworkers and students as a part-time adjunct professor at the Division of Structural Engineering during 1980 - 98 gave me the opportunity to consider crack formation and strain-softening also in young concrete.

Special acknowledgements are directed to Ingmar Svensk, Anders Hansson and Lars Nordström (Skanska Teknik AB). I am much obliged to Ingmar for his engaged support and for his active contributions to raising the necessary funding for this project. Much credit must be given to Anders for performing a major part of the computer analyses in connection with the case records described in the report and to Lars for having drawn most of the figures.

Furthermore, I must express my deep appreciation to my former colleagues at Skanska Teknik AB for their various contributions in the 1980-ties to the research work that has led forward to the present study, and in the absence of which the current project would not have been possible. In this context, I feel obliged to mention the names of the civil engineers Hasse Gustås, Ingvar Olofsson, Ingmar Svensk and Jan Olofsson.

I will also take this opportunity to extend my gratitude to Bernt Bernander (former UNDP General Secretary) for dedicating considerable time to reading the manuscript and for valuable editorial and linguistic advice. Thanks are also due to Phil Curtis, SYCON and Dr of eng. Keith Rush, M.Sc., (LTA Earthworks Ltd, South Africa) for having read and commented on the manuscript.

I am also aware of being indebted to many a colleague, who in discussion or even by opposing the novelty in some of my reasoning, have contributed to what I believe to be a further step in the development of concepts of brittle failures in natural slopes.

Last but not least, I am deeply grateful to my wife Sonja for the patience she has shown me and to my work in compiling this report.

Mölndal in April 2000

Stig Bernander

CONTENTS:

Pages

Abstract

General

The spread and final ground surface configuration of many landslides in soft Scandinavian clays cannot be explained on the basis of the commonly applied concept of perfectly plastic limit equilibrium. Conceivably because of this, the discrepancy between actual slide events and the results of back-analyses have in the past often provided fertile ground for failure concepts of rather imaginative and speculative nature. For instance, the great Tuve slide in Gothenburg generated some 10 different explanations of the slide events by engineers of the profession. (Cf SGI Reports No 10 (1981) and No 18 (1982).

In the conventional 'ideal-plastic failure' analysis (in this report referred to as I-PlFA), deformations inside and outside the studied soil volume are disregarded entirely – as it may seem for the sake of simplicity. This means that the soil in this context is presumed to be a perfectly plastic material.

An important contention in the current report is that inconsistency between theory and reality in this particular field of geotechnical engineering mainly derives from the fact that many soils are markedly strain-softening in the ranges of differential deformation that actually occur in the transition zone between an incipiently sliding soil mass and underlying ground. The issue relates in particular to potentially extensive slides in slopes with sensitive clayey sediments.

Deformation-softening

In the present document, the term *'deformation-softening'* denotes the loss of shear resistance both due to shear (deviator) strain in the developing failure zone and to concentrated excessive strain generated by large displacement and slip in the failure plane. The reason for this is related to the fact that failure in this context is represented by two simultaneous but basically different states (Stages I and II), simulating the conditions before and after the formation of a discrete slip surface or narrow shear band.

For the same reason, the constitutive stress-/strain/displacement properties are in the document generally referred to as *'stress-deformation'* relationships. (Cf e.g. Figure 4:4.2.)

The sensitivity of the soil material is a major factor in this context. There is in Sweden sometimes even a tendency to explain major landslides of the current type by simply referring to the presence of so called 'quick clay', which in Scandinavia is the term for clays with a sensitivity number of $St = c_u/c_{ur} \geq 50$, where c_{ur} denotes the residual shear strength of a completely remoulded (stirred) clay specimen.

However, there exist no established or generally recognized relationships between sensitivity – defined in this way – and the actual sensitivity of clay at impending failure in slowly developing real critical zones (and/or failure planes). This condition constitutes another highly complicating factor, contributing to the difficulty of understanding the nature of these slides.

The stirred shear resistance, as measured in laboratory (c_{ur}), is hardly likely to hold any fixed relationship with the resistance that is actually mobilized in a developing failure zone or slip surface in situ, considering the widely varying rates of stress and deformation change that can occur in the triggering phase of a landslide, as well as in the subsequent phases of its evolution.

This lack of proven compatibility is, in the present document, dealt with by distinguishing between the completely remoulded 'laboratory' shear strength (c_{ur}) and the actual un-drained residual strength parameter (c_{uR}) applicable to a *real* failure condition.

Since the effective residual shear resistance in a developing failure zone strongly depends on the rate of loading and locally prevailing drainage conditions, residual shear strength is in this document mostly referred to just as c_R.
Peak shear strength is generally denoted c, instead of c' or c_u, indicating that incipient failure conditions may typically neither be fully 'drained' nor 'un-drained'.

Analysis of failure in long slopes considering deformations
The current document focuses on the possibility of progressive or brittle failures occurring in slopes of strain-softening soil considering relevant deformations. A finite difference method (FDM) is applied for the numerical analysis of progressive failure (Pr F) formation.
The procedure resembles that of conventional (I-PlF) modelling in so far as the potential failure plane is initially presumed to be known, often readily identifiable by the sedimentary structure of the ground. Yet, the most critical condition may have to be found by 'trial and error'.
Nevertheless, the proposed analysis differs from ideal-plastic limit equilibrium methods in a number of key aspects:

- Whereas in the ideal-plastic failure approach, the equilibrium of the *entire* potentially sliding body of soil is investigated, the Pr F-analysis focuses on the equilibrium of each individual vertical element into which the body of soil is subdivided.

- The main deformations within and outside the potentially sliding soil mass are considered. Hence, axial downhill displacements due to earth pressure change in the slope are at all times maintained compatible with the shear deformations of the discrete vertical elements. Satisfying this criterion makes it possible to define the distribution of shear stress induced by local concentrated loading as well as the extent to which shear resistance can be mobilized along a potential failure plane. The fact that the analysis of shear deformations is 2-dimensional allows modelling of the *entire* incipient failure zone as a thick structural layer, and not just as a discrete failure surface (or shear band).
This is a **crucial feature** of the approach, as it is actually the resilience of the developing failure zone, in terms of its thickness and extension, that per se constitutes the mandatory requisite for the resistance to slope failure related to local additional loading or disturbance. Hence, it is the very nature and the properties of the soil structure in the shear zone that determine the magnitude of the critical load and the likelihood of progressive failure formation in slopes of sensitive clay. (For instance, the resistance of an extremely narrow 'quick clay' layer to progressive failure is bound to be negligible.)

- The shearing properties of the soil are defined by a full non-linear 'stress-strain-displacement' (or 'stress-deformation') relationship and not just by a discrete shear strength parameter as is the case in normal limit equilibrium calculations.
This constitutive relationship is subdivided into two stages (I and II), simulating the conditions before and after the formation of a slip surface.
The stress-deformation relationships are chosen so as to be compatible with the different phases of failure development. Thus, by adapting the stress-deformation relationships to the time-scale of load application and to the current rates of pore-water pressure dissipation (drainage conditions), it is possible to consider the effects of **time** in the analysis.

- Local horizontal or vertical loads as well as local features in slope geometry that may be conducive to progressive failure formation can be taken into account.

- Although the elevation of a potential failure plane is presumed to be known, the ultimate length of the failure plane and the extension of the passive zone, including the spread over level ground, emerge as results of the computations.

Safety criteria applicable to progressive failure analysis

Brittle progressive failure related to deformation-softening, due to additional loading or disturbance, is conceivable if in part of the slope – at some point in time – the residual shear strength (c_R) falls below the prevailing in situ shear stress (τ_o), i.e.

$$\mathbf{c_R(x) \leq \tau_o(x)}$$

Progressive failure may then be generated by a virtually dynamic redistribution of unbalanced forces (earth pressures) resulting from gradually increasing deformations and associated strain softening.

Alternatively, the residual shear strength (c_R) may remain in excess of the in situ stress (τ_o) throughout the duration of the impact of additional loading (which is probably the most common situation), i.e.

$$\mathbf{c_R(x) \geq \tau_o (x)}$$

If this is the case, the said redistribution of earth pressures will, instead of entering a dynamic phase, merely entail growing down-slope displacements, as the additional loading is increased. This failure process is of a ductile character and the current analysis, considering deformations within the soil volume, will be in agreement with conventional ideal-plastic analysis (I-PlFA) for a ratio of $\mathbf{c_R/c = 1}$.

The analysis proposed highlights the importance of considering deformations in potentially extensive landslides and indicates that neglecting to do so may result in total misjudgement of the stability conditions.

The results of the FDM-analysis enable identification of the most critical features of a slope, thus allowing possible remedial measures to focus on pertinent issues, such as location of the additional load and its distribution, sub-ground geometry below the load, rate of load application, measures promoting drainage conditions, piling reinforcement etc.

Revision of safety criteria – new safety factors

In the context of progressive failure analyses of landslide hazard, the conventional safety factors commonly used in stability investigations of long slopes are actually devoid of physical meaning.

Therefore new formulations, addressing the critical conditions in long slopes with regard to formation of progressive failure, are proposed in Sections 3, 8 and 11.

For instance, in respect of local triggering failure $\mathbf{F_s^I = N_{cr}/N = q_{cr}/q}$

and in respect of global failure $\mathbf{F_s^{II} = E_p /(E_{0x} + N_{max})}$ (Cf Section3)

Other implications of the proposed FDM approach

Effects of considering time

Considering time is of fundamental importance in this context. A crucial implication for the analysis of progressive slope failure is, among other, that accounting for time effects actually means that the slide events cannot be correctly studied as a *unique case* of *static* loading.

This is related to the fact that progressive failure develops time-wise in successive distinct phases, where each phase is controlled by specific but highly varying conditions as regards rates of loading, residual shear resistance, time duration, drainage and geometry.

In this document, it is distinguished between ***six*** different phases, of which only ***four*** are actually of a static nature. (Cf Sections 3.31 and 3.32.)

Phase 1 - the existing (or primordial) ***in situ stage***
Phase 2 - the ***disturbance phase***, subject to conditions relating to the agent triggering the slide.
Phase 3 - an intermediate, *virtually* ***dynamic stage of stress redistribution,*** when unbalanced up-slope forces are transmitted further down-slope to more stable ground.
Phase 4 - a ***transitory*** (or in some cases permanent) ***new state of equilibrium*** defining the related earth pressure distribution.
Phase 5 - ***final breakdown*** in passive failure, provided current passive resistance is exceeded in Phase 4. Phase 5 represents what is normally understood as the actual slide event.
Phase 6 - ***terminal state of equilibrium*** - resulting ground configuration.

In Bernander, (2008), (LuTU Report No: 2008:11), the first five of these separate phases of a fully developed progressive landslide are denoted '**Phases 1, 2, 3, 4** and **5**'. These denotations will be used henceforth.
In the current report, the ultimate state of equilibrium of a slide is referred to as **Phase 6**.

Consequently, the final outcome of a slope stability study (i.e. the potential degree of ultimate global failure) can eventuate in radically different ways if the conditions, in any of the intermediate phases, are altered.
For instance, if the conditions – such as time factors, sensitivity and geometry in the part of a slope that is engaged in the redistribution phase (Phase 3) – are only moderately different, an extensive landslide like the one in Tuve may instead end up just as a minor earth moment such as the 'landslide' in Rävekärr. (Cf Section 5).

Implications of the critical length parameter (L_{cr})
The fact that the distance down-slope of a local load – along which the additional shear stresses in the potential failure zone can be mobilized – is limited has a crucial implication. At a distance, defined as L_{cr} in Section 3.3, from the applied additional load, its effects can no longer be identified in terms of earth pressure or displacement. This circumstance actually rules out or diminishes the possibility of exploiting earth pressure resistance further downhill in less sloping ground for the stabilization of additional up-slope loading. The condition is basically valid prior to the initiation of progressive failure – i.e. provided the additional load is not applied at so slow a rate that long term creep affects the redistribution of load to a major degree. **([1])** (Cf Section 3.32, Regarding Phase 2.)

([1]) After the dynamic transfer of forces in Phase 3, passive down-slope resistance can effectively be mobilized further down-slope (i.e. in Phase 4) – in certain cases even forestalling continued slide development. (Cf the slide at Rävekärr, Section 5.)

The fact that passive resistance further down the slope cannot be mobilized for balancing additional up-slope loading is thus of great significance for the initiation and development of progressive slope failure. It means among other that resistance against failure along planes essentially following firm bottom or sedimentary strata is, subject to the degree of deformation-softening, considerably less than the resistances based on shorter failure planes surfacing in the sloping ground closer to the applied local load.
Notably, the proposed analysis considering deformations shows that this tendency may also apply to higher values of the brittleness ratio (c_R/c). In fact, in the initial stage it even applies

when fully plastic properties are ascribed to the soil. This is evident in view of the fact that mobilization of passive resistance requires sizable displacement.
(Cf Figure 3.33 in Section 3.3).

Hence, short failure planes and curved slip surfaces, i.e. failure modes for which the ideal-plastic approach may well be valid as such, seldom constitute the most critical failure modes in long slopes of deformation-softening soil. In many applications, this circumstance invalidates the use of the conventional ideal-plastic approach for identifying the initiating slide effect. The discrepancy in this respect tends to become more pronounced in varved clay deposits considering that sensitivity characteristics, and high pore water heads, are more likely to follow the sedimentary layers than across (or at some angle to) the same.

The proposed FDM-model for the analysis of progressive slope failure enables consideration also of deformations below the assumed failure plane. However, as indicated above, the fact that passive resistance further down-slope cannot be mobilized at a distance greater than L_{cr} for stabilizing local additional up-slope loads, implies that failure planes primarily tend to develop along the firmer bottom layers of soil, even to great depth below the ground surface.

Another point of interest in this context is that the ratio between the critical length L_{cr} and the total length of the prospective slide (L), offers an indication regarding the applicability of analyses based on ideal-plastic soil properties. This applies in particular to studies related to local additional loading.
Thus, for low values of L_{cr}/L, (i.e. < about 2) analyses based on full plasticity are prone to yield poor prediction of landslide hazard in soft sensitive clays. (Cf the slides at Surte, Tuve, Trestyckevattnet and Bekkelaget described in Chapter 5, Case records).
Consequently, slope stability investigations of long natural slopes in deformation-softening soils should at least include an estimate of the critical length L_{cr} even in cases when the use of conventional I-PlFA analysis is contemplated. The value of L should then represent the total length of the slope including a relevant portion of level ground beyond the foot of the slope.

Factors conducive to brittle slope failure
Progressive failure analysis according to Sections 3 and 4 also highlights the fact that there are several conditions, other than the inherent brittleness of the clay that are conducive to brittle slope failure. Such conditions, which are dealt with in Sections 9 and 11 are inter alia:
- Slope geometry and profile of the potential slip surface – 'geometric brittleness';
- Character and distribution of applied incremental loading or disturbance;
- Type, location and time-scale of the agents initiating failure. Rate of load application;
- Nature of local drainage in the zone subject to disturbance – the initiation zone;
- Hydrological conditions and hydrological history.

Landslide spread far beyond the foot of a slope
An unexplained feature, and a contentious issue, in many Scandinavian landslides has been the enormous spread of slides over virtually horizontal ground. This phenomenon is characterized by massive heave in passive Rankine failure extending to great depth below the ground surface. The issue is visualized in Figure 2:4.2b and dealt with at length in Sections 3.31 and 3.32 (Phase 4). This specific feature was strikingly manifest in the slides at Surte, Tuve and Bekkelaget. In the Tuve slide, for instance, about two thirds (i.e. some 160 000 m^2) of the ground involved in the main slide was plasticized down to a depth of about 35 m, resulting in a surface heave of up to 5 m.
A detailed exemplification of the mechanisms leading to vast landside spread over practically level ground is given in Bernander, (2008), LuTU 2008:11, Section 5.

Notably, progressive failure analysis according to the current FDM-approach not only predicts the possible incidence of this massive deformation of enormous volumes of soil but also explicitly indicates that events of this kind may derive solely from ***static*** forces – i.e. without taking dynamic effects and forces of inertia into account.

Why apply progressive failure analysis?
The stability conditions in natural slopes are closely related to their geological and hydrological history. Many clay slopes in western Sweden are made up of glacial and post-glacial sediments that emerged from the receding sea after the last glacial period. As the ground gradually rose above the sea level, the strength properties of the soils and the earth pressures in the slope gradually accommodated to the increasing loads by way of consolidation and creep. These loading effects may have resulted from retreating free water levels, falling ground water tables, long-time creep deformation and displacement, varying climatic conditions, ground water seepage and chemical deterioration.
In consequence, every existing slope is likely to be inherently stable by some undefined factor of safety that, in view of extreme precipitation and due ground water conditions in the past, at least by some measure may be assumed to exceed the value of unity under currently prevailing conditions.
Effects of time
The crucial challenge to the engineer responsible for investigating the stability of a slope is to study how it will respond to additional loading applied at rates, for which the '*time horizon'* is measured in terms of days, weeks or months instead of hundreds or thousands of years?
For instance, a fill deposited during a week may release a disastrous landslide, whereas the effects of an identical fill placed gradually in the time range of, say a few months, may pass totally unnoticed.
The proposed analysis, according to Section 4, provides a means of studying these issues.

Identification of type of landslide hazard
If local failure does take place, what *degree* of damage is likely to ensue? Will local instability merely result in earth pressure redistribution with minor cracking in the ground up-slope or will it terminate in a disastrous landslide displacing hundreds of meters of horizontal ground over great distances?

Progressive failure analyses explain in a straightforward way why, in many Scandinavian landslides, local disturbance caused by human activity has developed into comprehensive landslides, involving extensive areas of inherently stable ground. As mentioned, the specific ground configurations of the Tuve and the Surte slides, featuring immense passive zones in almost horizontal ground, materialize as *compelling* results of the FDM-analyses.

The fact that the likely extent of a potential landslide can be predicted is of great importance for assessing the risks and stakes involved, thus enabling evaluation of the scope and cost of measures designed to eliminate landslide hazard.

Identification of triggering agents
An important feature of this analysis is its ability to *pinpoint* and predict the possible consequences of man-made interference in critical portions of a slope.
Considering deformations and strain-softening in the assessment of slope stability normally results in a higher computed risk of slope failure than that emerging from the conventional ideal-plastic approach, depending in particular on the nature and the location of the applied additional load.

The decisive issue in this context is whether or not the conditions in the slope are such that a local disturbance agent is susceptible of inducing a critical state of deformation-softening in the soil – i.e. if the residual shear strength c_R may fall below the in-situ stress τ_o or not. Common disturbance agents are local additional loading (fills, stockpiling of materials), forced deformations, vibration (e.g. due to piling), blasting as well as extreme excess pore water pressure conditions.
These circumstances should be considered whenever soils exhibiting markedly deformation softening behaviour are encountered.

Although not difficult in principle, progressive failure analysis, as described in Section 4 may appear as an excessive complication of slope stability analysis to many a practicing geotechnical engineer. The valid constitutive relationships of the sensitive soil have to be known reasonably well, dependent as they are on various factors, among which the rate of loading, drainage conditions and the states of principal stress are of significant importance.

Yet, if we are serious in the purpose of making valid predictions of risk in terms of human life, property and other social economic losses, these complications should be addressed.

Computations
As may be concluded from the calculations demonstrated in Sections 4.4 & 7.2 and in Appendix I, hand calculations are, albeit simple in principle, too laborious to be practicable in dealing with slopes of complex nature. However, using computers, the time needed to perform the numerical computations, is insignificant. As regards the software in Windows C++, it may be noted that once appropriate in-put slope data have been entered, the complete computational study of a loading case, related to a specific failure plane, is a matter of only a few minutes.
Hence, the additional effort that may have to be dedicated to investigations of slope stability along these lines consists only to a minor extent of increased computational work.
The principal challenge lies in exploiting the enhanced possibilities of identifying the effec*ts* on slope stability of a number of factors, which ***by definition*** can only be determined by considering deformations and deformation-softening inside and outside the sliding body – for instance by using the proposed progressive FDM-approach.

Retrogressive or uphill progressive slides
Much of what has been stated above concerning downhill progressive landslides is applicable to uphill progressive slides. Even the basic equations apply with slight modification.

There are, however, some basic differences with regard to the factors leading to retrogressive landslide development. Moreover, the final disintegration of the soil mass in active failure (instead of passive failure) importantly affects the ultimate configuration of the ground surface of the area involved.

Whereas downhill progressive slides are usually triggered by some identifiable short–time disturbance agent, it is generally more difficult to pinpoint the true specific causes of uphill progressive landslides (often denoted as spreads). Retrogressive landslides are, according to this document, often related to change of the inherent conditions in the slope as regards stresses, earth pressures and deformations, including due ongoing creep movements – all mainly originating from long-time erosion processes.
Uphill progressive landslides are dealt with in Sections 6, 7 and 8.

Main conclusions
Landslide hazards in long natural slopes of soft sensitive clays may – on a strict structure-mechanical basis – only be reliably dealt with in terms of progressive failure analysis. There exist, for instance, *no fixed* relationships between safety factors based on the conventional limit equilibrium concept and those defining risk of progressive failure formation.
In consequence, the safety criteria have to be redefined for landslides in soft sensitive clays.

The proposed analysis renders it possible to identify the truly critical features of a slope, and thereby facilitate the choice of apt remedial preventive measures. The following aspects should be considered:

- The different phases of progressive landslides should be studied separately. Here it is distinguished between six different phases. The true risk of slope failure cannot be determined just in terms of a *singular static* case of loading, as each intervening phase of failure development is governed by widely differing conditions.

- Importantly, apart from defining the critical triggering load, the proposed FDM-approach also makes it possible to estimate the final spread or the degree of potential disaster in terms of static analysis. Notably the plasticization of enormous areas of level ground to great depth in Scandinavian landslides can be explained already in terms of *static* analysis – i.e. without considering the dynamic effects and forces of inertia in the slide proper.

- An interesting feature in this context is the fact that failure zones and slip surfaces tend to develop into level ground far (i.e. hundreds of meters) beyond the foot of a slope and that *prior to* the possible incidence of the general extensive passive spread failure.

- Progressive failure analyses show that slope failure in sensitive clay develops in direction down-slope rather than along slip circles surfacing in inclining ground near the additional load. This has e.g. the serious implication that a supporting embankment of the kind common in road construction can - acting as an effective triggering agent – per se initiate landslide disaster of much more serious nature than the one meant to be avoided by placing the embankment.

- In order to be able to make reasonable predictions of the impact of locally applied disturbance agents – capable of setting off large landslides – it is imperative to make adequate assessments of the effective residual shear resistance (c_R) that can be mobilized in a potential zone of local failure under the prevailing conditions of additional loading. In his context, time is a crucially important factor.

- Hence, reliable values of the residual shear strength c_R can only be established if the current rate of applying the additional load (or the disturbance) is considered. Moreover, the prevailing drainage conditions in the incipient failure zone have to be taken into account.

- Future research in this field of geotechnical engineering is urgently required if we really aspire to make adequately accurate predictions of landslide hazard in slopes of the kind subject to study in this document.

- Pending the results from such research, geotechnical engineers will have to resort to sensitivity analyses based on existing geotechnical knowledge and available experience. As indicated in Bernander, (2008) Appendices A, B and C, reasonably good prediction of

risk can be made already on present State-of-the-Art knowledge.
Yet, even if such an approach may seem imprecise, doing so will in any case provide better understanding and handling of landslide hazard in long slopes of soft clay than the application of the conventional limit equilibrium approach, based on perfectly plastic behaviour of the clay material.

Key phrases: *Down-hill progressive landslides in soft clays; Deformations in the soil mass; Deformation softening; Applicability of conventional ideal-plastic failure analysis; Modelling of progressive failure using a Finite Differences Approach; Residual shear strength in the incipient failure zone – a decisive parameter; Different phases in down-hill progressive slides; Analysis of slides occurred in terms of progressive failure; The Surte slide – a 'time bomb' ticking through millennia? Triggering disturbance load; Slide propagation over gently sloping ground; Development of failure zone and slip surface in the spread zone under level ground already* ***before*** *attaining passive Rankine resistance; Is 'quick clay' the only hazard in slopes of soft clay? Are shorter slip-circular failure modes relevant in long slopes of soft clays?; Brittleness related to nature of loading; Time effects; 'Geometric sensitivity'.*

Long-time evolution of retrogressive (uphill progressive) spread failure; loss of effective stress due to erosion; erosion-induced deformation and gradual loss of shear resistance over time; random and unpredictable slope failure.

Abstract in Swedish

Progressiva skred i långsträckta naturliga slänter

Orsaker, förlopp och utbredning hos skred i deformationsmjuknande jordar

Allmänt

Utbredningen och den slutliga topografin hos ett flertal i Skandinavien inträffade långsträckta skred kan inte förklaras med utgångspunkt från den inom praktisk geoteknik alltjämt ofta tillämpade jämviktsmetoden baserad på ideal-plastiska egenskaper hos jordmaterialet i brottstadiet. Enligt författarens uppfattning föreligger i många fall uppenbara brister i överensstämmelsen mellan, å ena sidan resultaten från analyser av inträffade skred och, å den andra vad som verkligen ägt rum under skredens förlopp. Detta förhållande synes utgöra en fruktbar grogrund för förklaringsmodeller av skilda slag. Exempelvis gav Tuveskredet upphov till ett tiotal olika förklaringar från geoteknisk expertis till detta skreds uppkomst och slutliga utbredning. (Jfr SGI:s Rapporter No 10 (1981) och No 18 (1982)).

Ett viktigt tema i föreliggande dokument är att bristande överensstämmelse mellan teori och verklighet på detta område av geotekniken härrör från det faktum, att många jordarter är utpräglat *deformationsmjuknande* inom ramen för de skjuvdeformationer och de förskjutningar i förhållande till underlaget som kan förekomma i den blivande brottzonen vid en begynnande skredrörelse. Detta gäller i synnerhet vid långsträckta flakskred i sensitiva jordar.

Vidare betonas deformationsmjuknandets tidsberoende – d v s inverkan av belastnings-hastighet och dräneringsförhållandena i den potentiella brottzonen.

Deformationsmjuknande - sensitivitet

Det kan redan inledningsvis framhållas att begreppet *'deformation-softening'* i föreliggande handling syftar på förlusten av skjuvmotstånd relaterad till såväl 'deviatorisk' töjning i den blivande brottzonen som till ren glidning (slip) i en etablerad glidyta. Anledningen härtill är att brott enligt föreliggande analysmetodik definieras av två *samtidigt* pågående tillstånd benämnda Stage I och Stage II, vilka simulerar rådande förhållanden dels *före*, och dels *efter* det att en diskret glidyta utbildats.

Graden av sensitivitet är en viktig faktor i detta sammanhang. I vårt land finns en tendens att ofta vilja förklara skred av ifrågavarande art genom att i all enkelhet referera till förekomsten av 'kvicklera', d v s lera med en sensitivitet $St = c_u / c_{ur} \geq 50$. Emellertid, hur den i laboratoriet bestämda sensitiviteten egentligen påverkar skeendet vid begynnande skred är i hög grad oklart och bidrar således på ett avgörande sätt till svårigheterna att bedöma skredrisk i detta sammanhang. Skjuvhållfastheten hos på laboratoriet omrörda lerprover – som i denna rapport betecknas c_{ur} – kan rimligen inte – under vilka betingelser som helst – överensstämma (eller utgöra ett entydigt samband) med den odränerade skjuvhållfastheten (c_{uR}) för samma lera vid begynnande brottutveckling i en verklig slänt.

Vidare, eftersom den *effektiva* resthållfastheten under reala betingelser måste vara starkt beroende av såväl pålastningshastighet som de i brott-zonen lokalt rådande dränerings-förhållandena, betecknas densamma i det följande bara som c_R – något som således är ett uttryck för tidsfaktorns avgörande betydelse i sammanhanget. I föreliggande framställning görs således en distinktion mellan innebörden av parametrarna c_{ur}, c_{uR} och c_R. Av liknande skäl ersätts beteckningarna c' och c_u för 'peak shear strength' med enbart c.

Vid konventionell skredanalys (i föreliggande dokument benämnd I-PlFA (= Ideal-Plastic Failure Analysis) bortser man, som det kan förefalla, för enkelhets skull från såväl deformationerna inom den potentiella glidkroppen som från de relativa deformationerna mellan densamma och under brottzonen liggande fastare material. Detta innebär således att man i praktiken tillskriver jordmaterialet obegränsat plastiska egenskaper, något som för lösa postglaciala leror sällan gäller i verkligheten.

Beträffande extrema nederbördsförhållanden som orsak till skred
Vid många tidigare utredningar av denna typ av skred (t.ex. Surte, Rävekärr m. fl.) har brottorsaken tillskrivits extremt höga artesiska grundvattentryck och/eller utbredda hydrauliska brott (liquefaction) i lokala skikt av silt eller sand.
Även om dessa brottmodeller i och för sig är teoretiskt möjliga så kan de – särskilt i samband med mycket långsträckta skred – likväl ifrågasättas av olika skäl, såsom:

- De ifrågavarande skreden har utlösts i *direkt* samband med lokalt pågående verksamhet av mänsklig art.
- Sannolikheten för att den avgörande orsaken till skreden enbart skulle sammanhänga med höga artesiska vattentryck torde vara ringa, d v s under förutsättning att infiltrations-förhållandena inte på ett avgörande sätt förändrats genom mänskliga ingrepp. Statistiskt sett, bör nämligen ogynnsammare hydrologiska betingelser med stor sannolikhet ha förekommit tidigare i släntens historia.
- Utbredda och sammanhängande skikt av silt eller sand av den art dessa brottmodeller förutsätter har i nämnda fall inte påvisats.
- Vidare har höga artesiska tryck eller porvattenövertryck av den storleksordning och utbredning som brottmodellerna förutsätter inte heller dokumenterats.
- Hydrauliska brott (liquefaction) genom *skjuvning* är på rent geotekniska grunder föga sannolika i jordlager som under lång tid undergått avsevärda skjuvdeformationer på grund av krypning och konsolidering i samband med att slänterna successivt anpassat sig till land-höjningen under senglacial och postglacial tid. **([1])**

([1]) Ovanstående utesluter givetvis inte att artesiska tryckförhållanden och lokala porvattenövertryck kan bidra till risken för progressiva skred. Lastökning och deformationer på grund av lokala hydrauliska brott i lager av friktionsjord, orsakade av stötar och vibrationer i samband med t.ex. pålning, sprängning, jordpackning, utgör ofta förekommande anledningar till att dylika skred utlösas.

Analys av stabilitet i långa slänter med hänsynstagande till relevanta deformationer
I denna handling ställs möjligheten av progressiv brottbildning i fokus, något som motiveras av ett antal inträffade skred med uppenbara indikationer på att spröda brottmekanismer varit för handen. En numerisk beräkningsmetod baserad på finita differenser (Finite Difference Method = FDM) tillämpas vid analysen av deformationernas och deformationsmjuknandets inverkan på släntstabiliteten.
Förfarandet liknar konventionell skredanalys i så motto att brottzonen och den presumtiva glidytans sträckning under markytan antas vara känd, frånsett dess bortre avgränsning. Emellertid, även om läget för den potentiella brottzonen ofta är given med ledning av sedimentlagrens struktur kan alternativa lägen för densamma behöva undersökas.

Den föreslagna analysmetodiken avviker dock från den konventionella i flera betydelsefulla avseenden enligt nedan:

- Under det att man vid gängse beräkningsmetoder (I-PlFA) begränsar sig till att studera jämvikten för den tänkta glidkroppen i sin *helhet*, tillämpas jämviktvillkoret vid analys av progressiv brottbildning (PrFA) på *vart och ett* av de vertikala element i vilka glidkroppen indelats.

- Vidare beaktas deformationerna inom och utom den presumtiva glidkroppen. Härvid tillses att den axiella deformationen i släntriktningen – på grund av ändrad jordtrycksfördelning i samband med lasttillägg – i varje sektion är förenlig med skjuvdeformationen i motsvarande vertikala delelement. Härigenom kan fördelningen av skjuvspänningar av t.ex. lokal tilläggslast bestämmas samt på vilken längd i släntriktningen lerans skjuvmotstånd tas i anspråk för upptagande av lasten ifråga.
Eftersom den här tillämpade FDM-analysen är två-dimensionell kan den begynnande brottzonen modelleras i *sin helhet* och ej endast som en glidyta (eller ett diskret s.k. 'shear-band').
Denna omständighet utgör en avgörande punkt i föreliggande analys. Brottzonens deformerbarhet, eller eftergivlighet, är nämligen i sig själva förutsättningen för att koncentrerad tilläggsbelastning skall kunna fördelas på någon längre sträcka.
Med andra ord, den skjuvade zonens utbredning i höjd och längdled avgör storleken på den koncentrerade belastning som kan påföras slänten utan att lokalt brott utlöses.
Det är således *brottzonens uppbyggnad* och jordlagrens egenskaper *inom* densamma som – under i övrigt likartade förhållanden – avgör benägenheten till progressiv brottbildning. **([2])**

([2]) En obetydlig koncentrerad lasteffekt skulle exempelvis med lätthet kunna generera progressiv brottbildning i ett tunt lager av 'kvicklera'.

- Jordens egenskaper vid skjuvning definieras medelst ett fullständigt spännings/deformationssamband och ej endast med ett enstaka värde på skjuvhållfastheten såsom vid gängse beräkningsmetoder.
De konstitutiva sambanden indelas i två skilda stadier benämnda 'Stage I' och 'Stage II', vilka simulerar förhållandena före respektive efter utbildandet av en diskret glidyta. De konstitutiva sambanden kan varieras och anpassas alltefter de i släntens jordlager och i brottsprocessen rådande förhållandena.

- Genom att relatera nämnda spännings/deformationsegenskaper till olika tidshorisonter vid påförandet av tilläggslast, (eller till tidsförhållandena vid andra skredutlösande orsaker) samt till de olika skeendena under själva skredförloppet, kan hänsynstagande till tidsfaktorn införas i analysen. (Se nedan.)

- Olika typer av lastfördelning samt specifika förhållanden i släntens och fasta bottnens geometri, vilka ofta starkt påverkar skredrisk och benägenhet till progressiv brottbildning, kan beaktas.

- Som nämnts antas brottzonens höjdläge i varje enskild beräkning vara given, men skredets slutliga utbredning i släntriktningen och passivzonens längd – d v s en uppskattning av skredets slutliga omfattning och grad av katastrof – erhålls som resultat av beräkningarna.

Olika faser i utvecklingen av progressiva skred
Möjligheten att, som ovan nämnts, beakta tidsfaktorn vid analys av skred innebär att skredrisken inte – såsom vid plastisk brottbildning – kan baseras på en entydig brottsituation

av statisk karaktär. Från och med tidigt 1980-tal har författaren därför distingerat mellan olika faser hos progressiva skred. I denna rapport har detta skett enligt följande:

Fas 1 - Rådande ***tillstånd in situ***;
Fas 2 - ***Störningsfasen*****,** d v s det skede som kännetecknar den lasteffekt som utlöser skredet
Fas 3 - Ett (i princip) ***dynamiskt övergångsskede*** då krafter p g a bristande jämvikt i släntens övre del överförs till stabilare mark längre ner i sluttningen;
Fas 4 - Ett ***övergående*** (eller i vissa fall ***bestående***) ***nytt jämviktstillstånd*** med därtill hörande kraftspel;
Fas 5 - ***Dynamiskt sammanbrott*** om passivt Rankine motstånd överskrids i det nya jämviktsläget. Denna fas utgör det som vanligen uppfattas som det egentliga skredet;
Fas 6 - ***Slutligt jämviktstillstånd***. **([3])**

([3]) I Rapport LuTU 2008:11 har de fem första av dessa skilda faser i utvecklingen av progressiva skred benämnts *'Phases 1, 2, 3, 4 and 5*'. I föreliggande handling betecknas det slutliga tillståndet i jämvikt som *'Phase 6'*.

De olika faserna karakteriseras sinsemellan av i hög grad varierande tidsförhållanden
- dels i samband med störande inverkan av tillskottslast.
- dels i samband med uppkommande spänningsändringar och vid fortsatt brottbildning.

Varierande geometri, materialegenskaper, dräneringsförhållanden och portrycksutveckling i de olika faserna längs med det område som omfattas av skredrörelsen är också av *avgörande* betydelse för brottutvecklingen.
Dessa betingelser kan således medföra att inverkan av en initialt skredutlösande faktor upphör i ett senare skede av brottutvecklingen – d v s att en begynnande skredrörelse kan avstanna inom vilken som helst av Faserna 2, 3 och 4.

Brottkriterier vid progressiv brottbildning
Resultaten från den föreslagna analysmetoden understryker nödvändigheten av att beakta deformationerna i jordmassan vid skred i långa slänter med deformationsmjuknande jord. Underlåtenhet härvidlag kan leda till allvarlig felbedömning av risken för *lokalt brott* i slänten och i synnerhet av omfattningen hos det *slutliga* skred som därmed kan utlösas. Analysen möjliggör identifiering av de verkligt kritiska förhållandena i en slänt med hänsyn tagen till lastfördelning, geometri och lokala egenskaper hos jordmaterialet.

Risk för progressivt brott föreligger om jordens resthållfasthet (c_R) i någon del av en slänt vid någon tidpunkt kan komma att understiga rådande in situ spänningar d v s
$\mathbf{c_R(t,x) < \tau_o(x)}$ (Betr. beteckningar se 'Notations')

Ändrade kriterier för brottsäkerhet
I samband med den föreslagna metodiken för analys av skred, vid vilken deformationerna beaktas, blir gängse sätt att definiera brottsäkerheten *utan fysikalisk mening* i de fall då resthållfastheten $\mathbf{c_R < \tau_o}$. Följaktligen måste i dessa sammanhang säkerheten mot brott omformuleras med hänsyn till de villkor som är avgörande för uppkomst och utveckling av progressiv brottbildning. Följande brottvillkor vid koncentrerad tilläggslast föreslås i Sections 3, 8 and 11:

Med avseende på uppkomst av lokalt brott i del av slänten: $\mathbf{F_s^I = N_{cr}/N = q_{cr}/q}$

Med avseende på uppkomst av omfattande totalt skred $\mathbf{F_s^{II} = E_p/(E_{0x} + N_{max})}$
(Jämför Notations)

Om däremot $\mathbf{c_R > \tau_o}$ kan säkerhetsfaktorn formuleras på gängse vis på basis av mobiliserbar medelskjuvhållfasthet. Skjuvspänningsfördelningen i brottstadiet kan därvid beräknas med hjälp av den föreslagna progressiva beräkningsmodellen.

Skreds utbredning över plan mark
En omdiskuterad och mindre väl utredd frågeställning beträffande vissa skred i lösa leror, har varit deras väldiga utbredning, karakteriserad av att passivzonen ofta sträckt sig hundratals meter bortom släntfoten varvid marken under hävning deformeras plastiskt till stort djup. Vid skreden i Surte och Tuve utgjordes exempelvis ca 50 resp. 60 % av den yta som omfattades av initialskreden av svagt sluttande mark. I Tuve deformerades exempelvis ca 16 hektar mark ned till ca 35 m:s djup i passivzonen varvid hävningen uppgick till ca 5 m.
En detaljerad redovisning av de mekanismer som kan leda till dylik utbredning av skred i sensitiva lösa leror ges i Bernander, (2008), LuTU 2008:11, Section 5.
Vidare visas där att:
a) … utbredningen över plan mark vid skred i lösa leror klart förutsägs genom den använda analysmetoden (FDM) och att detta fenomen kan förklaras med rent ***statiska*** belastnings-förhållanden - d v s utan beaktande av de dynamiska effekter och tröghetskrafter som kan uppkomma i skredets slutskede, (’Phase 5’).
b) .....att brottzon och glidyta tenderar att utbildas hundratals meter bortom släntfoten, redan ***innan*** eventuellt sammanbrott av passiv-zonen *eventuellt* äger rum.
c) .....att vid brott i markerat deformationsmjuknande jord sträcker sig brottzon, glidyta och därmed sammanhängande markrörelser ofta långt (d v s 100-tals meter) ***bortom gränsen*** för synligt passivt markbrott – eller med andra ord långt utanför vad som normalt uppfattas som det egentliga skredområdet.
d) .....att skredens utbredning över nästan horisontell mark inte med nödvändighet förutsätter förekomst av kvicklera i hela skredområdet. Lerorna under dalbottnen, såväl i Surte som i Tuve, uppvisade normal, låg sensitivitet med c_u/c_{ur} omkring 10 à 15.
e) .....att brottmodeller baserade på cirkulär-cylindriska glidytor (mynnande i slänten) med stor sannolikhet ej har någon relevans vid analys av skred i långa naturliga lerslänter av den typ som avhandlas i föreliggande dokument. Detta gäller dock inte om djupet till den potentiella brottzonen är ringa.

Andra konsekvenser av hänsynstagandet till deformationer i jordmassan vid analys av skred enligt föreslagen FDM- metod.
Den omständigheten att skjuvspänningarna p g a en lokal tilläggslast endast mobiliseras på en begränsad sträcka räknat från lastens angreppspunkt, kan i många fall vara av avgörande betydelse.
På ett avstånd definierat som L_{cr} (enligt ’Section 3.3’) från en lokal tilläggslast är lastens inverkan på spänningar, jordtryck och deformationer försumbar. Detta utesluter eller minskar de facto möjligheten att i skredets initiala skede tillgodoräkna sig ökande passivt motstånd längre ner i slänten för stabilisering av tilläggslasten. Man kan uttrycka förhållandet så, att jorden nedanför den sektion som definieras av avståndet L_{cr} från tilläggslasten, inte ’vet om’ eller ’känner av’ när brott vid lastens angreppspunkt är nära förestående.

Vid den i princip dynamiska omfördelningen av jordtrycken i samband med senare progressiv brottbildning kan dock givetvis fullt passivt motstånd mobiliseras vilket också sker i samband med fullbordade skred.
Beaktandet av jordens deformationsmjuknande medför att i de fall då $\mathbf{c_R}$ är *mindre* än $\boldsymbol{\tau_o}$ blir den påverkan som kan utlösa progressivt brott markant lägre än den som skulle erhållas enligt konventionella beräkningar.
Man bör emellertid i detta sammanhang notera att resthållfastheten (c_R) merendels förblir större än rådande skjuvspänningar in situ – d v s ($\mathbf{c_R > \tau_o}$). Detta tillstånd medför då en segare 'statisk' brottyp av progressiv karaktär, vid vilken överensstämmelse med konventionell ideal-plastisk analys inträffar för det gränsfall då kvoten mellan resthållfasthet och maximal skjuvhållfasthet = 1.

Avgörande för brottutvecklingen är givetvis i vilken utsträckning c_R under densamma reduceras på grund av tilltagande deformationer och därmed sammanhängande deformationsmjuknande – något som i sin tur på ett avgörande sätt påverkas av tidsramarna för brottprocessen respektive av dräneringsförhållandena i brottzonen och i glidytans närmaste omgivning.

Brottutveckling i sluttande terräng
En viktig konsekvens av den ovan nämnda begränsade möjligheten att initialt mobilisera passiva jordtryck längre ned i slänten blir, beroende på graden av deformationsmjuknande, att brottmotståndet längs plan parallella med markytan eller längs med fast botten parallella sedimentplan som nämnts är avsevärt *mindre* än motståndet baserat på glidytor som utmynnar i sluttningen närmare lasten.
I princip gäller detta förhållande även i initialskedet hos skred då $c_R > \tau_o$ eftersom betydande förskjutningar i släntriktningen måste äga rum innan de passiva jordmotstånd, som vid konventionella beräkningar förutsätts bidra till stabiliteten, kan mobiliseras.

Det förhåller sig med andra ord så att kortare glidytor i sluttande mark, för vilka konventionell ideal-plastisk analys som sådan kunde anses vara giltig, sällan representerar det farligaste sättet för brottbildning. (Bernander, 1981). Skillnaden mellan resultaten från progressiv brottanalys (PrFA) och konventionell ideal-plastisk brottanalys (I-PlFA) kan vara betydande. Bedömning av skredrisk enligt I-PlFA kan följaktligen i många situationer bli mycket 'på osäkra sidan'. (Jfr Bernander LuTU 2008:11, Appendix A, B & C.) **([4])**
([4]) Detta förhållande kullkastar en utbredd föreställning att ideal-plastisk analys - trots eventuellt erkända brister – ändock äger tillämplighet vid fastställande av s.k. 'initialskred', varmed man i allmänhet avser instabilitet med avseende på någon lokal glidyta i ett brant parti av slänten.

Nämnda avvikelse mellan utvärdering av initierande brottorsak under hänsynstagande till deformationerna å ena sidan och resultat från konventionella beräkningar å den andra, kan dessutom bli än allvarligare i skiktade jordar och varviga leror. Detta sammanhänger med att höga porvattenövertryck med större sannolikhet utbreder sig längs sedimentskikten än i vinkel mot desamma.
Den föreslagna FDM-modellen för framåtgripande progressiv brottbildning medger också hänsynstagande till deformationer under den presumtiva glidytan. Som framgår av ovanstående medför emellertid de begränsade möjligheterna att mobilisera passiva tryck längre ner i sluttningen att brott i slänter uppvisar en markerad tendens att följa sedimentlagren och/eller i stort sett lutningen hos fast botten till avsevärt djup under markytan. Vid Tuve skredet synes exempelvis glidytan i huvudsak vara parallell med fast botten ända ned till c:a 35 m:s djup. Beaktande av deformationerna under brottzonen torde

därför i många fall ej ha någon större inverkan vid bestämning av den last som kan initiera en skredrörelse.

Betydelsen av förhållandet L_{cr}/L
En annan parameter av betydelse i detta sammanhang utgörs av relationen mellan den kritiska längden (L_{cr}) och släntens totala längd (L) vari en del av marken framför släntfoten även bör inräknas. Förhållandet (L_{cr}/L) kan sägas utgöra ett mått på tillämpligheten av konventionell analys i en aktuell situation, i synnerhet när det är fråga om påförande av lokala tilläggslaster högre upp i sluttningen.
Om förhållandet L_{cr}/L är mindre än ett värde av – säg 2 – föreligger sannolik risk för progressiv brottbildning. Stabilitetsundersökningar i samband med påförande av belastning i långa slänter bör med hänsyn härtill regelmässigt inbegripa en uppskattning av den kritiska längden (L_{cr}) och motsvarande kritisk last med hänsyn till läget för den aktuellt tillkommande belastningen.

Faktorer som inverkar på benägenheten till sprödbrott i naturliga slänter
Deformationsanalysen enligt kapitel 4 visar klart att även andra förhållanden än jordens sprödhet kan ha stor inverkan på benägenheten till progressiv brottbildning. Till dessa faktorer, som belyses särskilt i kapitlen 9 och 10, kan räknas:

- Markytans, sedimentskiktens och fasta bottnens geometri – 'geometrisk sprödhet'
- Typ och läge av påförd belastning eller störning
- Tidsförhållanden för dito
- Dräneringsförhållandena i brottzon och i eventuell glidytas omedelbara närhet
- Hydrologiska förhållanden och hydrologisk historia

***Varför tillämpa progressiv brottanalys*?**
Stabilitetsförhållandena i en naturlig slänt är nära förbundna med dess geologiska och hydrologiska historia. Många lerslänter i Västsverige är uppbyggda av glaciala och postglaciala sediment som rest sig ur det regredierande havet under efteristiden. Allteftersom marken höjt sig över havsytans medelnivå har jordens hållfasthet och jordtrycken i slänten, genom konsolidering och kryprörelser, kommit att successivt anpassa sig till de ökande påfrestningar, som blivit följden av sjunkande grundvattenytor, klimatologiska variationer, krypdeformationer, kemiska förändringar och urlakning.
Följaktligen är varje naturlig slänt stabil i den meningen att den existerat under årtusenden. Med hänsyn till att slänten under denna tidsrymd med viss marginal förblivit stabil i situationer med extrema porvattenövertryck, bör 'säkerhetsfaktorn 'vis à vis skred under normalt rådande betingelser vara större än 1.
Emellertid, den avgörande frågeställningen vid bedömning av risken för skred blir i stället hur stabiliteten kan komma att påverkas av tilläggslaster eller störningskällor, för vilka tidshorisonten mäts i *timmar, dagar, veckor* eller *månader* i stället för *århundraden* respektive *årtusenden*?
Med andra ord, vad blir således följderna om en lokal instabilitet skulle uppkomma p g a ovan nämnda störningskällor? Kommer eventuellt lokalt brott endast att resultera i en markspricka vid släntkrönet eller kan det föranleda ett katastrofalt skred varvid hundratals meter av i och för sig stabil (eller horisontell) mark, undergår våldsam hävning och förskjutning.

Analysen enligt kapitel 4 & 5, vilken beaktar deformationerna i jordmassan erbjuder just strukturmekaniskt logiska förklaringar till varför ett antal katastrofala skred i Skandinavien kunnat utlösas p g a vad som i sammanhanget bedömts vara obetydliga störningseffekter. Ifrågavarande slänter har således kunnat förbli stabila under tusentals år sedan marken en gång höjde sig ur det post-glaciala havet.
Ändock har skred, innebärande markförskjutning och markhävning med vidsträckt utbredning över svagt sluttande mark ofta inträffat i samband med vad som kan uppfattas som mindre mänskliga ingrepp av lokal natur.
Progressiv brottanalys visar emellertid att detta är *just* vad som kan hända, även vid obetydlig störning av ett ömtåligt parti i en dylik slänt. Analysmetoden bör således vara av betydelse vid bland annat kartering av potentiell skredrisk.

Såsom nämnts medför hänsynstagandet till ett jordmaterials deformationsmjuknande i allmänhet betydligt större beräknad risk för skred p g a koncentrerad last respektive lokala störningsmoment än vid tillämpning av konventionell analys baserad på ideal-plastiska egenskaper hos jorden – och det givetvis i synnerhet om $\mathbf{c_R}$ i något avsnitt kan bli $< \boldsymbol{\tau_0}$.
I kritiska fall kan det således vara välbetänkt att utföra s.k. känslighetsanalyser genom att inom ramen för vad som kan anses rimligt på geotekniska grunder variera jordens konstitutiva egenskaper.

Beräkningar
Även om beräkningarna enligt den i kapitel 4 föreslagna metoden för analys av progressiva skred i princip är tämligen enkla, kan de förefalla komplicerade i jämförelse med gängse metoder för bedömning av släntstabilitet. Det gäller exempelvis att välja tillämpliga konstitutiva samband för den aktuella jordarten, varvid tidsramen för påförande av eventuell tilläggslast, hydrologiska betingelser, dräneringsförhållanden, OCR och huvudspänningstillstånd utgör några av de inverkande kriterierna.

Dock vill man uppnå säkrare *förutsägelser* beträffande skredrisk med hänsyn till människoliv, samhällsekonomiska konsekvenser och egendom måste man enligt författarens mening ta itu med dessa svårigheter.

Som framgår av exemplifieringen av FDM-metoden enligt kapitlen 4 & 5 medför handberäkningar – ehuru enkla i princip – omfattande beräkningsarbete vid godtycklig släntgeometri. Med hjälp av datorkraft blir dock tidsåtgången för beräkningarnas genomförande obetydlig. Sedan man väl definierat och matat in ingående parametrar kan den egentliga beräkningstiden för erforderliga passningsberäkningar mätas i minuter.

Såsom påvisats i LuTU 2008:11 kan man med en alternativ programvara i Excel lättvindigt analysera *kritisk last* och utbredningen av skred i slänter med konstant lutning och konstant djup till brottzonen. Metoden kan lämpa sig för att snabbt utforska huruvida påtaglig risk för progressiv brottbildning föreligger i – exempelvis – det övre brantare partiet av en slänt. Excel-programmet lämpar sig också väl för undervisning eftersom användaren snabbt kommer till insikt om de komplicerade förhållanden som styr progressiv brottbildning i sensitiv lera.

Ifrågavarande programvara kan emellertid även användas för slänter med godtycklig geometri men blir då avsevärt mer arbetskrävande. (Jfr LuTU 2008:11, Appendix A, B & C.)

Den extra arbetsinsats som geoteknikern måste ägna släntstabilitetsundersökningar enligt föreliggande metodik behöver dock inte utgöras av i oöverstiglig grad ökat beräkningsarbete. Den huvudsakliga *utmaningen* för geoteknikern består snarare i att kunna utnyttja möjligheterna att studera hur släntstabilitet påverkas av ett antal faktorer, vilkas inverkan per definition inte kan identifieras med de konventionella metoder som grundar sig på obegränsat plastiska egenskaper.
Denna inverkan måste i stället baseras på beaktandet av jordens *deformationer, deformationsmjuknande egenskaper,* brottsprocessernas *tidsramar* och släntens *geometri*.

Nyckel-uttryck: *Framåtgripande skred i lösa leror; Deformationer i jordmassan; Deformations-mjuknande; Plasticitetsteorins tillämplighet; Modellering av progressiv brottbildning med finita differenser; Resthållfasthet i den begynnande brottzonen – en avgörande parameter; Olika faser i framåtgripande progressiva skred; Analys av inträffade skred som exempel på progressiv brottbildning; Surteskredet – en tidsinställd bomb tickande genom årtusendena? Utlösande störningsfaktorer; Skredens utbredning över svagt sluttande mark – Utbildning av brottzon resp. glidyta långt inunder möjligen uppkommande passivzon redan före passivt sammanbrott med tillhörande hävning; Är 'kvicklera' det enda riskmomentet vid skred i sensitiva leror? Har analys av mindre skred baserad på circulär-cylindriska glidytor någon relevans i långsträckta slänter? Inverkan av tilläggslastens natur – koncentration och belastningshastighet; Tidsfaktorns inverkan; Geometrisk sprödhet.*

Långtidsutveckling av bakåtgripande skred ('uphill progressive landslides'); Reduktion av effektivtryck genom erosion; Av erosion orsakade deformationer, förskjutningar och kryprörelser; Deformationsmjuknade över tid; Slumpartad och tidsmässigt svårbedömd brottutveckling.

Symbols and notations

In the present document, the term *'deformation-softening'* denotes the loss of shear resistance both due to shear (deviator) strain in the developing failure zone and to concentrated excessive strain generated by large displacement and slip in the failure plane. The reason for this is related to the fact that failure in this context is represented by two simultaneous but basically different states (Stages I and II), simulating the conditions before and after the formation of a discrete slip surface or narrow shear band.
For the same reason, the constitutive stress-/strain/displacement properties are in the document simply referred to as *'stress-deformation'* relationships.

Greek letters:

α	Coefficient defining the elevation of the earth pressure resultant
αH_x	Level at which the down-slope displacement (δ_{ave}) is valid
β, β (x), β_x	Slope gradient at coordinate x
γ, γ (x,z), $\gamma_{x,z}$	Deviator strain, (angular strain) as a function of x and z
γ_{el}	Deviator strain, (angular strain) at elastic limit
γ_f	Deviator strain, (angular strain) at failure stress
$\varphi' = \varphi_i$	Angle of internal friction, drained conditions
φ	Angle of internal friction
$\delta_x = \delta(x)$	Down-slope displacement
δ_N	Down-slope displacement in terms of axial deformation generated by forces N_x
δ_τ	Down-slope displacement in terms of deviator deformation
$\Delta\delta$	Differential of δ
Δx	Differential of x coordinate
δ_S, δ_S (x),$\delta_{S,x}$	Post peak slip deformation in the slip surface in relation to the sub-ground
$\delta_{S\,(CR)}$	Post peak slip in slip surface at ultimate residual shear strength c_R
$\delta_{S\,100}$, $\delta_{S\,300}$	Post peak slip in slip surface = 100 mm = 0.1 m or = 300 mm = 0.3 m
δ_{ave}	Average down-slope displacement of the soil above the potential slip surface
ε	Longitudinal strain
ν	Poisson's ratio
Ω	Coefficient relating the modulus of elasticity to the undrained shear strength
ρ , $\rho(z)$	Soil density ($Mg/m^3 = ton/m^3$)
σ_1,	Major principal stress in tests
σ_3,	Minor principal stress in tests
σ_v	Vertical normal stress
σ_h	Horizontal (down-slope) normal stress
σ_x, $\sigma(x)$, σ_x	Mean incremental down-slope axial stress corresponding to N
τ_{el}	Shear stress (deviator stress) at elastic limit
τ_o,τ_o(x,o), $\tau_{ox,o}$	In situ shear stress at failure plane (z = 0)
τ, τ(x,o), $\tau_{x,o}$	Total shear stress at failure plane (z = 0)
τ_o,τ_o(x,z),$\tau_{ox,z}$	In situ shear stress
τ , τ(x,z), $\tau_{x,z}$	Total shear stress (deviator stress)

Roman letters:

b, b(x), b_x	Width of element
c	Shear strength of clay in the current time scale (or rate of loading)
c_o	Adhesion for $\varphi' = 0$ - drained shear strength

$c_u = c_u(\gamma_f)$	Undrained shear strength
$c_{u,mean}$	Mean undrained shear strength of the soil above the failure plane
$c_R = c_R(x)$	Residual shear strength at a point (x) for post peak slip of $\delta_{S,x}$ in slip surface
c_{uR}	Un-drained residual shear strength at (x) for post peak slip of $\delta_{S,x}$.
$c_R(t,x)$	Residual shear strength at a point (x) at time (t)
c'	Drained shear strength
g	9.81 m/sec^2
q(x)	Additional vertical load
t(x)	Additional horizontal load
w	Natural water content (%)
w_L	Liquid limit (%)
w_P	Limit of plasticity (%)
x	Horizontal (or down-slope) coordinate
z	Vertical coordinate
D_W	Submerged depth (when slope borders river or lake)
E, E (x), E_x	Down-slope earth pressure at point x, i.e. ($E_x = E_{ox} + N_x$) or ($E_x = E_{ox} + \Delta E_x$)
E_o, $E_o(x)$, E_{ox}	In situ earth pressure at point x
E_a	Active earth pressure
$E_{el,o}$	Elastic modulus of structural element at z = 0
E_{el}, $E_{el,mean}$	Mean secant elastic modulus in down-slope compression of a vertical structural element $H \cdot \Delta x$, i.e. $E_{el,mean} = \Omega \cdot c_{u,mean}$
E_p	Passive earth pressure
$E_p^{Rankine}$	Critical down-slope earth pressure resistance at passive Rankine failure
$\Delta E = N$	Incremental down-slope earth pressure at point x due to additional loading
F_s	Safety factor
G, G_{el}	Elastic modulus in shear
G_o,$G_{el,o}$	Elastic modulus in shear of structural element at elevation z = 0
H, H(x)	Height of element, (from slip surface to ground surface)
K_o	Ratio σ_h / σ_v – or where applicable – between minor and major principal stress, or ratio of horizontal earth pressures at rest, $E(\varphi')/E(\varphi' = 0)$
L_{cr}	Limit length of mobilization of shear stress at N_{cr}
L_{instab}	Limit length at which slope fails for $N_i = 0$
$L_p = L_{E>E(Rankine)}$	Length of the passive Rankine zone at the foot of the slope
N, N(x), N_x	Earth pressure increment due to additional load or progressive failure formation at point x
N_i	Load effect of agent initiating local slope failure
N_{cr}	Critical load effect initiating local slope failure

Abbreviations:

ICSMFE	International Conference on Soil Mechanics and Foundation Engineering
ISL	International Symposium on Landslides
I-PlF	Ideal-plastic failure
I-PlFA	Ideal-plastic failure analysis
NGM	Nordic Geotechnical Meeting
OCR	Over-consolidated ratio
Pr F, PrFA	Progressive failure, Progressive failure analysis
SGI	Swedish Geotechnical Institute

1. Introduction – historical background

1.1 *Historical background*

Aspects on the topic of progressive failures in clays, silts and sands have been treated by Taylor (1948), Terzaghi & Peck (1948), Terzaghi (1950), Kjellman (1954), Skempton, (1964) and (1977), Haefeli (1965), Peck (1967), Turnbull & Hvorslev (1967), Bjerrum (1954, 1961, 1967), Bishop (1967), Skempton & Hutchinsson, State-of the Art report (1969), Suklje (1969), Christian & Whitman (1969), Palmer & Rice (1973), Lefebvre & La Rochelle (1973), Bernander et al (1978-1989), P. Hansbo et al (1984), Wiberg et al (1990), Chen et al (1997), Alén (1998), Tiande et al (1999) and others. Much of this material refers to strongly over-consolidated clays and clay shale. However, specific papers, reports and writings, which are considered to relate more closely than others to the key issues highlighted in the present report, are briefly commented on below.

1.11 Early research

Terzaghi & Peck (1948) emphasized the risk of progressive failures in brittle soils, but when exemplifying these phenomena in normally consolidated soft clays they seem to have limited their interest to bottle-neck slides, clay flows, successively retrogressive slides and to spontaneous liquefaction in loose sands or silts. Considering the enormous scope of the writings of these two authors, their rather modest contributions in this field of soil mechanics may indicate that they did not regard brittleness in normally consolidated clays as an important problem in the sense conceived in this report.

In the late 1960's Bjerrum (1967) lectured on retrogressive brittle failures in cemented Tertiary clays. However, in response to a direct question by the author of this report as to whether progressive failure formation could be a conceivable issue also in normally consolidated Scandinavian clays, Bjerrum firmly stated that in his opinion this was not the case.

Kjellman (1954) discussed 'progressive failure mechanisms' in connection with large Swedish landslides, and some important features of his failure concept coincide in principle with the progressive failure mechanisms of large landslides dealt with in this document. However, although Kjellman discussed the effects of down-slope axial deformations on strain- and deformation softening in the slip surface proper, his model did not consider the deformations in highly strained zones adjacent to the failure plane. This implied that his approach seriously exaggerated the risk of incidence of progressive failure phenomena. In the article referred to, no quantitative analyses were made of key issues in this context - e.g. the vertical distribution of downhill shear deformations within the sliding body. Nor were critical parameters such as modified safety criteria and other phenomena arising from considering deformations in the soil mass identified.
Furthermore, Kjellman did not address the rate of loading on shear strength or the role of the time factor in general, thus also neglecting the important impact of creep in this context.

However, Kjellman interestingly argued that progressive failure formation should not be limited to 'quick' clays, as it may be liable to occur also in other normally consolidated soft clays of sensitive nature. The author of this document subscribes to this opinion.

With special reference to Skempton's and Bjerrum's reports on slope failures in over-consolidated clays and clay shales, Christian and Whitman (1969) proposed a method of

analysis for a specific mode of retrogressive (or upward progressive) failure, in which the sliding soil mass moves as an integral block owing to failing down-slope support. The paper is interesting in the current context because it addresses some of the issues highlighted in this document. However, their one-dimensional model is very simplistic, the slope gradient and depth of the sliding soil block being assumed to be constant in the model.
The most problematic feature of this approach is the fact that the stress-deformation relationship, defining the properties of the shear band joining the sliding soil body to the sub-base, cannot be derived directly from conventional soil parameters without the use of specific 'field observations'. It is therefore difficult to conceive how this crucial parameter is to be determined in practice, for instance when investigating potential slope failures or slides that have already occurred.

Lo and Lee (1973) studied the effects of strain-softening on progressive failure in steep slopes of London clay applying FEM-analysis. The approach resembles the analytic approach in the present document in so far as a full stress-strain relationship is used.
However, the stress-strain relationship assumed features sharply jointed straight linear components, and as the method of analysis is focussed on steep, short slopes of over-consolidated clay ($H/L \approx 1$: 2.5 to 3), the results of the analyses performed have little relevance to the long natural gentle slopes that are subject to study in the current document.

P. Hansbo et al (1984), de Beer & van Impe (1984) and Wiberg et al (1990) performed studies of progressive failures in slopes. All of these studies were essentially based on the simplistic model adopted by Bernander & Olofsson (1981) for *investigative* purposes. This approach implied that the shear deformations were confined to a specific sensitive soil layer of given thickness. The basic weakness of this approach was obviously that the appropriate thickness and the integral shear deformation of this layer were difficult to define – especially as the one-dimensional model provided no information about the distribution of the deformations within the failure zone.
In order to address this problem, an improved version of the analytical model was later developed, whereby the shear deformations in the entire failure zone are modelled in a two-dimensional analysis by applying a relevant constitutive shear stress-strain (-deformation) relationship. Bernander et al (1984 &1989).

1.12 Examples of more recent research
A valuable contribution to the analysis of progressive landslides has been presented by S.Y.Chen, X.S. Zhang and W.S. Tang (1997). The safety factor is by Chen et al defined as the ratio between the peak strength and the mobilized *mean* shear stress, which in turn emerges from an analysis considering the deformations *in the slip surface* using a relationship related to stress/displacement. The approach resembles that of Skempton and other workers, as discussed in more detail in the next section. The progressive failure process is then studied by gradual increase of the relative displacements along the slip surface. The method offers a good understanding of the progressive failure mechanisms. However, as the authors themselves point out, the accuracy of the results may be affected by the fact that the development of the failure process is linked with the distribution of the incremental displacements, which are not uniquely defined by the method presented.

The progressive failure development is by Chen et al denoted as 'dynamic' in the sense that the method of analysis involves a progressively changing scenario. However, as time and inertia forces do not enter into their computations, the failure mode is *not* dynamic in a true mechanical sense, as demonstrated in the Figures 5:1.9 to 5:1.17. (Cf Section 5.)

Moreover, the one-dimensional method of analysis lacks some of the main characteristics of the method of analysis defined in Section 1:3 below.

Alén (1998) proposed a 'shear beam model', which in some essential respects is similar to the model adopted by Bernander et al (1981, 1984, 1989) and therefore exhibits several features in common with the approach adopted in this document. The model allows studying effects of progressive failure, particularly in steep slopes. Yet, the global safety factor is still defined as a weighted mean value of local safety margins, roughly in accordance with formulations used by other investigators of progressive failure formation.

Tiande, Chongwu and Shengzhi (1999) have proposed a model for progressive failure, by which the strain softening of the soil is defined as a rheological Maxwell relationship. In this approach, the effect of strain softening on failure propagation is calculated considering its effects on inter-slice forces. The model, which is applied to failures propagating up-slope, appears to be intended for steep slopes and over-consolidated clays.

1.13 Research after 2000 and current research on downhill and uphill progressive landslides
Research on progressive slope failure is going on in many countries e.g.:

Canada:	- Leroueil, S (2001, 2004). - Locat, A (2007). - Quinn, P., Diederichs, M.S. Hutchinsson, D.J. and Rowe, R.K. (2007). - Quinn, P. (2009).
Italy:	- Urciuoli, G. (2002). - Urciuoli, G., Picarelli, L. and Leroueil, S. (2007).
Norway	- Andresen, L. and Jostad, H.P. (2004, 2007). -Thakur, V. (2007). - Nordal, S. (2008). - Grimstad, G. (2004). - Grimstad et al (2005, 2010). - Gylland et al (2010, 2011).
Sweden:	- Bernander, S. (2008).
Switzer-land	- Puzrin, A.M. and Germanovitch, L.N. (2005). - Puzrin et al (2006 and 2010). - Saurer, E. and Puzrin, A. M. (2007, 2008, 2010). - Saurer, E. (2009).

Interesting State-of-the Art reviews are given in the cited theses by Thakur (2007), Quinn (2009) and Saurer (2009).

1.2 *Definitions of 'progressive failure'*

In this context it may be of interest to observe that the term 'progressive failure' often has different meanings for individual researchers.
In some papers, the term designates a failure process, which is progressive in a *spatial* sense, i.e. the slip surface formation starts at some point in the incipient slide and propagates towards the boundaries. The gradual loss of shear strength of the soil is then mainly expressed in terms of the development of *displacements.* The analysis should therefore consider, at least in some measure, the relative deformations in the failure zone as in the papers by Christian & Whitman (1969), Chen et al (1997) and Bernander (1981-1989).

In case records of slides in strongly over-consolidated clays, as for instance described by Skempton in his famous Rankine Lecture (1964) and by Tiande et al (1999), the mechanical processes leading to deformation softening and failure propagation are essentially governed by *time*, often in terms of decades. However, the safety factor in these studies is still defined as a *mean strength to mean stress ratio* (c_R/τ_{mean}), in accordance with the normal practice in conventional analysis based on plastic equilibrium. Hence, the loss of *mean shear strength* in

the developing slip plane and the consequential risk of sliding are essentially manifested as time related displacement.

Furthermore, the term ‘progressive failure’ is sometimes used as opposed to ‘retrogressive failure’, whereas in other contexts, the expression only refers to the mechanism leading to a ‘retrogressive failure’.
For instance, the types of slide referred to by Skempton (1964), Christian & Whitman (1969) and Tiande et al (1999), are undoubtedly set off by failing down-slope support considering the fact that stress concentrations tend to build up at the toes of steep slopes. These slide categories may by some be regarded as being ‘up-hill progressive’, retrogressive or spreads (e.g. A Locat), whereas others like Skempton designate them as ‘progressive’.

Progressive failure in the sense adopted in the present document is defined in the following section.

1.3 *Key features of the present report*

In the late 1960’s and the early 1970’s a number of large planar landslides took place in southwestern Sweden, some of which are accounted for in more detail in Section 5.
On inspecting the sites of some of these slides, the author of this document observed that the topography of the finished slides was actually distinctly inconsistent with the failure mechanism based on ideal-plastic limit equilibrium, by which practicing engineers traditionally still predict potential slide hazards. This particular issue is dealt with in more detail in Section 2.4. In the current context, suffice it to say that the upheaval of the passive zone provides clear evidence of immense unbalanced down-slope forces acting in the course of the slide. The enormity of these forces, which may readily be estimated by back analysis of a slide, is totally *inconsistent* with an ideal-plastic failure process.

The progressive landslides described in the present document have taken place in Quaternary deposits of normally consolidated or slightly over-consolidated, more or less sensitive clays, in which the implications of strain- and deformation-softening are generally radically different from those in highly over-consolidated clays.

In addition, the landslides dealt with in Section 5 have been triggered by specific *additional loading* or disturbing agents, which are basically local in *time* and *space* and usually brought about by human activities.

(By contrast, in the type of slides documented by e.g. Skempton in highly over-consolidated clays, the total load was gravitational and essentially invariable, as well as being more evenly distributed. Hence, the main cause of slope failure is related to long-time deformation softening, and not to any decisive effect of additional loading immediately preceding the slide event. The magnitude and distribution of earth pressures in the slope do not apparently form an important part of the analysis).

In the present document, the *magnitude* and *distribution* of earth pressures along the slope, including those defining the in situ condition, are results targeted in the analysis and constitute the key parameters in the assessment of safety factors against both *local* and *global* slope failure.
Moreover, the distribution of *shear stresses* and down-slope *displacements* are accounted for. It has therefore seemed appropriate to define the term ‘progressive failure’ as failure propagating along the potential slip surface in strict accordance with the *requirement* of *compatibility* regarding the displacements within and outside the potentially sliding body of

soil. The deformations are determined using relevant constitutive *stress-strain and stress-displacement* relationships – generally denoted just stress-deformation relationships. In doing so, the deformations in the *entire* failure zone (i.e. not only in the shear band) are accounted for by two-dimensional modelling of the crucial deformations in the potentially sliding soil mass.

The most important issues in this document may be summarized as follows:

– The document focuses on *brittle dynamic slope failure*, which may ensue if the residual shear strength, as a result of some disturbance agent, falls below the in situ shear stress, i.e. $\mathbf{c_R \leq \tau_o}$

– Six distinct phases in the development of a complete progressive failure are defined. (Cf Section 3). New formulations of the safety factors, which are related to the specific key issues in progressive failure analysis, are presented. (Cf Bernander & Gustås, 1984).

– An important circumstance, which is highlighted in connection with this type of progressive slope failure, is the limited distance down-slope of a local load along which additional shear stresses in the potential failure zone can be mobilized. Thus, at some distance from the point of load application, the effect on the earth pressures of this load has not yet materialized when the progressive failure further up the slope begins. For the current type of progressive failure, this has the crucial implication of reducing the possibility to utilize increased earth pressure resistance in less sloping ground as a means of stabilizing additional loading further up-slope.

– Brittle or dynamic failures of the kind referred to *cannot* take place if the residual shear strength remains greater than the in situ stress – i.e. when $\mathbf{c_R \geq \tau_o}$.
In the proposed analysis, considering deformations and deformation-softening, this condition leads to a more ductile failure mode, which is compatible with the conventional I-PlFA analysis in the limit case when the ratio of residual strength to peak strength is equal to unity. (i.e. $c_R/c = 1$). This failure mode is discussed in more detail in Section 3.4.

– As the assumed shear/deformation properties of the clay can be adapted to the rate of loading and to ambient drainage conditions, the impact of time may be considered in the analysis. This important feature renders it possible to distinguish between different phases in the development of extensive landslides of the current type.

– Since 1984 it has been proposed that the following stages of progressive landslide formation may be defined as follows:

- The existing ***in situ stage*** **(Phase 1)**;
- The ***disturbance phase***, subject to conditions relating to the agent triggering the slide **(Phase 2)**;
- An intermediate, *virtually* ***dynamic stage of stress redistribution,*** when unbalanced up-slope forces are transmitted further down-slope to more stable ground **(Phase 3)**;
- A ***transitory*** (or in some cases permanent) ***new state of equilibrium*** defining the resulting earth pressure distribution **(Phase 4)**;
- ***Final collapse*** in passive failure, provided valid passive resistance is exceeded in this new state of equilibrium. (Cf Section 3). This phase represents what is normally conceived as the actual slide movement **(Phase 5)**;
- ***Terminal state of equilibrium,*** post-slide configuration **(Phase 6)**.

– Slides of the kind subject to study in this document cannot therefore be analysed just as one singular mechanically static event considering that such a slide actually represents a series of consecutive - and therefore not simultaneous - phases of static and dynamic instability.
These phases are characterized by radically differing conditions in respect of the type of disturbance agent, type of loading and rates of load application.
The response of soft clays to time and drainage factors may also vary widely between the different phases.

1. 4 *Earlier publications by the author on the current topic*

The apparent inconsistencies in explaining the development and the final configuration of large planar landslides led to specific research and studies by the author in this field of geotechnical engineering. The progress of this work was presented to a larger audience in some fifteen publications in Swedish and English during the period 1978 to 1989. The various reports reflect different aspects of the problem with brittle failures in soils as well as different stages in the development of an engineering approach. In particular, contributions were made to the ICSMFE conferences 1981, 1985 and 1989. An important phase of the development of the analytical approach was presented at NGM (1984 and 1988) and at the Symposium on Landslides in Toronto, (ISL 1984).
A licentiate report was presented in 2000 the object of which was to synthesize essential principles and findings that had motivated the publications mentioned.

2. On the applicability of ideal-plastic failure analysis (I-PlFA) to strain-softening clays

2. 1 *General*

Analysis of the stability of natural slopes is in engineering practice normally based on the supposition of unlimited plastic properties of the soil material. The equilibrium of the potentially sliding mass – regarded as a rigid body – is at failure determined assuming:

a) Fully mobilized shear strength along the slip surfaces confining the moving soil mass;
b) Partial mobilization of the shear resistance in the 'service condition' in terms of a mean stress level (τ_{mean} /c_{mean}) along the potential failure surfaces.

Hence, the safety factor (F_s) is defined as

$F_s = c_{mean} / \tau_{mean}$ ……Eq. 2:1

where c_{mean} denotes the mean shear strength of the soil and

τ_{mean} denotes the presumed mean shear stress in the slip surfaces corresponding to the studied case of loading.

When conditions are un-drained $c = c_u$ and under drained conditions $c = c_d = c' + \sigma' \cdot \tan \varphi'$.

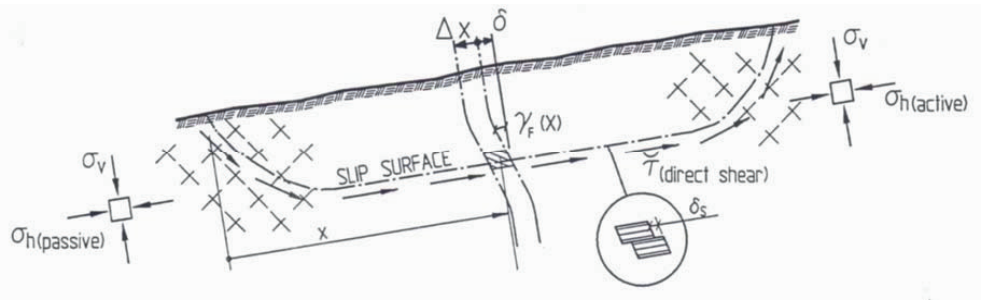

Figure 2:1.1 Shear deformation and shear stresses in a vertical plane of a potentially sliding soil mass. In ideal-plastic failure analysis (I-PlFA) based on unlimited plasticity, the effects of deformations in the soil mass on stress distribution are disregarded.

From a structure-mechanical point of view, this methodology is highly simplified, since the deformations within (and outside) the sliding body are not considered. (Figure 2:1.1) This means that – already by definition – the way in which the distribution of load, in situ stresses, stiffness properties and geometry affect the stress distribution in the potential failure zone (and slip surface) cannot be accounted for. Neither can the different phases of progressive slide development be identified or studied appropriately. For instance, the important impact of the distribution of the in-situ earth pressure along the slope does not affect the results of stability analysis based on unlimited plasticity. However, when the method was once introduced it was a big step forward, see e.g. Fellenius (1918) and Eklöf (1979).

Admittedly, the I-PlF method of analysis may not claim to model the true behaviour and the stress distribution in the 'serviceability limit state' but it does claim to provide a defined degree of safety against slope failure that is very uncertain in deformation-softening soils.

But also in more general terms of soil mechanics, there are a number of questionable approximations that tend to undermine the validity of conventional analysis of slope stability.

In general, the un-drained shear strength and the failure strain of clays are in practical engineering looked upon as material properties. Yet, this is done notwithstanding the recognized facts that both shear strength and ductility of clays intimately depend on a number of ambient conditions in the soil structure. Such conditions are, for instance, the state and magnitude of principal stresses, the effective stress situation (OCR), and the level of shear strain and deformation. The time scale and the rate of loading are also of paramount importance to the strength characteristics of soft clays that are therefore often of a transitory nature.
For instance, laboratory shear tests according to current practices are often carried out at strain rates in the range of 0.3 to 0.5 % per hour although the rate of strain (or deformation) may vary widely in the different phases of a slide. A major landslide such as the Tuve slide, (cf Section 5.1) covering some eight hundred meters in length of ground, may well begin as local and gradual acceleration of an ongoing slow creep deformation, but the subsequent phases of the event can take place within a few minutes in sensitive clays.

It stands to reason that, in deformation-softening soils, the actual response of the soil in the time scale of the different phases of a progressive landslide is bound to be relevant for the prediction of its time-related development and ultimate extension.

In conclusion, only laboratory testing consistent with the rates of deformation actually occurring during a slide will allow valid predictions with regard to the triggering failure mechanisms, failure propagation and the final spread of a fully developed slide.

The decisive importance of the shear-deformation properties of brittle clays is further discussed in Section 9.

2.2 *Prerequisite conditions for the validity of 'ideal-plastic' failure analysis (I-PlFA) in engineering practice*

If conventional analysis, based on fully plastic behaviour of soils, is to apply, at least one of the following conditions must be fulfilled:
1) The soil in the failure zone can be subjected to virtually unlimited deformation without substantial loss of strength.
2) The deformations within the sliding body due to an additional load are small compared to the strain range ($\Delta\gamma_f$ in Fig. 2:2.1), within which the assumed shear strength is valid – i.e. the sliding body is considered to be practically rigid.
3) The distribution of the *incremental* stress leading to potential slope failure corresponds with the distribution of in situ stresses and shear capacity in the failure zone.

Condition **No 1** normally applies to drained conditions in normally consolidated clays and cohesion-less soils. In engineering practice, this requirement has – in a general way – traditionally been taken to be met also under un-drained conditions for normally consolidated plastic clays. However, in sensitive soils, the validity of this assumption is bound to be questionable for potentially sliding bodies of soil of great length.

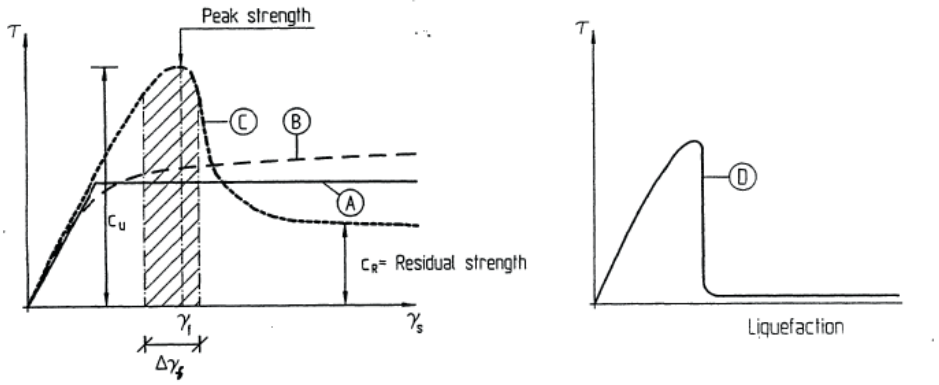

Figure 2:2.1 Examples of shear stress/deformation relationships
- A) Ideally elastic/plastic material
- B) Tough clay at low strain rate – drained conditions
- C) Sensitive strain-softening and importantly deformation-softening clay, un-drained conditions
- D) Loosely layered saturated silts, sands or silty sands. Sands or gravels with interstices filled with under-consolidated clayey material.

Condition **No 2** is usually presumed to apply even in moderately sensitive clays, when the length to height ratio (L/H) as well as the extension of the sliding body is reasonable, as is normally the case in the design of steep inclines, retention walls and sheet pile excavations. Also in slopes of minor extension, the applicability of Condition 2 may be limited by the L/H-ratio. Hence, the length of a sliding body for which I-PlF-analysis applies is limited by the current depth (H) to the slip surface.
However, no generally accepted recommendations in this respect exist.

Condition **No 3** may be fulfilled in natural slopes, considering that long- time creep in a slope is likely to result in a condition, where the stress levels (τ/c_u) are roughly constant along the potential failure zone owing to gradual adaptation of in situ earth pressures, and the shear stresses in strained zones, over time.
It will be shown in this document that long term progressive failure FDM-analysis, assuming fully plastic creep conditions, confirms and quantifies the transfer of load over time from highly stressed zones to more stable areas. Yet, a crucial requirement in this context is then that any short term incremental load must induce a stress field that agrees reasonably well with the in situ stress distribution in the potentially critical zones.

In practice, this may approximately apply when the additional stresses are induced by load placed evenly over the area susceptible to sliding. It may also apply when excess pore water pressures in a soil layer tend to rise by about the same amount in all parts of the potential slide area.

However, it may be noted that progressive landslides of the kind discussed are – although the main cause of the slide is linked with identified man-made activity – often triggered in conjunction with spells of sustained rainfall. (Cf e.g. Section 5.7.)

2.3 *Accuracy of basic assumptions with regard to the application of I-PlFA*

In the preceding section, some essential prerequisites for applying conventional stability analysis in practical engineering have been listed.
However, it is evident that in very sensitive clays the likelihood of these conditions being satisfied is negligible for long slopes.
As will be demonstrated later in this document, conventional analysis based on 'ideal' or full plasticity may, in markedly deformation-softening soils, lead to highly erroneous factors of safety. It may also result in serious misjudgement as to the eventual spread of a slide, and hence to the potential degree of disaster resulting from a local up-slope failure.

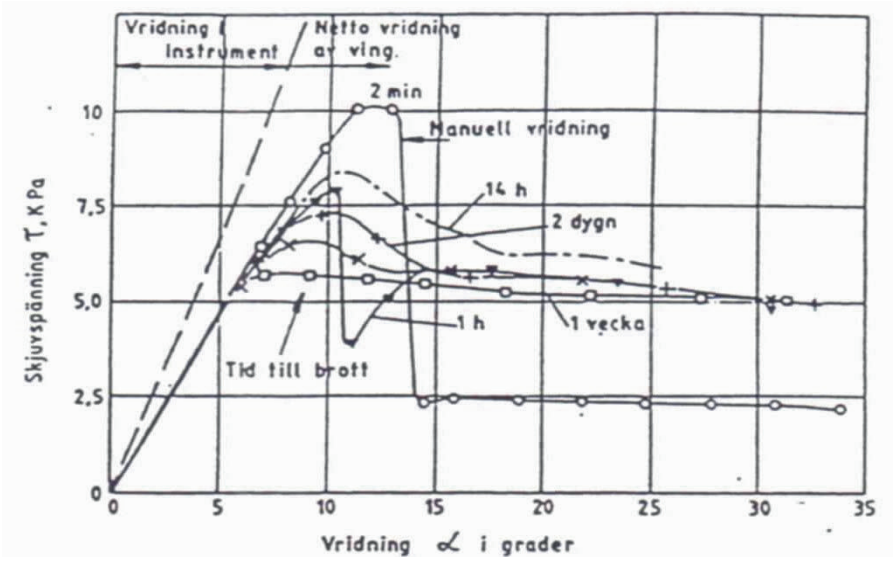

Figure 2:3.1 Stress/strain (deformation) curves for consolidated, un-drained vane tests at different strain rates (Aas, 1966).
Legend: Brott = failure, vridning = torsion, dygn = day, vecka = week, grader = degrees.

In the following, the applicability of Conditions No 1 through 3 (in Section 2.2) to sensitive clays will be scrutinized.
Note that the term 'deformation-softening' is here used both for the strain-softening in the developing failure zone, and for the loss of shear resistance in an established failure plane. (Cf Figures 2:3.2 and 4:4.2)

a) In sensitive deformation-softening clays, normally with water contents significantly above the liquid limit, Condition No 1 regarding unlimited ductility without substantial loss of strength is not likely to be fulfilled under un-drained circumstances. Figures 2:3.1 and 2:3.2 illustrate how stress/strain relationships and residual shear strengths are significantly affected by stress levels and the rate of loading, and if applicable by the effective stress ratio (OCR).

b) Condition No 2 demands that the differential deformations within the limits of sliding soil volume are sufficiently small. The probability of this requirement being met at all times must be considered to be negligible both in longitudinally (i.e. downhill) and laterally extensive natural slopes.

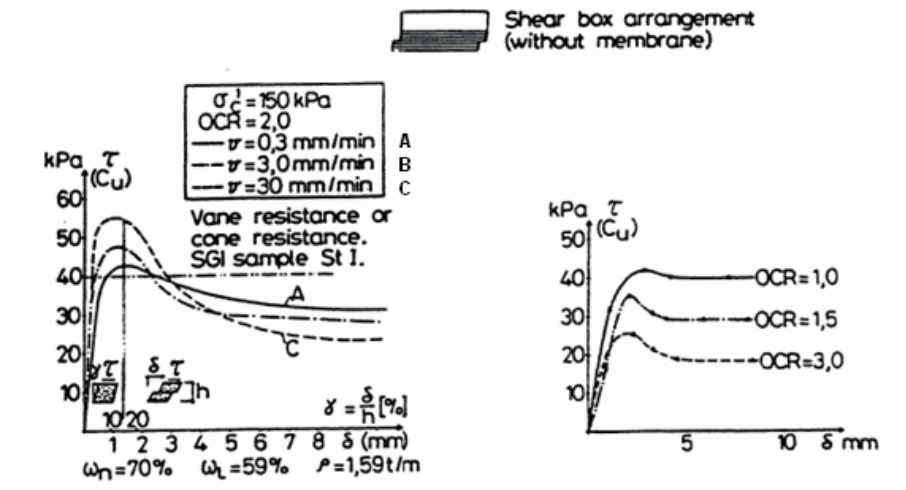

Figure 2:3.2 Typical test results from consolidated un-drained direct shear tests on a soft Swedish clay. Note that deformation on the horizontal axis is represented both in terms of angular strain and slip displacement in mm. (Cf Bernander & Svensk, 1985)

Assuming for instance that the maximum horizontal shear strain immediately prior to failure in the soil is γ_f, and that the width of a slide is b m, then the differential down-slope displacement may well amount to at least $\Delta\delta = \gamma_f \cdot b/4$, before the lateral boundaries of the slide manifest themselves and the soil mass begins to move as an integral block. (Cf Figure 2:3.3a). Taking for instance $\gamma_f = 5$ % and b = 50 m, then $\Delta\delta$ will be in the order of 0.625 m.

When investigating a slide, involving some 500 m by 180 m of ground, at the construction site of the Kotmale dam (Sri Lanka, 1981), the author of this document observed a differential displacement across the slide area of about 7 m as per Figure 2:3.3b. The observation was made at a stage, when failure at the boundary DF was incipient and the signs of impending rupture were still hardly detectable.

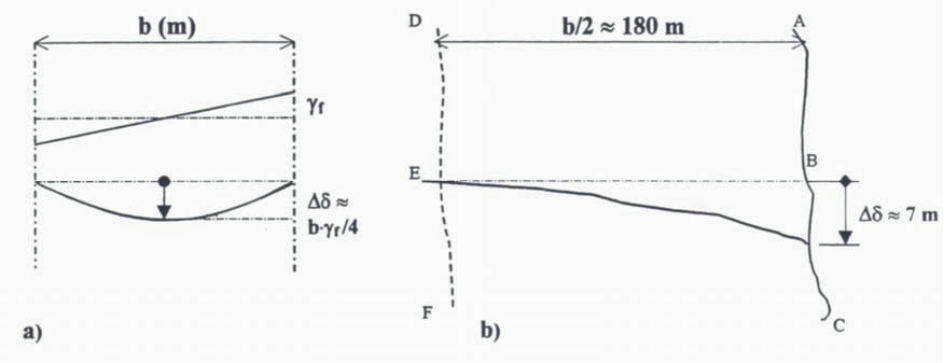

Figure 2:3.3 a) Conceivable range of down-slope displacement prior to the actual slide movement of the soil mass as an integral block.
b) Documented differences in down-slope displacement in a slide at the Kotmale Dam site (Sri Lanka, 1981)

The recorded displacements correspond to a maximum horizontal shear strain ranging from about $\gamma_f = \Delta\delta/(b/3)$ to $\Delta\delta/(b/4) = 7/120 \approx 6$ % to $7/90 \approx 8$ %, depending on the distribution of horizontal strain across the line BE.

The implication of these observations, is that the down-slope movement relative to the sub-base in a potentially sliding soil mass may locally adopt any value between displacements corresponding to the maximum angular strain (γ_f), and slip deformations in the order of several meters prior to the formation of the lateral boundaries of the slide – i.e. before the soil mass actually assumes the global kinematic behaviour of the assumed analytical model. This means in turn that the maximum shear stress that can be mobilized along major portions of the horizontal slip surface area is actually limited to the residual shear strength (c_R), i.e. a condition obviously invalidating the use of conventional analysis based on the peak shear strength of markedly strain softening soils.

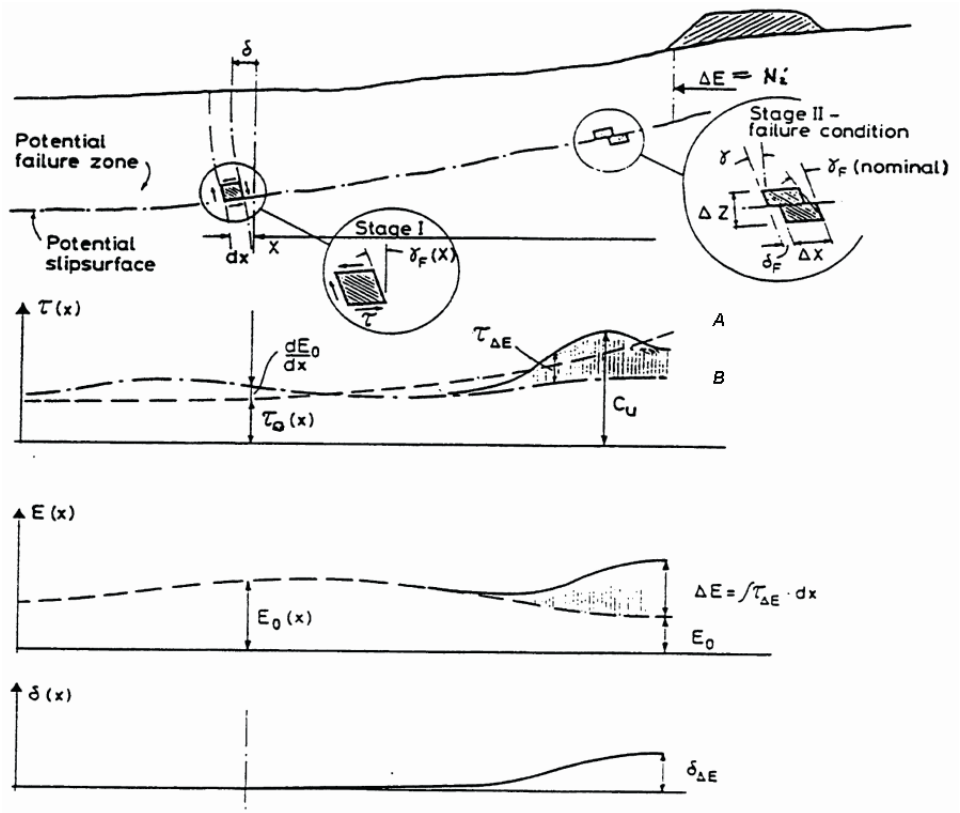

Figure 2:3.4 Shear stress field from local fill at the crest of a slope.
Curve A: Shear stress (τ_{ox}) – corresponding to slope gradient
Curve B: Shear stress (τ_{ox} + dE/dx) – corrected for earth pressure distribution (E_{ox}) in the in situ condition.

c) The prerequisite Condition No 3 states that the stress field due to the incremental load, causing a slope failure, should at least in principle conform to the prevailing in situ stress distribution. This condition is rarely fulfilled. Landslides in western Sweden are – more often than not – triggered by agents, the effects of which are far from being evenly distributed over the area of the prospective slide. In fact, a considerable number of landslides have been set off by construction work such as pile driving, heavy vibration, excavation, placing up-slope earth fills or stock piling of waste material – i.e. activities locally affecting stress levels, earth pressures, deformations, excess pore water pressures, hydrologic systems, etc.

Yet as mentioned, even in the cases where human interference constitutes the major cause of a landslide, sustained raining often turns out to be an additional triggering factor.

Figure 2:3.4 illustrates the short-term shear stress distribution in a case, where a local fill has been placed near the crest of sloping ground. The instantaneous effect of the fill will be local increase of the shear stresses immediately down-slope of the fill.
Experience shows that slides resulting from this kind of additional loading are, in sensitive clays, likely to engage the entire slope including large areas of level ground. Hence, if a plastic failure assessment (I-PlFA) of slope stability is based on slip surfaces comprising the whole slope, Condition No 3 is not likely to be fulfilled. (Cf Case records – Section 5).

However, if the fill is established over a long period of time, Condition No 3 not being satisfied initially may not be a problem. This is because the redistribution of earth pressures owing to creep, as well as to the consolidation generated by gradual excess pore water pressure dissipation.
Yet, if the local additional load is applied at such a rate that un-drained (or partially drained) conditions prevail, then analysis according to the ideal-plastic approach is not likely to be applicable in markedly strain-softening clays.

2.4 *Relationship between the features of a finished slide and the mechanisms acting during the slide event*

2.41 Downhill progressive slides
The final morphology of landslides in Scandinavia often exhibits extensive zones at the foot of the slope or over the valley floor, where the ground has heaved in passive failure. As demonstrated below, this feature is not compatible with the ideal-plastic failure concept.
If the laws of force equilibrium are applied to the soil element shown in Figure 2:4.1, we get:
$N + \Delta N = N + \rho \cdot g \cdot H \cdot \Delta x \cdot \cos\beta \cdot \sin\beta - c_u(\gamma) \cdot \Delta x$ i.e.

$$\mathbf{\Delta N} = \rho \cdot g \cdot H \cdot (\sin 2\beta)/2 \cdot \Delta x - c_u(\gamma) \cdot \Delta x = \mathbf{[\tau_o - c_u(\gamma)] \cdot \Delta x} \qquad \ldots\ldots\ldots\ldots\ldots\ldots \quad 2{:}2$$

where:
$c_u(\gamma)$ = the shear (or the residual) strength of the soil as defined by the stress strain Curves P or D;
τ_o = prevailing stress due to forces acting downhill;
Other notations according to Figure 2:4.1.

Case a) *Ideal-plastic failure* (I-PlF, Curve P in Figure 2:4.1)
It follows directly from Equation 2:2 that, in the case of ideal-plastic failure, $c_u(\gamma) = c_u^{max}$ for all values of $\gamma > \gamma_F$ and $F_c = c_u^{max}/\tau_o = 1$. Thus substituting $c_u(\gamma) = c_u^{max}$ by τ_o in Equation 2:2 it

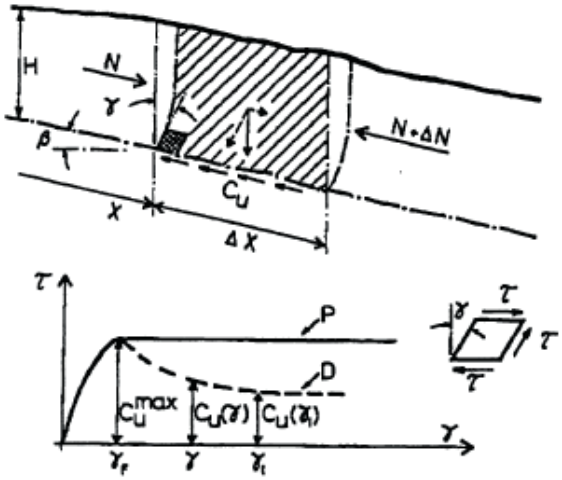

Figure 2:4.1 Earth pressure development in a uniform slope at failure. N is the force increment that may result from deformation-softening according to the shown constitutive relationship. Curve P = Plastic failure. Curve D = Deformation-softening failure. From Bernander (1984).

is evident that $\Delta N \approx 0$ even for large post-failure deformations. This means that no significant build-up of earth pressures ($\Sigma\Delta N$) can take place down the slope.

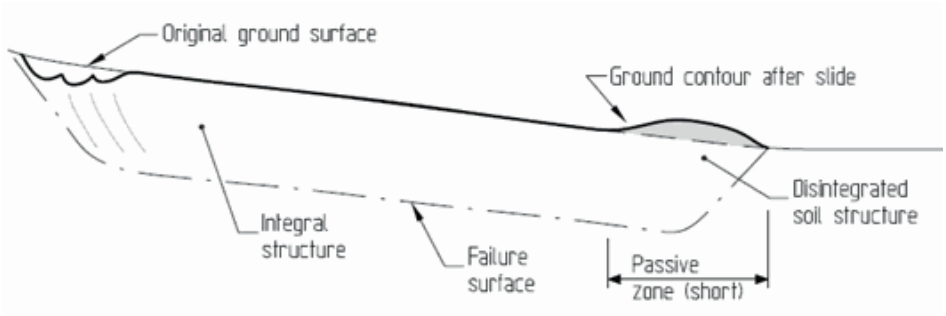

Figure 2:4.2a Slide in ideal-plastic soil featuring a small passive Rankine zone at the foot of the slope and insignificant build-up of down-slope forces. (Bernander, 1984).

Case b) *Deformation-softening failure*
If, on the other hand, the soil exhibits deformation-softening properties as for instance according to Curve D in Figure 2:4.1, then $\Delta N > 0$ from the very moment γ exceeds γ_F. Hence:

$N = \int \Delta N = \int [\tau_o - c_u(\gamma)] \cdot dx \; \mathbf{> 0}$ as soon as $c_u(\gamma) < \tau_o$.

The force increment N due to deformation-softening may thus bring about a significant build-up of the static down-slope earth pressures as well as an un-balanced movement of the soil masses. Both these phenomena originate from the inherent strain-softening properties of the soil.

The conclusion to be drawn is that the build-up of static earth pressures and the accumulation of kinetic energy during a landslide are in principle conceivable only when the failure process deviates from perfect plastic behaviour. Hence, when landslides exhibit evidence of passive failure having taken place over vast areas of gently sloping ground at the foot of a slope, the failure mechanism is evidently the result of significant deformation-softening in the progressive phase of the slide. In the Tuve slide, for instance, some 60 % of the area affected by the main slide covered the almost horizontal valley floor.

In short, already the final appearance and configuration of a landslide offer important clues to the mechanisms explaining the event.

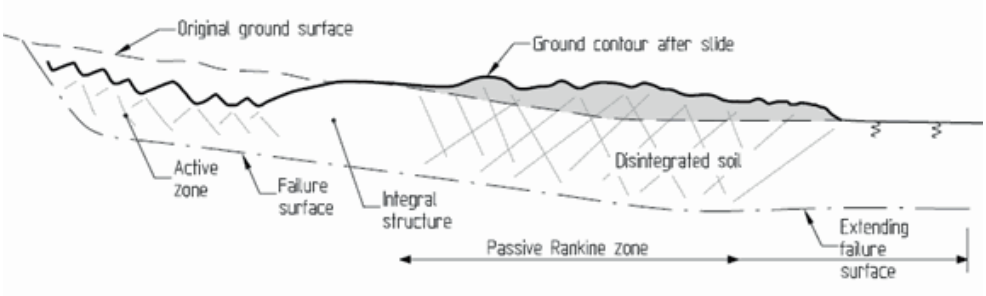

Figure 2:4.2b Final phase of slide in deformation-softening soil featuring an extensive passive zone due to massive build-up of down-slope static and dynamic earth pressures. (Bernander, 1984). Note the failure surface extension ahead of the lower limit of the slide proper.

2.42 Retrogressive or uphill progressive slides

In uphill progressive slides, the development of down-slope earth pressures is radically different from that in downhill progressive landslides. The retrogressive failure results by its very nature in reduced down-slope support, and instead of the passive pressure build-up – typical of most downhill progressive failures – active earth pressures tend to develop. In the final phase the entire slope may disintegrate in a state of active Rankine failure, often denoted as a spread failure.
Hence, the final configuration of the ground surface often displays the typical saw-toothed appearance with 'horsts' and 'grabens', which typically characterize retrogressive landslides. (See Figure 2.4.2c). The extension in the downhill direction resulting from the slide movement takes place along a continuous *preformed* failure surface. (Cf the slides along the Lidan River (Sköttorp) and along the Nor River, Section 8.)

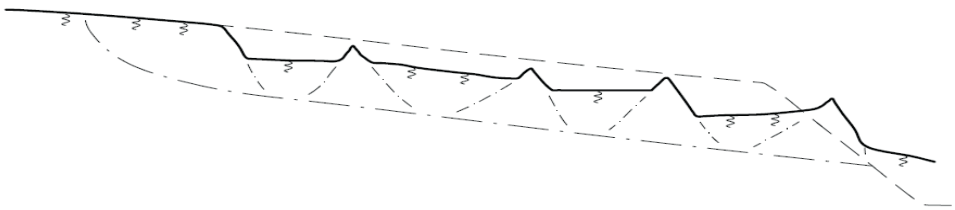

Figure 2:4.2c Retrogressive landslide (or spread failure) featuring extensive active Rankine failure covering all of the slide area. (Cf e.g. the Nor River Slide, Section 8.5).

However, in many cases the disintegration of the soil mass takes place in the form of a series of cylindrical active slides generated by successively vanishing down-slope support as shown in Figure 2.4.2d. It is important to note that these *'serial active'* slides do not arise from a continuous process. Instead, they typically take place at random intervals in such a way that the energies released in the individual slides are not contemporary or cumulative.
Yet, in the two retrogressive slides referred to above, the energies released in the slide were so enormous that they cannot be accounted for by intermittent serial events.
Thus, in the Lidan slide, the width of which amounted to some 300 m, the river channel was blocked by soil debris 200 m upstream and downstream of the slide limits – i.e. in total about 800 m. (Odenstad (1941)
Similarly, in the Nor slide, the Nor River was dammed up 750 m – also in this case 200 m up- and downstream of the slide boundaries. An eyewitness claimed to have witnessed how a small islet of clay with a couple of tall spruce trees moved slowly like a sailing ship up the Nor River. (Cf Lindskog & Wager (1970).)

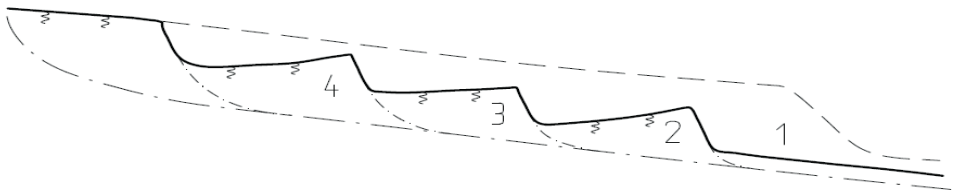

Figure 2:4.2d Serial retrogressive intermittent slip-circular failures due to successively failing down-slope support.

In other words, the disintegration process in neither of the two mentioned slides along Lidan and Nor is likely to have developed as a distinctly 'serial' retrogressive slide, according to the definition given in Section 6.1. Instead, they must have developed as continuous dynamic movements, during which most of the total potential energy was released. (Cf Section 8.)

By contrast, in numerous singular local riverbank slides of normal size in Sweden, such extremely wide spreads of disintegrated soil up and down the river channels have not been recorded.

2.5 *Conclusions - progressive or brittle slope failures*

The discussion in Section 2.3 above implies that, in markedly deformation-softening soils, the relative displacement between the soil mass involved in a potential slide and its sub-base vary significantly in the slide area. Hence, while the shear stresses in parts of the failure zone range from zero to peak shear strength, stresses corresponding to the residual shear strength may prevail in other major portions of the failure plane.

The conclusion in this context is that considering brittle or progressive failure mechanisms in slope stability analysis is in fact mandatory.
For instance, additional load in the uphill part of a slope (denoted Part 1) causes stress increase and strain softening – a fact calling for more support from the neighbouring downhill element of soil (Part 2). Yet, this event generates in turn a shear stress increase and strain-

softening in Part 2 as well as more strain-softening in Part 1. This course of events entails again stress increase in the next downhill element (Part 3) and further strain-softening in Parts 1 and 2 … and so on in neighbouring downhill elements, which themselves may be affected by additional stress and strain softening.
It is reasonable to assume that the soil properties and the prevailing conditions in a slope, now and again, can be such that the described interactive strain softening process leads to local up-slope failure that eventually develops into a veritable landslide disaster.

In consequence, the prospect of progressive failure should be addressed in the analysis of slope stability in markedly sensitive clays.

It may be noted in this context that, although factors conducive to brittleness in soils are treated to some extent in Section 9, it is not within the scope of this report to address the methods and procedures for establishing and documenting the constitutive stress/deformation properties of soils. This task will be up to future R & D and the investigating engineer to perform.

The subsequent sections of this document highlight the impact of deformation-softening on landslide hazard and present an analytical method of assessing the risk of local instability in a slope. Another important aim is to make a reasonable estimate of the final spread - i. e. the degree of disaster of the slide that may ensue.

As will be demonstrated in the following chapters, a slope with deformation softening soil layers, though reliably stable under long term drained conditions, may readily fail due to the effect of any powerful agent capable of inducing un-drained local failure in some highly strained porion of the slope.

2.51 Different types of failure in deformation-softening soils
Slope failure in deformation-softening soils is of a different character depending on how the in situ stresses (τ_o) relate to the residual shear strengths (c_R) that may develop as a result of the magnitude and the rate of strain and deformation induced by an additional loading effect or by other disturbing agents.

Case 1 $c_R < \tau_o$
In cases, where the deformations induced by the additional load cause the residual shear strength to fall below the prevailing in situ shear stress, a progressive failure of dynamic character may be triggered at a specific critical value of the additional loading effect. This is the type of progressive slope failure, on which the present document is focused.
(Cf Section 3.3).

Case 1a) Resulting down-slope earth pressures ***exceed*** current passive resistance causing a veritable landslide. (Cf e. g. the Surte and Tuve slides, Section 5.)

Case 1b) Resulting down-slope earth pressures do **not exceed** passive resistance, in which case displacement of earth masses will be moderate or insignificant.
(Cf the slide movement at Rävekärr, Section 5.)

Case 2 $c_R \geq \tau_o$
In contrast to Case 1, the residual shear strength (c_R) may remain in excess of the in situ stress (τ_o) throughout the duration of the impact of the additional load. The redistribution of earth

pressures related to the deformation-softening then, instead of triggering a dynamic phase, merely results in increasing down-slope displacements as the additional loading is increased. This failure process is of a ductile character and the ultimate load is no longer limited to the critical value as per Case 1. The conditions according to Case 2 probably represent the most frequent situation.
In Case 2, the subsequently proposed analysis considering the deformations in the soil will be in agreement with conventional ideal-plastic analysis (I-PFlA) in the limit case when the ratio of $c_R/c = 1$. (Case 2 is discussed in more detail in Section 3.4).
Analysis according to the FDM-approach can serve to assess the mean exploitation of shear capacity representing a more conventional safety factor:
$F_s = c_{mean} / \tau_{mean}$

2.52 Implications of progressive and retrogressive failure analysis for design philosophy
In the opinion of the author, progressive failure analysis entails the following advantages:

- It models the failure mechanisms more accurately than conventional analysis based on perfect plasticity, allowing more reliable predictions of the ultimate consequences of a local up-slope failure. Many features of slides in sensitive clays cannot, by definition, be explained or understood in terms of the plastic failure concept.
  In fact, the formulation of valid constitutive (stress/deformation) relationships is an indispensable prerequisite for reliable interpretation and prediction of landslide hazard in all kinds of deformation-softening soils.

- By means of progressive (retrogressive) failure analysis, the truly most critical conditions in a slope can be identified, enabling preventive or remedial measures to focus on the pertinent issues.

- A better understanding of the mechanisms leading to global failure in a slope will induce geotechnical engineers to focus R & D and exploratory investigations on topics that are relevant in the context of progressive failure formation.

- The analysis explains the phenomenon of vast spread in terms of passive failure over gently sloping (or horizontal) ground extending to great depths, even not considering dynamic effects and forces of inertia.
  It also predicts the presence of a failure zone reaching far ahead (i.e. hundreds of meters) of the visible slide limit. (Cf Figures 2.4.2b and 3:3.5)

The Tuve slide described in Section 5.1 substantiates the importance of the statements made above. Although conventional I-PlFA analysis predicts, by safety factors of about 2.4 to 3.0 that the slide would not extend as far as ≈ 270 m over the almost horizontal valley ground, this was indeed what **actually** happened. (Cf Figure 5:1.2 in Section 5.)

By contrast, progressive failure analysis explicitly indicates that the vast spread of the tongue of the slide over level ground is precisely what should be expected if local up-slope failure was conceivable.

As opposed to conventional I-PlFA analysis, progressive failure analysis also explains the remarkable phenomenon of a soil volume of about 16 hectares by 35 m (≈ 5 600 000 m^3) being squeezed in passive failure to the effect of raising the ground level in the area by 4 to 5 m. This applies in principle also to the great slide in Surte (1950). (Cf Section 5.2.)

In the current context, it is also of interest to note the typical extension of the failure zone and the associated slip surface beyond the actual slide limit, as illustrated in Figure 3:3.5 in Section 3.33.

Reference may also be made to the well documented slide at Bekkelaget (Norway) described in Section 5.3, where the slide took place along the longest slip surface that in fact rendered the highest safety factor according to the traditional analytical I-PlFA approach.
(Cf Aas, 1983 & Karlsrud, 1984).

3. Different types and phases of downhill progressive failures in natural slopes – exemplification

3.1 *General*

The modeling of brittle failure in natural slopes is an issue of considerable complexity, and it is not within the scope of this report to deal with every aspect of the problem. The analytical model presented in this section is primarily tailored for slopes in markedly sensitive normally consolidated clays, but applies in principle to any material that is deformation-softening in shear.
The term **'deformation-softening'** refers in this document to the loss of shear resistance both due to shear (deviator) strain in the developing failure zone and to concentrated excessive strain related to large displacements (or slip) in a developed failure surface.

An important and puzzling issue in the investigations of many landslides in western Sweden has been the fact that the slides have extended over large areas of gently sloping ground, deforming the sub-ground to great depths.
A further strange phenomenon related to these slides is the astonishingly trivial nature of the disturbance agents, capable of destabilizing these vast areas of ground that had remained stable for thousands of years.

The main reason why investigations of landslides occurred in soft sensitive clays have frequently remained inconclusive, and intrigued many a geotechnical expert, appears to be mainly due to the fact that deformations within and outside the potentially sliding soil mass were not considered in the post-slide analyses.

Furthermore, there is a common tendency to explain landslides of the current kind by just referring to the presence of so called 'quick clay', which in Scandinavia is the term for clays with a sensitivity number $St = c_u/c_{ur} \geq 50$. However, the fact that there are no established or generally recognized relationships between the sensitivity – defined in this way – and the actual sensitivity of clays in developing failure zones constitutes another serious complication contributing to the difficulty of understanding the nature these slides.
The shear strength of a completely remoulded (stirred) clay specimen (c_{ur}), as measured in laboratory, is hardly likely to be generally applicable to the true resistance that is mobilized in real failure zones or slip surfaces developing at widely varying rates of strain and displacement in the different phases of a landslide.
This lack of proven compatibility is, in the present document, dealt with by distinguishing between the completely remoulded laboratory shear strength (c_{ur}) and the un-drained residual strength parameter (c_{uR}) that is applicable to the true failure condition.

Drained or un-drained analysis
Traditionally, shear strength is mostly determined under either un-drained or fully drained conditions although, in reality, the conditions are mostly neither one nor the other – i.e. normally just partially drained.
Since the effective residual shear strength in a developing failure zone strongly depends on the rate of loading and prevailing drainage conditions, the current residual shear strength is in this document generally denoted as c_R, thus implying that the effect of time is of particular importance to this strength parameter and must therefore be considered in the analysis.
The peak shear strength is generally denoted c, instead of c' or c_u, indicating that incipient failure conditions are typically neither 'drained' nor 'un-drained'.

Another condition, the effect of which escapes attention in the normally used perfectly plastic failure analysis (termed I-PFlA in this document), is the way in which geometric features between the upper and lower limits of a studied soil volume affects the true risk of slope failure. The term used by the present author for this phenomenon is 'geometric sensitivity'.

3.11 Slope failure in deformation-softening soils

As mentioned in Section 2.51, slope failure in deformation-softening soils develops differently depending on how the in situ stresses (τ_o) relate to the residual shear strengths (c_R) resulting from deformation (and rate of deformation) induced by additional loading or other kinds of disturbance.

Case 1 $\mathbf{c_R < \tau_o}$

In cases, where the deformations generated by the additional load cause the residual shear resistance (c_R) to fall below the prevailing in situ shear stress (τ_o), a redistribution of earth pressures in the slope has to take place in order to maintain overall equilibrium. Hence, a progressive failure of dynamic nature may be triggered at a specific critical value of the additional loading effect as discussed in Section 2.4. This type of brittle, dynamic progressive slope failure is dealt with in more detail in Section 3.3 below.

Case 2 $\mathbf{c_R \geq \tau_o}$

In contrast to Case 1, the residual shear strength (c_R) may remain in excess of the in-situ stress (τ_o) throughout the duration of the impact of the additional loading. The redistribution of earth pressures due to deformation-softening will then merely eventuate in limited down-slope displacements instead of inducing a virtually dynamic phase. This failure process is essentially of a ductile character, and the ultimate load is no longer limited to the critical value as per Case 1. In general, the conditions according to Case 2 may be assumed to represent a normally valid situation.

3.2 *Different types of progressive failure*

Progressive failures in natural slopes may be classified as:

a) *Downhill progressive landslides*, where an initial local instability in the upper part of a slope propagates down the slope generating a major increase in horizontal earth pressures in less inclining ground further downhill. If, there and then, the total pressure exceeds the current passive resistance, a global ground displacement takes place, typically involving large areas of inherently stable ground ahead of the foot of the slope proper. Downhill progressive landslides are characterized by significant growth of the mean axial stress – i.e. in this context the normal stress acting in the downhill direction.

b) *Uphill progressive or retrogressive slides*, (often denoted 'spreads') where local instability in the lower part of a slope propagates uphill, eventually leading to monolithic displacement of the soil mass, which finally disintegrates in various active failure modes. These may develop as saw-toothed patterns of so called 'horsts' and 'grabens' or as piece by piece serial retrogressive slides or merely just in the form of earth flows.
Thus, retrogressive slides are characterized by tension and significant decrease of the in situ earth pressures resulting in active failure. A typical failure mode in this context can be the 'column failure' described by Janbu, (1979).
(Cf Gould, (1960), Skempton, (1964), Bjerrum, (1966), Carson, (1977), Lefebvre, (1981), Leroueil, (2001), Urciuoli, (2002), Locat, (2007), Quinn, (2009).)

c) *Laterally progressive slides,* where local instability anywhere in a slope propagates sideways along the elevation contours. In this case the destabilizing forces are transferred to

initially stable parts of the potential slide area by horizontal shear in vertical planes in the direction of the slide. Slides with significantly larger width than length in the direction of movement are likely to be of a laterally progressive nature.
Laterally progressive slides can be controlled by ensuring adequate safety against failure for the most critical section in the direction of the slope. (Cf Bernander ICSMFE, 1989)
Many major landslides combine more than one of the three Categories a), b) and c) – an example being the Rissa slide, Norway, described by Gregersen, (1981).

3.3 *Stability conditions in slopes susceptible to downhill progressive failure formation i. e. when $c_R < \tau_o$*

3.31 Different stages in the development of a progressive slide - limiting criteria
Most landslides of a progressive nature in Sweden belong to the *category* a) 'downhill progressive slides' as defined in the previous section. The analytical model dealt with in Sections 3 and 4 is focused on this specific type of brittle failure.
In order to facilitate the understanding of the analytical model presented in Section 4, the specific features and stages of a progressive failure in a slope are highlighted in an example presented in this section. Reference is here made to Figures 2:3.4, 4:2.1 and 4:2.2, illustrating the main principles of the FDM-analysis applied in the example. **([1])**

Downhill progressive failures in natural slopes exhibit several distinct phases that may be defined as follows. The figures 3:3.2 through 3:3.5 illustrate different critical stages in the development of a downhill progressive landslide related to deformation softening. **([2])**
It may in this context be mentioned that since NGM (Linköping, 1984) and ISL (Toronto, 1984) all publications by the author have pronouncedly distinguished between different stages of progressive landslide formation as follows ([3]):

- the existing (or primordial) ***in situ stage*** **(Phase 1).**
- the ***disturbance phase***, subject to conditions relating to the specific agent triggering the slide **(Phase 2)**.
- an intermediate, *virtually* ***dynamic stage of stress redistribution,*** when unbalanced up-slope forces are transmitted further down-slope to more stable ground **(Phase 3).**
- a ***transitory*** (or in some cases permanent) ***new state of equilibrium*** defining the related earth pressure distribution **(Phase 4).**
- ***final breakdown*** in passive failure, provided current passive resistance is exceeded in this new state of equilibrium. This phase represents what is normally understood as the actual slide event **(Phase 5).**
- ***terminal state of equilibrium*** - resulting ground configuration **(Phase 6).**

([1]) For denotations not defined here, the reader is referred to the general list of denotations in the introductory section named **'Symbols and notations'**.
([2]) The subdivision of progressive landslides into several distinct phases dates back to Bernander, (1984), (NGM and ISL).
([3]) In Bernander (2008), the first five of these separate phases of a fully developed progressive landslide are denoted '**Phases 1, 2, 3, 4** and **5**'. These denotations will be used henceforth. In the current report, the ultimate state of equilibrium of a slide is referred to as **Phase 6**.

The time factor
The different phases are between themselves characterized by very different time scales related to the disturbance agent, to stress change under continued failure formation and to excess pore water pressure development.

Varying material properties, changing geometry and drainage conditions in the soil mass in the different phases of slide movement are also of decisive importance to failure formation.

The methodology used in this report allows taking the factor of time into consideration. (Cf Bernander, ISL, (1984), ICSMFE XII (1989), LuTU 2000:16 & LuTU 2008:11.)
The necessity of dealing with slide development in highly strain-softening soils in different separate phases implies that a landslide of this kind cannot be studied as just a single case of static loading. The subject has been elaborated on in Bernander, (2008), (LuTU 2008:11, Section 3.2).

3.32 Exemplification
Figure 3:3.1 shows the stress/deformation) relationship assumed to be valid for the sensitive soil in the incipient failure zone in the following exemplification.

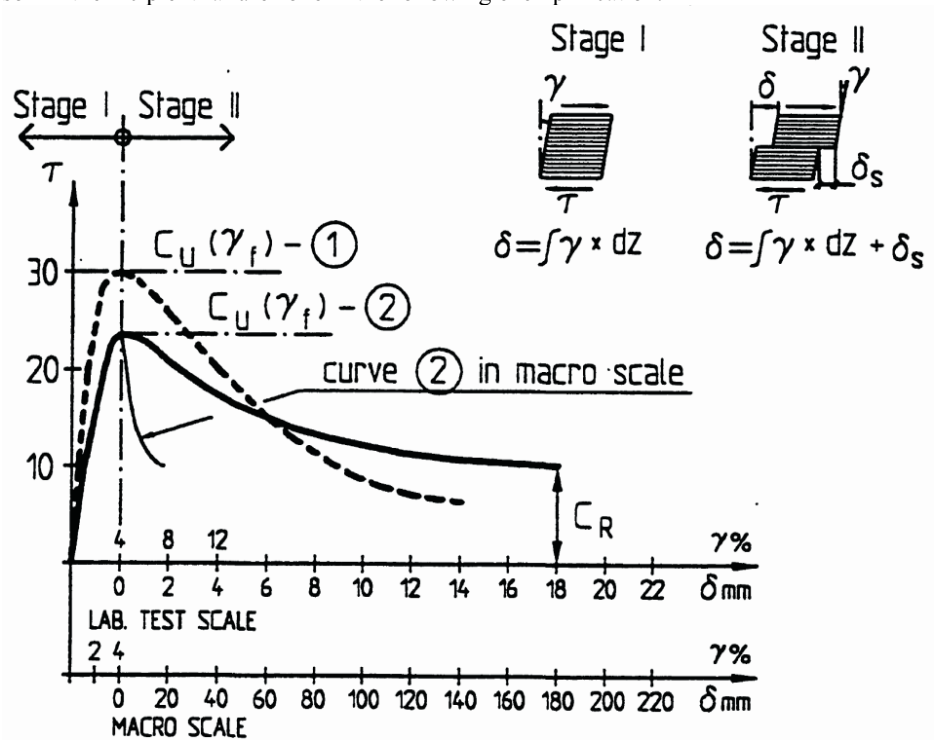

Figure 3:3.1 Assumed types of stress/deformation relationships $\tau(\gamma)$ and $c_R(\delta)$ of the soil in the example. Curves 1 and 2 exemplify such relationships at different rates of loading. c_R is the large deformation residual value of $c_R(\delta)$.

In-situ condition – Phase 1
For the sake of simplicity and pedagogics, the slope gradient is taken to be constant in the current case, and the ground below the presupposed failure zone to consist of firmer soil. The ratio of horizontal to vertical stresses ($K_o = \sigma_h'/\sigma_v'$) is also presumed to be constant. Hence, the in situ stress conditions are readily defined.
As will be evident in subsequent sections, these simplifications do not represent limitations to the FDM-analysis or affect the nature of the phenomena highlighted in the example.

Stability conditions prior to local failure - Phase 2

The weight of the earth fill generates an earth pressure increment (N_i) at the toe of the earth fill as shown in Figure 3:3.2. As the fill is being placed, the increasing force (N_i) gradually 'mobilizes' the remaining shear capacity in terms of the stress difference ($c - \tau_o$) in the potential failure zone, i.e. the 'shear capacity', which is not being exploited for stabilizing the sloping ground in the in situ condition. Figure 3:3.2 displays the situation, where the shear strength (c) and the shear strain (γ_f) are fully mobilized at point A.

Compatibility between the shear deformation – mainly generated in the failure zone – and the related down-slope displacements due to the additional earth pressures entails that the shear stress (τ) gradually decreases with growing distance from the point of application of the force (N_i). Hence, in Figure 3:3.2 the coordinate (x_1) defines the limited length along which the shear resistance required to balance the force N_i can be mobilized at this stage. **([4])**

([4]) Instructive results from a considerable number of studies of progressive failure and spread in this type of slope configuration are listed in Bernander, (2008), Appendices A & B.

The agent initiating slope failure in the studied case consists of an earth fill placed at such a rate that the soil response is of an un-drained or just slightly drained nature.**([5])**

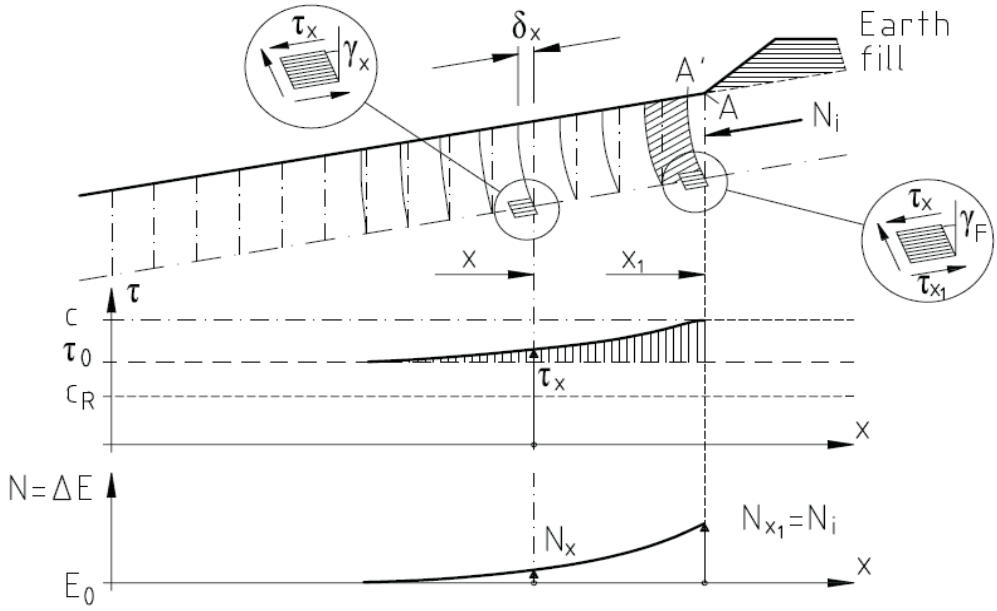

Figure 3:3.2 Stability situation prior to local failure, i.e. for $\gamma_x \leq \gamma_F$ and $\tau_x \leq c$. The figure illustrates a stage in the disturbing stage (Phase 2), when $N_i < N_{cr}$. N_x denotes the additional earth pressure force induced by N_i - in this case caused by an earth fill. ([4])

([5]) Comment: It may be pointed out in this context, that the line defined by the in situ stress $\tau_o(x)$ actually constitutes an asymptote to the curve $\tau(x)$, i.e. the point x, defined by the differential $(\tau_x - \tau_{o,x}) = 0$ being theoretically located at an infinite distance from A. In practice, this difficulty is overcome by locating 'Origo' (i.e. x = 0) at a point, where $(\tau_x - \tau_{ox})$ has a defined, but negligible value.

Triggering load and Critical length – Limiting condition in Phase 2.
This state constitutes the end of the disturbance Phase 2 as per Section 3:31and Section 3.33, (Synopsis). Further growth of the force (N_i) initiates local failure at A, and from this point on, the deformation in the failure zone between the points A and B in Figure 3:3.3 will consist of an additional component arising from the slip in the developing post-peak failure plane. Figure 3:3.3 depicts the situation where the in-situ stress (τ_o) is equal to the current post peak residual shear strength ($c_{R,x2}$), i.e. where $\mathbf{(c_{R,x2} - \tau_{o,x2}) = 0.}$ At this point, all available shear capacity is mobilized, and the stabilizing resistance ($N_{x2} = N_{cr}$) has attained its maximum value possible.

$\mathbf{N_{cr} = {}_o\int^{x2}(\tau(x) - \tau_o(x))\cdot dx}$ (for $0 \leq x \leq x_2$) ……Eq. 3:1
where $\tau(x)$ ranges from $\tau_{o,x=o} \rightarrow c$ and from $c \rightarrow \tau_{o,x2} = c_{R,x2}$

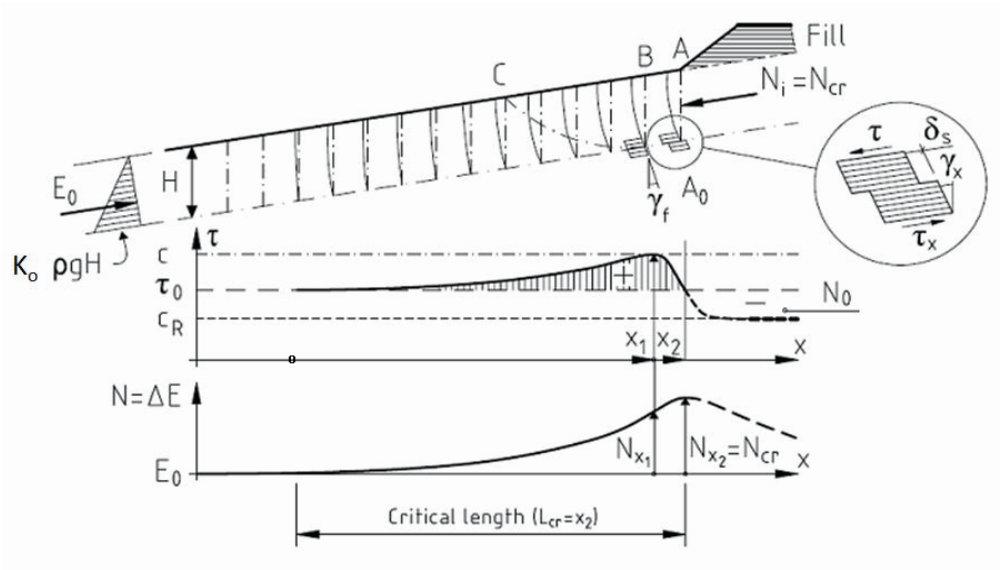

Figure 3:3.3 Effect of increasing the downhill active force (N_i) beyond the value corresponding to the peak shear strength at point A. When $(c_{R,x} - \tau_{o,x}) = 0$, the maximum resistance $N_{x2} = N_{cr}$ is reached. In the figure, the 'critical length' $L_{cr} = x_2$ is indicated. ([4])

The length (x_2) corresponding to $N_{cr,}$ along which shear strengths in excess of the in-situ stress (τ_o) can be mobilized is in the following denoted 'the critical length' (L_{cr}), as further deformation at A generates negative values of $(c_{R,x} - \tau_{o,x})$. This implies that unbalanced downhill forces may at this stage start acting at A. Hence, the critical length L_{cr} indicates in some measure the maximum length of a potential slide – induced by a concentrated load – that can be analyzed on the basis of ideal-plastic soil properties with any remote prospect of attaining a reasonable prediction of slide hazard. Yet, the implications of Comment no **([4])** above must be considered in this context.

The general condition that has to be fulfilled, lest a dynamic progressive failure (Pr F) be initiated, is therefore:

$\mathbf{c_R(x) - \tau_o(x) > 0}$ for values of $x > x_2$ ……Eq. 3:2

Another key criterion governing the possible occurrence of progressive failure, is that the earth pressure ($E_{cr} = N_{cr} + E_o(x_2)$) required to provoke failure in a zone of limited length (L_{cr}), oriented parallel to the ground surface or to the firm bottom, must be smaller than the resistance along a failure plane A_o-C (Figure 3:3.3), i.e.:

$$\mathbf{E_{cr}(x_2) = N_{cr} + E_o(x_2)} = N_{cr} + K_o \cdot \rho \cdot g \cdot H^2/2 \; < \; \mathbf{N_{Ao\text{-}C}} \approx \rho \cdot g \cdot H^2/2 + 2 \cdot \int_o^H c(z) \cdot dz \quad \text{……..Eq. 3:3}$$

where $N_{Ao\text{-}C}$ represents the force required to provoke local failure along the plane A_o-C Alternatively, Equation 3:3 may be written:

$$\mathbf{N_{cr} \leq \approx (1 - K_o)\, \rho \cdot g \cdot H^2/2 + 2 \cdot \int_o^H c(z) \cdot dz} \quad \text{.... ……..Eq. 3:3a}$$

The steeper the gradient, and the more the soil is deformation-softening, the more does the value of N_{cr} tend to fall below the resistance in failure planes such as (A_o- C) surfacing just ahead of the additional load. Analyses indicate that, in sensitive soils, the condition 3:3 (or 3:3a) is normally fulfilled even in gently sloping ground. For the slope studied in the example in Appendix I, N_{cr} is for instance = 221.9 kN/m, while the value of the force $N_{Ao\text{-}C}$ (for K_o = 0.7) may be estimated at 2000 kN/m >>> 221.9 kN/m. (Cf also Bernander, (2008), Appendix B, where this phenomenon is demonstrated for widely varying slope conditions.)

The inverse conclusion to be drawn from the above is that, in markedly sensitive clays, short slip surfaces engaging only the steeper portions of a long slope cannot be used for predicting landslide hazard. This is simply because such failure modes do not represent the lowest resistance against slide formation if the residual shear strength c_R drops below τ_o. Yet, the further development of a landslide will actually depend on the conditions controlling the subsequent phases of progressive failure formation.
In this context, it is therefore of utmost importance to consider the introductory comments in Section 3:1 regarding the vital effects on the true shear resistance in incipient failure zones of factors such as time, rate of load application and drainage conditions.

First dynamic phase – ***Phase 3.*** *Propagation and transfer of forces further downhill.*
Due to the build-up of unbalanced forces, the soil mass immediately ahead of the triggering agent, (i.e. the fill in the present case), passes into a state characterized by virtually dynamic increase of strain and deformation in the propagating failure zone, and by growing displacement in the rapidly extending slip surface. (Cf Sections 3:31 & 3:33.)

Of particular importance in this context is the fact that the increasing deformations extend the zone in the slope, where the in-situ down-slope forces, defined by the shear stress (τ_o), are no longer balanced by the post-peak shear strength, which soon attains its residual value of (c_R). (Cf. Figure 3:3.4).
The growing unbalanced down-slope driving force N_D can be written as

$$\mathbf{N_D(x > x_2) = N_i + \int_{x2}^{x} [\tau_o(x) - c_R(x)] \cdot dx} \quad \text{. ……Eq. 3:4}$$

The increasing force N_D causes the front of the developing slip surface to propagate downhill producing a significant change of the earth pressure distribution in the slope. However, this movement should not be understood as a regular slide but rather as a progressive pressure wave, by which unbalanced forces in the zones subject to deformation softening are transferred to more stable ground further down the slope.

The maximum velocity at which pressure change in the slope may propagate is theoretically:
$v_{max} = \sqrt{(E_{el}/\rho)}$ m/sec…. **([5])** **([5])** Relationship from basic wave theory.

If, for example $E_{el} = 200 \cdot c$ kN/m^2, c = 20 kN/m^2 and ρ = 1.6 kg/m^3, then v ≈ 50 m/sec. However, friction and time dependent processes in the rupture zones slow down the speed of failure propagation effectively, thus significantly reducing the virtually dynamic effects in this phase of progressive failure development. The duration of the progressive phase is subject to many factors. In extremely sensitive clays it may possibly be a matter of minutes or tens of seconds. (Cf slide at Rävekärr, 1971, Section 5.5)

Conclusion - The progressive failure in this dynamic phase represents a transmission of unbalanced shear forces in steeper ground to more stable, less inclining parts of the slope, where a dramatic growth of the total earth pressures may ensue.

Possible new state of equilibrium – Phase 4
As the progressive failure - or the pressure wave - propagates into less sloping or horizontal ground, the value of maximum resistance N_{cr} increases dramatically with falling values of τ_o, whereby a second stage of static equilibrium (Phase 4) becomes possible:

$$\mathbf{N_D(x_3) = N_i + \int_{x_2}^{x_3} [\tau_o(x) - c_R(x)] \cdot dx < N_{cr}} \qquad \text{See Figure 3:3.4} \qquad \text{.....Eq.3:4a}$$

In this phase, N_{cr} refers to the conditions at the foot of the slope. The progressive failure in the preceding dynamic phase only consists in a redistribution of unbalanced forces from un-stable areas up-slope to more stable ground further down the slope. (Cf Sections 3:31 & 3.33).

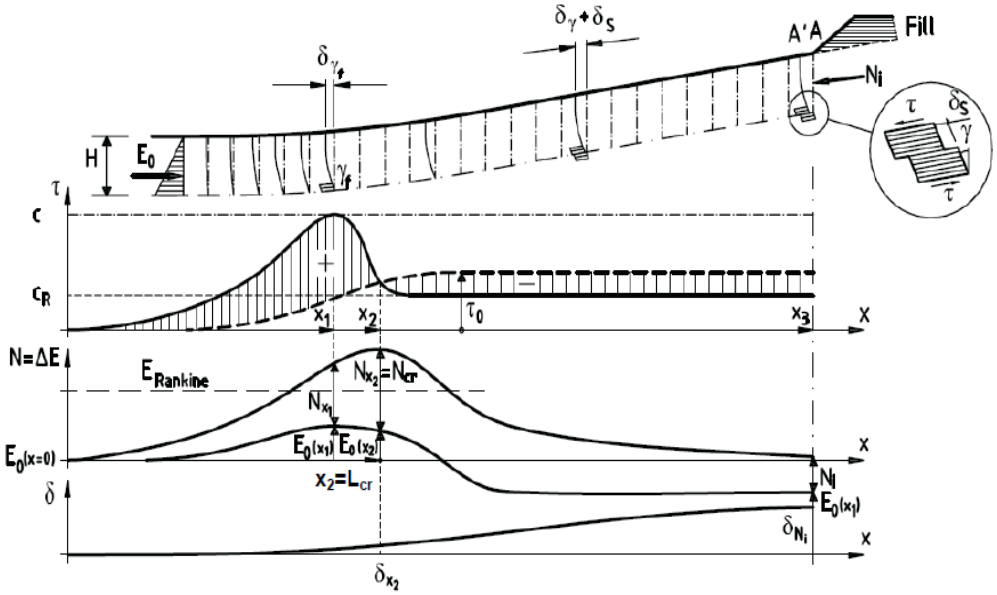

Figure 3:3.4 Possible new state of equilibrium (Phase 4) resulting from local up-slope failure and the ensuing earth pressure redistribution in Phase 3. (Cf Sections 3:31 & 3.33).
Note that, in this phase, it is presumed that the short-term passive earth pressure resistance may well transiently exceed passive resistance based on the shear strength derived from standard laboratory testing procedures.

It is therefore important to realize that the displacements (δ_x) at this stage are limited to the effects of axial compression of the soil mass, induced by the force N_D (x_3), and to the degree of the associated deformation-softening as defined by the value of c_R. This means that the total displacement at A may typically range from a few decimeters to a meter or two, depending on the length of the slope and the sensitivity of the clay. (Cf Bernander, (2008).

The earth pressure distribution in Phase 4 is:

$$\mathbf{E(x) = E_o(x) + N(x)} \qquad \text{……Eq, 3:5}$$

where N_x denotes the earth pressure increment resulting from the force $N_{D(x_3)}$, and
$E_o(x)$ is the prevailing in situ earth pressure.

In case the maximum earth pressure $E_{(x)}{}^{max}$ – after the progressive failure event – remains less than the current passive earth pressure resistance, the potentially sliding soil mass contained between $0 < x < x_3$ will remain in equilibrium and retain its monolithic structure.
Hence:

$$\mathbf{E_x{}^{max} = [E_o(x) + N(x)]^{max} = [K_o \cdot \rho \cdot g \cdot H_x^2/2) + N(x)]^{max} < E_p =}$$
$$\mathbf{= \rho \cdot g \cdot H_x^2/2 + {}_o\int^H 2 \cdot c(z) \cdot dz} \quad \text{or} \qquad \text{..……....Eq.3:5a}$$
$$\mathbf{N_x{}^{max} < (1 - K_o) \cdot \rho \cdot g \cdot H_x^2/2 + {}_o\int^H 2 \cdot c(z) \cdot dz} \qquad \text{..……....Eq.3:5a}_1$$

Equation 3:5a$_1$ illustrates the importance of making a reasonable assessment of the in-situ K_o-value. Considering time dependent creep, the value of K_o is likely to assume rather high values in the transition zone at the foot of the slope, where the gradient decreases.
Thus, if for instance $K_o = 1$, the criterion according to Equation 3:5a$_1$ is:
$N_x{}^{max} < {}_o\int^H 2 \cdot c(z) \cdot dz$

As long as the condition according to Equation 3:5a is valid, the slide movement is terminated at this stage. This implies that the fill generating the force N_i, is merely displaced a distance δ_{x3}, corresponding to the axial compression of the soil in the downhill direction.
The outcome may be a minor local active failure or moderate displacements and cracking up-slope of the fill. (Cf Section 5.5, the slide at Rävekärr, 1971,).

Assessment of passive resistance in Phase 4
A specific issue in this context is whether it is reasonable – in this state of equilibrium – to presume the presence of earth pressures (denoted $E_{ox}+N_x$ in Equations 3:5a & 3:5b) that are in excess of the passive Rankine resistance based on shear strength as derived from standard laboratory testing, and that over considerable distance sometimes measuring hundreds of meters.
Another question is whether locally developing passive failure may jeopardize the validity of the computed distribution of static earth pressure in Phase 4.

It is believed that Phase 4 represents a realistic and for the degree of potential disaster decisively important stage in the development of a progressive landslide in strain-softening clay. The reasons for this standpoint are as follows:
1) In the current context it is vital to appreciate that failure along the long progressively preformed slip surface with the associated failure zone is, for various reasons, of an entirely different nature than failure in a passive Rankine state.
1a) In the first place, the progressive FDM-analysis implies that the two failure phenomena are simply not concurrent.

Already before passive resistance is attained at the foot of the slope, the failure zone and the associated failure plane will – provided the depths to the same are sufficient (e.g. 10 to 30 m) – have developed far, often hundreds of meters, beyond the foot of the slope into more level ground. (Cf Figures 2:2.2b, 3:3.5 and 5:1.2.)

1b) Moreover, this implies that prior to the formation of potential failure along passive slip surfaces of limited length, an extensive failure zone and its concurrent slip surface already exist where large displacements and substantial deformation-softening have taken place. The mechanisms leading to this condition are highlighted in a detailed exemplification presented in Bernander, (2008), Section 5. In this exemplification, the extensive failure parallel to the gently sloping ground, is generated already at an increase of the prevailing in-situ earth pressure corresponding to 75 % of the passive Rankine resistance – i.e. if this is based on shear strength determined according to standard testing procedures.

2) In the current critical stages of progressive landslide formation (i. e. at the end of Phase 3 and in Phase 4), the shear stresses and associated earth pressures will, because of rapid rates of loading, temporarily attain considerably higher peak values than those corresponding to standard tests on clays. This implies that the short-term passive resistance is likely to exceed standard evaluation of passive earth pressure, implying that $E_{P\,(t=\Delta t)}$ may well transiently be considerably higher than $E_{P\,(t=\infty)}$ over a large distance in the potential spread area of the slide.

3) Regarding the earth pressure distribution in Phase 4, it is maintained that even if one assumes that passive failure may be initiated locally – i.e. in the area where the earth pressure ($E_{ox}+N_x$) has its maximum – the computed distribution of earth pressure will still not be significantly affected. This is because displacements and deformation-softening along the already existing failure zone and slip surface are considerable in this situation. In an extensive landslide, the balance between forces acting down-slope and residual stabilizing resistance then virtually constitutes an enormous external impact force, the magnitude of which is practically independent of beginning internal differential deformations within the soil mass. This implies that incipient local resilience in the passive zone actually has little impact on the transitory earth pressure distribution in Phase 4, or on the subsequent general failure conditions.
The configurations of fully developed progressive slides, such as those in Tuve and Surte corroborate the failure mode outlined in above.

The actual slide event – Phase 5. The second dynamic phase
The pressure build-up further down the slope may of course well exceed passive resistance by far, i.e:

$$\mathbf{E_x^{max} = [E_o(x) + N(x)]^{max} > E_p = \rho \cdot g \cdot H_x^2/2 + \int_o^H 2 \cdot c(z) \cdot dz} \qquad \text{.....Eq. 3:5 b}$$

or

$$\mathbf{N_x^{max} > (1 - K_o) \cdot \rho \cdot g \cdot H_x^2/2 + \int_o^H 2 \cdot c(z) \cdot dz} \qquad \text{.....Eq. 3.5 b}_1$$

Equation 3:5 b (or b_1) constitutes the critical criterion for the occurrence of a major slide due to progressive failure. If passive resistance is exceeded over some distance in the lower part of the slope, the consequences will be dramatic as the soil mass will then disintegrate in a state of passive failure, entailing substantial heave of the ground surface.

More important still, this ground heave forms the prerequisite condition for the inherently unstable up-slope soil masses to move downhill at an accelerating pace. It is at this point that the slide enters its truly dynamic phase, in which further events are governed by Newtons laws of motion. Hence, Phase 5 constitutes what is normally understood as the actual slide event. (Cf Section 5.1, the Tuve slide, dynamic analysis, and Section 5.2, the Surte slide).

In this context, it is important to note that gradually increasing sliding velocity tends to further reduce the residual shear resistance in the slip surfaces already formed, thus amplifying the unbalanced force N_D. This also applies to the parts of the failure zone involved in passive failure.
The final extension of the slide, in terms of static equilibrium, can roughly be estimated by basing the calculations on the residual shear resistance c_R that is compatible with the relative velocity, at which the soil actually slides along the slip surfaces.
Consequently, if we do want to predict the extent or degree of disaster of a potentially progressive landslide, it is imperative to use a set of soil parameters that is radically different from the ones normally used – e.g. for identifying the conditions leading to local up-slope failure. (Cf. Sections 9 to 10).
Yet, FDM-analysis based on static loading conditions can only predict minimum spread of the potential slide, since dynamic effects are not included in the computations.

Furthermore, it is essential to observe that, as indicated in Figure 3:3.5, the pre-formed failure zone and slip surface, as well as associated displacements, extend far ahead beyond the visible lower limit of the actual slide. (Cf Figure 3:3.5.)

Final state of equilibrium – Phase 6. *Configuration of the fully developed slide*
Provided sufficient passive resistance is available at the foot of a slope, a final state of equilibrium is possible. The additional growth of the force N_D, together with the dynamic inertia forces in the retardation phase, require that even more of the initially stable, less sloping ground may have to be engaged in order to attain a final state of equilibrium. However, if sufficient passive resistance cannot be mobilized further down the slope, no computable final state of equilibrium exists. The soil structure is then likely to disintegrate in a way typical of retrogressive landslides as discussed in Section 6 and Section 2.42.

3.33 Synopsis
The main conditions, under which local instability in a slope may develop into progressive failure, eventually leading to possible global collapse, are: **(6)**
a) The difference $\mathbf{(c_{R,x} - \tau_{o,x})}$ becomes less than zero (< 0) in a zone of local potential instability, **(6)** i.e. $\mathbf{N_i > N_{cr}}$

(6) Note: For values of $(c_{R,x} - \tau_{o,x}) > 0$, a kind of ductile progressive failure will be induced for increasing values of N_i. However, the vital difference is that the additional load N_i under such conditions is no longer limited to a specific critical value but tends to rise as the failure is progressively 'forced' down the slope. The ultimate limit of N_i is then, among other, related to the down-slope passive resistance. (Cf Section 3.4).

b) The earth pressure $E(x) = N_{cr} + E_o(x_2)$ falls below the resistance along a failure plane surfacing in the slope (e.g. the failure plane A_o- C shown in Figure 3:3.3), i.e.:
$\mathbf{E(x) = N_{cr} + E_o(x_2) < N_{Ao\text{-}C}}$,
where $N_{Ao\text{-}C}$ is the force required to provoke failure along the plane A_o- C

c) The example presented above indicates, and further analysis will highlight, that in a fully developed downhill progressive slide, four states of equilibrium and two intervening dynamic phases can be identified, some of which may have to be considered in careful studies of potential landslide hazard:

Phase 1 The existing ***in situ stage*** (often primordial) (Cf Sections 6.32 & 11.32.)

Phase 2 The ***disturbance phase***, subject to conditions relating to the agent triggering the slide. This is a state of static equilibrium as long as $\mathbf{N_i < N_{cr}}$ but which may become critical if the initiating agent generates a force exceeding N_{cr}, i.e. (See Figure 3:3.2 and 3:3.3)

Phase 3 The virtually ***dynamic load transfer***
If N_i exceeds N_{cr}, i.e. $\mathbf{N_i > N_{cr}}$, a downward progressive failure generates a virtually dynamic transfer of unbalanced up-slope forces entailing significant increment of earth pressures in more stable ground further down the slope. As maintained by the author, and particularly highlighted in Bernander, (2008), Section 5, the failure zone and slip surface may, already at the end of this phase, have developed far beyond the foot of the slope under the valley floor. (Cf Figures 2:4.2b, 3:3.5)

Phase 4 ***Permanent*** or ***transitory static state of equilibrium***
Phase 4a A possible state of static equilibrium may be reached if, subsequent to the downhill force transmission, the maximum earth pressures remain below current passive resistance, i.e:

$$\mathbf{E_{max} = [E_o(x) + N(x)]_{max} < E_p}$$

In this case, the progressive failure will only result in moderate cracking or a minor local active failure up-slope of the agent initiating the local failure.

Phase 4b On the other hand, the resulting maximum down-slope earth pressures may exceed passive resistance, i.e:

$$\mathbf{E(x) = (E_o(x) + N(x)) > E_p(x)}$$

If this is the case, ground upheaval in passive failure will take place. Hence, Phase 4b is inherently of a transient nature. Nevertheless, it defines in terms of static stability the length of the zone subject to passive failure before passing into the dynamic condition in Phase 5.

Phase 5 ***Final breakdown*** in passive failure if current passive resistance in the previous transitory state of equilibrium (Phase 4b) is exceeded.
This is when the slide proper takes place, resulting in large displacements of soil masses down the slope, as well as massive heave of the ground surface – often extending over level ground far beyond the foot of the slope, i.e:

$$\mathbf{N_i + N_D + N_{inertia} > E_p} \text{ (heave)} \qquad \ldots\ldots\ldots\ldots\ldots\text{Eq. 3:6}$$

Phase 6 The foregoing phase is of a dynamic nature, and will end up in the final state of equilibrium of the finished slide, provided sufficient passive resistance can be mobilized. This equilibrium is attained, when both static forces and forces of inertia are ultimately balanced by the passive resistance generated by ground upheaval and increase of earth pressure in the ground ahead of the visible slide limit. (Cf Figure 3:3.5).

The heave of the ground surface may roughly be estimated by equating the potential energy (W) released by the slide to the energy required to raise the center of gravity of the soil masses in the passive zone, i.e:

$$W_{\text{potential energy}} \approx \Sigma_o^{Lp} [\rho \cdot g \cdot H_x^{\text{heave}} \cdot \Delta x] \cdot (H_x^{\text{heave}} - H_x)/2 \qquad \text{..... Eq. 3:7}$$

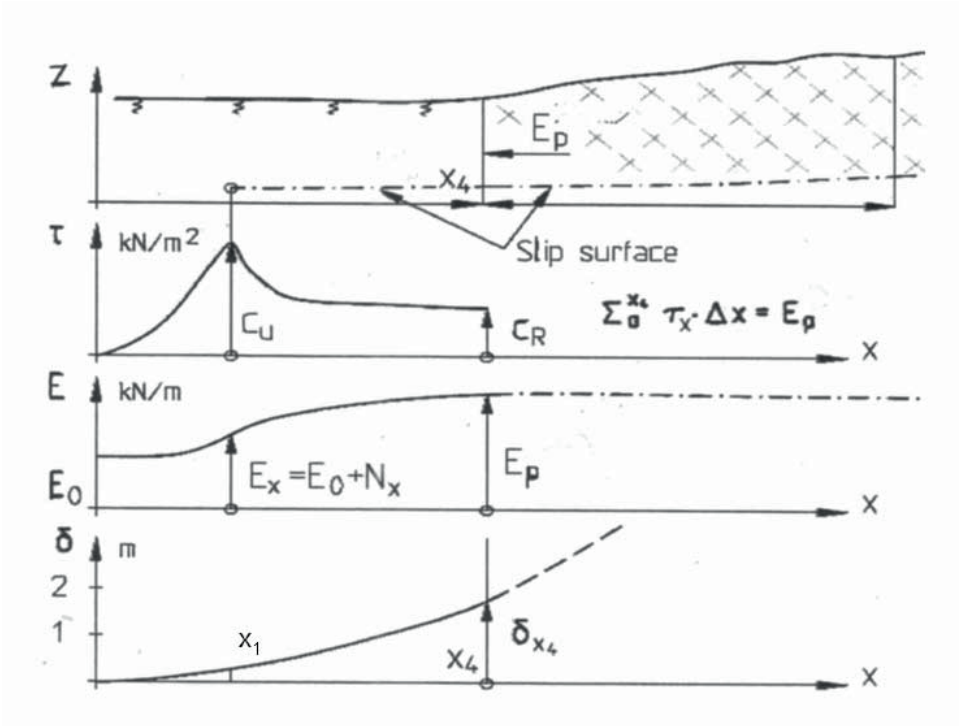

Figure 3:3.5 Conditions at the far end of a downward progressive landslide. Note displacement and considerable extension of failure zone and slip surface outside the limit of the slide proper.

The potential energy (W) has to be determined by iteration procedures. Equation 3:7 does not consider energy lost in the slip surfaces during the passive failure process. In very sensitive soils, this energy is likely to be small compared to the total energy released in the main slide event.

As already mentioned, FDM-analysis predicts that the shear failure zone and the associated slip surface, including related ground displacements, can extend far ahead (i.e. hundreds of meters) beyond what is normally understood as being the slide limit.
As indicated in Figure 3:3.5, the slide extends a distance x_4 outside the lower boundary of the passive zone. The length of x_4 may be estimated as:

$$E_p = E_o + {}_o\int^{x1}(\tau_x - \tau_{o,x}) \cdot dx + {}_{x1}\int^{x4} c_{R(x)} \cdot dx \qquad \text{..... Eq. 3:7a}$$

As demonstrated in an example in Bernander, (2008), Section 5, the failure zone and slip surface tend to develop prior to the incidence of passive Rankine failure, extending in the example some 200 m into the level ground ahead of the foot of the slope.

3.34 Safety factors – new formulations

The previous discussion indicates that the traditional way of defining the risk of slope failure, – i.e. $F_S = c_{mean}/\tau_{mean}$ – is not relevant for the prediction of slide hazard in long slopes of sensitive clay. Instead, the following criteria are considered to be pertinent.
(Bernander & Gustås, 1984)

Local failure – Regarding the prevention of initial local failure, the triggering force N_i should not exceed the local maximum stabilizing resistance N_{cr}, i.e. the safety factor

$$\mathbf{F_s^I = N_{cr} / N_i > 1} \qquad \text{…… Eq. 3:8}$$

or, if the additional loads (q,t) shown in Figure 4:2.1 are also considered,

$$\mathbf{F_s^I = (N_i,q,t)_{cr}/(N_i,q,t) > 1} \qquad \text{…… Eq..3:8a}$$

where $(N_i,q,t)_{cr}$ denotes a critical combination of the additional loading.

Global failure – With regard to the general failure that may result from local up-slope instability, triggering progressive failure, the ultimate earth pressure after the redistribution of forces in Phase 4b must not exceed passive Rankine resistance, i.e.

$$\mathbf{F_s^{II} = E_p/(E_{ox} + N_x)^{max} > 1} \qquad \text{…… Eq. 3:9}$$

or

$$\mathbf{F_s^{II} = \left[(1- K_o)\cdot\rho\cdot g\cdot H^2/2 + \int_o^H 2\cdot c_{u(z)}\cdot dz\right] / N_x^{max} > 1} \qquad \text{..…… Eq. 3:9 a}$$

As already mentioned, the resistance in Phase 4b may transiently exceed the passive resistance based on shear strength determined by standard laboratory procedures.

3.35 Slope failure in sensitive soils – *a phenomenon analogous to buckling*

It may thus be concluded that, once the initiating force N_i exceeds the value of N_{cr}, static equilibrium is no longer mechanically possible. The work performed by the force initiating progressive failure can be expressed as

$$W_{cr\ I} = \int_o^{x2} N_x \cdot d\delta_x \qquad \text{..…… Eq. 3:10}$$

where both N_x and δ_x are functions of the coordinate x

As may be concluded from Figures 3:3.4 and 4:2.4a, a situation may arise, in which the force required to set off a progressive failure is equal to zero. Hence, Equation 3:10 applies also to the case, when a forced displacement corresponding to $N_i = 0$, is applied, i.e.

$$W_{cr\ II} = \int_o^{Linstab} N_x \cdot d\delta_x \qquad \text{..…… Eq. 3:10a}$$

Interestingly, Equation 3:10a signifies that, when a certain forced displacement (δ_{Ni}) is applied, e.g. by driving soil displacing piles, the slope may fail despite the fact that there is no sustained active force N_i maintaining the failure process. In other words, the failure criterion

here is related to the total energy or to displacement generated by the agent causing the initiating failure. (See Figure 4:2.4a, where the length L_{instab} in Equation 3:10a is defined.) Accordingly, slope stability may be considered as a problem analogous to 'buckling stability' in a structure-mechanical sense. As in the case of an axially loaded strut, static equilibrium is no longer possible once the limiting critical load is reached at a certain initial or applied mid-point deflection.

The stability of a slope may therefore metaphorically be thought of as being similar to the stability of a ball – weighing (m·g) kN – placed in a depression on top of a cone as shown in Figure 3:3.6. Here, if the work applied to the ball by a displacing agent N_i is greater than $W = m \cdot g \cdot \Delta h$, the ball is lifted over the rim of the depression and static equilibrium is out of the question.

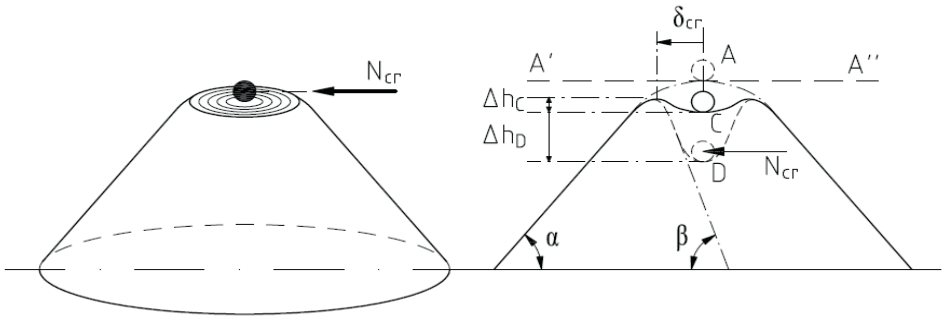

Figure 3:3.6 Metaphorical representation of slope stability in deformation softening soils.
The value of N_{cr} is in the analogy related to the depth and the steepest gradient of the sides of the depression ($N_{cr}^{max} = m \cdot g \cdot \tan\beta$), while the gradient ($\alpha$) of the exterior sides of the cone may be said to correspond to the degree of deformation softening of the soil.
Hence, in this model, ideal plastic equilibrium will correspond to the special case when the gradient of the sides of the cone becomes infinitely small so that the exterior surfaces of the cone form a horizontal plane A' – A'', as indicated in Figure 3.3.6.

3:4 *Ductile slope failure in deformation-softening soils – ($c_R > \tau_o$)*

In contrast to the condition valid for the kind of brittle progressive failure featured in Section 3.3, the residual shear resistance (c_R) may well remain higher than the in situ stress (τ_o) throughout the duration of the additional loading effect exerted by the disturbing agent. The redistribution of earth pressures related to the deformation-softening – instead of entering a dynamic phase – then only results in growing down-slope displacements as the additional loading is increased. This failure process is of a ductile character, and the ultimate load is no longer limited to the critical value according to Section 3.3. The condition $c_R > \tau_o$ is likely to be valid in most instances.
The subsequently proposed analysis considering deformations and deformation-softening in the soil correlates with conventional ideal-plastic analysis (I-PlFA) in the special case when the ratio of $\mathbf{c_R/c = 1}$.

In situ stress conditions
The FDM-approach may conveniently be used for assessing the stress distribution in current states of loading, including modified serviceability conditions.

An important condition in the analysis of brittle slope failure is that assessment of the distribution of in situ stresses and earth pressures can be made by applying an appropriate long-term stress/strain relationship.

3:5 *Factors conducive to brittle slope failure*

Local slope failure may lead to total collapse of not only the entire slope, but also of large areas of adjoining inherently stable ground subject to a number of factors such as:

Soil sensitivity	See	Section	9.1
Slope geometry	"	"	9.2
Creep deformations	"	"	9.3
State of stress	"	"	9.4
Distribution and location of incremental loading	"	"	9.5
Rate of load application	"	"	9.5
Hydrological conditions	"	"	9.6

Section 5 deals with a number of case records, where the morphology of fully developed slides, as maintained by the author, can only be explained using a progressive failure model.

In subsequent sections, examples of the application of a FDM-model will be provided, demonstrating that analysis based on 'ideal-plastic' properties cannot, in very sensitive soils, yield reasonably accurate predictions of slide hazard related to locally acting disturbance agents.

3.6 Orientation of coordinate axes

The x- and the z-coordinate axes are normally oriented in the horizontal and vertical directions respectively. However, for illustrative purpose the x- and the z-axes may also be oriented parallel and perpendicular to an irregularly sloping failure plane as for instance in Figures 4:2.2 and 4:4.1.

The difference between these approaches is insignificant for two reasons:

1) Firstly, the gradients (β) of the failure plane are in the current context rather small, implying that the values of $\cos \beta$ are very close to 1.
(E.g. for a gradient of 10:100, the value of $\cos \beta$ is 0,995. Yet, a gradient of 10% is a high value for failure planes in long natural slopes of soft sensitive clay.)

2) Secondly, the choice of coordinate axes does not affect the total weight of the soil mass or the shear stress distribution. A soil volume may just as well be subdivided into rectangles as into parallelograms.

4. An analytical FDM-model for downhill progressive slides - theory

4.1 *General*

The model for progressive failure analysis described below is a further development of an earlier approach published at the Xth ICSMFE (Stockholm, 1981). The improved model was presented at the XI th and XII th ICSMFE (San Fransisco, 1985 and Rio de Janeiro, 1989).

Ideally, slope stability analysis should unambiguously define the critical conditions in a slope directly on the basis of available input data. Yet, such an analysis would, apart from being more complicated, in most cases also be unnecessarily laborious, as the critical failure planes can mostly be reasonably well identified by the morphology of a slope and the stratification of the soils. In fact, the analysis proposed below predicts that failure planes primarily tend to develop along the steep of firm bottom or along firmer soil layers, even to great depth below the ground surface.

The approach to slope stability analysis presented below does not form an integral 'closed' analysis with the critical zones and failure planes emerging directly from the computations. The method of analysis resembles conventional limit plastic equilibrium modelling in so far as the potential failure plane is presumed to be known. The most critical condition – as in conventional stability calculations – may therefore have to be found by iteration involving alternative assumptions regarding the potential failure plane. This implies that the failure planes related to potential landslide risk in a slope can readily be identified beforehand.

Nevertheless, the proposed analysis differs from the fully plastic limit equilibrium methods in a number of important ways:
a - Whereas, in the 'ideal-plastic' failure approach (I-PlFA), the equilibrium of the entire potential sliding body of soil is investigated, the presented progressive failure analysis (Pr FA) focuses on the equilibrium of each individual element into which the potentially sliding body of soil is subdivided.

b - Furthermore, the main deformations within and outside the potentially sliding soil mass are considered. Hence, the axial displacements in the slide direction due to earth pressure changes in the slope are at all times maintained compatible with the shear deformations of the discrete vertical elements. In doing so, it is possible to model the distribution of shear stresses and the extent to which the shear capacity can be mobilized in the forming failure zone and slip surface. The differential equations are integrated and solved numerically.

c - The shear properties of the soil are defined by a full non-linear stress/strain curve, and not only by a discrete shear strength parameter, as in traditional calculations based on perfect plasticity. (Cf Figures 3:3.1, 4:2.4b and 4:4.2.)
The constitutive relationship being separated into two stages (I and II), the conditions before and after the formation of a slip surface can be simulated – e.g. in accordance with direct shear tests of the kind shown in Figures 2:3.2 and 4:2.1. The stress/deformation relationships, defining the degree of deformation-softening, may be chosen so that they correspond to the actual rates of loading and to other inherent conditions (such as e.g. drainage) in different parts of the slope. **([1])**

([1]) The term **'deformation-softening'** refers in this document to loss of shear resistance both due to shear (deviator) strain and to local displacement (or slip) in a failure plane.

d - By using different stress/deformation relationships, relating to different time scales of load (or stress) application, the time factor can be included in the analysis.

However, considering the time factor necessitates studying slope failure in markedly strain softening soils in distinctly separate phases. This is simply due to the fact that the stress-strain properties, and especially the residual resistance, of sensitive clays may vary significantly in the different stages of a progressive landslide. (Cf Sections 3.31 to 3.33.)
This is a feature of paramount importance. It makes it possible, among other, to define the in situ earth pressure conditions prior to the application of additional loading.

e - Local horizontal or vertical loads, as well as local features in the slope structure that may be conducive to failure formation can be taken into account – i.e. brittleness relating to the sedimentary structure and to specific geometric features in a slope can be accounted for.

f - Although the position of the potential failure plane is assumed to be given, the final extension of a slide and the length of the passive zone, emerge as results of the computations.

4.2 *Soil model - derivation of formulae*

4.21 Basic assumptions - drainage conditions
A progressive landslide may initially begin as a drained, partially drained or un-drained local failure depending on the rate at which the agents causing the limited zone of instability intervene. The soil strength parameters used for defining the critical condition, susceptible of initiating progressive failure in a slope, must therefore be selected in accordance with the nature of the additional load being investigated. The simultaneously prevailing drainage conditions in the incipient failure zone also have to be taken into account.

Yet, even when a potentially drained local failure has started to develop, time-dependent deformation-softening, and minor load increment, may gradually generate partially un-drained or even completely un-drained response in the failure zone.
Hence, although total stress parameters are used in the structure-mechanical analysis of the slide events, strength parameters (including the constitutive stress-deformation relationships) based on the partially drained or un-drained soil behaviour may have to be considered.
Temporary variation of ground water levels and possible artesian pressure can enter into the analysis by considering the OCR-ratio.

Furthermore, the soils of the entire slope profile are taken to be saturated. This means that the seepage pressures due to percolation of ground water down the slope are accounted for, even in cases with highly permeable soil strata.
If the slope is partially submerged, the stabilizing effect of horizontal hydraulic pressure can be considered in the model.

4.22 Basic assumptions in the analytical model
Some of the general notations applied in the adopted model for slope failure are shown in Figure 4:2.1. The figure depicts in principle a slide in progress and does not represent any of the particular phases of equilibrium defined in Section 3.3.

The basic mathematical approach used is that of finite differences in a two-dimensional model – denoted the FDM-approach for short. Nevertheless, any desired three-dimensional shape of the sliding body can be accommodated by varying the width b(x). As indicated in Figure

4:2.2, the potentially sliding soil volume is subdivided into vertical elements of length Δx with the coordinate (x) taken positive in the up-slope direction. In the derivation below, the x-axis is oriented along the potential slip surface, which is justified as long as cos β ≈1.

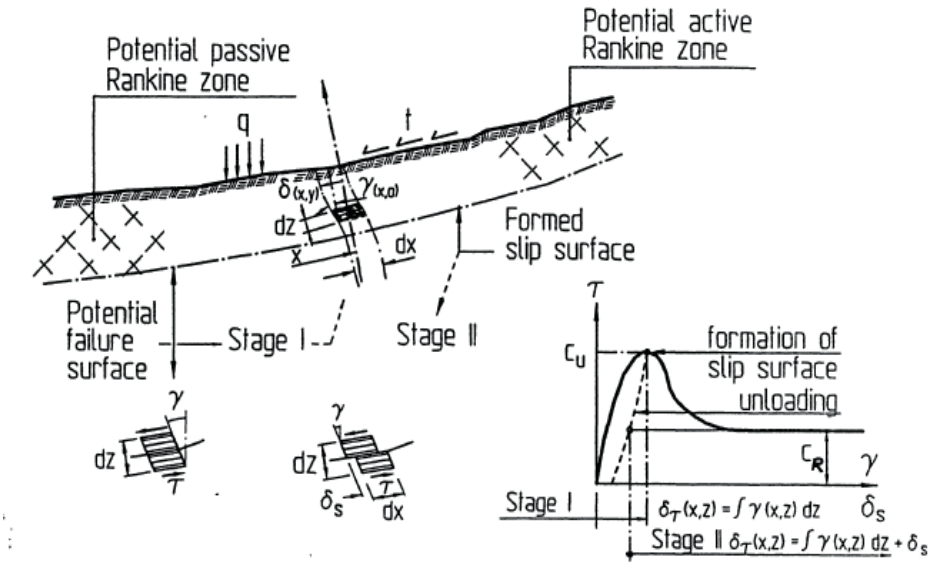

Figure 4:2.1 Structure and development of a down-slope progressive landslide – notations and principles.

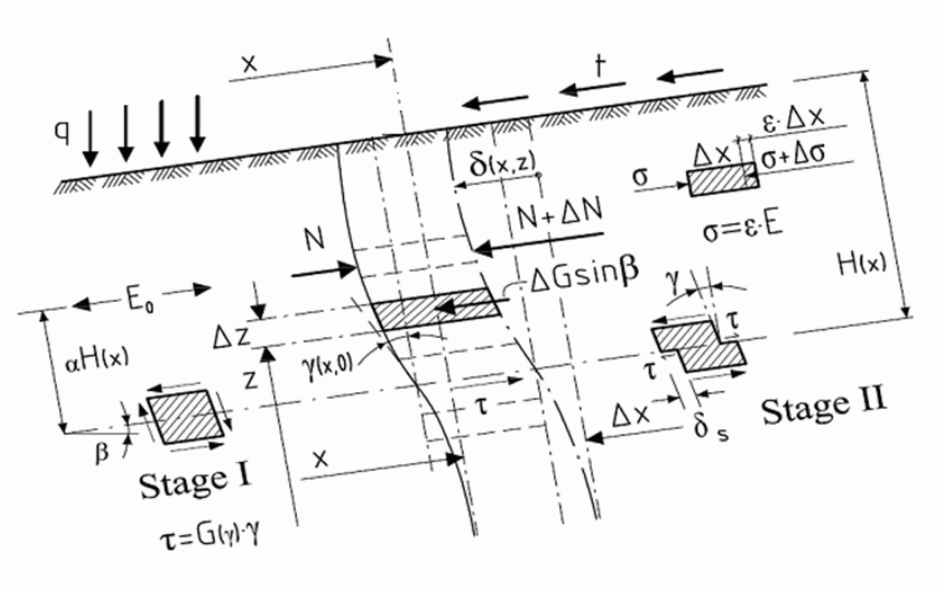

Figure 4:2.2 FDM - model – denotations. (From Bernander et al, 1988, 1989), E_o indicates the in-situ earth pressure condition. For illustrative and practical purposes H_x and Δz are taken perpendicular to the failure plane. As regards the orientation of x- and z-axes, confer Section 3.6

Each vertical slice is subdivided into a number of rectangular elements of height Δz in the z - direction, thus permitting modelling of the deviatory deformations within and outside the soil profile, and in particular the deformations developing in the zones adjacent to both the potential and the already formed slip surfaces.
This is a cardinal feature in the current FDM-approach because the incipient failure zone contributes to an overwhelmingly major part of the accumulated shear displacement of a vertical soil element before the incidence of local failure – and that notably prior to the formation of an extended failure plane or slip surface in the ensuing dynamic phase, defined as Phase 3 in Section 3.
This is therefore a crucial feature in the current context, as the resilience of the shear failure zone actually constitutes the prerequisite condition for an effective and calculable resistance to slope failure by concentrated loading. (Cf Figure 3:3.3)
Or to phrase the issue somewhat differently, the critical parameters N_{cr}, L_{cr} and δ_{cr}, related to triggering of progressive failure, depend directly on the total resilience of the entire zone subject to shear deformation. In fact, if the resilience of the failure zone were negligible, any minor load concentration could release slope failure. (Cf Equation 4:1b.)
(Cf comments regarding Kjellman's approach to progressive failure in Section 1.11.)

The denotations used in the subsequent derivation of Equations 4:1 to 4:7, are defined in Figure 4:2.2 and as follows:

δ_x	Average down-slope displacement of the soil above the potential slip surface
$\delta_{x,z}$	Down-slope displacement of element ($\Delta x \cdot \Delta z$) in shear
αH_x	Level at which the down-slope displacement is considered to be valid
$E_o(x)$	In situ earth pressure at point x
N (x)	Earth pressure increment due to additional load or to progressive failure formation
E(x)	$= E_o(x) + N(x)$
τ (x,z)	Total shear stress in section x at elevation z
τ (x,o)	Total shear stress at failure plane (z = 0)
$\tau_o(x,z)$	In situ shear stress in section x at elevation z
$\tau_o(x,o)$	In situ shear stress at failure plane (z = 0)
γ (x,z)	Deviator (shear) strain in point (x,z)
$\sigma(x)$	Mean incremental down-slope axial stress
q(x)	Additional vertical load
t(x)	Additional load in the down-slope direction
H(x)	Height of element
b(x)	Width of element
E_{el}	Secant elastic modulus in down-slope compression
G	Secant modulus in shear in the range τ (x ,z)$\rightarrow$ τ (x ,z)+ $\Delta\tau$ (x ,z)
$\beta(x)$	Slope gradient at coordinate x
$\delta_S(x)$	Off-set (slip) in the failure surface in relation to the sub-ground (slip deformation)
L_{cr}	Limit length of mobilization of shear stress at N_{cr}
N_{cr}	Critical load effect initiating local slope failure
δ_{cr}	Critical displacement in terms of axial deformation at N_{cr}

(For denotations not given here, see the introductory section named 'Notations'.)

4.23 Basic differential equations

Derivation of formulae valid in Stage I, i.e. for values of $\gamma(x) < \gamma_f$

The equilibrium of an element [H(x)· b(x)·Δx] in the down-slope direction requires that

Change of shear stress *Vertical load* *Down-slope load*

$$\Delta N = [\tau(x,o) - \tau_o(x,o)]\cdot b(x)\cdot\Delta x - q(x)\cdot b(x)\cdot \sin\beta(x)\cdot\Delta x - t(x)\cdot b(x)\cdot\Delta x \quad \text{....……Eq. 4:1}$$

Hence: $N_x = \Sigma_o^x \Delta N$ and …….. ... Eq. 4:1a

$N_{cr} = \Sigma_o^{Lcr} \Delta N$ …..…... Eq. 4:1b

.

The in situ shear stress at the potential slip surface level may for non-submerged conditions be written as

Gravitational load *Change of in situ stress*

$$\tau_o(x,o) = \Sigma_o^{H(x)}\, g\cdot\rho(z)\cdot\Delta z\cdot\sin\beta(x) - \Delta E_o(x)/(b(x)\cdot\Delta x) \quad \text{……. Eq.4:2}$$

(**Note:** x is positive in the up-slope direction, implying that ΔE_o is negative for decreasing earth pressure in the direction of x, thus counteracting the down-slope gravitational load.)

The axial compression of an element in the x direction may be written as

$$\Delta\delta_N = (N+\Delta N/2)\cdot\Delta x /[E_{el}\cdot H(x)\cdot b(x)] \quad \text{…… Eq. 4:3}$$

where $\Delta\delta_N$ is the incremental mean down-slope displacement due to the compression of an element.

However, the total mean down-slope displacement (δ_N), to which a vertical element is subjected, must be compatible with the shear deformation of the same element relative to the ground below the slip surface. This condition may be expressed as

$$\delta_\tau(x) = \Sigma_o^{\alpha H(x)} [(\tau(x,z)/ G(x,z,\tau) - \tau_o(x,z)/ G(x,z,\tau)]\cdot\Delta z + \delta_S(x,o) \quad \text{……Eq. 4:4}$$

$$= \Sigma_o^{\alpha H(x)} [(\gamma(x,z,\tau) - \gamma_o(x,z,\tau_o)]\cdot\Delta z + \delta_S(x,o) \quad \text{……Eq. 4:4a}$$

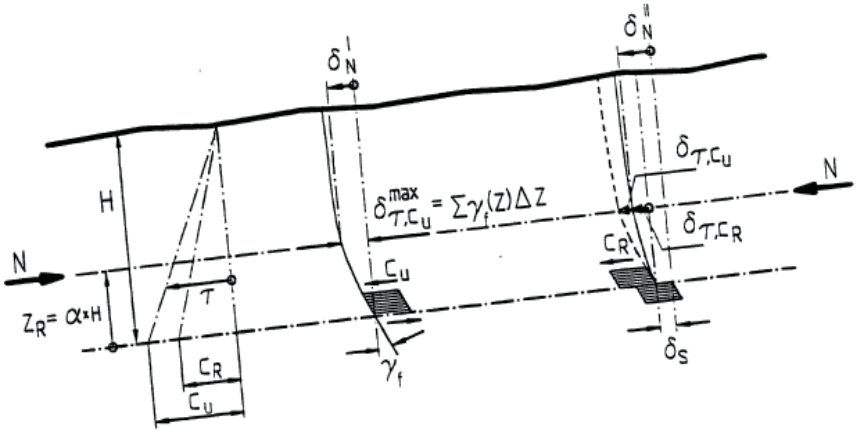

Figure 4:2.3 The down-slope axial displacement of a soil element must be compatible with the integral shear deformation of the same element in relation to the sub-ground.

The compatibility criterion with regard to down-slope displacement demands that

$\delta_{N(x)} = \Sigma_o^x (\Delta\delta_N) = \delta_{\tau(x)}$ When $\gamma(x,z) < \gamma_f$, then $\delta_S(x,o) = 0$ ……. Eq. 4:5

The known constitutive relationship defined by the shear stress/deformation curve is expressed as

$\tau(x,z) = \phi(\gamma(x,z), \delta_S, d\delta_S/dt)$ or inversely, ……Eq. 4:6

$\gamma(x,z, \delta_S, d\delta_S/dt) = \phi_1(\tau(x,z))$ ……Eq. 4:6 a

Thus, the shear stress $\tau(x,z)$ is a function of the deviatory strain $\gamma(x,z)$ and the displacement δ_S in the slip surface. If these functions are known, the differential Equations 4:1 to 4:6 can be integrated numerically yielding the states of stress, strains and displacements for any chosen mode of mobilizing the resistance to failure propagation - and that in any chosen portion of the slope. (See Figure 4:2.4a & b.)

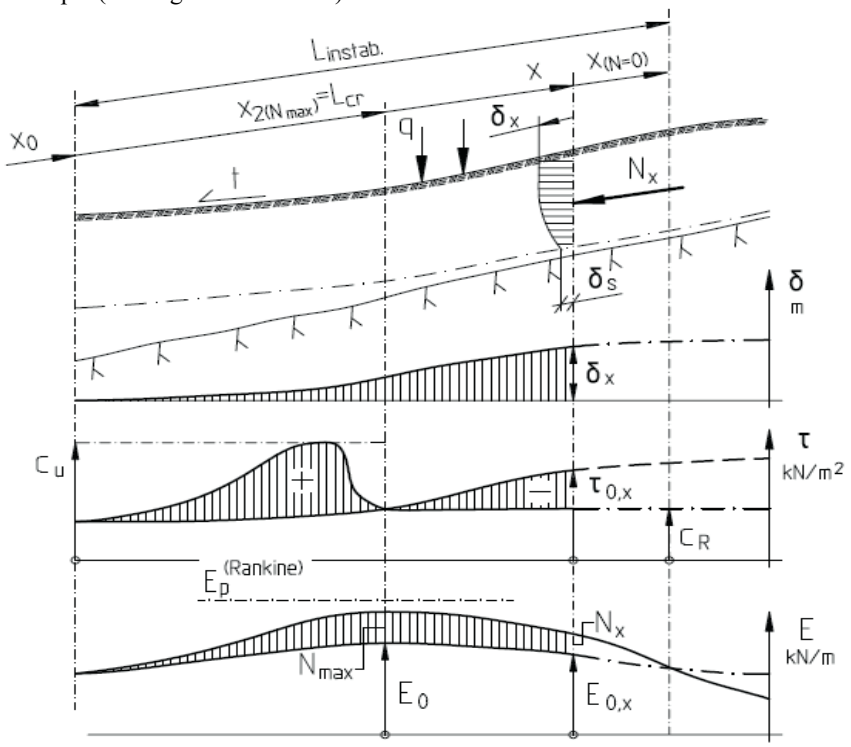

Figure 4:2.4a Principal results from downward progressive failure analysis according to Equation 4:1 to 4:6. – Notations.

Equation valid in stage II, i.e. for values of $\delta_{S(x)} > \delta_{S(cR)}$

When the residual shear strength is attained in the slip surface, the Equation 4:1c is substituted for Equation 4:1.

$\Delta N = [c_R(x,o) - \tau_o(x,o)] \cdot b(x) \cdot \Delta x - q(x) \cdot b(x) \cdot \sin\beta(x) \cdot \Delta x - t(x) \cdot b(x) \cdot \Delta x$ ……..Eq. 4:1c

where τ_o is defined as before

$\tau_o(x,o) = [\Sigma_o^{H(x)} g \cdot \rho(z) \cdot \Delta z] \cdot \sin\beta(x) - g \cdot \rho_W \cdot D_W(x) \cdot \sin\beta(x) - \Delta E_o(x) / b(x) \cdot \Delta x$ and

$c_R(x,o)$ = the residual large deformation shear strength at z = 0, and/or if applicable, the high deformation rate residual resistance of the soil at z = 0.

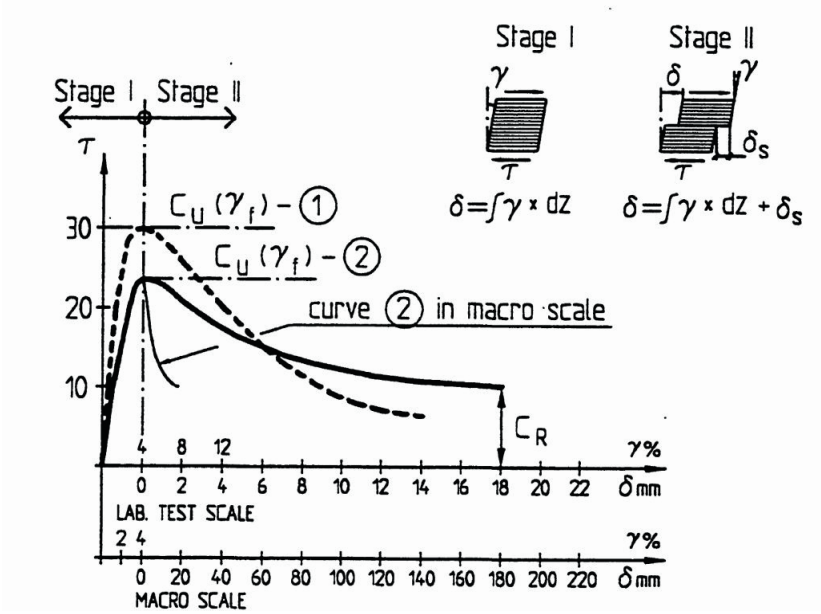

Figure 4:2.4b Time dependent stress-strain relationship $\tau = \phi(\gamma, d\gamma/dt, \delta_S, d\delta_S/dt)$. Laboratory test curve compared with the same curve translated to the real dimensions of the soil structure. Note the apparent difference in brittleness. Curves 1 and 2 exemplify stress/deformation relationships at different rates of loading. (Earlier also presented as Figure 3:3.1)

4.24 Modulus of elasticity

Young's modulus of elasticity (E_{el}) enters into the analysis (Equation 4:3) when evaluating the displacement of a vertical section in the down-slope direction. Referring to the constitutive relationship shown in Figure 4:4.2, the initial shear modulus, which is valid below the elastic limit defined by (τ_{el}) and (γ_{el}), can be expressed as $G_{el} = \tau_{el}/\gamma_{el}$ and the corresponding E-modulus is then according to basic theory

$E_{el} = 2(1+\nu)\cdot G_{el} = \Omega \cdot c$

where Ω is a coefficient relating the E-modulus to the shear strength.

As the elastic modulus in cohesive materials is often expressed in terms of the shear strength, the sought mean elastic modulus (E_{el}) may thus be put as:

$E_{el,mean} = \Omega \cdot c_{mean} = \Omega \cdot 1/H \cdot \int_o^H c(z) \cdot dz$ ……Eq. 4:7

For example, if in a specific case $c_{z=o} = 30$ kN/m^2, $c_{mean} = 25$ kN/m^2, $\tau_{el} = 20$ kN/m^2, $\gamma_{el} = 1$ % and $\nu = 0.5$ then

$G_{el,o} = 20/0.01 = 2000$ kN/m^2

$E_{el,o} = 2(1+0.5)\cdot 2000 = 6000$ kN/m^2 $= 200 \cdot c$ (i.e. $\Omega = 200$)

$E_{el,mean} = 200 \cdot c_{mean} = 200 \cdot 25 = 5000$ kN/m^2

For low shear stresses in the elastic or quasi-elastic range, the problem of time dependency of the modulus is not acute, since the ratio of G/E will largely be independent of time. However, at high shear stress levels in the potential failure zone, time dependency of the deviatory strains is more pronounced while the displacements determined by $E_{el,mean}$ may still be largely elastic. Hence, time dependent phenomena in the zone of initial failure have to be

modelled by appropriate constitutive relationships, selected in accordance with the time range of the event or agent jeopardizing the stability of the slope.

4.25 Regarding distribution of vertical shear stress

The value of α in Equation 4:4 may require special consideration. The analytical model illustrated in Figures 4:2.2 and 4:2.3 may metaphorically be thought of as a structure composed of a massive compression member in the slope direction connected to the sub-base by vertical shear elements (or 'shear keys') measuring $\Delta x \cdot \alpha H$.

Hence, in this model, the soil mass in the slope is stabilized partly by axial compression in the slope direction and partly by shear of the vertical elements connecting the potentially movable soil mass to firm bottom or to firmer soil strata.

Now if, hypothetically, this compression member of massive soil were to be replaced by a strut or a beam with the same stiffness as the soil, compatibility would require that the strut be located at the elevation of the earth pressure resultant. Thus, the value of α is taken to be equal to z_R/H, where z_R denotes the z-coordinate of the earth pressure force resultant.

The fact that z_R and α are not constant along the slope may constitute a complication in the proposed analysis. However, the variation of the value of α is not very significant. For instance, in the case of normally consolidated Swedish clays, the following values of α would be valid for total stress analysis:

	H = 10 m	H = 20 m
At active earth pressure	$\alpha = 0.27$	$\alpha = 0.30$
For values of $K_o \approx 1.0$	$\alpha = 0.33$	$\alpha = 0.33$
At passive earth pressure	$\alpha = 0.37$	$\alpha = 0.35$

Furthermore, the outcome of the analysis is largely insensitive to variation of α, which is partly due to the non-linear behaviour of soils at high stress levels. (See further comment at the end of the following paragraph).

In conclusion, although the method of analysis can accommodate any α-value deemed to be appropriate, a value of 0.33 can in practice be applied within the ranges of normally prevailing earth pressures in slopes.

4.26 Vertical shear stress distribution closer to the failure zone

An important point in this context is the vertical distribution of shear stress in the vertical elements constituting the shear keys.

Shear in these elements originates mainly from four different sources, namely

a) Shear due to direct gravitational load related to slope inclination;
b) Shear due to other existing external loads at the studied section;
c) Shear stress increase resulting from specific additional local load acting at some distance from the section studied;
d) Internal shear due to forced down-slope displacement - also emanating from action some distance away from the section studied. (E.g. driving of soil displacing piles)

In slope stability issues, the overwhelmingly dominant condition is **Case a**, in which the shear stress basically increases linearly with depth.

In **Case b**, the distribution of shear stress depends on the type and point of application of the load.

In **Case c**, the shear stress distribution is somewhat more complicated. For typical additional loads, such as the local fill shown in e.g. Figure 4:7.1, the distribution of shear stress immediately down-slope of the loaded area is basically linear, i.e.

$\Delta\tau_{x,z} = \Delta\tau_{x,H} \cdot z/H$ …… Eq.4:7a
where $\Delta\tau_{x,z}$ is the shear stress from additional load in section (x) as function of (z),
and $\Delta\tau_{x,H}$ is the corresponding shear stress at the potential slip surface, i.e.
$\Delta\tau_{x,H} = (\tau_{x,z} - \tau_{x,o})$ according to Equation 4:4.

However, at some distance away from the additional load, the downhill axial (normal) stress originating from this load may be presumed to be distributed in proportion to the stiffness of the clay layers in the soil structure.
Hence, assuming the stiffness to be proportional to the peak shear strength as per Eq. 4:7, the shear stress distribution can be derived to be:
$\Delta\tau_{x,z} = \Delta\tau_{x,H}\cdot[c_S\cdot z/H + 1/2(c_H - c_S)\cdot(z/H)^2]\cdot 2/(c_H + c_S)$ …… Eq.4:7b
where c_S = Shear strength at ground surface
c_H = Shear strength at potential slip surface level.

(For example, if $c_S = 20$ kN/m^2 and $c_H = 30$ kN/m^2, then
$\Delta\tau_{x,z} = \Delta\tau_{x,H}\cdot[0.8\cdot z/H + 0.2\cdot(z/H)^2]$, i.e:
$\Delta\tau_{x,z} = \Delta\tau_{x,H}$ for z = H, at the potential failure plane, and
$\Delta\tau_{x,z} = 0$ for z = 0, at the ground surface).
In the computer software mentioned in Section 4.5, Equation 4:7a is applied, whereas in the Excel spread-sheet presented in Bernander 2008, (Appendices A, B and C), the shear stress distribution from the additional load is optional.
Yet, numerous practical applications indicate that the difference between the results from using the distribution according to either Equation 4:7a or 4:7b is negligible – the difference between the values of, e.g. the critical force N_{cr}, often being less than 0.5 %.

In **Case d**, regarding imposed displacement, the internal shear stress distribution may be taken to be linear for the same reasons as in Case c.
Again, results from analyses performed appear to be insensitive to inaccuracy in respect of the distribution of shear stress from additional load in the zone limited by the coordinates z = 0 and $z = z_R = 0.33H$. The reason for this is largely related to the markedly non-linear behaviour of clays at high shear stress levels and, of course when applicable, even more so to the effects of slip in an already formed failure surface.
In other words, large shear deformations in the incipient failure zone, or slip in the developed failure plane, tend to eclipse the consequences of possible inaccuracy as regards the shear stress distribution with depth. For practical purposes, therefore, this relationship may be assumed to be linear as per Equation 4:7a.

4.3 *Computation procedure*

The aim of the following exercise is to determine the effects of the additional forces (N_i, q, t) in terms of stresses and deformations of significance down to a chosen location (x=0) further down the slope, taking relevant stress/deformation relationships into account. Additional forces, likely to trigger downhill progressive landslides, are typically located in a steep uphill portion of the slope.
As discussed in more detail in Section 3.3 and in Section 11, the objective of the present analysis is to identify the critical limiting conditions in slopes, where progressive failures are prone to develop. The criterion, likely to trigger progressive failure in natural slopes is, for instance, $N_i \geq N_{cr.}$ (Cf Equation 3.8).
Integration of the differential Equations 4:1 to 4:6 can be made by the following step-by-step procedure, which may be used for manual as well as computer analysis.

Step 1:

Step 1a Beginning at some point x = 0, which is selected to suit the aim of the analysis, the shear stress is increased by a value $\Delta\tau$, so that $\tau_1 = \tau_o + \Delta\tau_1$. The value of τ_o is defined by Equation 4:2. The corresponding abscissa of the studied section is then $x_1 = 0 + \Delta x_1$.
The choice of the location for the point x = 0 may be regarded as the down-slope boundary condition, as it constitutes the one point, where the effects of the additional load on the sought parameters N_x, δ_N, δ_τ, $(\tau_x - \tau_o)$ are negligible, and where $E_{o,x}$ is known or definable using State-of-the Art soil mechanics. The significance of where in the slope the point x = 0 is located is therefore that the subsequent computations will yield the additional force N_x, that must not be exceeded at the location defined by (x), lest the point x= 0, (i.e. Origo) has to be relocated further down-slope **([2])** (Cf Appendix I; Section I.1)

([2]) Again, it should be observed that the line defined by the in situ stress $\tau_o(x)$ actually constitutes an asymptote to the curve $\tau(x)$ - the point x, defined by the differential $(\tau_x - \tau_{o,x}) = 0$ being theoretically located at an infinite distance from the location of N_i. This difficulty is overcome by locating origo (i.e. x = 0) at a point where $(\tau_x - \tau_{ox})$ has a defined, but negligible value.)

The up-slope boundary condition is therefore that N_x has to be equal to the additional force N_i at the upper limit of the presumptive slide.
In the critical condition $\mathbf{N_x = N_i = N_{cr.}}$

Step 1b Equation 4:1 gives the value of $\Delta N_1 = N_1$ in terms of Δx_1.
Step 1c Equation 4:3 yields the corresponding value of the displacement δ_{N1}, while $\delta_{\tau 1}$ is computed from Equation 4:4a.
Step 1d The value of Δx_1 is then obtained by the compatibility criterion (Equation 4:5), which is solved with respect to Δx_1
Step 1e ΔN_1 may then be computed from Equation 4:1 and δ_N from Equation 4:3.
Step 1f The analyzed section is then advanced a distance of Δx_1, i.e. $x_2 = x_1 + \Delta x_2$.

Step 2 From this point and on, the calculation proceeds by repeating steps 1a) to 1f) for each vertical element and by advancing in steps of suitably chosen values of $\Delta\tau$ and Δx. The values of δ_N and δ_τ can then be expressed in terms of the assumed values of $\Delta\tau$ and Δx, and the correlating values of Δx and $\Delta\tau$ in each iterative step cycle have to be found by iteration so that the compatibility equation 4:5 is satisfied, i.e.

$\delta_N = \Sigma_o^x(\Delta\delta_N) = \delta_\tau$ (Eq. 4:5)

The computation procedure is further demonstrated in Section 4.4 as well as in the practical example given in Appendix I. (Cf also Bernander, (2008), appendices A, B and C.)

4.4 *Exemplification of the numerical procedure for a calculation step involving one slope element of length Δx*

The objective in this section is to demonstrate the method of solving Equations 4:1 to 4:6 using an iterative procedure. The calculations may appear prohibitively laborious, but it should be realized that using computers, the time required to perform the computational work is insignificant.

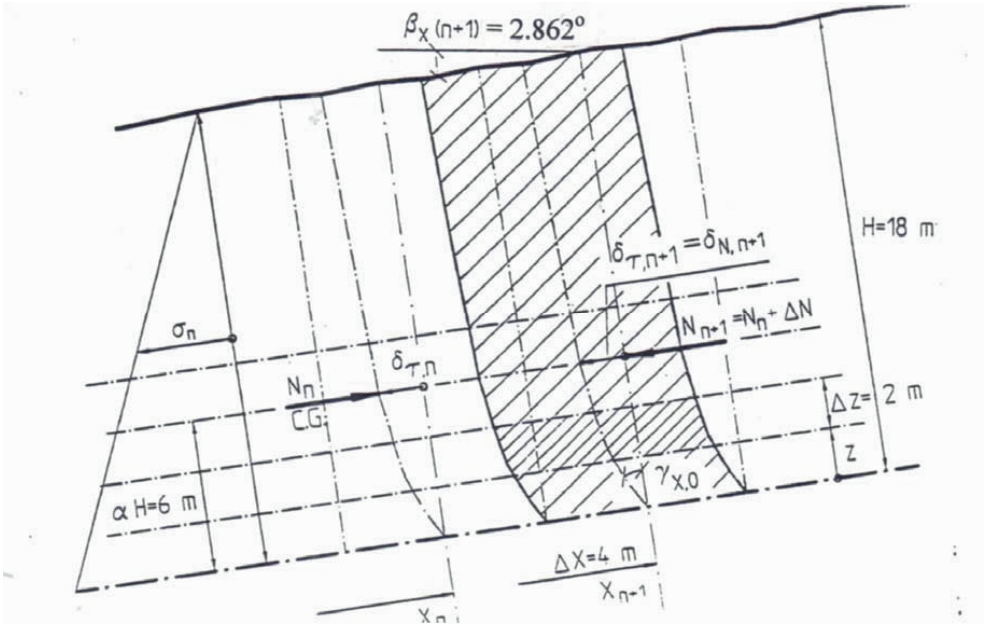

Figure 4:4.1 Section of the slope being analyzed in the example.

Assumed data in the current exemplification:

$\rho \cdot g$ = 15.5 kN/m^3 $K_{o,n} = K_{o,n+1} = \sigma_h/\sigma_v \approx$ constant $\therefore\ \Delta E_o/\Delta x \approx 0$

H = 18.0 m b = 1 m $\beta_n = \beta_{n+1} = 2.862$ °

q(x) = 0 t(x) = 0

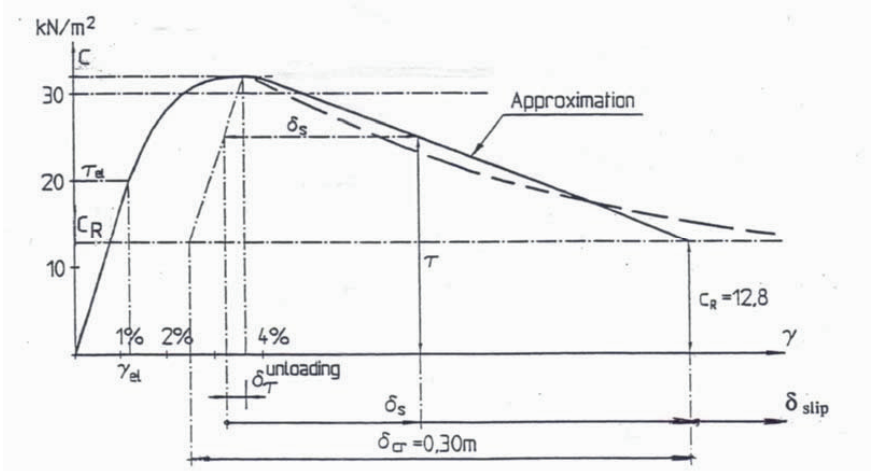

Figure 4:4.2 Constitutive shear stress/deformation relationships. It may be noted that the ratio of τ_{el}/c is assumed to be constant when c_u varies with the coordinate (z). Cf also Section 3.6.
(Note: The parabolic relationship to the power of 2 between τ_{el} and c, which is used here only for practical reasons, may be substituted for any other desired relationship, deemed appropriate by the investigating engineer. However, the issue has little impact on the essential results of the analysis.)

4.41 Constitutive relationships:

The general constitutive relationship $\tau_{x,z} = \phi\,(\gamma_{x,z}, \delta_F, d\delta_F/dt)$ in Equation. 4:6, may in the range $0 < \gamma < \gamma_f$ be defined by the inverse expression $\gamma_{x,z} = \phi_1\,(\tau_{x,z})$ ……4:6a

Assumed data in the current example are ($\nu = 0.5$):

$c_{z=o}$ = 32 kN/m^2 c_R/c = 0.40 τ_{el} = 20 kN/m^2 $G_{el,o}$ = 1333 kN/m^2

$c_{surface}$ = 16 kN/m^2 γ_f = 3.3 % γ_{el} = 1.50 % $E_{el,o} = 125 \cdot c_u$ = 4000 kN/m^2

c_{mean} = 24 kN/m^2 $E_{el,mean} = 125 \cdot c_{u,mean}$ = 3000 kN/m^2 ($E_{el} = G_{el} \cdot 2(1+\nu)$)

Elastic range.

In the range $0 < \gamma_{x,z} < \gamma_{el}$ (for $0 < \tau_{xz} < \tau_{el}$), the relationship between shear stress and deviator strain is taken to be linear.

$\tau_x = G \cdot \gamma_x$ or $\gamma_x = \tau_x / G$ ……Eq. I:1

$\mathbf{\Delta\gamma_{x,z} = \Delta\tau_{x,z} / G}$ ……Eq. I:1a

where $G = \tau_{el}/\gamma_{el}$ (τ_{el} and γ_{el} denote shear stress and shear strain at the elastic limit as defined in Figure 4:4.2)

Non-linear range $\gamma_{el} < \gamma_{x,z} < \gamma_f$

In the non-linear range, where $\gamma_{el} < \gamma_{x,z} < \gamma_f$ (i.e. for $\tau_{el} < \tau_{x,z} < c$), the relationship between shear stress and deviatory strain is taken to be a 2nd power parabolic relationship with its vertex in Point (γ_f,c) and sloping τ_{el}/γ_{el} at the elastic limit as shown in Figure 4:4.2.

As derived in Appendix I, Equation I:4 then applies:

$$\mathbf{\Delta\gamma_{x,z} = (\gamma_f - \gamma_{el}) \cdot [[1 - (\tau_{0(n),z} - \tau_{el})/(c - \tau_{el})]^{1/2} - [1 - (\tau_{x,z} - \tau_{el})/(c - \tau_{el})]^{1/2}]}$$ ..…….. Eq. I:4

where $\tau_{x(n),z}$ and $\tau_{x(n+1)z}$ denote the shear stresses in elements (n) and (n+1).

In the *transition range* between linear and non-linear behaviour, the combined expression in equation I:4a is valid.

$$\mathbf{\Delta\gamma_{x,z} = (\tau_{el} - \tau_{0(n),x})/G + (\gamma_f - \gamma_{el}) \cdot (1 - [1 - (\tau_{x,z} - \tau_{el})/(c_u - \tau_{el})]^{1/2})}$$ ……Eq. I:4a

4.42 Calculation procedure

In this particular example, the ratio of $\tau_{el}(z)/c(z)$ is kept constant. However if necessary, each individual element may in principle be attributed its own specific properties. In the interval $x_n \rightarrow x_{n+1}$, the slope angle and the depth to failure surface are unchanged, i.e. $\Delta E_o(x)/\Delta x = 0$.

Assume that in the course of the preceding computation, i.e. in Step No **(n)**, the following results have been obtained at location $x = x_n$.

Results from Step **(n)**:

$x = x_n$ $\tau_o,(x_n)$ = 13.93 kN/m^2 N_x =126.9 kN/m H = 18 m

$\tau\ (x_n)$ = 24.50 kN/m^2, $\delta_N = \delta_\tau$ = 0.03827 m

Step (n+1) Advance x by Δx = 4 m, i.e. $x_{n+1} = x_n + 4$ m

Applying Equation 4:2:

$\tau_o(x_{n+1}) = H \cdot g \cdot \rho \cdot \sin\beta(x) - \Delta E_o(x)/\Delta x = 18 \cdot 15.5 \cdot \sin(2.862°) + 0 = 13.93$ kN/m^2

Iteration No 1: Try $\mathbf{\Delta\tau = 3.0}$ kN/m^2 $\rightarrow$ $\tau_x\,(x_{n+1},o)$ = 27.5 kN/m^2

$\Delta N = [\,(\tau(x_{n+2},o) + \tau(x_n,o))/2 - \tau_o,(x_n)] \cdot b \cdot \Delta x =$

$= [(27.5+24.5)/2 - 13.93] \cdot 4$ = 48.28 kN/m …(Eq. 4:1)

$N_{n+1} = N_n + \Delta N$

= 126.9.0 + 48.28 = 175.18 kN/m

$\Delta\delta_N$ = (126.90 + 48.28/2)·4/3000/18 = 0.01119 m ….(Eq. 4:3)

$\boldsymbol{\delta_N}$ = $\sum\Delta\delta_N$ = 0.0.03827 + 0.01119 = **0.04946** m

Note: 4/3000/18 is the same as 4/(3000·18)

Proceed to calculate $\boldsymbol{\delta_\tau}$ in Table 4:4.1 according to Equation 4:6a (i.e. Eq.I:1a, I:4 or I:4 a in Appendix I). As $\tau_o(x_{n+1},z) < \tau_{el}$, Equation I:4a is valid in this step. τ_o and τ vary linearly with z.

Table 4:4.1 x = x_{n+1} , $\boldsymbol{\Delta\tau}$ **= 3.0** kN/m^2

z (m)	$\tau_o(x_{n+1},z)$	$\tau(x_n,z)$	$\Delta\tau$	$\tau(x_{n+1},z)$	$\Delta\gamma_z\cdot10$ (Eq.I:4a)	Δz	$(\Delta\gamma_{z=n}+\Delta\gamma_{z=n+1})/2\cdot\Delta z$ (Mean value)
0	13.93	24.50	3.000	27.500	0.1153	0.9	
0.9	13.24	23.28	2.865	26.140	0.1093	0.9	0.01010 = $(\Delta\gamma_{z=o}+\Delta\gamma_{z=o,9})/2$
1.8	12.54	22.05	2.730	24.780	0.1035	0.9	0.00958 = $(\Delta\gamma_{z=o,9}+\Delta\gamma_{z=1,8})/2$
2.7	11.84	20.83	2.595	23.420	0.0980	0.9	0.00907
3.6	11.15	19.60	2.460	22.060	0.0926	0.9	0.00858
4.5	10.45	18.38	2.325	20.700	0.0874	0.9	0.00810
5.4	9.75	17.15	2.190	19.340	0.0822	0.9	0.00763
6.0	9.29	16.33	2.100	18.429	0.0789	0.9	0.00486

$\delta_\tau = \Sigma_o^{1/3H}\Delta\gamma_{x,z}\cdot\Delta z$ = **0.05791 m**

Result from iteration No 1:

$\boldsymbol{\delta_\tau}$= 0.05791 m > $\boldsymbol{\delta_N}$ = 0.04946 m ……. (Eq. 4:5)

Hence, Equation 4:5 is ***not*** satisfied. Try another value of $\Delta\tau$.

Iteration No 2: Try $\boldsymbol{\Delta\tau}$ **= 1.0** kN/m^2 → τ_x (x_{n+1},o) = 25,5 kN/m^2

ΔN = [(25.5+24.5)/2 – 13.93]·4 = 44.28 kN/m …… (Eq. 4:1)

N = 126.9 + 44.28 = 171.18 kN/m

$\Delta\delta_N$ = (126.90+44.28/2)·4/3000/18 = 0.01104 m …… (Eq. 4:3)

δ_N = $\sum\Delta\delta_N$= 0.03827 + 0.01104 **= 0.04931** m

Repeat calculation of $\delta_{\tau\ such}$ as in Table 4:4.1 using Equation I:4a for a value of $\Delta\tau$ = 1.0 kN/m^2.

Table 4:4.2 (not shown) will for $\Delta\tau$ = 1.0 kN/m^2 and Δx = 4 m render a value of $\delta_\tau = \Sigma_o^{1/3H}\Delta\gamma_{x,z}\cdot\Delta z$ = **0.04747** m

Hence, the result from iteration No 2 is:

$\boldsymbol{\delta_\tau}$ = 0.04747 m < $\boldsymbol{\delta_N}$ = 0.04931 m ……(Eq. 4:5)

Yet, Equation 4:5 is still ***not*** satisfied. Try another value of $\Delta\tau$ by proportioning between previous results.

Interpolation indicates that a value of $\Delta\tau$ = 1.378 may be appropriate.

Iteration No 3: Try $\boldsymbol{\Delta\tau}$ **= 1.378** kN/m^2 → τ_x (x_{n+1},o) = 25.878 kN/m^2

ΔN = [(25.878+24.5)/2 – 13.93]·4 = 45.04 kN/m …… (Eq. 4:1)

N = 126.90 + 45.04 = 171.94 kN/m

$\Delta\delta_N$ = (126.90 + 45.04/2)·4/3000/18 = 0.01107 m …… (Eq. 4:3)

δ_N = $\sum\Delta\delta_N$ = 0.03827 + 0.01107 **= 0.04934** m

Proceed to calculate δ_τ in Table 4:4.3 using Equation I:4a:

Table 4:4.3 $x = x_{n+1}$, $\Delta\tau$ = 1..378 kN/m^2 → $\tau_x\,(x_{n+1},o)$ = 25.878 kN/m^2

z (m)	$\tau_o(x_{n+1},z)$	$\tau(x_n,z)$	$\Delta\tau$	$\tau(x_{n+1},z)$	$\Delta\gamma_z \cdot 10$ (Eq.I:4a)	Δz	$(\Delta\gamma_{z=n}+\Delta\gamma_{z=n+1})/2\cdot\Delta z$ (Mean value)
0	13.93	24.50	3.000	25.878	0.0969	0.9	
0.9	13.24	23.28	2.865	24.591	0.0924	0.9	0.00852 = $(\Delta\gamma_{z=o}+\Delta\gamma_{z=o,9})/2$
1.8	12.54	22.05	2.730	23.304	0.0879	0.9	0.00811 = $(\Delta\gamma_{z=o,9}+\Delta\gamma_{z=1,8})/2$
2.7	11.84	20.83	2.595	22.017	0.0835	0.9	0.00771
3.6	11.15	19.60	2.460	20.730	0.0792	0.9	0.00732
4.5	10.45	18.38	2.325	19.443	0.0750	0.9	0.00694
5.4	9.75	17.15	2.190	18.156	0.0708	0.9	0.00656
6..0	9.29	16.33	2.100	17.294	0.0680	0.9	0.00418
					$\delta_\tau = \Sigma_o^{1/3H}\Delta\gamma_{x,z}\cdot\Delta z =$		**0.04934 m**

Result from iteration No 3:
δ_τ = 0.04934 m = **δ_N = 0.04934** m Equation 4:5 is satisfied.

Hence, the final results from step No (n+1), i.e. from **x = x_n** to **x = x_{n+1}** are:
$x_{n+1} = x_n + 4$ m $\tau_o,(x_n)$ = 24.500 kN/m^2 N_x = 171.93 kN/m
$\tau\,(x_{n+1})$ = 25.878 kN/m^2, $\delta_N = \delta_\tau$ = 0.04934 m

More information is given in Appendix I.

4.5 ***Objectives and overall procedures for performing stability investigations according to Section 4.*** (For more detail, cf Chapter 11.)

In Figure 4:2.4a, the principal parameters derived from the computations are shown. The down-slope force N_x denotes, as already mentioned, the earth pressure increment that may not be exceeded at the section defined by the coordinate x, lest the displacements induced by the force N_x propagate beyond the starting point ($x \approx 0$) of the calculations.
N_x will, therefore, assume different values depending on the extent to which, as defined by the point of reference x = 0, the resistance down-slope of N_x is mobilized. Hence, any chosen portion of the slope may be analyzed for any selected failure plane.

The different stages and limiting conditions in a downhill progressive landslide have been detailed in Chapter 3, according to which the analysis must focus especially on the two possible states of equilibrium, i.e. before and after the virtually dynamic redistribution of earth pressures (Phase 3) due to progressive failure development.

Another vital outcome of the proposed analysis is the possibility of establishing the initial earth pressure and stress conditions that, as suggested in Section 11.32 can be studied as an extremely slow progressive failure using the method presented in this section.

4.51 Safety criteria with regard to locally triggered failure
The limiting critical value of the force N_i, induced by the agent initiating local slope failure, may be defined by N_{cr}, as shown in Figure 3:3.3. The value of N_{cr} is computed by finding the position of the reference point (x = 0), rendering a value of $\tau_{x,} = c_{Rx} = \tau_{o,x,}$ at z=0,
i.e. when $\boldsymbol{\tau_{x,(z=0)} - \tau_{o\,x,(z=0)}} = 0$ at the location of N_i.
This necessitates a procedure of combined 'trial and error' and interpolation.

Although potential failure planes are often given by the soil structure, alternative failure planes may – as in conventional slope stability analysis – have to be investigated. Once the minimum value of N_{cr} at the location of the force N_i has been established, the safety factor against local failure may be expressed as:

$$\mathbf{F_s^I = N_{cr} / N_i < 1} \qquad \text{…....(Eq. 3:8, cf Section 3)}$$

or, if the additional loads (q and t) shown in Figures 4:2.1 and 4:2.2 are also considered,

$$\mathbf{F_s^I = (N_i,q,t)_{cr} / (N_i,q,t) < 1} \qquad \text{…….(Eq. 3:8a, cf Section 3)}$$

where $(N_i, q, t)_{cr}$ denotes a critical combination of the additional loads along the slope.

If the safety criterion, defined by Equation 3.8, is not satisfied, i.e. if $N_i \geq N_{cr}$, a dynamic phase (Phase 3) is triggered. However, as demonstrated in Chapter 3, a new state of equilibrium – at least a transient one – is then possible.

4.52 Criteria with regard to global slope failure

If, for some reason, local slope failure does in fact occur, the ensuing progressive failure results in the virtually dynamic transfer of unbalanced up-slope forces to more stable ground further downhill as is for instance illustrated in Figures 3:3.4 & 4:5.1.

At this point in the analysis, the reference point (x = 0) is defined by a boundary condition requiring that the computed value of N_x must be equal to $F_s^I \cdot N_i = N_{cr}$ precisely at its point of action, (F_s^I being the required safety factor in respect of local failure.).

Again, this exercise constitutes an iterative process of the kind mentioned above.

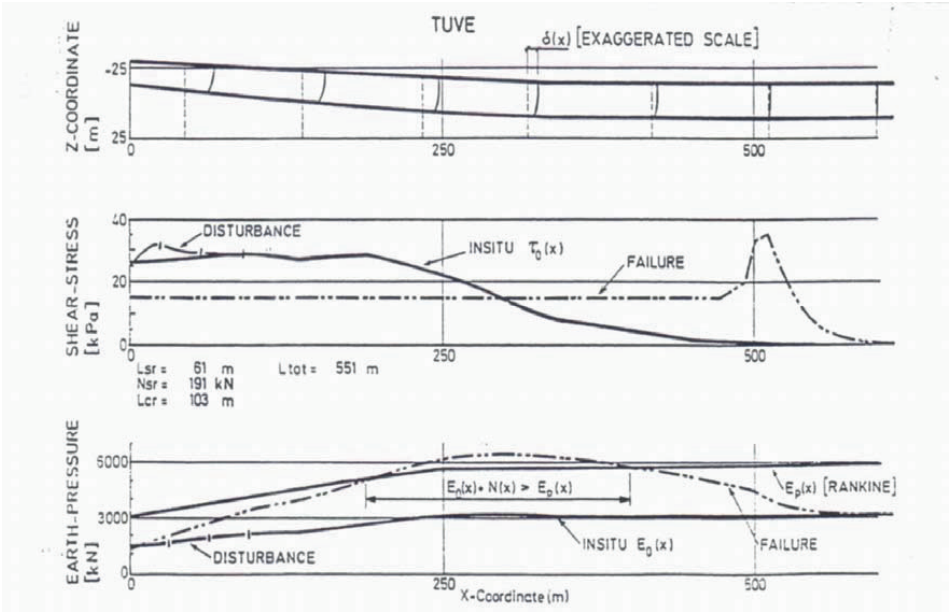

Figure 4:5.1 Graphic display from a computer analysis of the 'post-progressive' stage of equilibrium based on a ratio of $c_R/c_u = 0.42$. In this case – actually the Tuve slide – passive Rankine resistance is exceeded already by the static forces in the virtually horizontal ground, entailing extensive global slope failure. (Bernander et al, 1979 →1989).

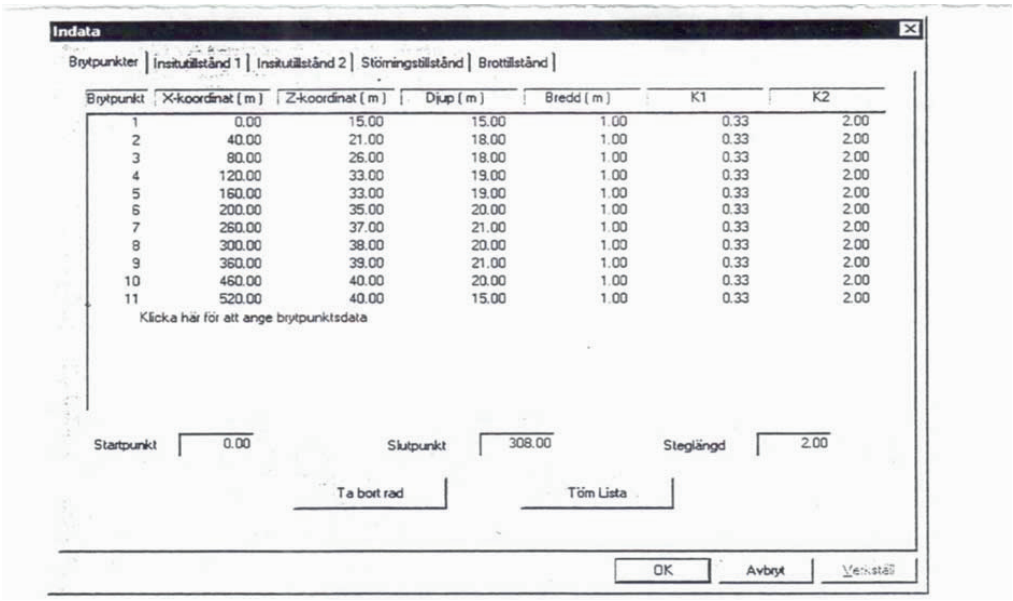

Figure 4:5.2 Table showing showing options and some of the main in-put data in the present version (2000) of computer software developed in 1984.

The critical condition to be satisfied in the *'post-dynamic'* state of equilibrium, lest global failure take place, is then (according to Sections 3.32 & 3.34):

$$F_s^{II} = E_p / (E_{ox} + N_x)^{max} > 1 \qquad \text{……..(Eq. 3:9)}$$

or

$$F_s^{II} = [(1 - K_o)\cdot\gamma\cdot H^2/2 + {}_o\int^H 2\cdot c_u(z)\cdot dz] / N_x^{max} > 1 \qquad \text{……..(Eq. 3:9a)}$$

Hence, the vital condition is that passive earth pressure resistance may not be exceeded anywhere in (or beyond) the lower part of the slope.

4.53 Computer programs

As mentioned, the presented calculation method involves iterative procedures, which make manual calculations very laborious. However, this problem is readily overcome using computers. Once input data have been installed, the time needed to carry out the numerical computations according to Equations 4:1 to 4:6 is insignificant.

Computer software following the outlines given above was prepared at the Department of Design and Engineering at Skanska West AB (Gothenburg) as early as in 1980. However, an improved two-dimensional version was developed in 1984. An updated version of the 1984 software in Windows C++ has been available since June, 2000.

Several studies of existing and failed slopes were carried out already in the 1980:s. In two cases of the long natural slopes investigated, preventive measures were taken in order to ameliorate safety with special regard to the risk of progressive failure formation.

Computer software in the form of an Excel spread sheet was established in 2005. Although applicable to arbitrary slope conditions, this software is more practicable for slopes with simple geometry, i.e. with constant inclination and depth to the failure surface.
The spread sheet is well suited for educational purposes.
(Cf Bernander (2008), Appendices A, B & C.)

4.6 *Conclusions*

The proposed model for studying downhill progressive failures in natural slopes has – in practical applications – proved to be a useful tool for evaluating in situ stresses, the additional effects of superimposed loading, as well as for assessing the conditions governing potential slope failure in markedly deformation-softening clays.

In any specific scenario, the stress/strain response of the soil may be related to the time scale of the current load increment, thus enabling studies of the stress conditions in stable slopes as well as in potentially unstable slopes in the different phases of progressive failure development – i.e. in the Phases 1- 6 as per Section 3.32.

It is of particular interest that the analysis makes it possible to study the long term in situ distribution of earth pressures and shear stresses, yielding values of the inter slice forces and of K_o ($= \sigma_h/\sigma_v$), a parameter on which engineers engaged in soil stability problems have focused their interest for decades. (Cf e.g. Janbu's method of constant stress levels, 1979).

The critical length (L_{cr}) corresponding to the critical load $N_{cr,}$ indicates in some measure the maximum length of a slide, that can be studied on the basis of 'ideal-plastic' soil properties with any prospect of attaining reasonable accuracy.
The fact, that there is a limit to the distance downhill of a local load, along which additional shear stresses can be fully mobilized, has another crucial implication. At a length of L_{cr} from a local load, the effects of loading no longer exist in terms of stress, earth pressure and deformation. (Cf e.g. Figure 4:6.1.)
In a short term perspective, this circumstance rules out or effectively limits the possibility of exploiting earth pressure resistance in less sloping ground further downhill for the purpose of stabilizing a local up-slope loading.

The implication of not being able to utilize available support in terms of passive resistance further down the slope is of decisive importance for another reason. The failure resistance along planes oriented along the slope of the firm base – or along firmer sedimentary layers – may, depending on the degree of deformation-softening and depth to failure plane, be radically less than that derived for slip circles surfacing in sloping ground closer to the additional local load.
(Cf Figures 4:6.1 & 4.6.2.)

$$N_{cr}^{BD} = {}_o\int^{Lcr} (\tau_x - \tau_o)\cdot dx \;<< E_p^{BC} - E_o \approx (1- K_o)\cdot\gamma\cdot H^2/2+2\sqrt{(1+c_a/c)}\cdot H\cdot c^{mean} \text{ (kN/m)}$$

Hence, short failure planes and slip circles – i.e. situations in which plastic failure analysis may still be valid (e.g. as discussed in Section 2.2.) – rarely represent the most critical failure modes in long slopes of deformation-softening soil.
The disparity between PrF- and I-PlF-analyses may even be more pronounced in varved clays, as excess pore water pressures are more likely to spread along sedimentary layers than across (or at some angle to) the same.

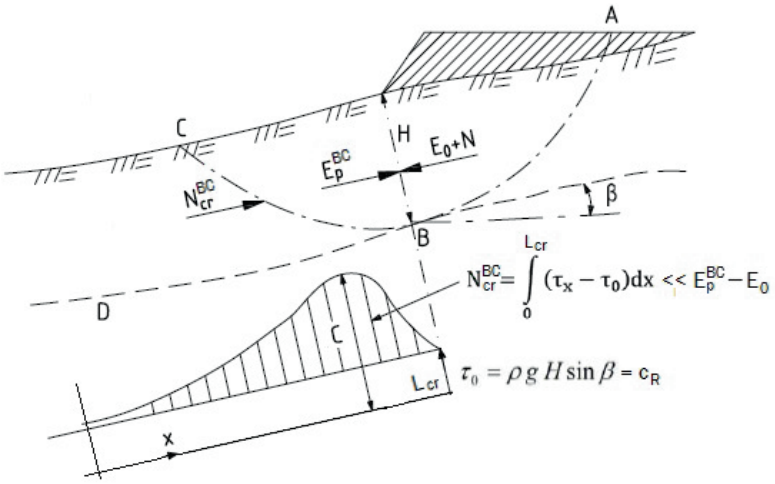

Figure 4:6.1 Maximum passive earth pressure that can be mobilized along the failure plane BD if deformations are considered. Note that, depending the depth (H), $\mathbf{N_{cr} << E_p^{BC} - E_o}$. (Bernander 1981)

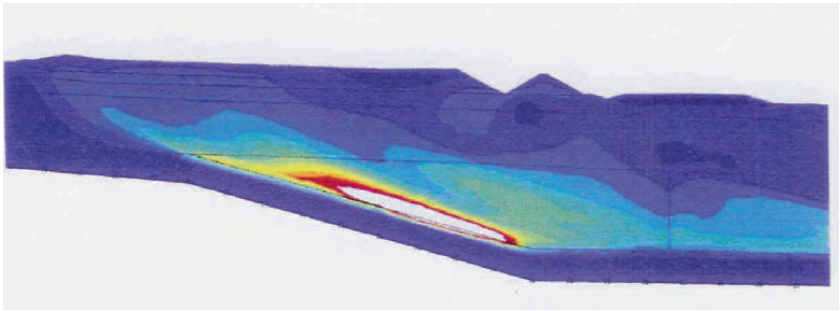

Figure 4:6.2 Illustration of how the failure zone tends to develop downhill along steeply inclining firmer soil layers. Analysis according to FEM, PLAXIS by Gustav Grimstad. From the Report, regarding the slide at Småröd (December 2006), of the Independent Investigatory Group of the Swedish Road Administration, IIG-SNRA (2007).

Figure 4:6.2 illustrates ostentatiously the tendency to failure propagation along inclining firm layers that is typical in deformation softening soils.

It may be noted that the described downhill evolution of stress and deformation also applies to higher values of the brittleness ratio (c_R/c). In fact, according to the FDM-analysis, the issue actually applies initially even in the ideal-plastic failure state, when deformations are considered.
The case records listed in Table 5:8.1 (Section 5) bear witness of the acute risk of potential disaster related to placing fills and embankments in up-slope areas, where the inclination of the ground surface and/or firm bottom are likely to generate high mobilization of local shear resistance. Consequently, considering deformations and deformation-softening in slope

stability assessment generally results in a considerably higher computed risk of slope failure than what emerges from the conventional ideal-plastic approach.

Progressive failure development in natural slopes is liable to take place for wide variation (within reason) of chosen constitutive relationships. The cardinal issue in this context is whether, or not, the conditions in the slope are such that a local disturbance agent is susceptible of inducing a critical degree of deformation-softening in a potentially vulnerable zone in the soil mass. Common disturbance agents are additional earth deposits, imposed deformation and vibration (e.g. due to piling and compaction), and extreme excess pore water pressure regimes.
These circumstances should be taken into account whenever soils exhibiting markedly deformation-softening behaviour are encountered.

Deformations below the potential failure plane
The proposed FDM-model for analysis of progressive downhill slope failure enables consideration of deformations below the assumed failure plane. However, as mentioned above, passive resistance further down-slope cannot possibly be mobilized at a distance greater than L_{cr} for stabilization local additional loads. This condition implies that failure planes primarily tend to develop in the direction of the firm bottom gradient, sometimes even to great depth below the ground surface. E.g. in the about 500 m long main slide in Tuve, the failure zone roughly followed firm bottom down to about 35 m below the ground surface ahead of the foot of the slope.
There is, therefore, often no particular need for considering deformations below the slip surface, which is why the computer program, referred to in Section 4.5, addresses this issue only in an approximate way.

In this computer program, the shear deformations below the slip surface may be taken into account as follows:
1) Referring to Figure 4:2.2, the shear deformation in the failure zone below the assumed potential slip surface is defined for soil columns of length Δx along the slope.
2) The effect of the additional shear deformation can then be accounted for by modifying the shear deformations in the failure zone above the potential failure plane by an amplification factor based on item 1) above. The value of this factor is then included in the set of in-put data for the computer program. Denoting the deformations above and below the potential failure surface $\delta_{\tau,o}$ and $\delta_{\tau,u}$ respectively, the factor to be inserted is taken as $(\delta_{\tau,u}+ \delta_{\tau,o})/ \delta_{\tau,o}$. (Cf Section 4.7 below.)

Final remarks
The analysis of progressive failure described in this section may appear complicated to practicing geotechnical engineers but is in fact very relevant and necessary considering the significantly increased landslide hazard related to additional local loading in slopes with clays of high sensitivity, and with adverse geometrical features.
The constitutive relationships of sensitive soils therefore have to be defined by special consideration of the rate of application of additional loads, time factors and drainage conditions in the incipient failure zone that are likely to initiate a progressive landslide.

Yet, complexity of analysis must be balanced against the imperative of making valid predictions of risk in terms of human life, property, social and economic values.

As can be concluded from the exemplifications in Section 4.4 and Appendix I, manual calculation may, although quite possible, be considered as being too laborious and impracticable for slopes with complex arbitrary geometry. However, computer analyses like the ones referred to in Section 4.5 render the results of the various mathematical expressions in almost no time. As mentioned, once the appropriate in-put data have been entered into the computer program – referred to in Figure 4:5.1 – the time required to carry out a complete study of a loading case is insignificant.

The additional effort devoted to slope stability investigations along these lines consists, therefore, only to a minor extent of increased computational work. The major challenge lies in exploiting the enhanced possibilities of identifying the effects on slope stability of a number of factors that by definition cannot be obtained using the conventional ideal-plastic failure approach.
It is of course imperative that appropriate input data are introduced, which requires experience in geology and soil mechanics in general. Adequately detailed field investigations, providing necessary information, are a prerequisite.

Future Research and development
It is important to note that many of the parameters needed for the analysis of brittle slope failures are not subject to routine investigation procedures in the present State-of-the-Art of Soil Mechanics, and are therefore not sufficiently well known or adequately defined. Future research in this field of geotechnical engineering is thus a vital issue.

4.7 *Alternative presentation of the FDM-approach defined in Sections 4.1 through 4.4*

4.71 Basic principles – **Stage I**
The model presented in the previous sections can also be described and explained structure-mechanically as follows:
1) In Figure 4:7.1, ABCD represents a plane slab in a state of equilibrium – at first only subjected to the prevailing in situ shear stress conditions defined by the curve for $\tau_{0,z}$

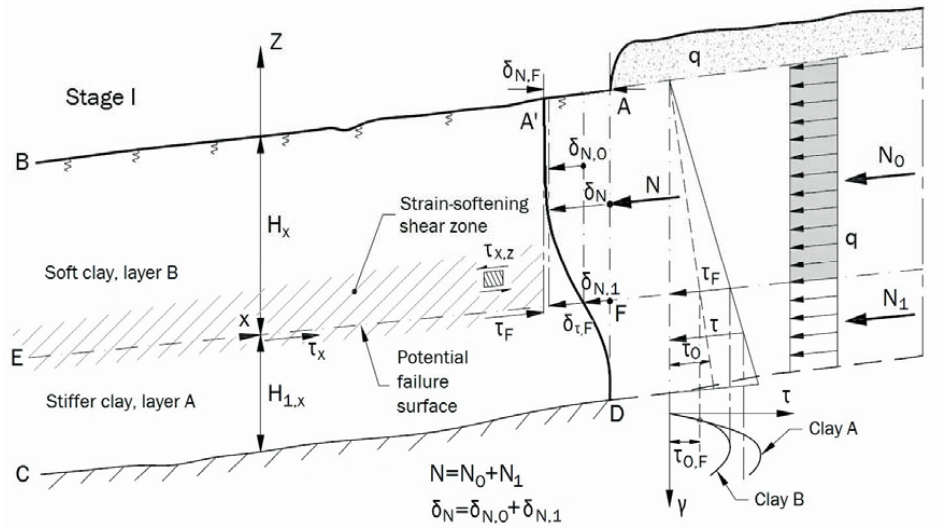

Figure 4:7.1 Figure illustrating an alternative presentation of the basic concept for the FDM-analysis of progressive slope failure according to (Bernander 1988, 1989, 2000).

2) A cut is made along line EF dividing the slab in two separate parts ABEF and FECD. However, existing in situ stresses in the cut surfaces (actions and reactions) are maintained, which means that the in situ state and the effects of existing restraint remain unchanged despite the hypothetical separation into two plane structures.

3) Apply the forces N_0 and N_1 (due to the load q) acting on the upper and the lower halves respectively of the split plane structures. Owing to restraint from the lower slab (FECD), the effect of the axial force N (in terms of N_x in slab ABEF) decreases in the downhill direction. In a similar way, the influence of the force N_1 abates in the lower slab FECD.

The distribution of the axial force in the upper slab can be defined as a function N_x and the related mean axial deformation in slab ABEF is $\delta_N(x) = {}_o\int^x N_x/(E_xH_x)\cdot dx$, giving a value of $\delta_{N,F}(L) = {}_o\int^L N_x/(E_xH_x)\cdot dx$ at Point F where x = L.
The corresponding mean axial deformation in the lower slab FECD can be defined as $\delta_{N,1}(x) = k_x\cdot{}_o\int^x N_1(x)/(E1_xH_{1,x})\cdot dx$, where the reduction factor k_x represents the restraining effect of firm bottom. Hence in general, the relative differential deformation between the two slabs $\delta_{N,F,}(x)$ along line EF to be considered consists of the difference between the mean deformations in the upper and lower slabs, i.e.
$\delta_N(x) - \delta_{N,1}(x) = {}_o\int^x N_x/(E_xH_x)\cdot dx - k_x\cdot{}_o\int^x N_1(x)/(E_{1,x}\cdot H_{1,x})\cdot dx$

For failure surfaces closer to firm bottom, the value $\delta_{N,1}(x) = k_x\cdot{}_o\int^x N_1/(E_{1,x}\cdot H_{1,x})\cdot dx$ tends to become insignificant. In the case shown in Figure 4:7.1, k_x may be set at about 1/3. **([3])**
Thus, if for instance, $H_{1,x}/H_x = 1/10$, $k_x = 1/3$ and $E_1/E = 1{,}5$ the ratio $\delta_{N,F}(L)/\delta_{N1,F}(L) \approx 1/45$, implying that the deformations below the potential failure surface can be neglected in many instances. This applies especially in the upper parts of a slope – i.e. in the zones, where progressive failure is most likely to be triggered.
Hence $\boldsymbol{\delta_N(x) \approx {}_o\int^x N_x/(E_xH_x)dx}$ ……Eq.4:8
and $\delta_{N,F} \approx {}_o\int^L N_x/(E_xH_x)dx$

([3]) The assumed value of k_x is therefore normally of minor importance in the current context.

4) If the two slabs are then reconnected along Line EF, vertical continuity is re-established by the differential shear deformations $\delta_{\tau,x}$ generated by the shear stresses $\tau_{x,z}$, whereby the difference in displacements between the upper and the lower slabs along line EF are compensated by elastic and - in particular - strain-softening shear deformations in the lower parts of slab ABEF and, normally, to less extent in the upper portions of slab FECD.

5) Equilibrium demands that at all times ${}_o\int^x (\tau_x - \tau_{o,x})\cdot b_x\cdot dx = N_x$ …… Eq.4: 9

Continuity demands that at all times $\delta_N(x) - \delta_{N,1}(x) = \delta_{\tau,x}$ **([4])** …….…… Eq.4:10

A boundary condition at Point F is ${}_o\int^L (\tau_x - \tau_{o,x})\cdot b_x\cdot dx = N$

Equilibrium also demands that ${}_o\int^H [\tau_{z,(FA)} - \tau_{o,z\,(FA)}]dz = N = q\cdot H$ ……. Eq.4:11

([4]) The axial deformation $\delta_{N,x}$ which is based on the E-modulus of the undisturbed soil mass is not greatly affected by the shear stresses resulting from the strain-softening behaviour of the soil in the highly sheared zone.

The shear/deformation relationships for Clays A and B in Figure 4:7.1 illustrate the conditions leading to the formation of a shear zone subject to intense strain softening. Once a strain softening zone of this kind has begun to form, it will inexorably progress

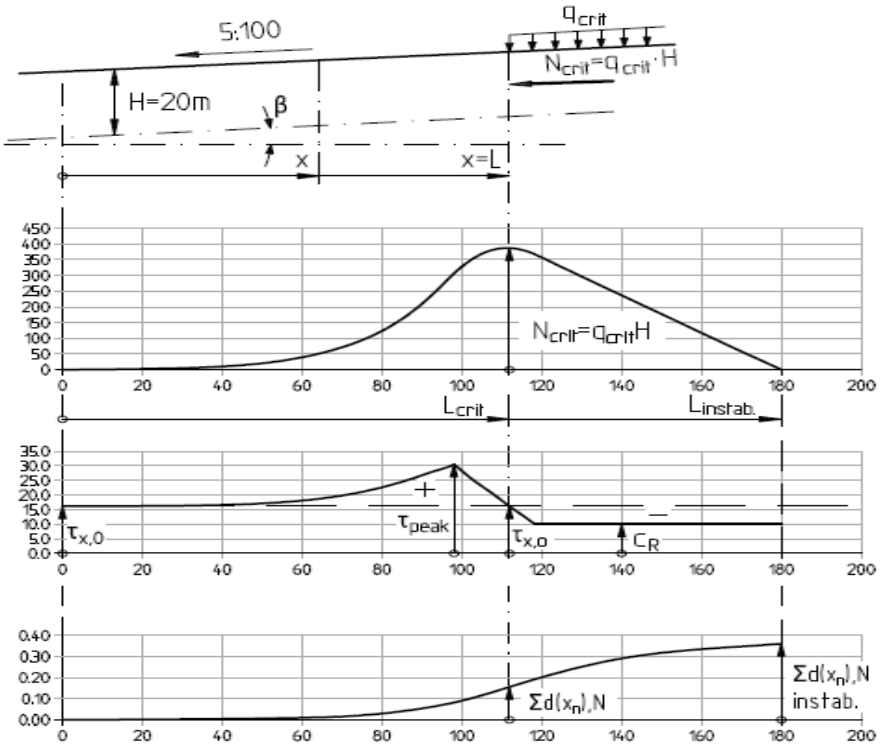

Figure 4:7.2 Results from progressive failure analysis showing the critical triggering load $N_{cr} = q_{cr} \cdot H$, the critical length (L_{cr}) and critical deformations in a slope. c = 30 kN/m^2, $c_R/c = 0.333$.

down-slope as loading is increased - i.e. the prospects of a new failure zone developing along another soil stratum being virtually zero. (Cf Figures 4:6.1 & 4:6.1.)

An approximate compensation for the loss of axial stiffness in slab ABEF, due to the plasticization of the failure zone, can be made by suitable adjustment of the E-modulus of the undisturbed soil mass. However, analyses performed indicate that this issue is of minor significance in progressive failure formation on account of the considerable strain softening in the failure zone. The approximation seems justified considering the uncertain character of many other parameters used in slope stability analysis. Sensitivity studies made on this issue corroborate this statement. (Cf comments in Section 4.26 regarding Case b.)

4.72 Basic principles – **Stage II**

A crucial feature in the FDM-approach presented in this document is distinguishing between two radically different conditions of stress and deformation – i.e. the Stages I and II.

In Stage II, the down-slope axial displacement corresponds to the accumulated deformation due to shear strain and slip in the failure surface. Equation 4.10 then becomes:

$\delta_N(x) - \delta_{N,1}(x) = \delta_{\tau,x} + \delta_{slip}$ ……Eq. 4.12

δ_{slip} is not shown in Figure 4:7.1

5. Case records – downhill progressive landslides

The following section deals with case records of downhill progressive landslides mainly from south western Sweden, all bearing the characteristics of progressive failure formation. The substance of the presentation will focus on features indicating that mechanisms related to deformation-softening have governed the initiation, the development and the final ground configuration of the slides.
The progressive nature of many of these slides is corroborated by application of the FDM-analysis presented in Sections 3 and 4 of this document.

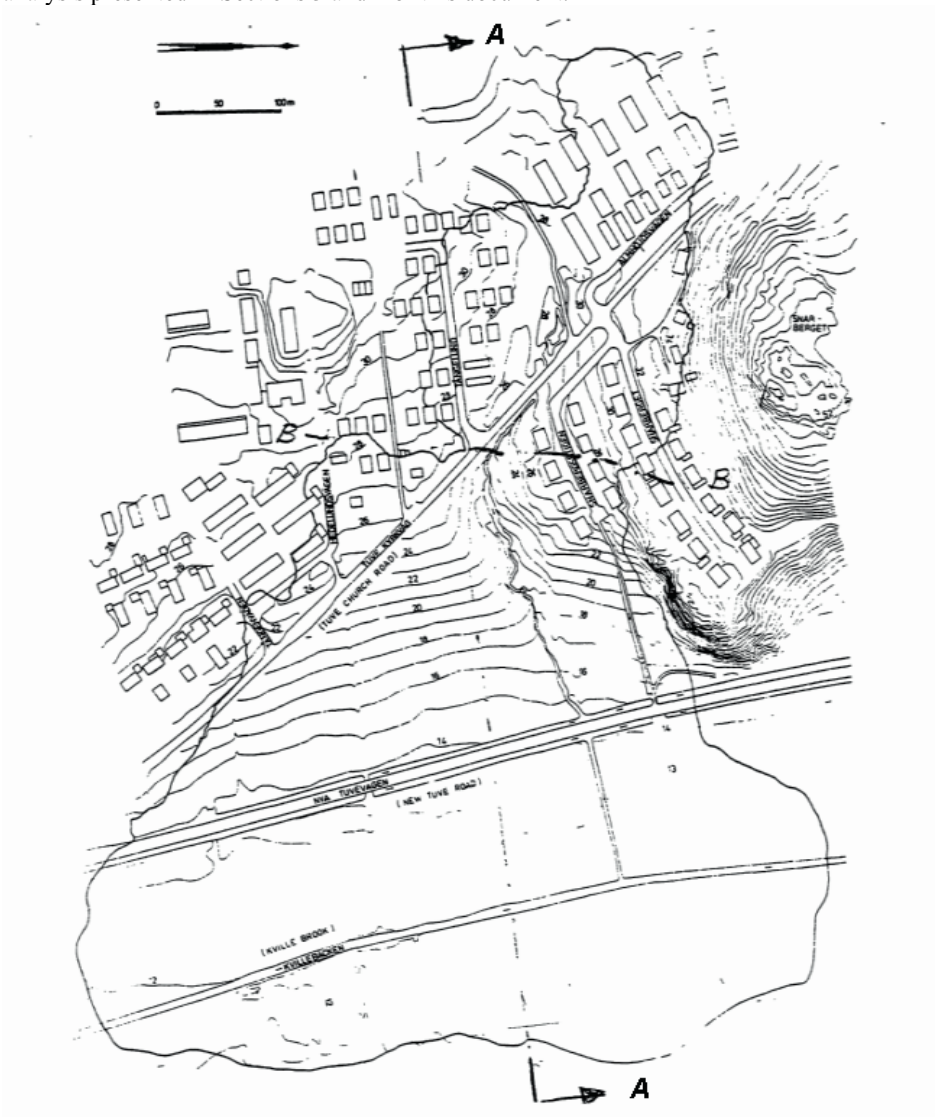

Figure 5:1.1 The landslide at Tuve, 1977. Topography of the valley before the slide and boundaries of the slide area.

The case records also serve to illustrate the shortcomings of analyses based on the concept of 'limit state plastic equilibrium', substantiating the need for more relevant methods of of predicting slope stability in highly deformation-softening soils – e.g. such as the one described in Section 4.
The official explanations of most landslides, including the famous ones in Surte (1950) and Tuve (1977) were, in the opinion of the author, incomplete and/or inconclusive.
For instance, the post-slide investigations did not – in terms of current structure-mechanical methodology – explain the fact that in both slides vast areas of horizontal or gently sloping ground were massively deformed in plastic failure down to great depth. In Surte about 14 hectares of ground were 'plasticized' to a depth of some 20 m. In Tuve, the corresponding numbers were 16 hectares and 35 m respectively. Both of these slides are examined in this section.
The conditions in Tuve, related to slope stability, have many basic features in common with those in the closely situated site of the Surte landslide, (1950) – i.e. in respect of geological history, slope characteristics and soil properties. Reference is therefore made to Section 5.2.

5.1 *The landslide in Tuve (1977), Sweden*

The landslide in Tuve, a community near Gothenburg, took place on the 30th of November, 1977, just after four o'clock in the afternoon – i.e. at a time that must have reduced the death toll significantly since people had not yet returned from work or from school. In all, the slide resulted in nine deaths, the total destruction of 65 family houses and a drastic change of the topography of some 270 000 m^2 of ground. Settlements in the active zone of about 10 m and horizontal displacements up to 200 m were recorded. Upheaval in the passive zone of about 5 m over a distance of about 300 m was noted.

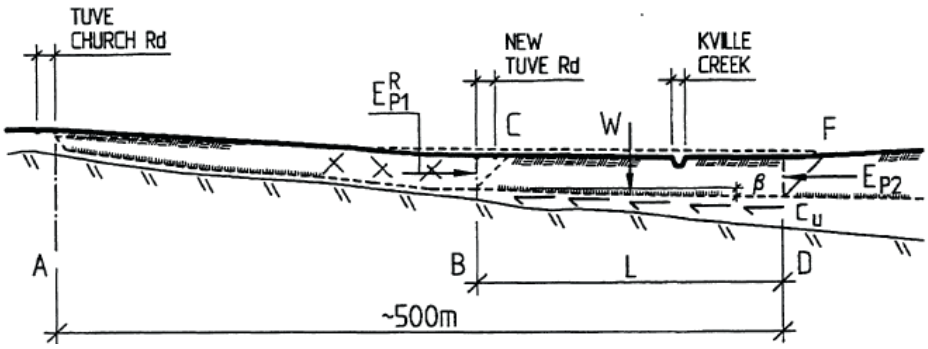

$c_{u(e)} = 0.12 \cdot \sigma_c$' (Empirical shear strength as assumed in SGI Report No 18)
$E_{p1} << R_{BDF} = \int_0^L c_{ux} \cdot b_x \cdot dx - w \cdot \sin\beta + E_{p2}$ Vert. scale = 2 x hor. scale
E.g. for $\beta = 0$, $b_1 = 400$ m, $b_2 = 600$ m and $L = 270$ m
For H = 20 m, $E^{Rankine} \approx 1520$ MN $<< R_{BDF} \approx 4560$ MN $F_s = 4560/1520 \approx 3.0$
H = 35 m, $E^{Rankine} \approx 4520$ MN $<< R_{BDF} \approx 10655$ MN $F_s = 10655/4520 \approx 2.4$

Figure 5:1.2 Section through the main slide. (Distorted vertical scale). - Forces required to provoke plastic failure over the valley floor according to I-PlF analysis. ($c_{u(e)} = 0.12 \cdot \sigma_c$'). From Bernander & Olofsson I, (1981). b_1 and b_2 denote the width of the slide at Points B and D.

The total length of the slide, i.e. including after-slides, was about 800 m. Two main phases could be identified, namely an initial slide event encompassing the ground east of line B-B in Figure 5:1.1 and a secondary retrogressive stage covering the area west of line B-B. The initial slide is presumed to having been triggered by a local instability in the steepest portions of the slope, i.e. near and up-slope of the Tuve Church road.
The length of the main slide measured some 500 m with a maximum width of the passive zone of about 600 m. According to SGI Report No 18, the main slide "occurred suddenly and the events that followed took place in rapid succession". The total duration was estimated to approximately 5 minutes.
A striking feature, which may be seen on the aerial photograph (Figure 5:1.3) is that about 60 % of the area engaged in the main slide consists of a passive upheaval zone extending over almost horizontal ground ahead of the foot of the slope. As the slip surface under the valley floor was found to be situated at a depth of about 35 m below ground surface, this means that more than 5 500 000 m^3 were virtually 'plasticized' in a state of passive failure. The force required to bring about a condition of this kind amounts to some 12 000 kN/m - i.e. in total 6,6 million kN. It is evident that any mode of failure analysis, not explaining the generation of forces of this magnitude, is simply not applicable to the prediction of slide hazard.
Referring to the discussion in Section 2.4 regarding the relationship between the features of a finished slide and insufficient plasticity of the soil, it must be concluded that the development of the Tuve landslide is bound to have been governed by highly deformation-softening soil properties.

Nevertheless, SGI Reports No:s 18 & 11a explain the Tuve slide only in terms of ideal-plastic failure analysis (I-PlFA). Assuming normal growth of shear resistance with depth, safety factors of 2.0 to 2.3 (un-drained analyses) and 2.6 (drained analysis) were initially presented. (Cf Figure 5:1.4).

Figure 5:1.3 Aerial photograph of the Tuve slide.

However, as these results failed to explain why the slide actually occurred, further stability investigations were focused on what was termed 'empirical shear strength, which meant applying the lowest alternative of drained and un-drained shear strengths to zones in active and direct shear. This empirical strength is here denoted as $c_{ue)}$, (where the letter 'e' signifies 'extension').
Thus, by taking the un-drained shear strength from direct shear tests (i.e. CK_oU-DSS tests according to the terminology of Ladd & Foot, 1974) as low as $c_{u(e)} = 0.12 \cdot \sigma_c$', safety factors of about 1.0 to 1,13 were obtained for slip surfaces, ranging in length from 80 to 180 m, and which were located in the upper third of the area involved in the main slide.
(Cf Figure 5:1.5).

Yet, this approach raises a number of questions, which were discussed in more detail in a critical study of Chapters 11 and 12 of SGI Report No 18. (Cf Bernander, 1983).

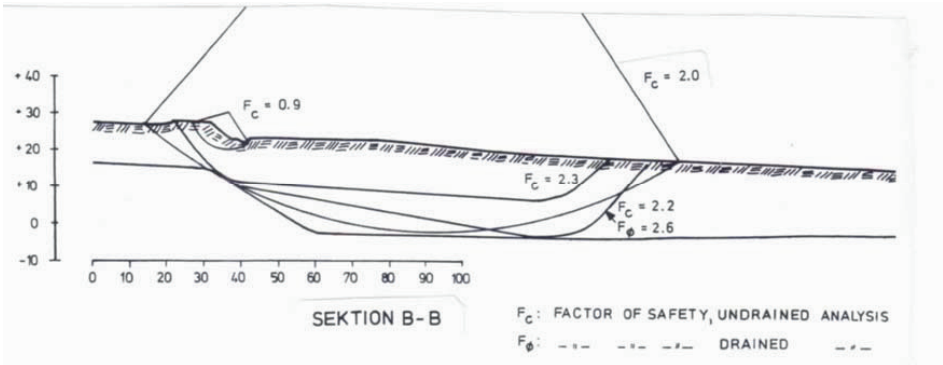

Figure 5:1.4 Results from stability calculations for a section through part of the 500 m long main slide assuming normal increase of shear strength with depth. (From SGI Report No 18, 1982).

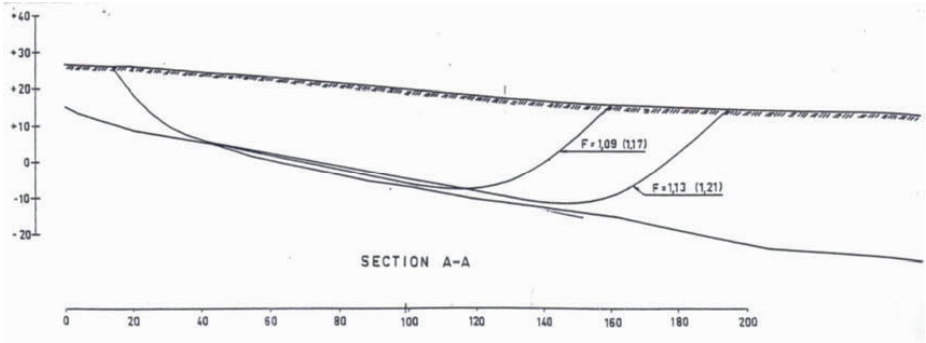

Figure 5:1.5 Results from stability calculations for a section through part of the 500 m long main slide (Section A-A in Figure 5:1.1) assuming 'empirical shear strengths' in the deep layers of silty clay. Bulk density of the clay was 16 – 19 kN/m^2. (From SGI Report No 18, 1982).

For one thing, it is questionable whether direct un-drained shear tests are representative of the actual conditions on the Tuve site, where the stress range from the in- situ state to the failure condition were likely to be quite different. (See Figure 5:1.6).

Hence, there is no adequate compatibility between these two cases of loading, as there are important differences between the principal stresses, drainage conditions and the stress paths in the two cases.
For instance, the soil material in the in-situ condition is, in reality, pre-consolidated for an effective normal stress state (σ'_1, σ'_3) corresponding to the prevailing shear stress τ_o in the slope. The stress range from τ_0 to shear failure (i.e. $\tau_0 < \tau < c_{u(e)}$) is very different from the stress range in the DSS-tests, where the shear stress varies from zero to a peak value, (i.e. $0 < \tau < c_{u(e)}$).
In addition the soil in the slope structure may be pre-consolidated for a somewhat different K_o-value than the test samples depending on where in the slope a sample originates.

In tests carried out at Skanska's geotechnical laboratory in Gothenburg, the difference in shear strengths between consolidated un-drained CK_oU-DSS tests and tests that may be denoted as consolidated 'pre-sheared' un-drained (CK_oPU-DSS) tests was measured. For clay with a liquid limit of 50 % and $\tau_o = 0.10 \cdot \sigma_c'$– roughly representative of the conditions in the failure zone of the Tuve slide – the following results were recorded:
$c_{uI} = 0.18 \cdot \sigma_c'$ and $c_{uII} = 0.26 \cdot \sigma_c'$, i.e. $c_{uII}/c_{uI} = 1.44$. (Cf Figure 5:1.6)

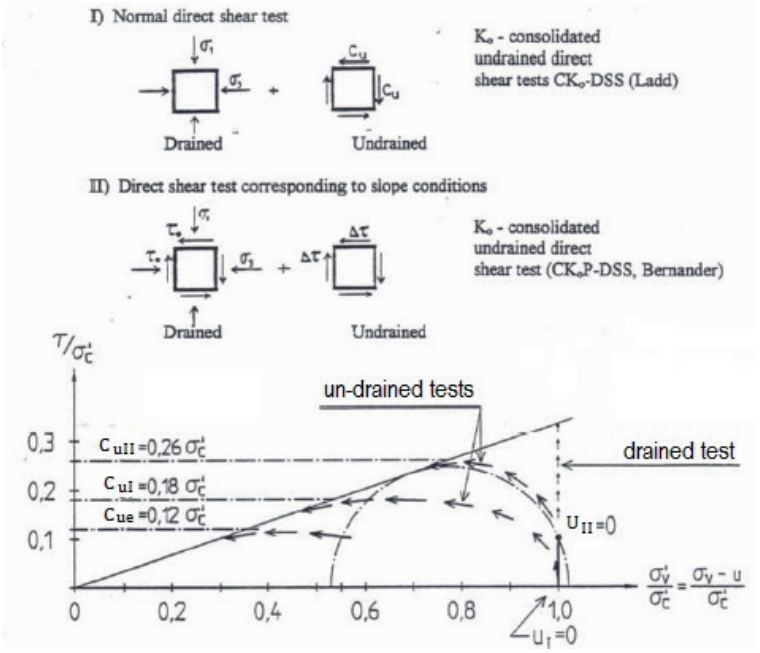

Figure 5:1.6 Difference between results from normal CK_oU-DSS tests and 'pre-sheared' CK_oPU-DSS tests. The latter tests would correspond more to the states of stress in the soil of the macro structure when loaded to failure.

Another indication that a value of $c_{u(e)} = 0.12 \cdot \sigma_c'$ may be an over-conservative assumption is that it corresponds to slope gradients in the range of 1:40 (2,3°) to 1:35 (2,83°), mainly depending on the density of the normally consolidated soft clays involved.

Considering that most natural slopes in glacial clays contain seams of sands, silts and clays with low plasticity, few of them would be able to stand steeper than 2 to 3 degrees with a safety factor equal to 1. In reality this is not the case.

The reasoning above implies that the safety factors related to the slip surfaces, which were identified as being critical according to SGI reports, may actually have been in a range between 1.4 and 1.5 instead of about 1. If that is the case, the role in the main slide of the slip surfaces shown in Figure 5:1.5 – involving only about a third of the length of the initial main slide – still remains unexplained even on the basis of the applied I-PlFA approach adopted in the SGI reports No:s 18 and 11a.

Another very important question that may be raised in this context is whether the strain rates used in the laboratory tests performed are really compatible with the long-time in situ state in combination with the differing rates of stress change prevailing during ongoing slide events. This is especially relevant when considering the effects of drainage conditions in the initial stages of a slope failure, as well as for the assessment of the likely extension of global failure.

5.11 The Tuve slide explained in terms of progressive failure

Yet, there is no doubt that the steepest up-slope portions of the main slide (close to Tuve Church Road) had low factors of safety in terms of conventional plastic failure analysis, as was also presumed by SGI. This condition was also documented by Sällfors, (1979, 1981) and Bernander & Olofsson, (1981).

Regarding spread of the slide over the valley floor

However, even accepting the low so called 'empirical shear strength' of $c_{u(e)} = 0.12 \cdot \sigma_c$', attributed to the silty clays in SGI Reports No 18 and No 11a, there is no explanation as to why most of the area, actually involved in the slide, consisted of virtually horizontal ground. Admittedly, Chapter 11 of the report No 18 contains some verbal reference to the possibility of progressive failure and dynamic effects, but in this respect there is no quantitative analysis or structure-mechanical explanation related to the vast spread of the slide over the valley beyond the foot of the slope proper.

It is, for instance, not consistent, as in Report No 18, to assume unlimited plastic properties in the soil, and then simultaneously explain paradoxical phenomena in the slide by referring to dynamic effects, that are not accounted for or quantified. If the computed safety factors in the order of $F_s \approx 1$ (shown in Figure 5:1.5) are to represent any physical reality, it follows that the sensitive lean clays in the failure zone – considering the inexorable downhill deformations in the extensive, potentially sliding soil mass – possessed unlimited plasticity.
This means in turn that, as demonstrated in Section 2.4, the enormous build-up of forces and kinetic energy required to generate the approximately 300 m long passive zone, have not been accounted for.
The vast spread of the slide over horizontal ground must therefore be attributed to brittle failure resulting from deformation-softening and due progressive failure mechanisms.

The numbers shown in Figure 5:1.2 indicate for instance that, applying conventional plastic failure analysis, the main slide could not possibly propagate beyond point C (the New Tuve Rd). This is due to the simple fact, that the passive Rankine resistance (E_{p1}) at point B only amounts to a small fraction of the resistance R_{BDF} along the failure plane BDF if the analysis is based on unlimited plastic clay properties.

Notably, this would apply even if the low shear strength of $c_{u(e)} = 0.12 \cdot \sigma_c$' were valid. Hence, Figure 5:1.2 suggests that the event that actually occurred, could not possibly take place according to conventional I-PlF-analysis, and that with 'safety margins' ranging from 2.4 to 3.0.

In conclusion, the Tuve slide raises serious doubts with regard to the application of ideal-plastic limit equilibrium methods (I-PlFA) for predicting the risk of failure in long slopes of sensitive soils.
Significant deformation-softening of the soil must have governed the main slide, being triggered by local instability in the steepest portions of the slope – i.e. near and up-slope of the Tuve Church Road. (Cf Bernander & Olofsson, (1981), SGI Report No 10 and Bernander, (2000.)

Progressive failure analysis of the Tuve slide
Progressive failure analysis of the Tuve slide has been performed according to the principles outlined in Section 4 in this document. The analysis corroborates many of the remarkable features of the slide, especially the spread over large areas of level ground, and the related plasticization of the soil mass to great depth. Referring to Figure 4:4.2, the in-put data given below were used in the computer analysis, from which some of the results are shown in Tables 5.1.1 to 5.1.3 and in Figure 5:1.7.

In the in situ state condition: (i.e. Phase 1 according to Sections 3.32 & 3.33)
$c_R/c_\infty = 1.00$ $\gamma_{el} = 2.5\ \%$ $\gamma_f = 7.5\ \%$, $G_o = \tau_{el}/\gamma_{el} = 480\ kN/m^2$
c_∞ * $= 24 \rightarrow 30\ kN/m^2$, $\tau_{el} = 12\ kN/m^2$ $E_o = 2(1+\nu)\ G_o = 3G_o \approx 1440\ kN/m^2 = 60\ c_\infty$
$K_o = 0.55$ $\tau_{el}/c_\infty = 0.5$ $E_{el,mean} = 60\ c_{\infty,mean}$
$\rho \cdot g = 16.5\ kN/m^3$
Note: In all calculations in Chapter 5, the curved portion of the constitutive relationship from γ_{el} to γ_f is a function of x^n with vertex at (c_u , γ_f) and connecting tangentially at (τ_{el} , γ_{el}).

In the disturbance condition: (i.e. Phase 2 according to Sections 3.32 & 3.33)
(Case No 4 from top in Table 5.1.2 below)
$c_R/c = 0.60$ $\gamma_{el} = 2\ \%$ $\gamma_f = 4.67\ \%$, $\delta_{cr} = 0.3$ m, G_o* $= \tau_{el}/\gamma_{el} = 810\ kN/m^2$
$c = 27$* $\rightarrow 33$** kN/m^2 $\tau_{el} = 16.2\ kN/m^2$ $E_{el,o} = 3G_o = 90 \cdot c \approx 2430\ kN/m^2$
K_o *** $\tau_{el}/c = 0.6$ $E_{el,mean} = 90\ c_{mean}$

In the global failure condition: (i.e. Phase 4 according to Sections 3.32 & 3.33)
(Case I in Table 5.1.3 below)
$c_R/c_u = 0.1 - 0.4$ $\gamma_{el} = 1\ \%$ $\gamma_f = 2.0\ \%$, $\delta_{cr} = 0.3$ m, G_o** $= \tau_{el}/\gamma_{el} = 2000\ kN/m^2$
$c_u = 30$* $\rightarrow 40$** kN/m^2, $\tau_{el} = 20\ kN/m^2$ $E_{el,o} = 3G_o \approx 6000\ kN/m^2$
K_o *** $\tau_{el}/c_u = 0.677$ $E_{el,mean} = 200\ c_{u,mean}$

* Mean values applying to the initiation zone. ** Mean values applying to the down-slope failure zone. *** As computed in the in-situ condition

It may be observed that shear strengths and E-moduli are varied along the slope in relation to the current mean shear strength of the soil profile.
In the disturbance condition, the shear deformations in the failure zone have been taken to be largely one-sided in relation to the incipient failure plane, which in the higher parts of the slope tends to follow the gradient of firm bottom.

However, at global failure, these deformations have been assumed to be symmetrical in relation to the potential failure plane in the parts of the slide area, where the depth to firm bottom is bigger than the depth from ground surface to the failure plane.

Table 5.1.1 ***The Tuve slide – results from PrF-analysis***

L indicates the extent of soil mass involved in the current failure condition and denotes a distance measured from the upper end of the slide, (or from the point of application of critical load. (Cf Figure 4:2.4a.)

The situ state condition: (Phase 1*)*

$c_R / c_\infty = 1.0$ $N_{max} = 671$ kN/m $L = 240$ m $E_o = 4169$ kN/m, $K_o = 0.64$

($\delta_{creep} = 6$ m) $\tau_{el}/c_\infty = 0.5$

Critical disturbance condition a) in Phase 2 – *Force initiated failure* Cf Section 3)

$c_R / c = 0.60$ $N_{cr} = 75.8$ kN/m $L_{cr} = 91.2$ m $E_x = 2572$ kN/m at $x = L_{cr}$

$\delta_{cr} = 0.055$ m $\tau_{el}/c = 0.6$

Critical disturbance condition b) in Phase 2 – *Deformation-initiated failure.*
(Cf Section 3.35)

$c_R / c = 0.60$ $N_{cr} = 0$ kN/m $L_{instab} = 135$ m* $E_x = 3025$ kN/m at $x = L_{instab}$

$\delta_{instab} = 0.105$ m $\tau_{el}/c = 0.6$ * (As defined in Figure 4:2.4a)

The in situ state condition – (Phase 1)
In the steepest part of the slope, available shear strengths do not match the in situ shear stress in terms of the joint effect of slope and gravitation, i.e. $\tau_o = \rho \cdot g \cdot H \cdot \sin\beta$. According to Equation 4:2 (Section 4) this implies that in the in situ condition the soil masses were shored up by incremental earth pressures in less inclined ground further down the slope, i.e. K_o increasing from 0.55 to (maximum) 0.64. See Table 5.1.1 and Figure 5:1.7.

Disturbance condition – *Force-initiated failure* – (Phase 2)
One of the main implications of applying the FDM-analysis according to Section 4 to a slope like the one in Tuve is that the length over which shear stresses and deformations can be induced by local load effects (N_i) is limited. (Cf. Section 4.6.)
The vital consequence of this is that, due to the fact that the deformations related to $N_i = N_{cr}$ in this case do not materialize beyond the distance of $L_{cr} = 91.2$ m down-slope of the load, passive resistance there cannot be utilized for balancing the additional local load N_{cr}, even in the state of impending progressive failure.

This means in fact that the progressive failure approach to analysing the stability of long slopes eliminates profiting from support related to potential passive resistance further downhill. This applies in particular to an extensive slope such as the one in Tuve, measuring at least 300 meters, and where the soils were very sensitive in the upper parts.

For instance, the implication of the plastic failure modes shown in Figures 5:1.4 and 5:1.5 is full exploitation of down-slope passive resistance balancing the forces that initiated the main slide in the steep part near the Old Tuve Church Road. The computed safety factors, based on the I-PlF-analysis, indicated in Figures 5:1.4 & 5:1.5 are therefore not likely to be relevant.

The assessment of the load effect (q_{cr}), capable of initiating local failure, is of course radically affected by the limitations mentioned. The weight of fill required to provoke progressive slope failure applying the methods outlined in Section 4 is generally much less than that computed using conventional short slip circles surfacing in the sloping ground. E.g. according to Table 5.1.1, the critical load (N_{cr}) sufficient to initiate local failure in the steepest part of the slope, only amounts to 75.8 kN/m.

Although the Tuve slide is not believed to have been brought about solely by the weight of an applied fill, it may still be of interest to observe that – assuming fully un-drained conditions in the disturbance phase – the value of N_{cr} merely corresponds to a distributed load on the ground surface (q_{cr}) of about $75.8/17 \approx 4.5$ kN/m^2.
By contrast, ideal-plastic failure analysis, based on local slip surfaces, indicates a corresponding value of $q_{cr} \approx 90$ kN/m^2 – i.e. a disparity between the two modes of analysis that can be expressed in terms of a factor of 20. (Cf. in this context also Figure 5:2.7 related to the Surte slide.)
Hence, according to I-PlF analysis $q_{failure}(min) \approx 90.0$ kN/m^2 (Short slip surfaces) **(1)**
According to Pr F analysis $q_{failure} = 75.8/17 \approx 4.5$ kN/m^2 (Slip surface in the direction of the gradient of firm bottom)

(1) The value of $q_{failure}$ is based on routine laboratory testing of shear strength and not on the extension value $c_{u(e)} = 0.12 \cdot \sigma_c$' adopted in SGI Report No 18.

However, in this context it is vital to consider that, depending on drainage conditions and rates of load application, the residual shear resistance may vary widely. The locally developing failure zone is normally not likely to be fully un-drained. If partial drainage prevails during failure development, the values of N_{cr} can be substantially greater.

Sensitivity study
The effect of varying some of the in-put parameters on N_{cr}, L_{cr}, δ_{cr}, $q_{failure}$ is demonstrated in Table 5.1.2 below. As may be concluded, changing the input parameters as they are defined in the table, the progressive failure approach importantly affects the results of the analysis.

Table 5.1.2 ***The Tuve slide*** *– variation of parameters*

No	c_R/c_u	$E_{el,mean}$ kN/m^2	γ_{el} %	γ_f %	N_{cr} kN/m	L_{cr} m	δ_{cr} m	L_{instab} m	δ_{instab} m	$q_{failure}$ kN/m^2 (PrFA)	$q_{failure}$ kN/m^2 (I-PlFA)
1)	**1.00**	90 c_{mean}	2	4.67	152.0	113	0.094	203	0.244	8.9	90
2)	**0.80**	90 c_{mean}	2	4.67	99.5	100	0.072	175	0.195	6.0	90
3)	**0.70**	90 c_{mean}	2	4.67	84.9	95	0.064	155	0.140	5.0	90
4)	**0.60**	90 c_{mean}	2	4.67	75.8	91	0.055	135	0.105	4.5	90
5)	**0.50**	90 c_{mean}	2	4.67	71.0	89	0.050	124	0.090	4.2	90
6)	**0.40**	90 c_{mean}	2	4.67	67.9	87	0.046	118	0.080	4.0	90
7)	**0.30**	90 c_{mean}	2	4.67	66.1	85	0.043	113	0.075	3.9	90
8)	0.30	**180 c_{mean}**	2	4.67	105.4	131	0.049	180	0.089	7.7	90
9)	0.30	**180 c_{mean}**	**1**	**2.33**	129.0	142	0.035	218	0.070	7.6	90
10)	0.30	**90 c_{mean}**	**1**	**2.33**	90.3	98	0.035	145	0.068	7.6	90

Even so, it is interesting to note that the values of the critical force N_{cr}, the critical length L_{cr} and the critical load $q_{failure}$ are astonishly insensitive to variation of the values of the c_R/c -

ratio, γ_{el} and γ_f. For instance, in the studied case, the magnitude of N_{cr} deviates from its mean value by about – 6 % and + 8 % within a range of c_R /c between 0.3 and 0.6. (Cf Table 5.1.2.)

This is a circumstance that effectively contributes to the viability of progressive failure analysis, when evaluating the risk of local instability in slopes.
However, it may be noted that the disparity between PrF- and I-PlF-analyses highlighted above is valid for wide variation of the pertinent parameters. Even with residual shear strengths as high as c_R = 0.8 c, the critical length L_{cr} is only about 100 m, and the ratio of $q_{failure}$(I-PlFA)$q_{failure}$ to (PrFA) in the order of 10. **(2)** The crucial factor in this context mainly relates to the issue as to whether deformations are taken into account or not.

Moreover, the effects on N_{cr} and L_{cr} of reducing the constitutive parameters by 50 % – i.e. γ_{el} = 1 % instead of 2% and γ_f = 2.33 % instead of 4.67 % - are 36 % and 15 % respectively. (Cf Table 5.1.2, Items 6 and 9).

(2) Note that, as previously defined, $q_{failure}$(I-PlFA) relates to short failure planes surfacing in the slope near to the load – i.e. some 30 m in the case considered.

Conclusion: Despite the fact that the slope in Tuve had been stable over millennia, it was nevertheless, according to the PrF analysis performed, extremely sensitive to additional short-term loading or other disturbance agents inducing un-drained soil behaviour in critical portions of the slope.

Global failure condition – (Phase 4)
Figure 5:1.7 displays the calculated earth pressure distribution, shear stresses and displacements for a slip surface in accordance with boring logs in SGI Report No 18. The figure represents the situation at the end of the progressive redistribution phase, in which unbalanced shear forces in the steeper parts of the slope have been transferred further down-slope, resulting in tremendous build-up of earth pressures further down in the valley.
(Cf Figure 3:3.4 and Figures 5:1.3 and 5:1.7 in this section).

It should be observed that the earth pressures are calculated under the assumption that the potentially sliding soil volume essentially retains its geometrical shape before its possible disintegration in a state of passive Rankine failure. Hence, in cases where the resulting maximum earth pressure E_{max} exceeds $E_{Rankine(max)}$, the computed earth pressure scenario will represent a highly transient situation (Phase 4) that, in a fully developed landslide, shortly merges into the dynamics of the slide proper (Phase 5) as described in Section 3.

The significance of the earth pressure distribution in the transient stage of equilibrium denoted Phase 4 is that it constitutes a measure of the disaster that may ensue if local failure due to additional critical load is triggered in the disturbance condition – i.e. will the progressive failure result in a veritable landslide or not? **(3)**

The computations in *Case I* in Table 5:1.3 are based on residual shear strengths in proportion to the magnitude of displacement in the progressive failure phase, thus varying between $c_R = 0.10\ c_u$ and $c_R = 0.40\ c_u$ in different places along the slope.

(3) As stated in e.g. Section 3.32, no real landside will occur as long as earth pressures in Phase 4 do not exceed available passive resistance.

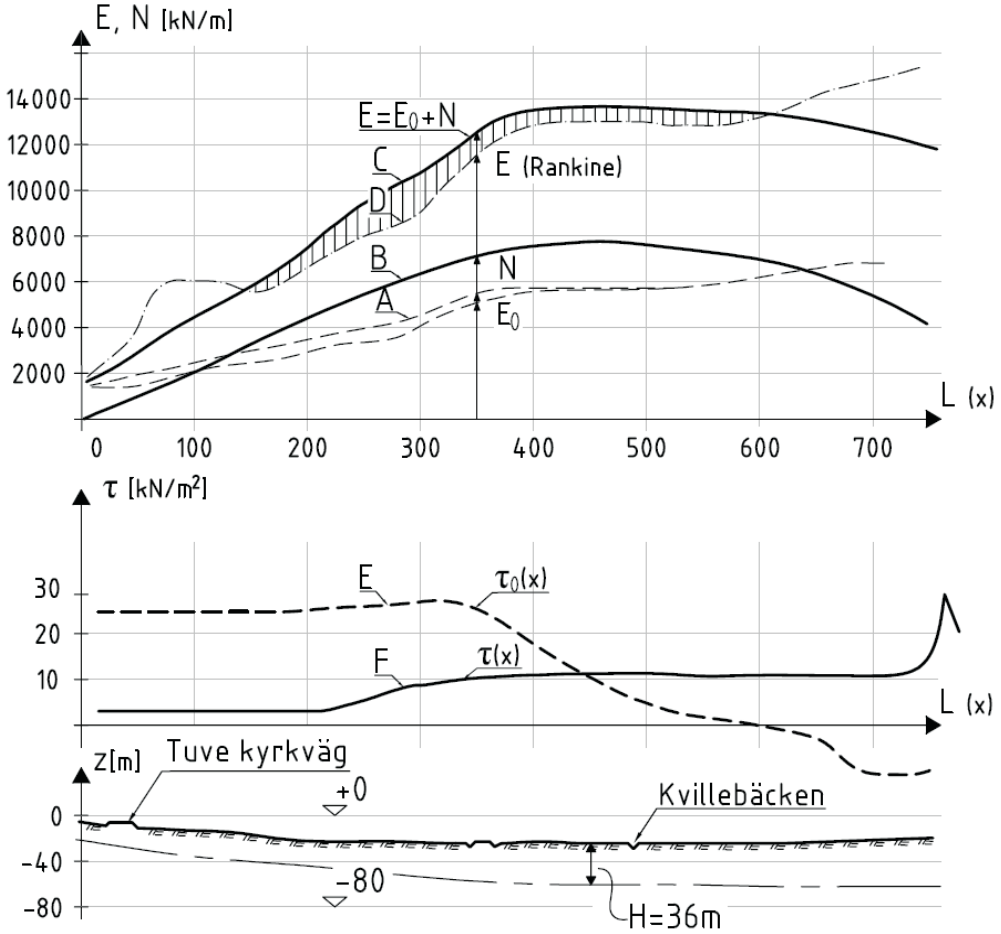

Figure 5:1.7 Static earth pressure distribution in the Tuve slide subsequent to the progressive failure phase but prior to the slide proper resulting in disintegration and heave in passive failure. (Phase 4). ***Case I:*** $\mathbf{c_R / c_u = 0.10\text{-}0.30}$**.** The figure indicates that the spread of the passive zone over almost horizontal ground can be ascribed solely to the static forces developed at the end of the dynamic progressive Phase 3 of the ground movement as explained in Section 3.3.

Curve A, $E_o(x)$ = In situ earth pressure prior to local failure, kN/m
Curve B, $N(x)$ = Earth pressure increment due to Pr F redistribution, kN/m
Curve C, $E(x)$ = $E_0(x) + N(x)$ = Earth pressure after Pr F redistribution, kN/m
Curve D, $E_p^{Rankine}$ = Passive Rankine resistance, kN/m
Curve E, $\tau_o(x)$ = In situ shear stress distribution before progressive failure, kN/m^2
Curve F, $\tau(x)$ = Shear stress distribution after progressive failure, kN/m^2

Table 5.1.3 ***The Tuve slide*** *- results from PrF analysis*
(L = distance from upper end of slide or point of application of critical load)

Global failure condition: - ***Case I***	E_{el}/G = **3**	(*Shown in Figure 5:1.7*)	
c_R/c_u = 0.10-0.40	N_{max} = 9128 kN/m	E_{max} = 15035 kN/m,	$E_{Rankine}$ = 12852 kN/m (varies)
$(E_{Rankine}/E)_{min}$ = 0.85	E_{el} = 200 $c_{u,\,mean}$	L_x = 486 m	$L_{E>E(Rankine)} \approx$ 410 m (4)
Global failure condition: - ***Case II***	E_{el}/G = **3**		
c_R/c_u = 0.20-0.40	N_{max} = 7709 kN/m	E_{max} = 13615 kN/m	$E_{Rankine}$ = 12852 kN/m (varies)
$(E_{Rankine}/E)_{min}$ = 0.944	E_{el} = 200 $c_{u,\,mean}$	L_x = 476 m	$L_{E>E(Rankine)} \approx$ 250 m (4)
Global failure condition: - ***Case III***	E_{el}/G = **3**		
c_R/c_u = 0.30-0.40	N_{max} = 6247 kN/m	E_{max} = 12152 kN/m	$E_{Rankine}$ = 12852kN/m
$(E_{Rankine}/E)_{min}$ = 1.06	E_{el} = 200 $c_{u,\,mean}$	L_x = 456 m	$L_{E>E(Rankine)}$ = 0 m (4)

(4) Length over which passive Rankine pressure is exceeded.

Considering the large deformations and rates of displacement involved already in the progressive phase, these values of c_R were in the evaluations considered to be appropriate for the soft clays at the Tuve site. As shown in Figure 5:1.7, (representing Phase 4), the earth pressures resulting from the redistribution of forces in Phase 3, entail that passive Rankine resistance is exceeded over a length ($L_{E>E(Rankine)}$) of some 450 m in gently sloping ground – i.e. a condition inevitably leading to total disintegration and heave in the lower areas of the slope and the valley, thus initiating the dynamic phase of the landslide proper (Phase 5).

Yet, in the Tuve slide the value of $L_{E>E(Rankine)}$ was actually about 360 m. This implies that, according to the estimates in respect of $L_{E>E(Rankine)}$ given in Table 5.1.3, a more appropriate assumption as regards the values of the residual shear resistances might have been:
c_R = 0.13 c and **c_R = 0.40 c** rather than c_R = 0.10 c and c_R = 0.40 c

Sensitivity studies
The effects of changing the c_R/c_u – ratios from 0.10-0.40 to 0.20-0.40 and to 0.30-0.40 are evident from the figures given in Table 5.1.3 above. Whereas the maximum *static* earth pressure exceeds passive Rankine resistance over a distance of 410 m in *Case I*, this does not occur in *Case III,* signifying that global failure with excessive heave of the passive zone is not likely to take place in the latter case.
The effect on the global failure condition of e.g. doubling the $E_{el,\,mean}/G_o$ – ratio (i.e. reducing the compressibility of the soil mass by 50 %) is rather insignificant. Thus, for c_R/c_u= 0.10-0.40 and $E_{el,mean}/G_o$= 6 instead of 3, the following values result:
E_{max} (max. earth pressure) becomes 13 474 kN/m at L = 456 m instead of 12 852 kN/m, and $L_{E>E(Rankine)} \approx$ 430 m instead of 410 m.
This follows from the assumption that the shear modulus and the modulus of elasticity are interrelated and, importantly, time dependent in a similar way.
Moreover, the effects on N_{cr} and L_{cr} of reducing the constitutive parameters by 50 % – i.e. γ_{el} = 1 % instead of 2% and γ_f = 2.33 % instead of 4.67 % - are 36 % and 15 % respectively. (Cf Table 5.1.2, Items 6 and 9).

Conclusions with regard to the Tuve slide
The progressive failure analysis performed indicates that the upper part of the slope was extremely vulnerable to additional short-term loading and unprecedented disturbance related to human activity of various kinds. The analysis also provides a logical and quantitatively consistent explanation of the vast spread of the slide over almost horizontal ground. Furthermore, the analysis also highlights the fact that landslide displacements in sensitive clay are not confined to its directly visible topographical appearance. The earth movements in the slide direction beyond its apparent down-slope boundary can be considerable, i.e. involving ground several hundreds of meters beyond the visible slide limit – in principle as illustrated in Figures 2:4.2 and 3:3.5. This particular phenomenon is, for instance, documented by the earth movement in Rävekärr described in Section 5.5.
The causes of the Tuve slide are in SGI Report No 11a, (1984) attributed to local disturbance generated by high ground water pressures due to prolonged precipitation in combination with the effects of additional load from a road embankment applied a few years before. Changes in the hydrological regime due to urban development were also believed to have contributed to local instability. The effect of local pore pressure increase related to human activity is exemplified in Section 5.26, Item **a)**.
The progressive failure analysis performed, indicates that disturbances of this nature may very well have been sufficient to trigger the landslide in Tuve.

5:12 Dynamic effects in a progressive landslide like the one in Tuve
With the intent of investigating the dynamic effects in a downhill progressive slide, both qualitatively and quantitatively, a study was carried out at Skanska Engineering Department, Gothenburg. (Cf Bernander & Gustås, 1984).
Although the slope examined was fictitious, the geometry, the mean gradient and the soil parameters were chosen so that they roughly corresponded with the conditions assumed in the mentioned analysis of the Tuve slide by Bernander & Olofsson, (1981).
The dynamic analysis consisted of step by step numerical calculations in the time domain applying Newton's laws of motion. The time interval between the discrete steps in the computations was about 1 second. The results of the investigation proved to be very instructive, and different phases of the slide event were presented as photocopies on a display board. (Cf Figures 5:1.8 to 5:1.17 below).

A selection of these photos were presented as photographic slides in discussions at the Nordic Geotechnical Conference (NGM 84), at the Symposium on Landslides (Toronto, 1984), and in a poster session at the XI th ICSMFE (San Fransisco, 1985). (Cf also Bernander, 2000.)
The photographic representations in Figures 5:1.8 to 5:1.17 depict various stages in a progressive slope failure, eventually resulting in a fully developed landslide. In the figures, escalating earth pressure development is simulated using different shades of yellow, green and black. Hence, earth pressure growth is presented in terms of increasing intensities of yellow → green → dark green → black, where black colour indicates that passive Rankine resistance is exceeded.
The dynamic effects in the active zone as well as on the final spread of the slide can be estimated by comparing the Figures 5:1.15 and 5.1.17.
According to the calculations, the time to failure is about 22 seconds. However, it is conceivable that, in reality, time dependent fracture and disintegration processes prolong the different phases of the slide. This a condition substantially reducing dynamic forces of inertia and kinetic energy, as these parameters are proportional to the square of the rate of displacement.

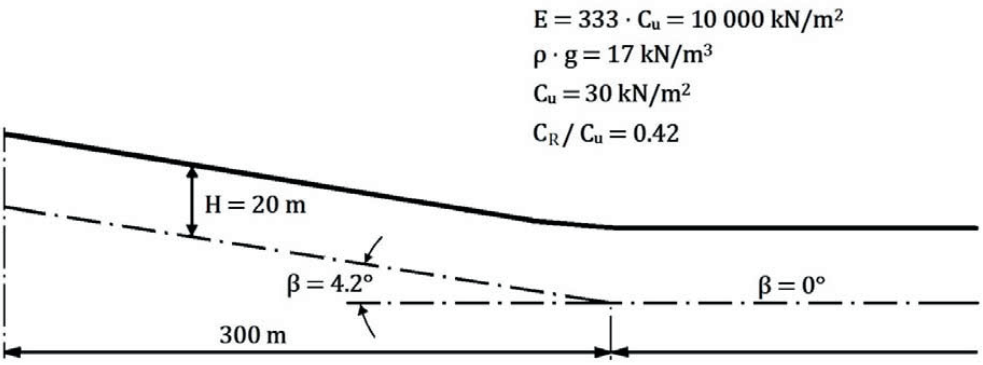

Figure 5:1.8 Main data of the slope studied

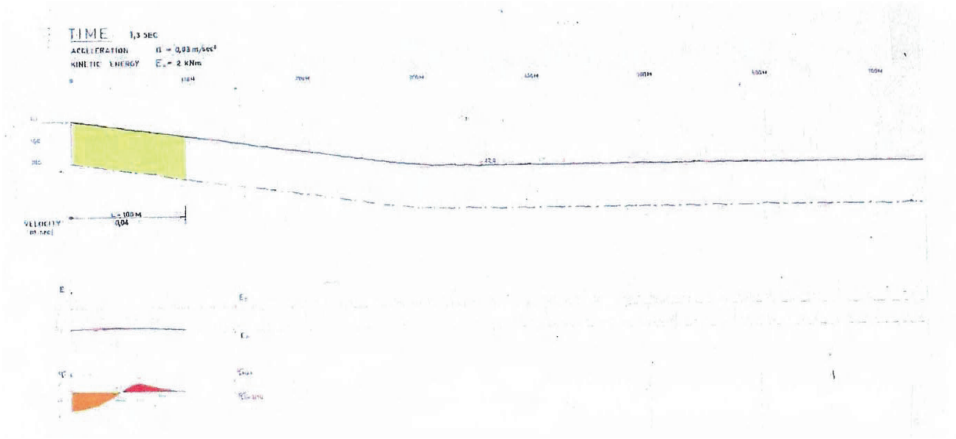

Figure 5:1.9 Progressive failure released by the additional force $N_i = N_{cr}$, dynamic phase I.
Time t = 1.3 sec. Deepening colours or shades indicate growth of down slope earth pressures. Phase 3 just after transition from Phase 2.

Acceleration =	0.02 m/sec^2	Max. velocity	≈ 0 m/sec
Kinetic energy	≈ 0 kNm	Total length, L	= 100 m

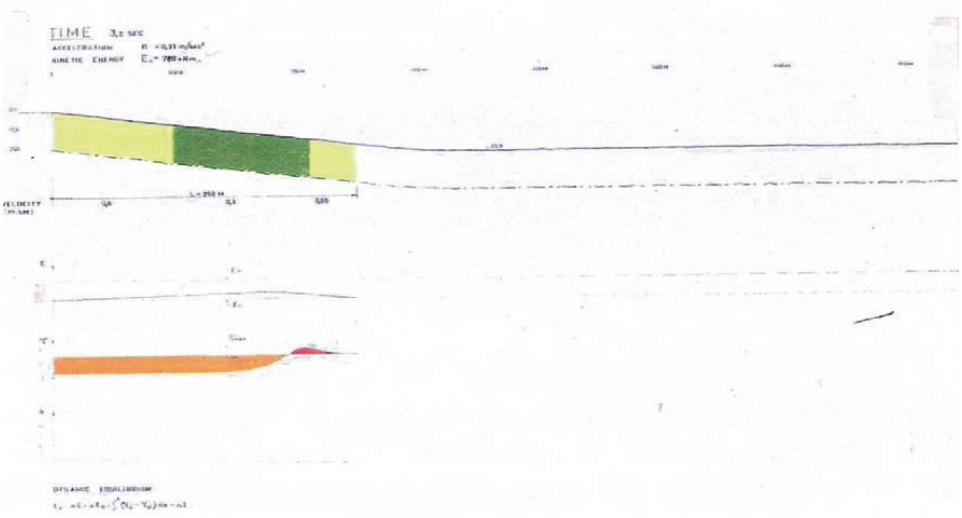

Figure 5:1.10 Progressive failure propagation down-slope, dynamic phase I. Phase 3.
Time t = 3.2 m/sec
Deepening colours or shades indicate growth of down slope earth pressures.
Acceleration = 0.20 m/sec^2 Max. velocity = 1.3 m/sec
Kinetic energy = 780 kNm Total length, L = 250 m

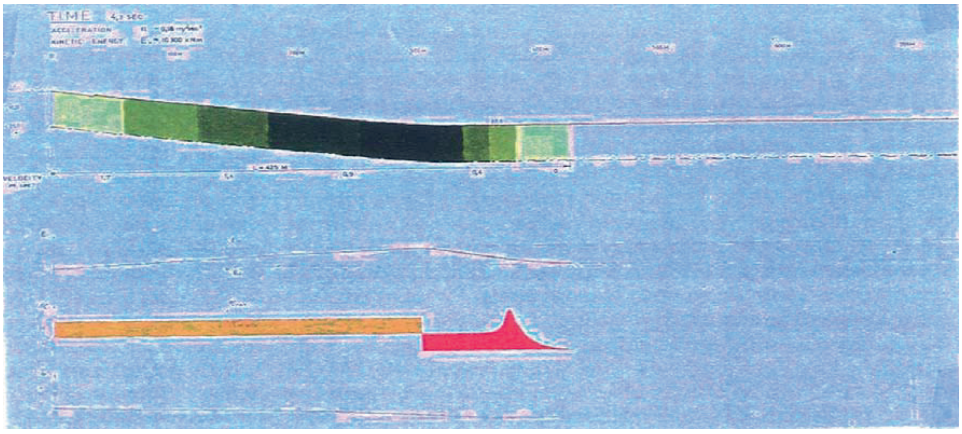

Figure 5:1.11 Progressive failure propagation down-slope, dynamic phase I continued.
Phase 3. **Time t = 4.3 sec**
Deepening colours or shades indicate growth of down slope earth pressures.
Acceleration = 0.18 m/sec^2 Max. velocity = 1.7 m/sec
Kinetic energy = 10 300 kNm Total length, L = 425 m

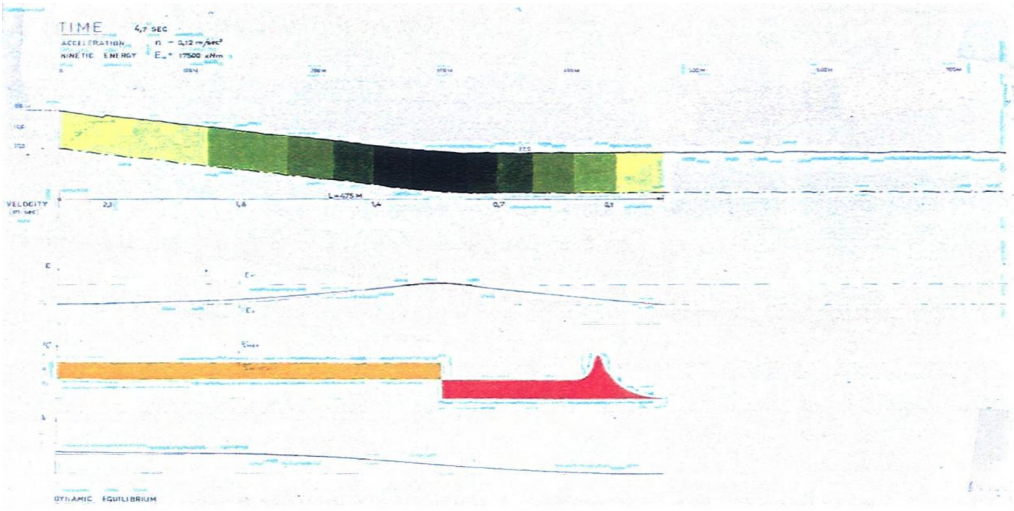

Figure 5:1.12 Progressive failure propagation down-slope, **transient** static phase, **Phase 4**.
Time t = 4.7 sec
If, however, E_p^{max} had been < $E_p^{Rankine}$, then the ground movement would have terminated at this point. (See slide at Rävekärr Section 5:5).
Deepening colours or shades indicate growth of down slope earth pressures.
Acceleration = 0.12 m/sec^2 Max. velocity = 2.1 m/sec
Kinetic energy = 17500 kNm Total length, L = 475 m

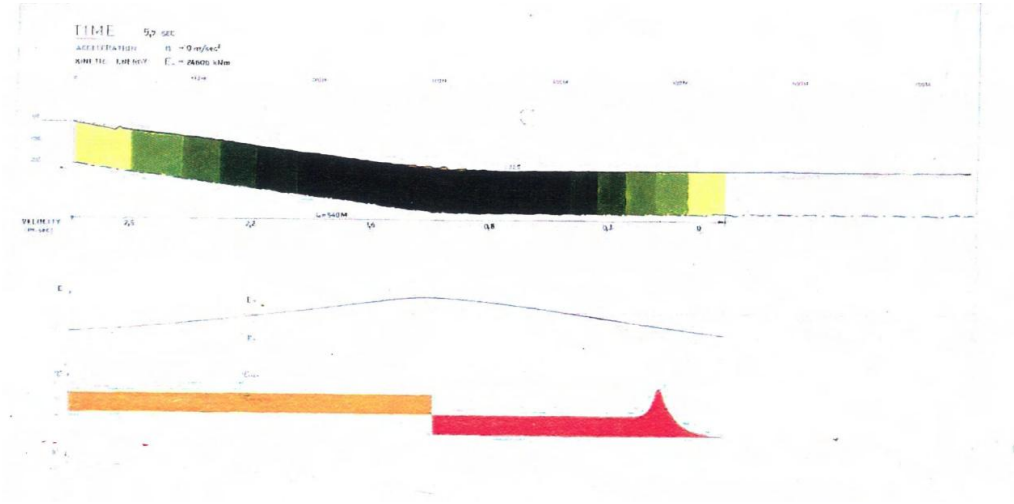

Figure 5:1.13 Progressive failure propagation accomplished and dynamic phase II begins.
Phase 5.
Time t = 5.7 sec. Deepening colours or shades indicate growth of down slope earth pressures. Phase 5.
Acceleration = 0 m/sec^2 Max. velocity = 2.5 m/sec
Kinetic energy = 24 600 kNm Total length, L = 540 m

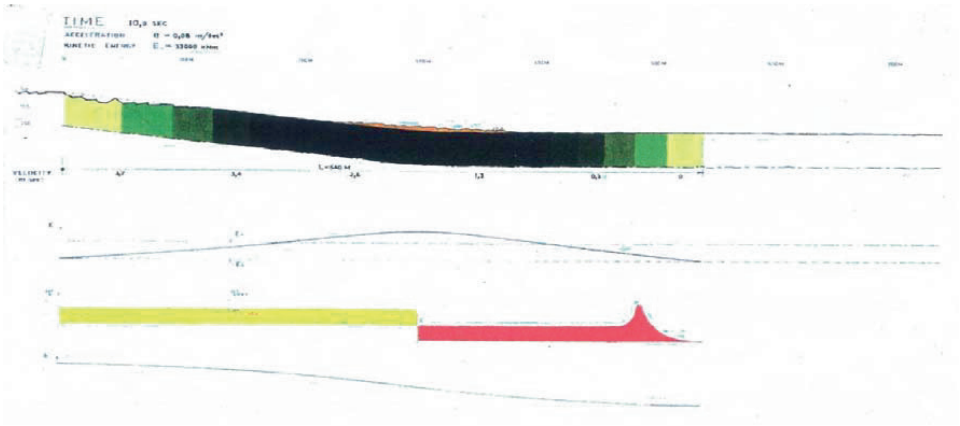

Figure 5:1.14 Incipient heave in the passive zone, dynamic phase II, Phase 5.
Time t = 10 sec.
Deepening colours or shades indicate growth of down slope earth pressures.
Acceleration = 0.08 m/sec^2 Max. velocity = 3.7 m/sec
Kinetic energy = 33 000 kNm Total length, L = 540 m

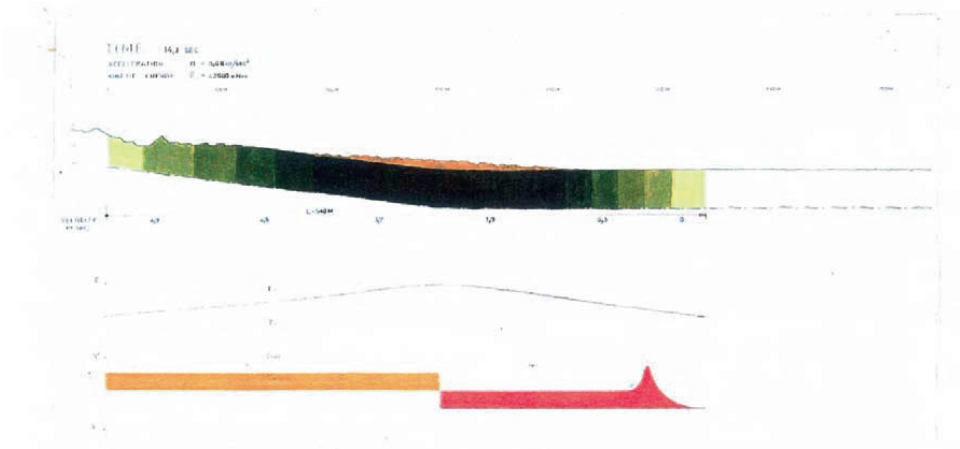

Figure 5:1.15 Heave in the passive zone due to static build-up of earth pressure forces almost completed. Observe development of the active zone. Phase 5. **Time t = 14.2 sec**
Retardation (retardation) = **-** 0.08 m/sec^2 Max. velocity = 4.9 m/sec
Kinetic energy = 42500 kNm Total length, L = 540 m

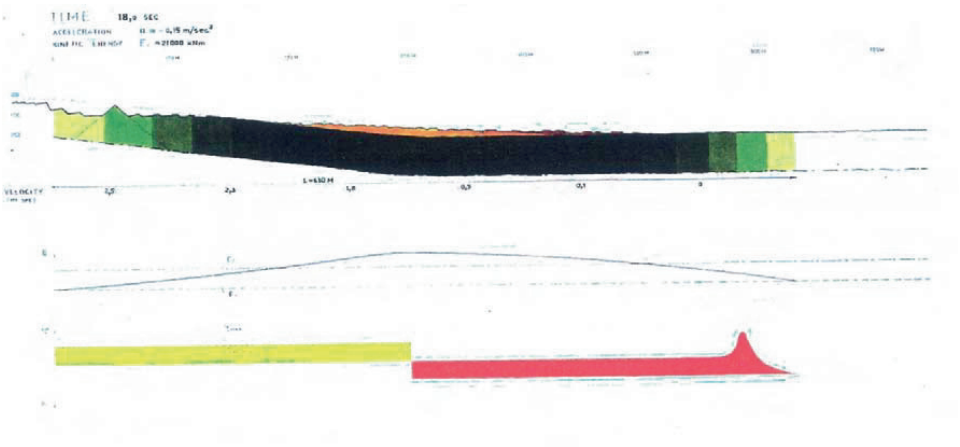

Figure 5:1.16 Retardation phase. Heave in the passive zone due to dynamic (inertia) forces. Deepening colours or shades indicate growth of down slope earth pressures. Phase 5.

Time t = 18 sec

Retardation	= - 0.15 m/sec^2	Max. velocity	= 2.5 m/sec
Kinetic energy	= 25 000 kNm	Total length, L	= 630 m

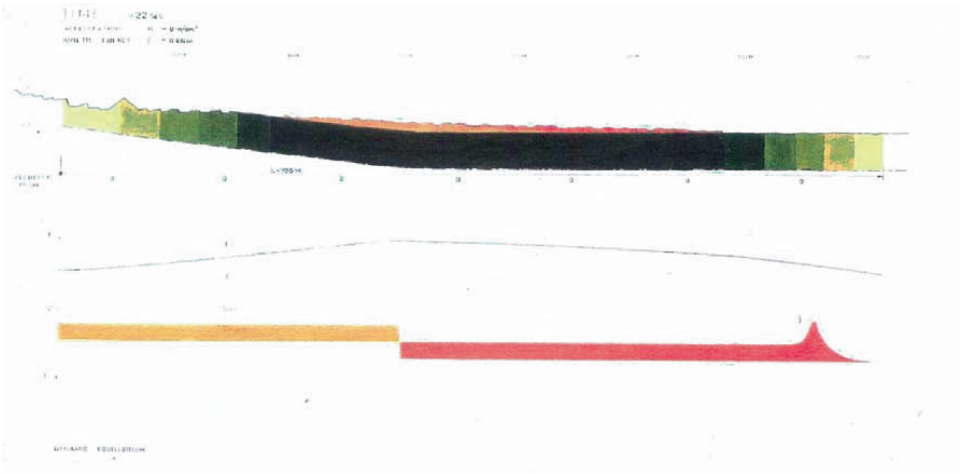

Figure 5:1.17 The slide is completed and has reached its final spread. Phase 6.

Time t = 22 sec

Deepening colours or shades indicate magnitude of down slope earth pressures.

Acceleration	= 0 m/sec^2	Max. velocity	= 0 m/sec
Kinetic energy	= 0 kNm	Total length, L	= 720 m

5.2 *The landslide in Surte (1950), Sweden*

5.21 General - history of a slope in the Göta River valley

The stability conditions in natural slopes are closely related to their geological and hydrological history. Clay slopes in western Sweden normally consist of glacial and post-glacial sediments that emerged from the regressing sea after the last glacial period. Hence, the sediments deposited in sea and fjords at the end of this period in what was later to become western Sweden, are now found in valleys and plains considerably above present sea level, forming deep layers of soft clays and varved silty clays.

As the ground gradually rose above the sea level, the strength properties of the soils and the earth pressures in the slope have, by way of consolidation and creep movement, accommodated over time to increasing loads and changing conditions. These may have resulted from the retreating free water level, falling ground water tables, varying climatic conditions and chemical deterioration.

In consequence, existing slopes are basically stable, as long as they remain undisturbed. Considering the effects of extreme high ground water events during past centuries and millennia, the nominal safety factor may – provided hydrology has remained unaffected by human interference – at least be assumed to exceed the value of 1.0 by some measure.

Yet, the true safety margin cannot, in long slopes of soft highly sensitive clays, be defined in the conventional way on the principle of plastic equilibrium, even under drained conditions. The real risk of slope failure can only be assessed by investigating the response of potential disturbing agents in terms of progressive failure, and will therefore mainly depend on the nature and magnitude of the additional load, to which the slope may be subjected.

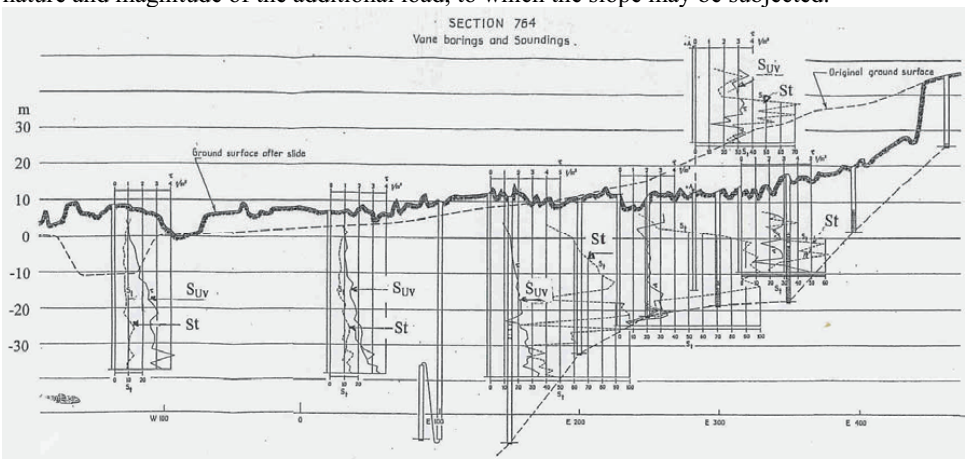

Figure 5:2.1 Section through the Surte slide area epitomizing common features in glacial and post-glacial clay deposits in western Sweden. (Vertical scale = 5 x Horizontal scale). Denotations in the figure: $\tau = S_{uv}$ = Vane shear strength ($\approx c_u$); St = Sensitivity = S_{uv}/S_{ur}. (From Jakobson (1952 a), modified regarding notations.)

A vital question, when investigating the stability of a slope of this kind, is therefore: "In what way will the slope respond to a local additional load or disturbance effect, for which the 'time horizon' is measured in terms of days, weeks or months instead of hundreds or thousands of years?" (Cf in this context Section 11.2. *History of a slope*)

For example, a specific gradually applied additional load or disturbance may be totally inconsequential in a six month scenario, whereas the same change of load happening in days or weeks may lead to a disastrous landslide. In other words, time is a crucially important factor in the assessment of slope stability in deposits of sensitive clay.
For instance, in what way does weather and climate change affect down-hill landslide hazard? Will extreme and extenuated periods of rainfall – generating higher pore water pressures than ever before in specific soil layers – result in slope failure? Or, will the properties of the soils involved gradually adapt to slowly changing environmental conditions, as has in fact been the case in existing natural slopes and slopes that have recently been destabilized by verifiable human activity?

And finally, if local failure due to additional load is conceivable, what kind of disaster is likely to ensue? Will such a failure, in a 'vulnerable' part of the slope, only result in creep movements and minor cracking in the up-slope active zone, or will it end up as a major landslide displacing hundreds of meters of horizontal ground over large distances? The basic preconditions leading to either of these scenarios are often not very different.

Aas (1982) discussed the hazards related to such primordial and potentially unfavourable conditions in natural slopes – yet without considering, as is done in this document, the effects of differential deformations within the sliding body of soil.

5.22 The Surte slide event

Figure 5:2.2 Aerial view of the Surte landslide in the valley of the Göta River some 10 km North of the city of Gothenburg, Sweden.

The Surte landslide took place soon after 8 a.m. on September 29, 1950. The main slide, involving some 24 hectares of ground, swept away 31 family houses and 10 outhouse units. Due to the hour - most residents already having gone to work elsewhere - the death toll was limited to one person.
The south-bound branch of the Göta River, which is navigable for heavy shipping transport, was blocked for two months. The north-bound railway and highway were displaced varying distances up to 150 m, blocking road and railway traffic for 10 and 19 days respectively. Transportation and industry incurred serious damage.
Figures 5:2.2 and 5:2.3 are aerial photos of the slide area. Figure 5:2.4 shows a plan and a longitudinal section of the slide.
The actual slide event was observed by a number of people within and outside the slide area, but as is often the case in dramatic circumstances of the current nature, most eye-witnesses only noticed incidents that were local in time and space.

However, one witness positioned outside the slide area gave an exceptionally coherent, continuous and time-wise extended description of the main events of the slide that can be considered to be of great value to anyone investigating the causes and the failure mechanisms of the landslide events. The witness, (Ture Berntsson), summed up his impressions as follows: (Quotations from Caldenius, C. & Lundström, R. (1955).

"The whole ground was moving rather slowly at a speed that can approximately be compared to that of the Bohus ferry. (Estimated speed a few metres per second.) The movement did not proceed at the same speed all the time - the speed increased progressively and the movement finally ceased when the ground piled up against the opposite side of the river. Then the ground rose and folded. However, folding had already begun during the first stage of the movement. House No 13 toppled very slowly when the slide was approaching the opposite side of the river. Water and clay were lifted very high. Cracks of various sizes were formed during the course of the slide. At first, the ground moved straight down towards the river but further down the slide widened, while the main part of the ground continued straight ahead."

Ture Berntsson's statement agrees very well with slide development as conceived by the progressive failure analysis used in this study.

Another important witness, (Hjördis Svensson), standing in her kitchen (Villaplatsen 2) and facing south, told among other things the following:
"She first noticed that a pile driving machine and the ground around it began to subside and that the men engaged in pile driving started to run away. Then she observed that the houses beyond were also moving. …….The pile driving machine did not topple until the last stage of the movement. A large number of cracks formed in the ground. The movement was wavelike and smooth. The houses seemed to sail along. "

5.23 Investigations and analyses after the slide
The Surte landslide was treated in two comprehensive reports by Jakobson et al (1952a), and by Caldenius & Lundström, (1955). In the latter report Lundström stood for the geotechnical assessments. The thorough field and laboratory investigations made in connection with these reports constitute valuable contributions to the knowledge of the behaviour of the types of soft clay involved in the slide.
However, in so far as the causes and the mechanisms that formed the slide event are concerned, both of these reports can be regarded as inconclusive, and at least from a strict structure-mechanical point of view the Surte slide has remained unexplained until recently. ([4])

([4]) A different explanation of the slide in terms of progressive failure development was presented by Bernander (2000), rendering a more plausible understanding of the remarkable features of this slide.

The reasons for this are as follows:
a) The two mentioned official reports are contradictory on essential issues – e.g. with regard to ground water conditions and piezo-metric levels, to the causes of the initial slide, as well as to the sequence of slide events and the failure mechanisms that formed the landslide.

b) In both reports, computational analyses of the various phases of the slide were based on the concept of plastic limit equilibrium. Hence, the differential deformations within the potentially sliding soil mass were not accounted for in any of the post-slide investigations.

Figure 5:2.3 Aerial photograph taken 13 days after the slide. From Caldenius & Lundström (1956).

In the author's experience, gained from comprehensive studies of progressive failure formation, the validity of the ideal-plastic failure concept (I-PlFA) is questionable as regards many kinds of additional loading in slopes of sensitive soft clays, and that already for lengths of the potential failure zone in the range of only 50 to a 70 m.
This condition applies of course in particular when, as in Jakobson's analysis, the length of the slide being investigated exceeded 400 m.

Lundström, on the other hand, considered effects of strain softening in attempting a verbal account of what he characterized as a 'progressive passive slide' over gently sloping ground – thereby implying that the slide propagated as a series of consecutive slip circular slides. It should be noted that the term 'progressive' is by Lundström used in an altogether different sense than that adopted in the present document.

c) Other points of discussion as described below.
Jakobson assumed in his report that the soil volume in the main slide, excluding the serial retrogressive after-slides, moved as a block towards the river. He also maintained that the critical cause of the slide was the presence of elevated artesian pore water pressure in the order of 7 m in the failure zone – a condition presumed to have been occasioned by high precipitation in the years 1949 and 1950.

It is true that high pore water pressures of this magnitude were recorded in deeper clay layers after the slide. The analytical model is of course also plausible as such but the problem with this approach is that it presupposes – without valid substantiation – that these high piezo-metric levels had existed prior to the slide event. In fact, no elevated artesian pressures of this extraordinary magnitude were registered in undisturbed ground anywhere else in the area. Nor were the measured pressure gradients compatible with a stable long-time ground water situation. Thus, Jakobson's assumptions, in respect of elevated artesian pressures of this magnitude before the slide, were not actually documented and were, incidentally, contested already by Lundström.

In the current context, it is essential to realize that, when soft and sensitive clays – i.e. basically collapsible soils – are excessively sheared, excess pore water pressures are generated by the very disturbance of the clay strata. These high water pressures tend to persist over long periods of time, transiently carrying part of the weight of the overburden. This phenomenon has been documented in other slides in soft sensitive clays.
The few pore pressure measurements actually made in the slide area indicate excess pore water pressures beginning at a depth of some 10 m below the ground level, and from there gradually rising to maximum values at a depth of about 20 m. As this was the level of the slip surface, the measured excess pore water pressures are indicative of disturbance due to shear deformation not only at the slip surface but in the entire zone subject to shear deformation.

Moreover, measurements of pore water pressure in the ground immediately outside the slide boundaries showed only about 50 % of the values mentioned previously, i.e. a maximum of some 3.5 m at the level corresponding to the failure surface. Yet, also these values were most likely induced by the slide itself, considering the close proximity of the pore pressure gauges to the lateral boundary of the slide.

Although Jakobson seems to have been aware of the fact that, during the thousands of years the slope had existed, more extreme ground water conditions must have prevailed time and

time again, he does not present any argument or reason as to why the slide happened to be set off on that particular day in September, 1950.

In the intense discussion of the immediate causes of the slide that followed the landslide event, Jakobson made no reference to the fact that prefabricated concrete piles were being driven in a steep part of the sloping ground. (Cf Figure 5.2.4). This is noteworthy since the pile driving activity was the only notable disturbance at the time of the slide event and which, as far as was known, had never taken place before in the steeper portions of the slope. Family houses in the area involved in the slide did not rest on piles.

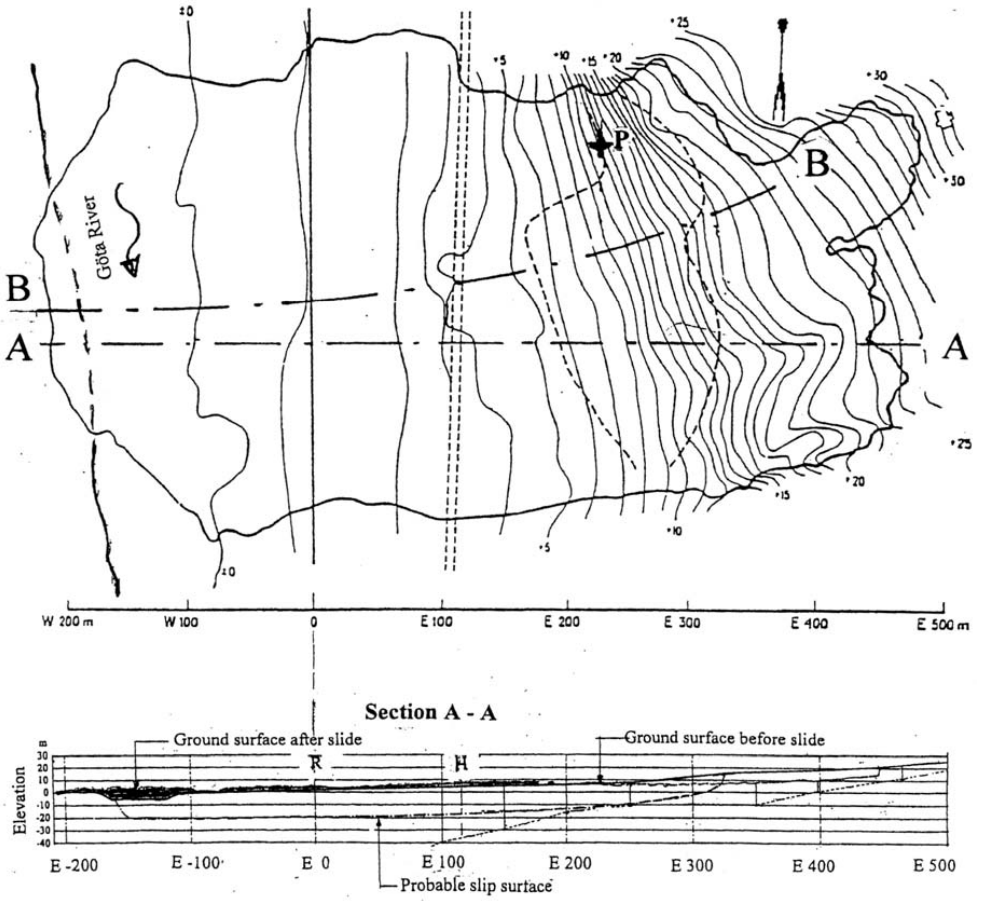

Figure 5:2.4 Plan of the slide area showing elevation contours and a longitudinal section A-A of the slide. From Jakobson (1952b). The point marked (P) on the plan is the location in the steepest portion of the slope, where piling operations were going on at the time of the slide occurrence. (Point P was not indicated in the source document. Section B-B marks the section being analyzed in Figure 5:2.8, and was not either shown on the original plan).

However, it may be noted here that Jakobson, (1952b), in response to critical comments on his report by Löfquist (Teknisk Tidskrift, 1952), as well as in the animated debate that followed in the aftermath of the slide (1953), argued that the immense spread of the slide may

have been due to some kind of progressive failure process. He then, as it appears, argued that the failure process may have been due to gradual loss of shear resistance as the slide propagated, yet without presenting any supporting analysis or computational documentation.
In the review of Jakobson's report mentioned above, Löfquist contended that the remarkable spread of the Surte slide must have been due to a near total loss of frictional resistance in a presupposed thin stratum of fine sand, thus establishing that failure in sensitive clay was not the decisive factor. He then had to assume that, in this layer, considerably higher artesian pressures than even those assumed by Jakobson must have prevailed before the slide.
Although also Löfquist's model for slope failure is viable as a theoretical concept, his approach must be regarded as highly speculative, as artesian pressures of this magnitude over a length of some 500 m had not ever been documented in this area. Nor were any continuous seams of fine sand shown to be present. **([5])**

([5]) In this context it is, in the opinion of the author of this document, important to point out that liquefaction in sandy or silty layers due to shear deformation is highly unlikely in slopes of this kind owing to the fact that, in the past, the soil structure has slowly been subjected to long-time shear deformation due to considerable downhill creep movements (i.e. in terms of several meters). This is a process that had been going on ever since the ground gradually emerged from the glacial sea.
Hence, according to basic soil mechanics, discrete seams of cohesion-less material will already long ago have attained their states of constant porosity in shear, in which case liquefaction generated by additional shear deformation is not a likely scenario.
However, this condition does not, of course, exclude liquefaction phenomena due to dynamic impact such as pile driving, rock blasting or the use of vibratory equipment. (Cf Section 5.6.)

Like Jakobson, Löfquist does not present any reason or argumentation as to why the piezometric levels in the sand layer assumed should have been higher than ever before at the time of the slide event.

Nature of the evolution of the slide
As opposed to Jakobson (1950), Lundström asserted that the slide developed as a rather complicated and interrelated series of smaller local slides with circular slip surfaces caused by an initial slide in the steeper part of the slope. From deliberations with regard to the kinetic energy released in this first rather local slide, he maintains that the same to some extent affected the practically horizontal ground ahead – i.e. by displacing it a certain distance towards the Göta River.
Yet, he then maintained that the impact of the first slide was not sufficient to bring about the continued slide movement all the way to the river. So, in order explain the further progression of the earth movement, he suggests that inertia forces originating from the retrogressive after-slides acted on the immense soil masses in the almost horizontal part of the valley, completing the passive heave of the ground as far as the river bank in terms of a series of smaller slip-circular slides.
Then in turn, the rising ground near the riverbank became unstable, thus ending the sequence of ground failures by eventually blocking the riverbed in a major local slip-circular slide of conventional type. Lundström's reason for contemplating this final slide event was presumably the fact that there was no heave (or subsidence for that matter) over a distance of about 20 m near the riverbed **([6])**. (Cf the longitudinal section in Figure 5.2.4.)

([6]) For the present author's explanation of this phenomenon, see Section 5.2.3 below – Global failure condition.

Lundström's reasoning seems complicated, circumstantial and mechanically disputable, but his explanation of the Surte slide has the merit of recognizing inertia forces as an important feature in slide propagation mechanisms. However, kinetic energies and forces of inertia are time-dependent dynamic phenomena and cannot be added algebraically unless they are perfectly concurrent.
Hence, the main difficulty in accepting Lundström's failure concept – i.e. when explaining the passive heave of the almost horizontal ground and the riverbed – consists mainly in the way that he compounds the dynamic effects of the retrogressive after-slides to those of the initial slide. These effects were in no way simultaneous.

However, importantly, Lundström ascribes the initiation of the slide to the pile driving activity that was going on in the steepest part of the slope, i.e. in Point P in Figure 5.2.4.

Conclusions
As may be concluded from the discussion above, the various explanations of the landslide in Surte emanating from the after-slide investigations do not yield plausible or structure-mechanically coherent descriptions of the initiation and development of this slide event.

A cardinal weakness in this context is the fact that differential deformations within and outside the extensive sliding body of soil (almost 600 m long) were not considered in the analysis.

Another important issue is that the piezo-metric levels presumed in Jacobson's and Löfquist's computations were not documented and do not appear to have existed before the slide.

Regarding Lundström's explanation of the extensive spread over level ground, it is difficult to conceive how the risk of potential spread failure in a similar geotechnical setting can be predicted by applying the complex arbitrary series of slip-circular failures and the related random sequence of events that characterize this failure concept.

In an article written in Swedish, Lundström (1997) has elaborated somewhat on his 1955 theory regarding the Surte slide events. However, even at this point his presentation does not address the possibility of progressive failure in accordance with concepts that have appeared in soil mechanics literature since 1955. In the absence of a coherent integral analysis in the time domain of both static and simultaneously acting dynamic forces in the ongoing slide, his specific explanation of the Surte slide remains rather circumstantial and inconclusive.

5.24 Explanation of the Surte landslide in terms of progressive failure formation
Fortunately for the art of slope stability analysis, the important issues are not as erratic or randomly structured as may be indicated by the failure concept previously described.

An investigation of the Surte landslide has been carried out using the progressive failure FDM-approach outlined in Sections 3 and 4 – i.e. considering in particular the differential deformations in the potentially sliding volume of soil.

A basic feature in the FDM-analysis described in Section 4 is that the deformations in the failure zone adjacent to the potential slip surface are modelled according to a constitutive shear stress/deformation relationship such as the one shown in Figure 5:2.5.
In the current case, deformations in the incipient failure zone are assumed to be symmetrical above and below the potential failure plane only where the slip surface is sufficiently distant

from the firm bottom contour. (Cf Section 4.7.) Shear strength and E-modulus are varied along the slope as interpreted from soils investigation data provided in the report by Jakobson, (1952a).

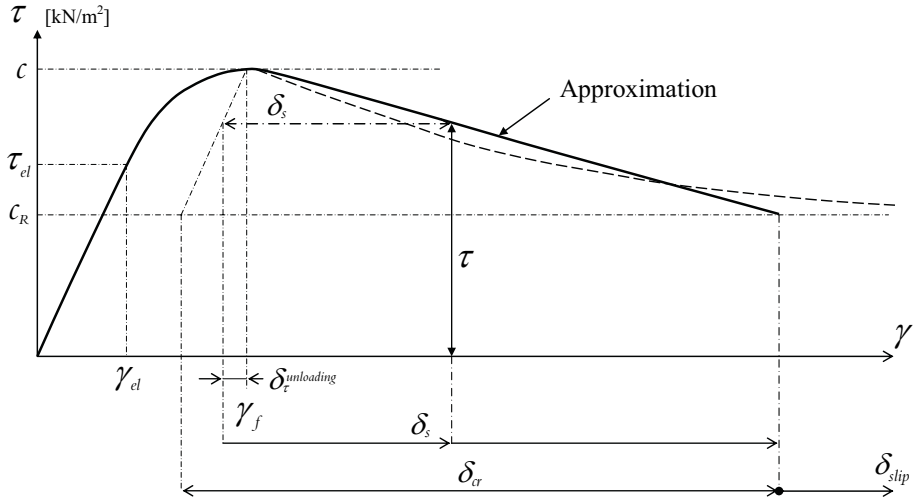

Figure 5:2.5 Constitutive stress/deformation relationship in principle. c_R denotes the residual shear resistance of the clay in the critical part of the slope when (and where) progressive failure is initiated. It may be noted that the ratio τ_{el}/c is in the current study assumed to be constant as c varies with the coordinate (x). The value of c_R is closely related to the rate of load application and to drainage conditions.

Input data
With reference to Figures 5:2.5 and 5:2.6, the following values of the characteristic parameters have been used in this study. c_R denotes the effective residual shear resistance under current rates of load application and ambient drainage conditions.

In situ state condition:
$c_{\infty R}/c_\infty = 1.00$ $\gamma_{el} = 3.75\ \%$ $\gamma_f = 7.5\ \%$ $G_{el,o} = \tau_{el}/\gamma_{el} = 480\ kN/m^2$
c_∞* $= 24\ kN/m^2$, $\tau_{el} = 18\ kN/m^2$ $E_{el,o} = 2(1+\nu)G_{el,o} = 60c_\infty = 1440\ kN/m^2$
$\rho \cdot g = 15.5\ kN/m^3$ $K_o = 0.55$ (for horizontal ground) $\nu = 0.5$ $E_{el,mean} = 60\ c_{\infty,mean}$
(* In the current state, c_∞ signifies the long time shear resistance – drained conditions.)

Disturbance Condition I – *failure initiation*
$c_R/c = 0.80$ ** $\gamma_{el} = 2\ \%$ $\gamma_f = 4.0\ \%$ $\delta_{cr} = 0.3$ m $G_{el,o} = \tau_{el}/\gamma_{el} = 1000\ kN/m^2$
c# $=30\ kN/m^2$ $\tau_{el} = 20\ kN/m^2$ $E_{el,o} = 3G_{el,o} = 100 \cdot c = 3000\ kN/m^2$
$\rho \cdot g = 15.5\ kN/m^3$ $k_o^{max} = 0{,}594$ (computed) $E_{el,mean} = 100\ c_{mean}$
Mean values applying to the initiation zone.

Disturbance Condition II – *failure initiation*
$c_R/c = 0.60$ ** $\gamma_{el} = 2\ \%$ $\gamma_f = 4.0\ \%$ $\delta_{cr} = 0.3$ m $G_{el,o} = \tau_{el}/\gamma_{el} = 1000\ kN/m^2$

** The values of c_R adapt to the rate of load application and estimated drainage conditions in the failure zone, and are here assumed to correspond to 0.8 (Condition I) and 0.6 (Condition II) of the shear resistance c. The parameters c_R and c_{uR} must not be confused with the completely remoulded shear strength c_{ur} as measured in laboratory.

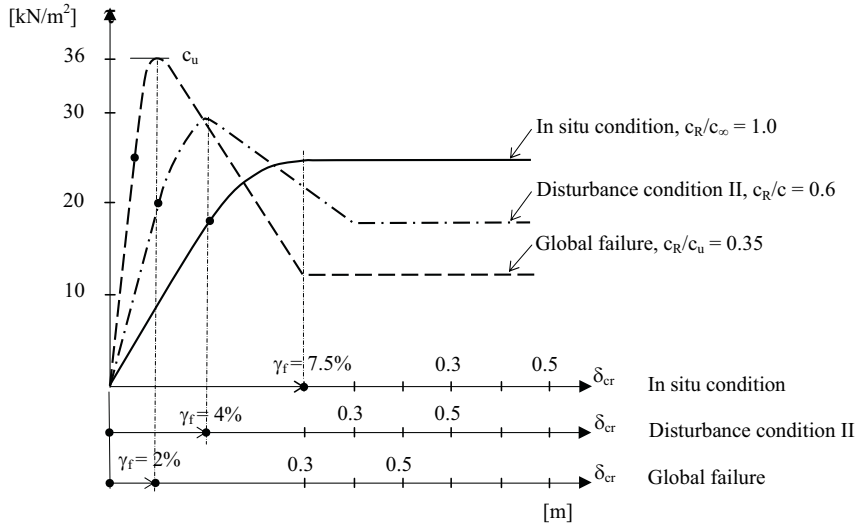

Figure 5:2.6 Assumed shear/deformation relationships for the three decisive phases of the Surte Landslide.

Global failure condition:
c_{uR}/c_u = 0.35-0.20 # γ_{el} = 1 % γ_f = 2 % , δ_{cr} = 0.3 m $G_{el,o} = \tau_{el}/\gamma_{el}$ = 2400 kN/m^2
$c_{u,o}$ = 36 kN/m^2 ## τ_{el} = 24 kN/m^2 $E_{el,o} = 3G_{el,o} = 200 \cdot c_{u,}$ = 7200 kN/m^2
K_o (as computed in the in situ condition) $E_{el,mean} = 200\ c_{u,mean}$
The un-drained residual shear resistance c_{uR} is in the current case assumed to vary between 0.35 and 0.20·c_u.
Mean value applying to the down-slope failure zone.

Note: In all of the calculations in Sections 5, and in Appendix I, the curved portion of the constitutive relationship from γ_{el} to γ_f is a function of x^2 with vertex at (c_u,γ_f) and connecting tangentially at (τ_{el} ,γ_{el}).

5.25 Results of the FDM-analysis

The results of the in situ FDM computations are given in Table 5.2.1 below.

The in situ state condition

In the steepest part of the slope, available shear strengths do not match the in situ shear stress in terms of $\tau_o = \rho \cdot g \cdot H \cdot \sin\beta$. This implies that already in the in situ condition, the soil masses were to some extent balanced by elevated earth pressures in less inclined ground further down the slope in accordance with Equation 4:2, (i.e. ΔE_o is positive).

$\tau_0\,(x,o) = \Sigma_o^{H(x)} \rho \cdot g \cdot H \cdot \sin\beta - \Delta E_o(x)/(b(x) \cdot \Delta x)$ i.e.……(Eq. 4:2.)

Table 5.2.1 *Results from FDM- analysis – In situ state condition.*

($L_{N,max}$ = distance to N_{max} from the point of application of the additional load)				
c_R/c_∞ = 1.0	N_{max} = 138 kN/m	$L_{N,max}$ = 120 m	E_{max} = 1673 kN/m	K_o = 0.594

The disturbance condition
The results of the analysis of disturbance Conditions I and II are presented in Table 5.2.2 ($L_{N,max}$ = distance to N_{max} from the point of application of the additional load).

Table 5.2.2 *Results from FDM- analysis – disturbance conditions.*

Disturbance Condition I – *Force-initiated failure*				
$c_R/c = 0.80$	$N_{cr} = 275$ kN/m	$L_{cr} = 140$ m	$E_{max} = 1748$ kN/m	$L_{N,max} = 0$ m
Disturbance Condition II – *Force-initiated failure*				
$c_R/c = 0.60$	$N_{cr} = 192$ kN/m	$L_{cr} = 114$ m	$E_{max} = 1665$ kN/m	$L_{N,max} = 0$ m
	$\delta_{cr} = 0.145$ m			
Disturbance Condition IIa – *Deformation- initiated failure*				
$c_R/c = 0.60$	$N_{cr} = 0$ kN/m		$E_{max} = 1770$ kN/m	$L_{N,max} = 50$ m
	$\delta_{instab} = 0.292$ m	$L_{instab} = 162$ m (As defined in Figure 4:2.4a)		

The critical load (N_{cr}), sufficient to initiate local failure in the steepest part of the slope amounts to 275 kN/m in Condition I and 192 kN/m in Condition II.

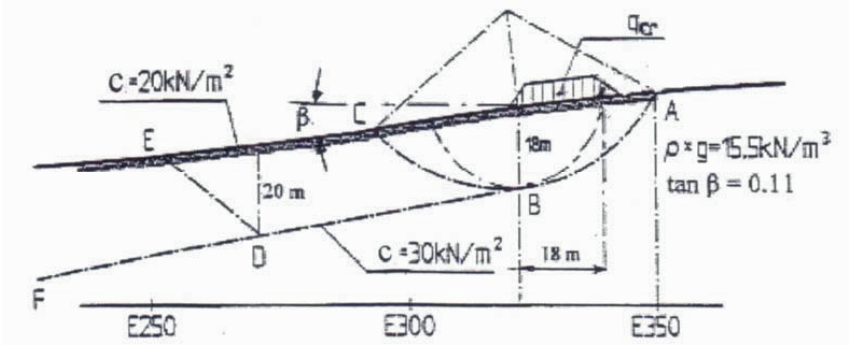

Condition I: $c_R/c = 0.80$
$q_{cr\,(Pr\,FA)} = q_{cr\,(ABDF)} \approx 15.3$ kN/m^2 << $q_{cr\,(I\text{-}PFA)} = q_{cr\,(ABC)} = 68$ kN/m^2 < $q_{cr\,(ABDE)} \approx 118$ kN/m^2

Condition II: $c_R/c = 0.60$
$q_{cr\,(Pr\,FA)} = q_{cr\,(ABDF)} \approx 10.6$ kN/m^2 << $q_{cr\,(I\text{-}PFA)} = q_{cr\,(ABC)} = 68$ kN/m^2 < $q_{cr\,(ABDE)} \approx 118$ kN/m^2

Figure 5:2.7 Comparison of progressive failure analysis (FDM) and ideal-plastic failure analysis (I-PlFA) with regard to a local distributed critical load q_{cr}, the extension of which roughly equals the depth to the slip surface. (Fully un-drained conditions are presumed.)

Although the Surte slide was not documented to have been triggered by the weight of a newly applied fill, it may still be of interest to note that – assuming totally un-drained conditions – the computed value of N_{cr} in disturbance Condition I would correspond to a rapidly applied overload of only $q_{cr} \approx 275/18 = 15.3$ kN/m^2 extending 18 m up-slope of Point B in Figure 5:2.7, or Point P in the real slope as shown in Figure 5:2.4). (7)

(7) It is important to observe in this context that if the additional load is applied gradually under long time – i.e. if conditions are drained or partially drained – progressive failure analysis would also result in considerably higher values of q_{cr}.

In disturbance Condition II, the same overload would be $q_{cr} \approx 10.6$ kN/m^2.

By contrast, ideal-plastic failure analysis (I-PlFA) based on local slip surfaces such as ABC in Figure 5.2.7 indicates a corresponding value of $q_{cr} \approx 68$ kN/m^2 – i.e. a difference that can be expressed by a factor of about 4.4 in disturbance Condition I.

This important discrepancy between the results from the ideal-plastic equilibrium approach on the one hand, and analyses considering deformations and deformation-softening on the other, stands out as the major reason why downhill progressive slides of the type dealt with in this document have long eluded convincing explanation in post-slide investigations of landslides that have occurred in Scandinavian soft sensitive clays.

The computed resistances in Table 5.2.2 are related to the disturbance condition – i.e. the end of Phase 2 as defined in Section 3.3 and immediately prior to the formation of a discrete failure plane or slip surface.
At this stage, both the modulus of elasticity and the shear modulus are time dependent in a similar way. In consequence, the analysis is not in this report very sensitive to the time factor considering that the ratio of E_{el}/G is largely constant and is not likely to vary widely. However, in order to estimate the sensitivity of the analysis to variation of the compressibility of the soil mass in the down-slope direction, the effect of doubling the value of E_{el} has been investigated and, other conditions unchanged, found to be as follows in disturbance Condition II: (Compare with Table 5.2.2)

$c_R/c = 0.60$ $N_{cr} = 274$ kN/m $L_{cr} = 163$ m $E_{max} = 1670$ kN/m at $L_{N,max} = 0$ m

Hence, doubling the E/G- ratio increases N_{cr} and L_{cr} by 43 %, while the value of E_{max} is virtually unaffected. It may be observed that an increase of N_{cr} of this magnitude has little impact on the issue highlighted in Figure 5:2.7. In fact, it would in principle remain unchanged even for much wider variation of the compression modulus of the soil in the slope.

Deformation- induced failure
As explained in more detail in Sections 3 and 4, there exists a critical value of deformation (δ_{instab}) forced upon an up-slope section that may result in global slope failure, even in the absence of an external force maintaining the failure process. In practice, such a situation can arise when driving soil-displacing piles, in which case no externally active sustained force will result from the operation.

As already mentioned, the Surte slide is for good reason suspected of having been triggered by ongoing pile driving for the foundation of a family house at the time of the slide event. Table 5.2.2 indicates a critical deformation value of $\delta_{instab} \approx 0.3$ m in disturbance Condition II a. However, as the number of piles in the foundation was not sufficient to generate a down-slope displacement of this magnitude, it may be concluded that soil displacement alone was not the only disturbance initiating the Surte slide.

It is thus very likely that the piling activities also locally induced high pore water pressures and loss of shear strength in possible local seams of coarser moraine out-wash in the clay formation. Such coarse strata commonly intermix with clay sediments in the vicinity of the ancient shores of the regressing post-glacial seas. (Cf Broms, 1983, Figure 9:2.2.).

It may be noted in this context that pile-driving is not an unusual agent causing slides in soft clays in Sweden. For instance, driving of only 6 prefabricated concrete piles for a family house released an earth movement at Rävekärr, involving roughly 15 hectares of ground south of Gothenburg in 1971. (Cf Section 5.5, The slide movement at Rävekärr.)
Numerous other examples of this phenomenon exist.

Lastly, regarding deformation-induced failure in disturbance Condition II a, doubling of the values of E_{el} in the slope has a moderate impact on the issue highlighted in Figure 5:2.7. Thus, although L_{instab} is increased by 41 %, E_{max} is only raised by 8 %.
$c_R/c = 0.60$ $N_{cr} = 0$ kN/m $L_{cr} =$ --- m $E_{max} = 1911$ kN/m at $L_{N,max} = 65$ m
$\delta_{instab} = 0.289$ m $L_{instab} = 228$ m

The global failure condition
The global failure condition is the stage subsequent to the redistribution (related to progressive failure) of up-slope unbalanced forces to the less sloping ground further downhill. Results from the FDM computations are shown in Table 5.2.3.
Figure 5:2.8, applying to the global failure condition Case I as per Table 5.2.3 below, displays calculated earth pressures, shear stresses and displacements along the slip surface defined by Jakobson (1952a) in the Surte slope.
The global failure condition illustrated in the figure represents the situation at the end of the progressive Phase 3 (as defined in Section 3.3), in which unbalanced forces in the steeper parts of the slope have been transferred further down-slope, resulting in massive build-up of earth pressures (Phase 4) in more level ground.

Table 5.2.3 *Global slope failure – results from FDM- analysis*

($L_{E,max}$ = distance to E_{max} from the point of application of the additional load)

Global failure condition: - *Case I*	E_{el}/G = **3**	E_{el}	$= 200 \cdot c_u$
c_{uR}/c_u = **0.35-0.20**	N_{max}= 3112 kN/m	E_{max} = 4969 kN/m	$E^P_{Rankine\ (max)}$ = 3900 kN/m
$E_{Rankine}/E_{max}$ = 0.785	$E_{el} = 206\ c_{u,\ mean}$	$L_{E,max}$ = 260 m	$L_{E>E(Rankine)}$ = 420 m #
Global failure condition: - *Case II*	E_{el}/G = **3**	E_{el}	$= 200 \cdot c_u$
c_{uR}/c_u = **0.40-0.25**	N_{max}= 2682 kN/m	E_{max} = 4554 kN/m	$E^P_{Rankine\ (max)}$ = 3900 kN/m
$E_{Rankine}/E_{max}$ = 0.856	$E_{el} = 206\ c_{u,\ mean}$	$L_{E,max}$ = 260 m	$L_{E>E(Rankine)}$ = 234 m #
Global failure condition: - *Case III*	E_{el}/G = **6**	E_{el}	$= 400 \cdot c_u$
c_{uR}/c_u = **0.40-0.25**	N_{max}= 2682 kN/m	E_{max} = 4558 kN/m	$E^P_{Rankine\ (max)}$ = 3900 kN/m
$E_{Rankine}/E_{max}$ = 0.855	$E_{el} = 412\ c_{u,\ mean}$	$L_{E,max}$ = 260 m	$L_{E>E(Rankine)}$ = 225 m #

$L_{E>E(Rankine)}$ = The length over which passive Rankine resistance is exceeded. Cf Figure 5.2.8.

It should be observed that the earth pressures in this phase are calculated on the assumption that the potentially sliding soil volume transiently retains its geometrical shape before possible disintegration in passive failure. This is justified because, as is demonstrated in detail in Section 3.3, the slip surface under the valley floor is fully developed far beyond the foot of the slope already in Phase 4 – i.e. prior to the potential final break-down of the passive zone in Phase 5 – and is therefore not concurrent with the final dramatic event constituting the actual landslide. (Cf Bernander, 2008, Chapter 5).

Hence, in cases where the resulting maximum earth pressure E_{max} exceeds $E^P_{Rankine\ (max)}$, the computed earth pressure scenario will represent a transitory stage that, in a fully developed

slide, later merges into the truly dynamic stage of the slide representing Phase 5 according to Section 3.3.
If, on the other hand, E_{max} had not exceeded $E^P_{Rankine}$, according to the computations, this would have indicated that the redistribution of earth pressures due to progressive failure would only have resulted in moderate ground displacements, such as in the ground movement at Rävekärr referred to above. (Cf Section 5.5.)

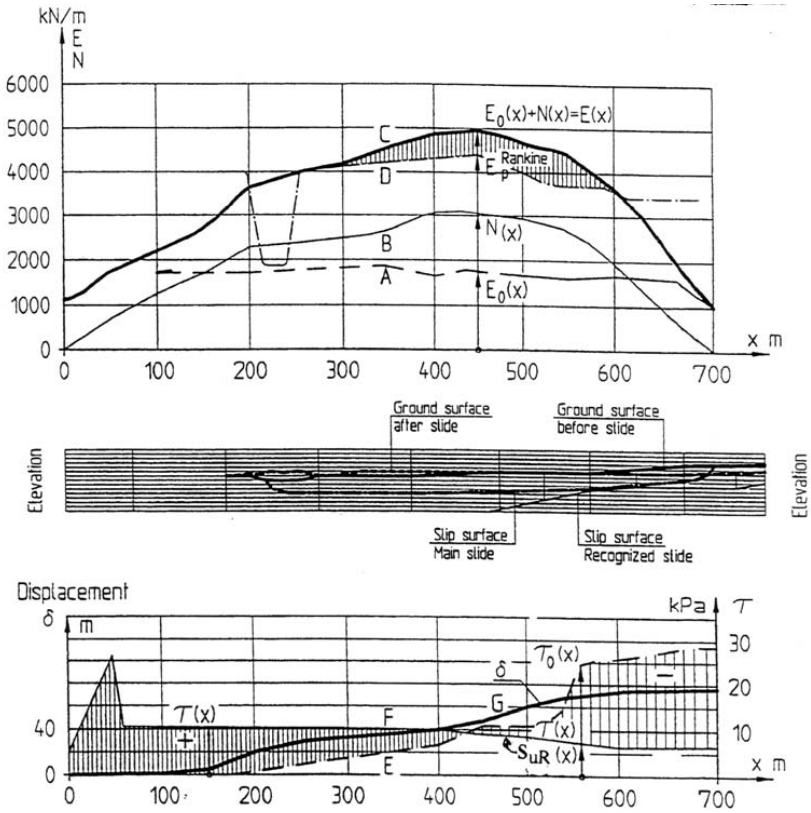

Figure 5:2.8 Static earth pressure distribution in the Surte slide subsequent to the progressive failure phase but prior to the slide proper resulting in disintegration and heave in a state of passive failure. The figure indicates that the static forces developed in the progressive phase of the ground movement suffice to explain the spread of the passive zone over almost horizontal ground. (Cf Sections 3 & 4.) Note $S_{uR} = c_{uR}$.

Global failure condition: Case I, $c_{uR}/c_u = 0.35\text{-}0.20$, $E_{el} = 200\ c_{u,\,mean}$
Curve A $E_o(x)$ = In situ earth pressure prior to local failure, kN/m
Curve B N(x)c = Earth pressure increment due to Pr F redistribution, kN/m
Curve C $E(x) = E_o(x) + N(x)$ = Earth pressure after Pr F redistribution (Phase 4), kN/m
Curve D $E^P_{Rankine}$ = Passive Rankine resistance, kN/m
Curve E $\tau_o(x)$ = In situ shear stress distribution before progressive failure, kN/m^2
Curve F $\tau(x)$ = Shear stress distribution after progressive failure Phase 4 – i.e. the situation prior to final disintegration in passive Rankine failure, kN/m^2
Curve G $\delta(x)$ = Displacement, m

Yet, it is important to note that also in this scenario the failure zone, including the failure surface, will have developed far beyond the foot of the slope into horizontal or less sloping ground.

The significance of the earth pressure distribution in the transient state of equilibrium, denoted Phase 4, is that it constitutes a measure of the disaster that may result if the critical load (N_{cr}) in the disturbance condition (Phase2) is exceeded. In other words, will the ensuing progressive failure lead to a veritable landslide, generating large displacements and heave over vast areas in passive failure, or will it only result in moderate deformations in the up-slope active zone?
As the formation of the slip surface is not contemporary with failure in the passive zone, the study of the transient condition in Phase 4 also provides information about how far ahead of the lower slide boundary the horizontal failure may have propagated into virtually level ground. Hence, the FDM-analysis performed indicates that this distance is in the order of some 400 m in the Surte slide.
Furthermore, Phase 4 renders information about the related displacements ahead of the visible lower boundary of the slide. (Cf Figure 3:3.5 in Section 3 and Figure 5:5.1 in Section 5.5.)

The calculations in *Case I* in Table 5.2.3 have been based on residual shear strengths roughly in proportion to the magnitude of the displacements in the progressive failure phase, and vary from $c_{uR} = 0.35 \cdot c_u$ to $c_{uR} = 0.20 \cdot c_u$ in different places along the slope. Yet, considering the significant displacements and the rates of stress change involved already in Phase 3, which is virtually of a dynamic nature, these values of c_{uR} may be considered as being high.
As shown in Figure 5.2.8, the earth pressures resulting from the progressive failure redistribution of forces entail that the calculated passive Rankine resistance based on these c_{uR}-values is exceeded over a distance of some 420 m of gently sloping ground including the riverbed. Thus, even if possible dynamic effects in the progressive phase are disregarded, the static condition alone would lead to total disintegration and heave in the lower areas of the slope and valley, inevitably eventuating in the final dynamic phase of the slide proper, which in Section 3 is defined as Phase 5. **([8])** (Cf Bernander, 2008, Chapter 5.)

([8]) Note. In the current context, Lundström's speculation mentioned in Section 5.23 regarding a possible final slip-circular slide near the Göta River, may be of interest. In the opinion of the present author, the absence of heave near the river did not, as suggested by Lundström, result from a local slip-circular slide. It was instead related to the fact that the in situ earth pressures were locally considerably much lower near the river scarp (i.e. close to active pressure) than elsewhere in the valley, in which case the probability of passive resistance being exceeded was locally considerably less. Yet, also this explanation, although different from Lundström's, relates in a way to reduced stability in the vicinity of the riverbed scarp.

Sensitivity studies
The effect of changing the c_{uR}/c_u – ratios from 0.35 – 0.20 to 0.40 – 0.25 is evidenced by the numbers given in Table 5.2.3 above. The maximum earth pressure only decreases from 4969 kN/m in Case I to 4554 kN/m in Case II, i.e. by a factor of 0.92, (i.e. by 8 %), whereas the length of the potential passive zone is substantially reduced from 420 m to 234 m.

However, for values of $c_{uR}/c_u > 0.6$ as in Case III, the value of E_{max} no longer exceeds $E_{Rankine}$ implying that global failure with excessive heave of the passive zone would not likely take place. Instead a 'Rävekärr type' of earth displacement would have occurred.

The effect on the global failure condition of doubling the mean elastic modulus ($E_{el,mean}$) – i.e. reducing the compressibility of the potentially sliding soil mass by 50 % – is insignificant as far as the maximum horizontal thrust is concerned. The effect on the length of the passive zone in heave is moderate.
Thus for c_{uR}/c_u = 0.40 to 0.25, and $E_{el,mean}$= 400 c_u instead of 200 c_u, the following values are obtained:
E_{max} becomes 4558 kN/m instead of 4554 kN/m, and
$L_{E>E(Rankine)}$ becomes 225 m instead of 265 m.

5.26 Conclusions from the progressive failure computations
The following conclusions may be drawn from the progressive failure FDM-analysis:

a) The critical force (N_{cr}) corresponding to full mobilization of the shear capacity in the steep part of the slope was remarkably small, and may very well have been exceeded by the impact of the ongoing piling activity and/or local placement of even a minor earth fill.
(Cf Table 5.2.2 and Figure 5:2.7).

Consider for instance the possible existence of an inclining local layer of cohesion-less soil in the steepest part of the slope where driving of prefabricated piles was going on, and that this activity generated an increase of pore water pressure in this layer of $\gamma_{H2O}\cdot\Delta H$ kN/m^2.
(Cf in this context Section 9.22, (Figure 9:2.2)
Taking the angle of internal friction in the soil layer to be φ, the temporary loss of effective shear resistance would be at least $\Delta c = 10\cdot\Delta H\cdot\tan\varphi$ kN/m^2. If the stirred layer of cohesion-less material measures ΔL m in the slope direction, the corresponding additional load acting downhill would be $\Delta N = \Delta L\cdot 10\cdot\Delta H\cdot\tan\varphi$ kN/m. Hence, the pore water pressure increase related to the critical force N_{cr} would amount to:
$\Delta H = N_{cr}/(10\cdot\Delta L\cdot\tan\varphi)$ m
Assuming $\varphi = 30^o$ and ΔL = 15 m (about size of the family house for which piles were being driven), the pore pressure rise corresponding to N_{cr} = 275 kN/m (according to Table 5.2.2) is:
$\Delta H = 275/(10\cdot 15\cdot\tan 30) \approx 3.18$ m.
Thus, according to the Pr F-analysis, a rise of the piezo-metric head of some 3.2 m in the area affected by piling would have been sufficient to set off the Surte slide. According to experience from actual measurements of the rise of piezo-metric head in connection with piling operations considerably higher values than 3.2 m are usually observed.

b) The limited length of mobilization of shear stress, defined as L_{cr} in Figure 3:3.3, is conducive to the formation of progressive failure planes following firm bottom or firmer sediments – i.e. in direction A-B-D-F in Figure 5:2.7 – instead of passive failure planes directly to ground surface such as A-B-C and A-B-D-E in the same figure.
Or to phrase it differently, the example emphasizes the issue dealt with in Section 4.6 that – in soft deformation-softening clays – slip-circular failures do not readily develop and surface in sloping ground. (Cf Bernander (1981b).
The striking discrepancy, demonstrated in Figure 5:2.7, between the results of the ideal-plastic equilibrium approach on the one hand, and the FDM-analyses considering combined deformation and deformation-softening on the other, clearly stands out as the main reason why downhill progressive slides of the type dealt with in this document have been difficult to explain convincingly by means of conventional methods of analyzing slope stability.
For instance, even with the high c_{uR}/c value of 0.80, as in disturbance Condition I, the ratio between $q_{cr\,(ABDF)}$ and $q_{cr\,(ABC)}$ still only amounts to 0.23. (Cf Bernander, 2008, Appendix B).

c) The static redistribution and build-up of earth pressures in the progressive phase of the initial slide were sufficient to make the slide propagate all the way to the Göta River. (Cf Figure 5:2.8 and Table 5.2.3).

However, obviously, dynamic forces in the final break-down phase (Phase 5) are liable to extend the passive zone and enhance the heave effect as shown in Figures 5:1.16 and 5:1.17.

The analyses also emphasize the fact that the different consecutive phases of progressive landslide failure must be dealt with separately and not as one singular case of static equilibrium. (Cf Section 3.3 and Bernander, (2000), Chapter 3.2).

The mentioned investigatory reports by Jakobson (1952a) and Caldenius & Lundström (1956) make no reference to any earth fills on the pile driving site, a situation that nonetheless is plausible as such. As shown in Figure 5:2.7, even a minor fill could, depending largely on the size of the loaded area, have been a contributing factor to the initiation of the slide.

However, at the time of the slide event, prefabricated concrete piles were, as already stated, being driven in the steepest portion of the slope (i.e. in Point P in Figure 5:2.4).
The estimates made in item **a)** above, indicate that the impact of the ongoing piling activity alone was quite sufficient to generate the critical degree of additional disturbance in terms of a temporary increase of the hydraulic head.
Sensitivity analyses based on reasonable variation of the crucial parameters indicate that, once the initial local failure at the pile driving site had formed, the stability of the entire slope was inexorably lost. **([9])**

The Surte slide may readily be explained as a fully developed progressive failure of the kind described in Sections 3 and 4. The dynamic phases (Phases 3 and 5) of the slide event may be understood as having been similar to those depicted in Figures 5:1.9 to 5:1.17 related to the Tuve slide described in Section 5.1.

([9]) (Note: To the reader, who may find the progressive FDM failure analysis made as somewhat arbitrary as regards the different assumptions made in respect of the shear/deformation properties of the clay, it may be emphasized that the characteristic outcome of the Pr F-analysis, compared to the I-PlF-analysis, mainly relates to the fact that the deformations in the soil mass are considered in the computations. Many of the important issues are namely remarkably insensitive to moderate variation of properties such as $\gamma_{el,}$ γ_f, δ_{cr}, and within reason even to the ratios of c_R/c_∞, c_R/c and c_{uR}/c_u. The impact of varying the properties of deformation-softening clays have been demonstrated in numerous exemplifications in Bernander, (2008), Appendices A and B.

Final comment to the Surte slide event
A primary objective of the FDM-analysis made of the Surte slide has been to demonstrate the impact of applying an analysis accounting for the differing deformations and the related deformation-softening in the sliding soil mass.
Another important objective was to highlight how even a local, seemingly trivial disturbance in a vulnerable part of the slope, had the potential of developing into a great disaster, massively destabilizing about 240 000 m^2 of ground that had remained stable for thousands of years.
And yet, hypothetically, the slope may have remained stable to this day if the piling job had not taken place, or if it had been carried out in a different way.

5.3 The landslide at Bekkelaget (1953), Norway

The landslide at Bekkelaget, close to the Oslo fjord, has been documented by Eide & Bjerrum (1954, 1955). The slide, which took place in quick clay, encompassed some 20 000 m^2 of ground, of which about 70 % had a surface gradient of only 2 to 3° in the north-easterly direction towards the fjord. The event was triggered by the placement of an earth fill designed to widen an existing road running parallel to a railway track.

Figure 5:3.1 presents the major features of the slide area and the computed safety factors for three of the investigated slip surfaces as reported by Aas (1983). The safety factors for the shortest and the longest failure surfaces are defined as 0.87 and 1.32 respectively.

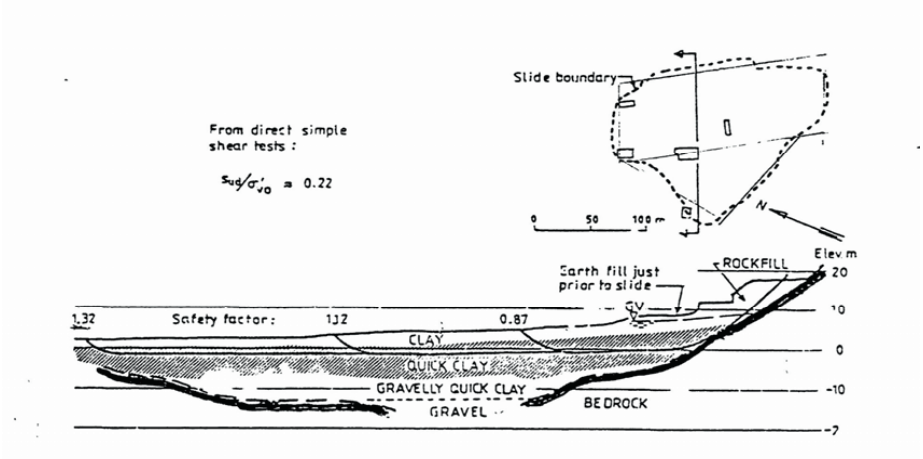

Figure 5:3.1 Main characteristics of the slide at Bekkelaget, Norway. Computed safety factors for three different potential failure surfaces. (Aas, 1983).

The odd circumstance here, from a conventional design point of view, is the fact that the slide actually developed along the ≈ 200 m long failure surface having a safety factor 1.52 times greater than that for shortest one. This is obviously entirely inconsistent with the prevalent plastic equilibrium approach used for slope stability analysis – suggesting that applying the same in long slopes of soft sensitive clays is actually not justified. (Cf e.g. Table 5.7.1.)

By contrast, the current phenomenon is explicitly predicted by the progressive failure FDM-analyses as per Section 4 when applied to slopes of deformation-softening clays. This approach also highlights the fact that the resistance along failure planes following firm bottom (or firmer sedimentary layers) will, in strain-softening soils, normally be considerably smaller than the resistance along short failure planes surfacing in sloping ground closer to the local additional load. (Cf Eq. 3:3, Figures 4:6.1 and 5:2.7.)

Hence, a specific lesson to be learnt from the Bekkelaget slide (and many others) is – with special reference to road construction – that the widespread practice of placing earth fills, designed to balance the weight of a road embankment, is a notoriously risky arrangement, as it is inherently likely to cause far greater inconvenience than the one intended to be avoided by the supporting fill. In highly deformation-softening soils, this applies even when the slope gradient is small. The Bekkelaget slide clearly accentuates the importance of progressive failure analysis for the assessment of slide hazard in slopes with sensitive clays.

5.4 The landslide at Rollsbo (1967), Sweden

A landslide involving some 20 000 m^2 of ground took place in 1967 at Rollsbo, some 20 km north of Gothenburg. Figure 5:4.1 shows a section through the slide. Although conventional calculations based on I-PlFA indicated a minimum safety factor of 2.3, the slide was triggered while sand drains were being driven at the up-slope end of the area involved in the slide.

The slide is of particular interest because both the sand drain driving operations and the soil conditions – before as well as after the slide event – were well documented. In view of the soil conditions, the triggering agent and the specific features of this slide, there is little doubt about this slide being a clear case of a downhill progressive failure.

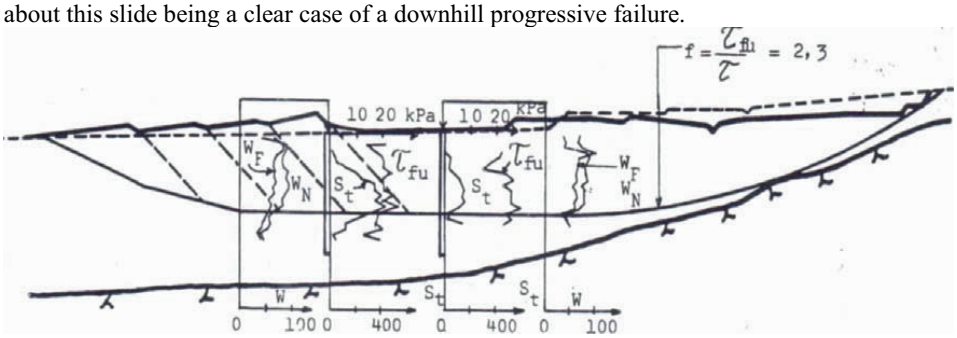

Figure 5:4.1 Section through the landslide at Rollsbo, (Kungälv), 1967

5.5 The slide movement at Rävekärr (1971), Sweden

5.51 Description of the site and the slide movement

The slide took place at Rävekärr, 8 km South of Gothenburg in the gently sloping ground of a side valley opening out into the Mölndal River valley. Figure 5:5.1 shows a plan and a representative section of the 550 m wide slide area.

This slide movement has been mentioned earlier in the document because of its specific and notable features. It serves as an unusually well documented example of what can be denoted as an 'un-finished slide' – i.e. a slide in which passive earth pressure resistance has not been exceeded in the lower part of the area involved.

It is also a striking example of the extreme sensibility of some slopes in south-western Sweden to potential disturbance from driving of soil displacing piles.

Thus, in 1971 a minor piling project for a family house was started. When the sixth pile was being driven a crack in the ground suddenly appeared. The crack propagated at a speed, judged by an eyewitness to be about the pace of a running person, some 130 m northwards, where it halted against an outcrop of firm ground. In the opposite direction, the crack in the ground passed through an area of family housing following the contour lines of the slope and came to a stop some 420 m from where it had started.

The final width of the crack and the related vertical off-set due to local active failure was only 0.2 to 0.3 m. The total area, subject to documented down-slope displacement in this order of magnitude, was about 150 000 m^2.

5.52 Interpretation of the slide in terms of progressive failure development

The interpretation of the evolution of the slide considering the progressive failure mode described in the preceding sections of this document is as follows:

- Although the ground down-slope of the crack was somewhat displaced, no passive zone with associated heave was observed, implying that the crack originated from deformations related to the redistribution of stresses and earth pressures in accordance with the dynamic phase (Phase 3) of a progressive failure, as described in Section 3.3. Before the slide event, elevated ground up-slope had essentially been stabilized by shear forces. The redistribution in Phase 3 meant that the up-slope loss of shear strength was compensated by a corresponding build-up of earth pressures in the down-slope area. Hence, the documented displacements forming the slide relate to this transfer of forces of a virtually dynamic nature.

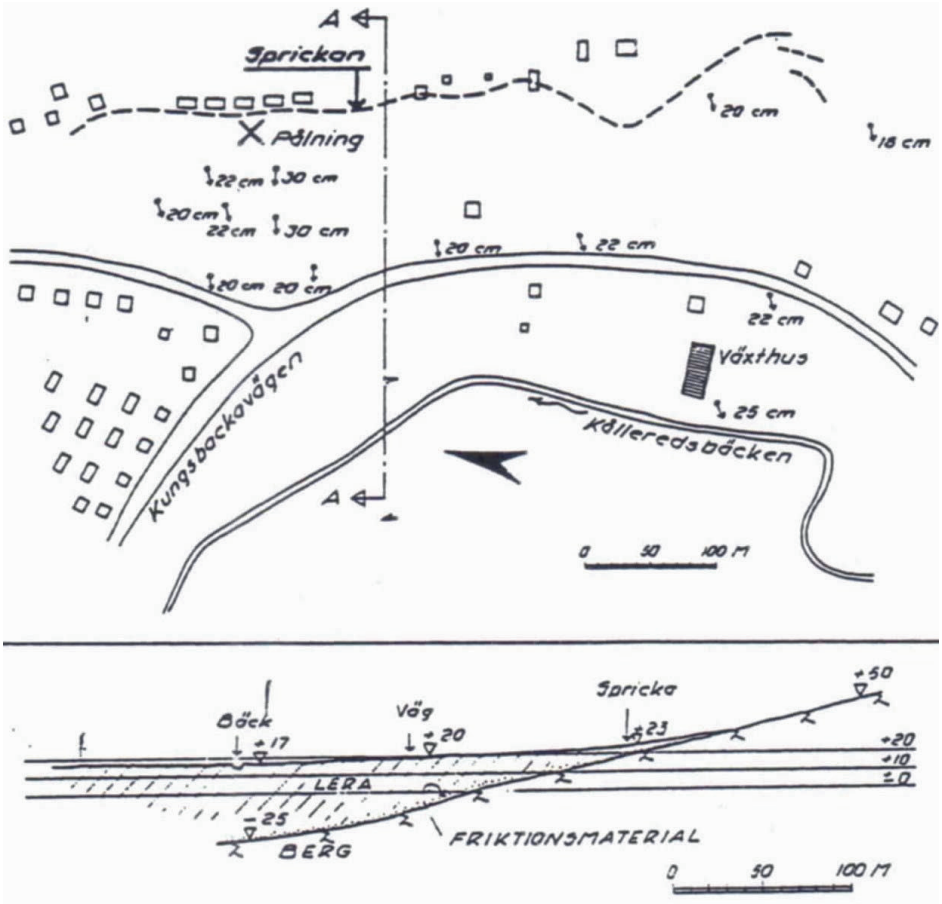

Figure 5: 5.1 Section through slide area at Rävekärr. Observe the gentle slope gradient. Slip surfaces were documented at depths of 5 -7 m in the upper part of the slide and angular deformations were recorded at 13 m and 33 m depth in the lower parts of the valley. Pile driving took place at the point marked **x.** (Löfquist 1973). Legend: Pålning = Pile driving, Bäck = Creek, Väg = Road, Spricka = Crack, Lera = Clay, Berg = Rock, Friktion = Friction.

- Hence, referring to Section 3.3, the slide at Rävekärr represents a case, where the earth pressure increase in the 'post progressive' state of equilibrium (Phase 4) remained smaller than the passive Rankine resistance at the foot of the slope, as defined by Equation 3:5a in Section 3.
This specific condition, i.e. $(E_o+N)_{max} < E_{Rankine}$, was manifestly confirmed by computations based on the current FDM-approach.

Discussion
The slide movement at Rävekärr was reported by Löfquist, (1973). Löfquist classified the slide as a 'clay slide by hydraulic uplift', i.e. caused by reduced vertical effective stresses in the clay or in seams of silt and silty sand. Löfquist's explanation may have some relevance to the initiation zone of the slide, as the soil profiles at the crack location contained discrete seams of moraine out-wash that had contaminated the clay during the sedimentation process.

However, the area actually affected by the piling activity can be estimated at some 100 m^2, which is only a minute fraction (i.e.1/1500) of the total area of about 150 000 m^2 involved in the slide. In view of this, and the fact that the slope had existed for centuries it seems very unlikely that high artesian conditions in the entire slide area constituted a major agent in the earth movement. If that had been the case, the slide would, in all probability, have taken place long before at some previous extreme hydrological situation in the past and not at the precise point of time when a few piles were being driven. (Cf in this context Note **([5])** in Section 5.23) Yet, Löfquist maintained, rightly in principle, that high pore water pressures due to intense rainfall or piling operations may be conducive to slope failure.

In his appraisal, Löfquist presents an aspect on slide mechanisms of a rather speculative nature. His notion of progressive degradation of soil strength over time due to creep deformation does not apply to normally or slightly over-consolidated clays. It disregards, for instance, the effects of re-consolidation and the basic behaviour of soft cohesive and cohesion-less soils, as documented by consolidated/un-drained direct shear tests, (CU-DSS tests).

However, back-analyses according to the FDM-method described in Section 4 show that the documented crack width (δ_{cr}), associated displacements and the down-slope earth pressure condition (i.e. $(E_o+N)/E_{Rankine} < 1$) can readily be explained by the progressive failure FDM-analysis used in this document.

It does not therefore seem necessary to resort to unlikely events such as a sudden rise of pore water pressure in possibly existing silt layers all over 15 hectares of ground, solely due to pile driving in minute corner of the vast area involved in the slide.
Moreover, continuous silt or sand layers in the soil profile, consistent with the dimensions of the slide area, were not documented. Nor were any exceptionally high pore water pressure conditions recorded at the time of the slide event.

The observed velocity, at which the crack propagated parallel to the contour lines, offers an interesting clue to the time scale of Pr F formation, i.e. as to how fast the related stress redistribution wave can travel down the slope. Hence, the slide at Rävekärr indicates that the time range for progressive failure of this type to take place can be a matter of tens of seconds or a few minutes.

Conclusion
The ground movement at Rävekärr may be classified as an 'unfinished landslide' where, owing to the low slope gradient and/or moderate sensitivity of the soil, the progressive failure did not terminate in massive upheaval of the passive zone in Rankine failure.

Furthermore, the slide confirms pile driving activity as being a well documented triggering agent in progressive landslide formation – a condition with specific bearing on the Surte slide.

5.51 Other 'unfinished slides' in Gothenburg suspected of being of a similar nature:
On September 28, 1905, a similar almost 1 km long crack is reported to have formed from Klockaregården in the north to Ättestupan in the south, not far from a hill called Ramberget on the island of Hisingen, Gothenburg. Many houses were damaged by ground subsidence.

Another unfinished slide of this kind, causing a crack, 50 to 100 mm wide and about 150 m long, occurred at the Björlanda Road (Hisingen) in Gothenburg proper in 1972. Also, in this case, the ground movement was triggered by pile driving activity in the outskirts of the slide area.

5.6 The landslide at Tre-styckevattnet (1990), Sweden.

5.61 Description of the site and of the slide
About 80 km north of Gothenburg, not far from the city of Uddevalla, another slide exhibiting the typical features of progressive failure formation took place in connection with the construction of a berm designed to provide additional stability to an embankment for the E6 highway.

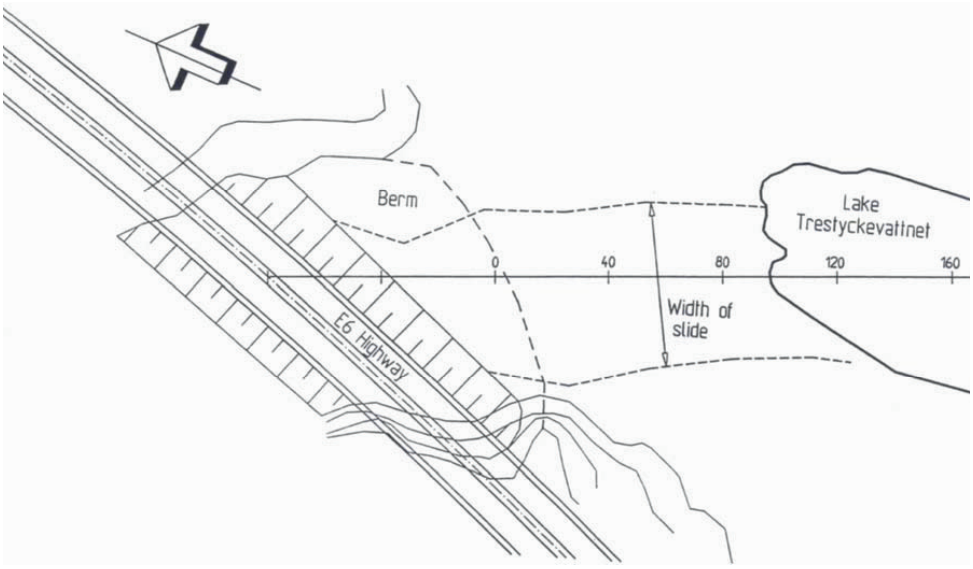

Figure 5:6.1 Plan of the slide area also indicating the position of the longitudinal section shown in Figure 5:6.2. The slide measured about 70 m in width and at least 140 m in length.

Figure 5:6.1 shows a plan view of the slide area and Figure 5:6.2 exhibits a section of the slide. The ground, above the water level of the lake 'Tre-styckevattnet', actually involved in the slide measured about 70 m in width and visibly 140 m in length. How far the slide extended into the lake was not investigated. The lateral boundaries of the slide were essentially parallel.
The original ground surface gradient from the toe of the highway embankment to the shore of the lake was uniform and remarkably small (≈ 1°), thus strongly indicating that the cause of the slide was related to the ongoing construction work rather than to inherent instability.

The embankment for the highway proper was not involved in the slide, as it had been founded on a compacted rock waste fill, replacing excavated loose soils down to competent base.
The roughly 5 m high supporting bank (or berm) had been placed already in the fall of 1989 but was completed about a year later by adding a layer of topsoil for vegetation. The topsoil was placed using bulldozers and compacted by means of a heavy vibratory roller.

It was at this point, when only two or three loads of topsoil remained to be levelled and compacted that the slide occurred.

5.62 Interpretation of the slide in respect of initiation and development

The heavy berm had thus remained stable for more than a year, and during this period the underlying soil had been subject to drainage and consolidation. It seems, therefore, very unlikely that the slide was initiated solely by the weight of the thin layer of humus-rich top-soil, constituting only some 5 % of the total weight of fill that had already been placed more than a year before. Hence, the impact of the heavy vibratory roller on the subsoil is assumed to have been the triggering agent in the slide initiation process.

However, the cardinal issue here is that the failure mode was not compatible with ideal-plastic equilibrium analysis, according to which the critical failure mode would follow a slip surface of the kind indicated by the curved line ABC in Figure 5:6.2. Instead, at least 140 m of almost horizontal ground was displaced towards the lake, thus overcoming not only the resistance along the horizontal slip surface but also the lateral shear resistance mobilized in the two 140 m long sides of the sliding soil volume.
Although no casualties or damage to housing resulted from the slide, a group of geotechnical engineers involved in the road project decided that the unusual features and circumstances of the slide merited closer investigation. The group included representatives of the following bodies:
The Swedish Geotechnical Institute, SGI, (Gothenburg department),
The Swedish National Road Administration, KM Consulting AB, (Ltd) and
Skanska Teknik AB, (Ltd) (Contractor's Engineering Division).

It was agreed within the group that the slide area should be surveyed and that sufficient documentation of the ground profile and of soil properties should be secured immediately in order to allow future studies of the slide.

Soil conditions
The vegetation in the slide area consisted of full-grown pine and spruce, some of which had been felled in connection with the construction of the highway. Under a top layer of humus, the soil consisted of peat to a depth varying between 4 and 7 m, the smallest value being valid at the front edge of the berm.

The soil underlying the peat was soft sensitive clay with water content almost invariably of about 60 %, yet with some local peaks of approximately 70 %. The liquid limit in the failure zone was typically 40 to 47 %. In two bore holes located about 80 m from the edge of the berm, the liquid limit at the critical level was locally as low as 25 % in layers classified as sandy respectively silty clay. The sensitivity number (cone tests) in the failure zone varied between 90 and 103 with an estimated mean value of 95 indicating marked deformation-softening properties.
The depth to firm bottom below the clay formation varied from 13 m to 20 m, the lower value applying near the front edge of the berm.

Progressive failure analysis
The failure zone was identified by the conspicuous drops in the sensitivity of the tested clay samples and was deemed to be located in the upper strata of the sensitive clay formation. The depth of the slip surface below ground level was thus about 7 m. The following input data were assumed for the Pr F analysis: **([10])**

The in situ state condition:
$c_\infty/c = 0.94$ $\gamma_{el} = 2.5\ \%$ $\gamma_f = 7.5\ \%$, $\delta_{cr} = 0.3$ m, $G_{el,o} = \tau_{el}/\gamma_{el} = 200$ kN/m^2
$c^* = 9.9$ kN/m^2 $\tau_{el} = 5.0$ kN/m^2 $E_{el,o} = 60 \cdot c_{\infty,mean} = 600$ kN/m^2
The disturbance condition:
$c_R/c = 0.80$ $\gamma_{el} = 2\ \%$ $\gamma_f = 5.5\ \%$, $\delta_{cr} = 0.3$ m, $G_{el,o} = \tau_{el}/\gamma_{el} = 275$ kN/m^2
$c^* = 11.0$ kN/m^2 $\tau_{el} = 7$ kN/m^2 $E_{el,o} = 75 \cdot c_{,mean} = 825$ kN/m^2

The global failure condition:
$c_R/c_u = 0.40$ $\gamma_{el} = 1\ \%$ $\gamma_f = 3\ \%$, $\delta_{cr} = 0.3$ m, $G_{el,o} = \tau_{el}/\gamma_{el} = 700$ kN/m^2
c_u ** $= 14$ kN/m^2 $\tau_{el} = 7$ kN/m^2 $E_{el,o} = 150 \cdot c_{u,mean} = 2100$ kN/m^2

* Mean values applying to the initiation zone.
** Mean value applying to the extended failure zone.

([10]) In all calculations in Section 5, the curved portion of the constitutive relationship from γ_{el} to γ_f is a parabolic function to the power of 2 with vertex at (c_{max},γ_f) and connecting tangentially at (τ_{el}, γ_{el}).

5.63 Outcome of progressive failure computations
The in situ state:
$c_R/c_\infty = 1.00$ $N_{cr} =$ --- kN/m $L_{cr} = 144$ m $E_o = 661$ kN/m, $K_o^{max} = 1.84$
c_∞ * $= 9.9$ kN/m^2 $c_R = 9.9$ kN/m^2

As may be concluded from the relationship between Curve A and Curve D in Figure 5:6.2, the Pr F-analysis performed indicates that the slope was 'globally' stable after the placement of the earth berm – the term 'global failure' being used in the sense defined in this document for the final phases of progressive failure.
However, passive Rankine resistance was exceeded over a distance of some 50 m ahead of the toe of the fill. It therefore seems likely that the ground surface actually heaved in passive failure already when the fill was being placed in 1989.
Yet, this phenomenon may have been very gradual, thus escaping much attention.
Measurements after the slide documented a heave of the ground in this area of about 1 m, but it has not been established if this upheaval existed before the final global slide in 1990 or not.

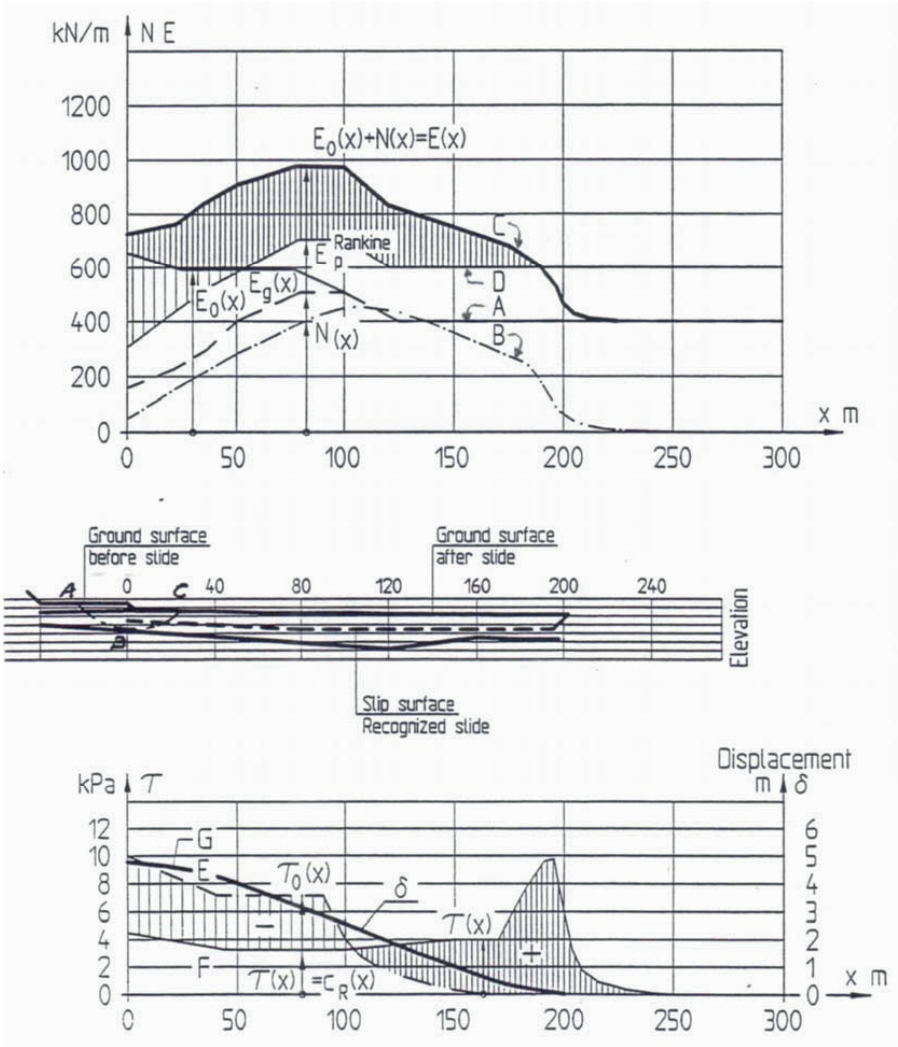

Curve A, $E_o(x)$ = In situ earth pressure prior to placing of topsoil layer, kN/m
Curve B, $N(x)$ = Earth pressure increment due to Pr F redistribution, kN/m
Curve C, $E(x)$ = $E_o(x)$ + $N(x)$ = Total earth pressure after Pr F redistribution, kN/m
Curve D, $E_p^{Rankine}$ = Passive Rankine resistance, kN/m
Curve E, $\tau_{o(x)}$ = In situ shear stress distribution before progressive failure, kN/m^2
Curve F, $\tau_{(x)}$ = Shear stress distribution after progressive failure, kN/m^2
Curve G, δ = Displacement, m

Figure 5:6.2 Shear stress and static earth pressure distribution (Phase 4) in the slide at Trestycke-vattnet subsequent to the progressive failure phase but prior to the global failure (Phase 5). The figure indicates that the spread of the passive zone over almost horizontal ground can be ascribed solely to the build-up of static forces developed in progressive Phase 3 of the ground movement as explained in Section 3.3.

An explanation as to why the ground resistance had actually been higher than the computed values may be the fact that the peat formation was heavily interlaced with thick roots from tall pine and spruce trees, thus strongly reinforcing the inherently weak peat layer. This condition was evidenced along the lateral boundaries of the slide, where thick broken roots protruded from the exposed surfaces.

Furthermore, the viscous character of the peat layer may have effectively mitigated the effects of strain concentration and of uneven force transmission to the underlying sensitive clay stratum. Anyway, the ground remained in fact stable for more than a year.

It may be noted in this context that, as in the Bekkelaget case, safety factors based on conventional plastic failure analysis of short slip circles surfacing close to the berm limit proved to be less than 1.0. Nevertheless, failure took place along a plane more than 140 m of length.

The disturbance condition:

$c_R / c = 0.80$ $N_{cr} = 40$ kN/m $L_{cr} = 95$ m $E_o = 661$ kN/m $E_o + N = 701$ kN/m
$c^* = 11$ kN/m^2 $c_R = 8.8$ kN/m^2 $F_s = N_{cr} / N_i \approx 1.0$

The critical load according to the Pr F analysis required to trigger the planar progressive failure is $N_{cr} = 40$ kN/m. Assuming un-drained conditions, this corresponds to a distributed surface load of $q_{cr} \approx 6.7$ kN/m^2 that in turn equals the weight of a soil layer of about 0.4 m.

The global failure condition:

$c_R / c_u = 0.40$ $N_{max} = 448$ kN/m $L_{Rankine} = 300$ m, $E_{max} = E_o + N_{80} = 972$ kN/m
c_u ** $= 14$ kN/m^2 $L_{N,max} = 104$ m $E_{Rankine} = 700$ kN/m $L_{E,max} = 80$ m
$c_R = 5.6$ kN/m^2 $F_s = E_{Rankine} / E_{,mx} = 0.72$

* Mean values applying to the initiation zone.
** Mean value applying to the extended failure zone.

Figure 5:6.2 shows shear stresses and earth pressures before and after progressive failure has taken place. As mentioned, Curve A representing the in situ condition indicates a low factor of safety already before the application and compaction of the topsoil layer.
These activities apparently induced deformations entailing softening of the clay below and down-slope of the berm, so that the residual shear strength dropped below 0.8 c_R – i.e. the value used for the disturbance condition.
A further gradual drop in shear strength to e.g. 0.4 c_R would according to the analysis by a wide margin explain the remarkable spread of the slide all the way down into the lake.

The fact that most of the sliding soil consisted of peat makes it difficult to estimate the correct compressibility of the material in terms of an E-modulus for the global failure analysis. The chosen values, which would apply to very soft clay, may therefore seem to be too high. However, using lower values of the E-modulus would according to the FDM-analysis only further promote the prospect of global failure.

5.64 Conclusive remarks

The progressive failure analysis suggests that the slide at Tre-styckevattnet was initiated already in the final stages of constructing the berm in 1989. However, for reasons given above, the slope remained globally stable until the topsoil layer was placed more than a year later.

The safety factor at this stage being close to 1.0, the application of the comparatively insignificant weight of the 0.3 m thick topsoil layer critically reduced the safety margin – thus increasing the risk of local failure.

However, the slide event actually coincided with ongoing compaction of the top-soil layer on the berm using heavy vibratory equipment. This activity, therefore, stands out as the disturbance agent that triggered the initial failure (Phase 2). The ensuing global slide, i.e. Phase 4, presumably extended far into lake Tre-styckevattnet.

As already mentioned, the safety factor based on conventional slip circle analysis near the fill was also less than 1. However, the crucial issue in this context is the fact that the slide did not develop along any kind of local slip circle such as ABC in Figure 5:6.2. Instead, an area of at least 150 by 70 m^2 of ground above the water level in the lake was displaced.

This is a condition highlighting the inadequacy of conventional ideal-plastic failure analysis for predicting the development, events and outcome of landslides in strain-softening clays.

5.6a The landslide at Småröd (2006), Sweden

On December 20, 2006, a large slide took place in Småröd south of Munkedal in western Sweden. Several hundred meters of road E6, the railway and Taske stream were destroyed, IIG-SNRA (2007), Nordal et al (2008). A progressive failure analysis according to the methods presented in this document was in good agreement with these after-slide investigation, Bernander (2007, 2008).

5.7 Triggering Agents

In the preceding sections, evidence is given of comprehensive slope failures having been triggered by local instability due to human activities such as pile driving, construction of embankments, compaction with heavy equipment etc. The impact of triggering agents of this kind is therefore of cardinal importance when assessing the risk of failure in slopes of sensitive clay.

Notable examples of downhill progressive landslides in soft sensitive clays are presented in Table 5.7.1. The listed slides are all typical of the kind of massive spread slope failures that have frequently occurred in the soft sensitive clays of Scandinavia. They generally exhibit the following characteristics – some of which can be deduced directly from items in the table.

- The landslides in question have occurred in long natural slopes that had remained stable during millennia. Nonetheless, they have all been destabilized by some – in view of the extensive and disastrous consequences – seemingly trivial human factor.

Figure 5.7.1 represents a typical example of this phenomenon, where a minor local fill (only a few meters wide) triggered a 150 m long landslide in connection with the widening of a narrow road bank.

It is thus important to note that the listed landslides all relate in some way to human activities, mostly in connection with road construction or operations involving some sort of dynamic impact. The listed events – possibly excepting the Tuve slide – are directly linked with either stock-piling of earth or rock debris, placing of supporting embankments, pile-driving, use of vibratory equipment or rock blasting.**([11])**

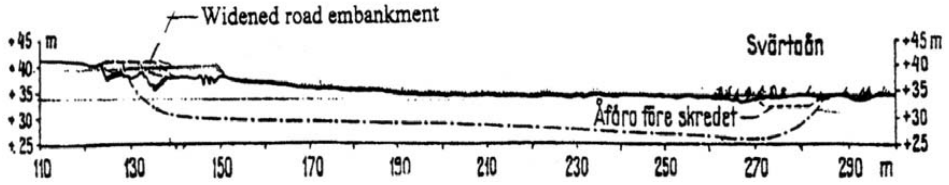

Figure 5.7.1 The landslide at the Svärta River (Sweden) 1938 featuring typical traits in the slides listed in Table 5.7.1. Bygg (1972).

Analysis considering strain and deformation in a sensitive soil predicts that placing of a load in sloping ground inexorably brings about displacements in the downhill direction. This movement in turn inevitably generates extension and cracking under – and in particular behind (i.e. up-slope of) – the additional load as illustrated in Figure 5:7.2.

Table 5.7.1 ***Examples of down-hill progressive landslides.***

Locality	**Year**	**Slide length [m]**	**Area [hec-tares]**	**Triggering agent**
The Svärta River	1938	160	2	Local road embankment (Cf figure)
Surte	1950	600	24	Pile driving for a family house
Beckelaget, Norway	1953	160	2	Widening of railway bank up-slope
Rollsbo Kungälv, Sweden	1967		2	Driving of pipes for sand drains
Rödbo, Kungälv Municipalaty	1968		1	Stock piling of blasted rock
Jordbro, V:a Haninge	1972			Local up-slope earth fill
Rävekärr, Mölndal	1971	≈300	15	Pile driving for a family house
Sem, Norway	1974	120		Local earth fill up-slope
Tuve, Göteborg ([11])	1977	800	26	Widening of road embankment etc
Rissa, Norway, slide C ([12])	1978	800	27	Retrogressive initial slide
Kotmale dam site, Sri Lanka	1981	500	9	Stockpiling of concrete aggregate
Trestyckevattnet, Uddevalla	1990	400	2	Vibration of road embankment
Saint-Fabien, Quebec, Canada	2004			Widening of an up-slope railway embankment
Småröd, Munkedal	2006	230	ca 10	Local up-slope earth fill
Namsos, Norway	2009			Rock blasting

([11]) The Tuve slide may differ somewhat in this respect but according to SGI-Report No 18 (1982), the causes attributed to the Tuve slide were disturbances generated by elevated ground water pressures in combination with the weight of an additional road embankment constructed some years before the slide event. Man-made changes of the hydrological regime due to urbanization further up-slope were believed to have contributed to elevated pore water pressures and due local instability. Hence, also for the Tuve slide, it may be concluded that human activity was an important triggering factor.

([12]) Slide C in Rissa was initiated by a retrogressive slide caused by human activity, (Gregersen 1981).

As regards available information and experience of the impact of precipitation on extensive slides in long natural slopes, the following may be concluded:

- The actual slide event may, or may not, coincide with high precipitation – and certainly not by necessity with highly extreme rainfall conditions. Generally, these slopes had been stable over very long periods of time, and in all probability been exposed to extreme peak pore water pressure situations in the past. In none of the cases presented, precipitation was likely, or was documented, to have been more exceptional than ever before in the history of the slope.

- Hence, the impact of heavy rainfall under long-time undisturbed in-situ conditions appears to constitute a secondary factor for the incidence of slides of the current type.

Yet, many of the listed slides have actually occurred during spells of abundant and continuous rainfall. However, for reasons given below, this is notably due to quite different phenomena that, nevertheless, are still related to human activity.

- The effects of long spells of raining are – in the current context – much more likely to be related to destabilizing forces, acting in temporarily water-filled cracks (above the normal ground water level) in the incipient active zone, rather than to the incidence of e.g. a 1000-year extreme pore water pressure acting in some deep layer in the ground soil profile.

- Furthermore, when a fill such as the one shown in Figure 5:7.2 is saturated because of abundant and prolonged raining, two additional aggravating conditions come about:

a) The weight of the fill is substantially increased by saturation. For instance, if the pore volume of non-compacted soil is e.g. 40 %, the weight of the fill will be raised by 4 kN/m^3

b) The horizontal 'splitting' active earth pressure in the fill that taken alone may constitute a major destabilizing agent will in a saturated state increase by a value in the order of $\Delta F_2 = \gamma_{H2O} \cdot H^2/2$, where H is the height from top of the fill to ground surface.

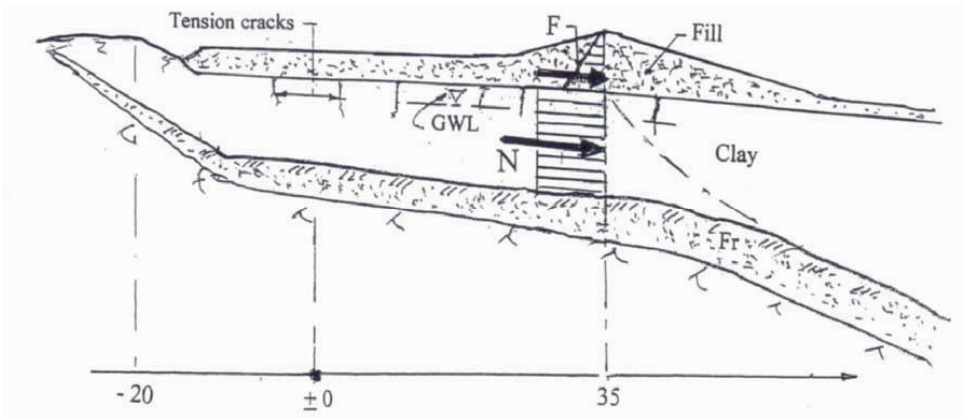

Figur 5:7.2 Destabilizing 'splitting' forces, partly from active earth pressures within the fill and partly from hydraulic water pressure due to saturation. Furthermore, water-filled cracks in the active zone above ground water level can under rain of long duration function as veritable destabilizing 'jacks' acting in the down-slope direction. In addition, also the weight increase of the bank due to water saturation has to be considered. The chosen section depicts the conditions presumed to have caused the great Småröd slide in December 2006. (Cf Bernander (2008) and Section 5.6a.)

c) Water-filled cracks in the active zone above the ground water level can, under ample persistent raining, function as veritable destabilizing 'jacks' acting forcefully in the downhill direction.

Exemplification

Incidentally, the fill depicted in Figure 5:7.2 actually corresponds to the embankment, which is believed to have set off the slide at Småröd about 80 km North of Gothenburg in December 2006. (Cf Bernander, 2008, Chapter 1, Introduction.)

Assuming that the porosity of the non-compacted fill was e.g. 38 % renders a dry density of 16.5 kN/m^3, and a corresponding wet density in saturated state of $\gamma^{wet} = 20.3$ kN/m^3. The mean height of the fill above ground surface (in the central part) is taken to be $H \approx 4$ m (with a peak value of 5 m). The depth to ground water level (GWL) ΔH is 2 m.

Dry conditions

The splitting active earth pressure within the fill will then be in the order of

$\Delta F_1 \approx 0.3 \cdot \gamma^d \cdot H^2/2 = 0.3 \cdot 16.5 \cdot 4^2/2 \approx 39.6$ kN/m

The down-slope load acting on underlying clay layers due to the weight of fill will, assuming a mean fill height of 4 m, correspond to a destabilizing load of

$N^d = 4{,}0 \cdot \gamma^d \cdot D$, where D the depth of the clay layers below ground surface.

Thus if D = 8 m, $N^d = 4.0 \cdot 16.5 \cdot 8 = 528$ kN/m

The total horizontal destabilizing load due to fill under dry conditions is then

$F_{total,dry} = \Delta F_1 + N^d = 39.6 + 528 = 567.6$ kN/m

Wet (saturated) fill conditions

The splitting destabilizing force F in fully saturated fill can approximately amount to

$\Delta F_2 \approx 0.3 \cdot \gamma^1 \cdot H^2/2 + \gamma^{H2O} \cdot H^2/2 = 0.3 \cdot (20.3\text{–}10) \cdot 4^2/2 + 10 \cdot 4^2/2 \approx 104.7$ kN/m

The downhill load due to the wet weight of fill, acting on underlying clay layers, will in a similar way correspond to a destabilizing load

$N^{wet} = 4.0 \cdot \gamma^{wet} \cdot D = 4.0 \cdot 20.3 \cdot 8 = 649.6$ kN/m

$F_{total,wet} = \Delta F_2 + N^{wet} = 104.7 + 649.6 = 754.3$ kN/m

The change of the horizontal destabilizing force F_{total} resulting from full saturation of the fill is then:

$\Delta F_{total} = 754.3 - 567.6 = 186.7$ kN/m

Assuming for instance that the width of the supporting embankment is 40 m, the total *increase* due to saturation ($b \cdot \Delta F_{total}$) can amount to:

$\Delta F_{total} = 40 \cdot 186.7 = 7468$ kN

Hence, full saturation entails a substantial increase of the destabilizing force related to the fill of 7468 kN, i.e. an increase of 33 % of the corresponding force under dry conditions.

Conclusion: The example highlights a most plausible reason why slopes affected by additional loading – especially in the form of earth deposits – tend to fail during extended spells of continuous precipitation.

The example also emphasizes the importance of considering the jacking effect of water in cracks that normally develop in the active zone under – as well as up-slope of – any kind of local additional load.

Hence, also the destabilizing effect of precipitation on progressive slope failure is usually heavily linked with human activity.

5.8 Conclusions from 'Case Records'

It is evident from the discussion in Section 2.2 that all extensive landslides do not necessarily occur as a result of progressive failure (Pr F) formation. The crucial criterion lest a brittle progressive failure be set off is, as mentioned previously that the residual shear strength (c_R) remains in excess of the prevailing in situ shear stresses (τ_o) at all times, i.e. $\mathbf{c_R > \tau_o}$.
However, the landslides listed in Table 5.7.1 are all believed by the author to belong to the downhill progressive failure category – i.e. when $\mathbf{c_R < \tau_o}$ and that for the following reasons:

a) Analyses based on 'ideal-plastic' limit equilibrium principles do not explain the extent as well as many other features of these landslides. In fact, subsequent application of conventional analysis, based on perfectly plastic behaviour of the clay usually indicates ample computed safety against slope failure – a fact suggesting instead the incidence of fracture-mechanical phenomena.

b) The slides were triggered by known, locally acting agen*ts* such as earth fills, pile driving, heavy vibratory soil compaction, rock blasting – sometimes but far from always in combination with documented spells of heavy rainfall.

c) Unprecedented kinds of local additional loading, inducing un-drained behaviour in strain-softening soils, may in particular be conducive to the initiation of progressive failure in natural slopes, and that irrespective of the fact that they have been stable for thousands of years.

d) The finished landslides feature vast areas of gently sloping ground being heaved and deformed to great depth already as a result of static build-up of earth pressures exceeding passive resistance.
As demonstrated in Section 2.4 and illustrated in Figure 2:4.2 b, this is typical of the immense release of potential energy and the build-up of static as well as dynamic forces associated with slides in markedly deformation-softening soil deposits.
The analogy of slope stability in deformation-softening soils to 'buckling stability', as described in Section 3.34 is striking in these case records.
Thus vast areas of inherently stable ground may become engaged in extensive landslides often triggered by some seemingly trivial local disturbance agent.
Progressive failure analysis has the potential of identifying dormant disasters of this kind.

e) Failure modes based on slip-surfaces emerging in the slope proper, near the additional load, normally have little relevance in slopes of sensitive clay. This phenomenon is of particular interest in connection with the use of supporting embankments in road construction. When investigating the impact on stability of earth deposits of this kind, the effects of water saturation in connection with continuous rainfall, should be considered.

6. Uphill Progressive or Retrogressive Landslides

6.1 *Definitions*

In the following, the terms 'uphill progressive' and 'retrogressive' are both applied to the reverse of downhill (or downward) progressive landslides – i.e. to slides initiated by instability in the vicinity of the foot of a long natural slope, often due the presence of a steep scarp or a river canyon.
In this document, therefore, the term ***retrogressive*** is defined as being synonymous with the term ***uphill progressive.*** In Canada, where uphill progressive landslides occur frequently in the highly over-consolidated Champlain clays, they are usually designated as *'spreads'*.

However, the term 'retrogressive landslides' (in Swedish: bakåtgripande skred) is often used for consecutive local slides spreading backwards from a steep scarp – usually created in connection with a previously occurred major slide. Events of this kind will in the following be referred to as ***serial retrogressive slides***. (Cf Figure 2:4.2d)

6.2 *Introduction*

As opposed to downhill progressive landslides, retrogressive (or uphill progressive) landslides are in principle triggered by the loss of support at the foot of the slope, generated by locally changing conditions or disturbance of some kind.
The loss of support may be caused by gradual erosion of a riverbank, degeneration of soil resistance due to decreasing effective stresses, seismic tremor or by man-made activities such as excavations, adverse hydrological intervention, vibrator activity or pile driving.

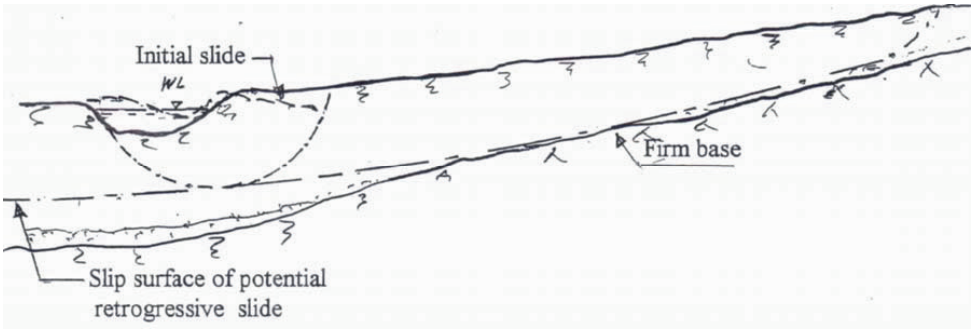

Figure 6:2.1 Slope liable to develop retrogressive (or uphill progressive) failure.

A crucial point in this context is the fact that retrogressive slides normally occur in over-consolidated clay formations. This is simply because hard clay is a pre-requisite condition for the formation of high steep scarps and deep river canyons. Another important issue is that disturbance or imbalance, e.g. due to deformation-induced loss of shear resistance ($c - c_R$), is in over-consolidated clays *not recoverable* over time by reconsolidation, as is in general the case in normally consolidated (or slightly over-consolidated) clays.
These preconditions are of major importance for the evolution of retrogressive landslides. (Cf Figure 7:1.1.)

As in the case of downhill progressive failure, the development of a retrogressive slide is closely related to the geometry of potential slip surfaces, usually as defined by the

sedimentary structure of the soil deposit and, in particular, by the interface between layers of strain softening clay and firmer sediments or what may generally be denoted as firm bottom. As mentioned, sites prone to developing uphill progressive failure normally differ from those conducive to downhill progressive sliding in respect of the presence of a steep scarp or a river canyon at the down-slope end of the incline as shown in Figure 6:2.1. Hence, retrogressive landslides develop as a result of failing or insufficient support in terms of passive earth pressure resistance in the lower parts of the slope.

The important implication of this is that, in retrogressive slope failure, there exists as a rule no definable 'post-dynamic' second state of equilibrium of the kind typical of downhill progressive slides, where, as emphasized in previous sections, predictable states of equilibrium (Phases 4 or 6) are normally possible due to the build-up of passive resistance over more level ground. (Cf Figures 3:3.4, 4:5.1, 5:1.7, 5:1.17 and 5:2.8).
This entails in turn that the mode of final disintegration of the soil mass is uncertain in retrogressive slides, and that the configuration of the after-slide ground surface is practically unpredictable. (Cf Section 6.4 and Chapter 8.)

However, even if FDM-analyses of the kind exemplified in Figures 6:3.1, 6:3.2, 7:4.1 and 8:3.3 predict that imminent retrogressive failure is likely, it may nonetheless be of major importance to study the different possible modes of ultimate disintegration of the unstable soil masses involved – i.e. actually defining the degree of ultimate disaster.
(Cf Section 6.4 below.)
An additional advantage of such a study is that, considering the way in which the soil structure disintegrates may render a clue to the nature and causes of the slide. (Cf e.g. Odenstad (1951), Bernander (NGM 1984).)

In Section 2.4 of the present document, it is demonstrated how the configuration of a finished landslide actually discloses the mechanisms acting during a slide – indicating, for instance, whether deformation-softening of the clay has been a governing factor in the event or not.

6.3 *Different phases in retrogressive landslides – the time factor*

6.31 Time dependency
When studying the impact of a disturbing agent such as additional load on a natural slope it is necessary to distinguish between its long-term effect over time and the transient, un-drained response of the soil structure during, and some time after, the application of the additional load. This applies in particular to loading of local character affecting only part of the slope. (Cf e.g. Section 2.3, Item c.)

As has already been emphasized in this document, the strength and deformation properties of sensitive clays exhibit strong strain-rate dependency relating importantly to the permeability of the clay and to the local drainage conditions in the potential failure zone.
(Cf Sections 2.2, 2.3, 4.1 and 4.2).

In view of the fact that the finite difference Retrogressive Failure Approach (ReFA) proposed in Chapter 7 can cope with any applicable time-dependent stress/strain relationship, the effect of time can in principle be incorporated into the analysis. An important requirement in this context is therefore that the stress/strain (deformation) relationship to be applied is compatible with the rate of loading of the currently studied disturbance agent, as well as with the locally prevailing drainage conditions in the developing failure zone.

Hence, also in retrogressive failure analysis, it is of interest to distinguish between the following conditions and phases of a potential landslide:

Phase 1 *The long-time in situ* shear stress and earth pressure conditions as per Section 6.32 below.

Phase 2 *The disturbance condition* – i.e. the analysis of uphill failure propagation set off by agents applied at varying rates of loading or acting during specific shorter periods of time. The disturbance may be related to a wide range of phenomena:

2a **-** Disturbance generated by *short time effects* like seismic tremor or human activities such as excavation, vibratory compaction and pile driving. Man-made interference with the hydrological regime, resulting in higher peak pore water pressures than ever before also belongs to this category.

2b **-** Disturbance related to long-time degradation such as weathering and loss of shear strength due to *chemical* change.

- Disturbance related to increased mobilization of shear resistance due to *erosion* and permanent adverse changes of the down-slope support and/or of the hydrological regime.

- Disturbance related to deformation-induced loss of shear resistance in highly over-consolidated clays because of reduced *effective stress* conditions (e.g. by erosion) and possible formation of slip planes and slicken-sided surfaces.

Phase 3 *Dynamic disintegration phase* – As mentioned above, no well-defined post-dynamic state of equilibrium is normally to be expected in retrogressive landslides because of insufficient passive earth pressure resistance at the foot of the slope. Instead, the mode of dynamic disintegration of the soil mass is likely to exhibit erratic and essentially unpredictable features. The issue is treated separately in Section 6.4.

6.32 <u>In situ state condition</u>

As already stressed in the analysis of downhill progressive slides, it is mandatory also in the study of retrogressive slides to establish a reasonably correct estimate of the prevailing in-situ state of stress prior to assessing the effects on the slope of possible destabilizing agents. **([1])**

If the inclination of a slope is uniform (the slope angle β being constant), the in situ state of shear stress is simply:

$\tau_o = \rho \cdot g \cdot H \cdot \sin(\arctan(dz/dx)) \approx \rho \cdot g \cdot H \cdot \sin\beta$ (i.e. for $\cos\beta \approx 1{,}0$) …….Eq. 6:1

([1]) This in-situ stress condition is sometimes termed 'the eigen-stresses'.

By contrast, when the slope gradient (β) varies, as e.g. exemplified in Figures 6:3.1 and 6:3.2, defining the in situ stress conditions is more complicated. The inclination of the potential slip surface is normally significantly steeper uphill than in more level ground further down-slope. As shown in Figure 6:3.1, the in situ shear stress is then

$\tau_{o,x} = \rho \cdot g \cdot H_x \cdot \sin\beta_x - dE_{o,x}/dx$ (again, $\cos\beta \approx 1{,}0$) ……..Eq. 6:2

where the parameters H_x, β_x and $E_{o,x}$ are variables and $\beta_x = \arctan dz/dx$

The parameters H_x, and β_x are known, but an estimate of the earth pressure distribution $E_{o,x}$ based on progressive failure analysis has to be established. Starting from the long-time stress/strain relationship considered to be valid, the earth pressure redistribution along the slope due to creep deformations can be estimated assuming that the deformations in the soil mass manifest themselves as a long-time progressive movement that may be studied e.g. by means of the FDM-analysis.

The key issue in this context is that the long-time constitutive stress-strain relationship used in the analysis is compatible with the loading conditions considered. If necessary, this relationship may have to be determined by long-time direct shear tests.

As can be concluded from Figure 6:3.1, the second term in Equation 6.2 may have a decisive influence on the distribution of the in situ shear stresses and earth pressures. Results from analyses, not taking these effects into account, are likely to be unreliable.

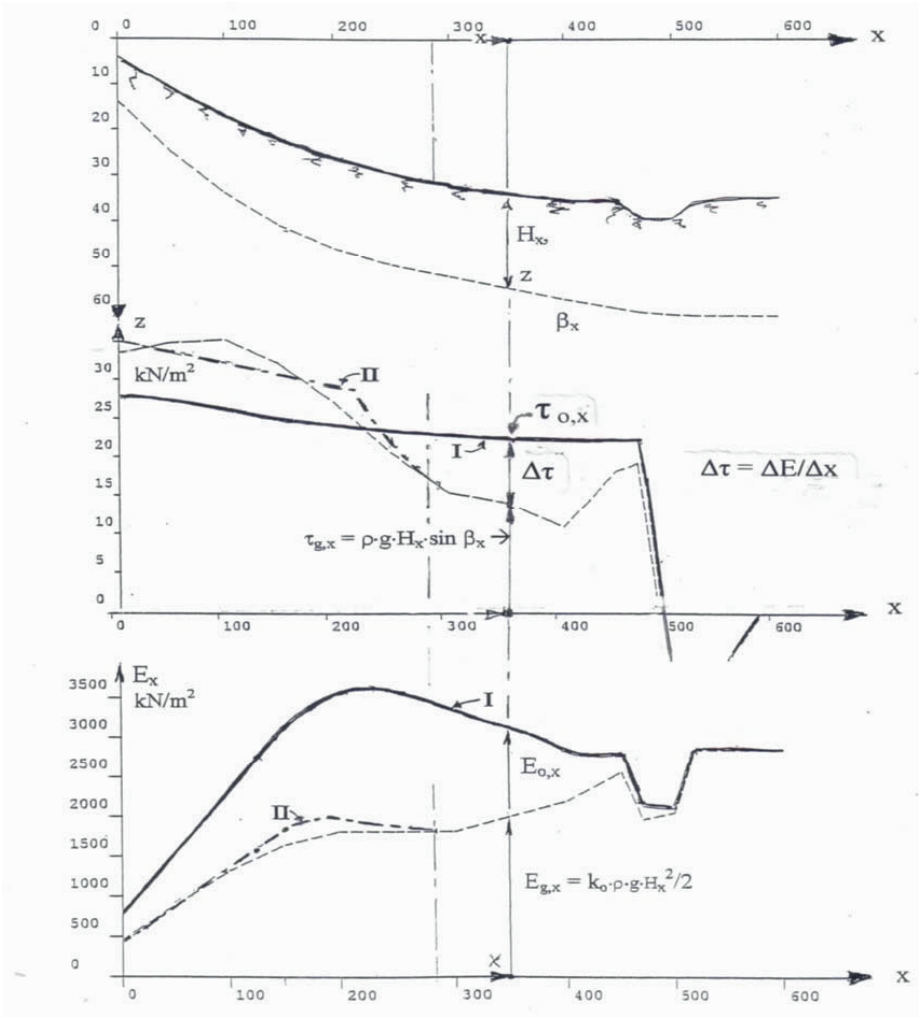

Figure 6:3.1 Diagram demonstrating two cases (I and II) of the effect of creep deformation on the in situ distribution (dashed lines) of earth pressures and shear stresses in a slope with varying depth to firm bottom. As is often the case, the inclination of the ground surface and that of the potential slip zone are steeper uphill than below the valley floor. The slope is identical to the one dealt with in Figure 6:3.2. The diagram illustrates the effect of a difference in magnitude of the prevailing shear resistance by 25 % – i.e. for a ratio of $c^{II}/ c^{I} = 1.25$. Note the considerable difference in the two cases as regards the mobilization of down-slope support. Conditions are typical of the slide in Sköttorp (C.f. Section 8.4).

The term $dE_{o,x}/dx$ represents the difference between Curves I and II for shear stress in Figure 6:3.1, illustrating the considerable redistribution of shear stresses that may result from creep deformation over time, and how this phenomenon affects the long-term distribution of earth pressure along the slope.

The notable feature in Case I is that the soil mass in the steep part of the slope – being unstable in a long term perspective – actually 'leans' on the more stable ground further downhill.
In fact, for most slopes with this geometry, there is a tendency to 'long-time' shear strength ($c^{t=\infty}$) being fully mobilized in their steepest parts, resulting in transfer of forces by creep deformation. However, it is important to observe that this condition, per se, is not necessarily an indication of impending global instability in view of the possible reserves of support available further down the slope.

Conclusions:
– In order to evaluate the impact of a disturbance agent with the potential of triggering a retrogressive slide, it is imperative to define the prevailing shear stress distribution, particularly in the area affected by the disturbance.
– The in situ distribution of earth pressures and shear stresses can be determined by the FDM-approach, which means taking the differential deformations in soil mass into account. For natural slopes, the creep process may in the current context be understood as an extremely slow downhill progressive failure condition based on the stress-deformation relationships that correspond to long-time creep deformation in the soil.
Finite element analyses (FEM) are likely to very be useful in this context.

6.33 Disturbance Condition **2a** - *short term stability conditions*
The key reason for the necessity of studying short term disturbance conditions in slopes – and that even if the disturbance as such is of a permanent nature – is that rapid loading and fast strain rates tend to induce low post-peak residual resistance (c_R) in clays, especially in sensitive ones. (Cf Section 3.11, Case 1, where $c_R < \tau_o$).
Deformations provoked by the disturbance may well transform a fully drained condition in parts of a slope into a more or less un-drained one, for which the strength parameters defined by standard laboratory procedures may no longer apply at all.
Furthermore, the pronounced dependence of the stress/deformation properties of clays on the rate of deformation entails that the effects of loads acting in different spaces of time cannot be directly superimposed, at least not without actually accounting for how the deformations intervene in the time domain.

In other words, this means that slopes, which – including the additional permanent load – would be inherently stable under drained conditions, may very well fail in a 'transitory' more or less 'un-drained' state generated by deformations related to a more hurried application of the very same additional load.
Like in downhill progressive failures, the major factor here consists in the significant loss of residual shear strength, as the deformations within a potentially unstable part of the slope increase. (Cf the Kotmale slide, Section 2.3)

The basics of the analytical approach to the modelling of retrogressive failure analysis (ReFA) are dealt with in Section 7. It is shown there that the finite difference model (FDM), valid for downhill progressive failure as described in Section 4, can readily be applied to retrogressive failure, provided that the sign of the additional down-slope earth pressure change (N) in the downhill direction is reversed – i.e. positive +N denoting tension instead of compression.

The fact that the computed additional earth pressure (N_x) represents a tensile force implies de-loading of the down-slope earth pressures, i.e. contrary to the typical earth pressure build-up in downhill progressive failure development. The well-known effects of variation of the ratio of horizontal stress to vertical stress (σ_H/σ_V) on the stress/deformation properties of clays is an important issue to be considered in this context.

The FDM calculation procedure derived in Section 7 is exemplified in Figure 6:3.2, applying to a slope with decreasing gradient towards the river canyon. The figure shows results from the retrogressive failure analysis (ReFA).

The curves in Figure 6:3.2 represent the maximum possible additional load in terms of N_x that can be applied at the coordinate x, lest the failure propagates further uphill. As may be noticed, the curves are somewhat dissimilar depending on the choice of the starting point defined by x = 0. The reason for this is of course that for a certain choice of the location of x = 0, the portion of the slope subject to study is only partially the same as for another chosen value of (x).

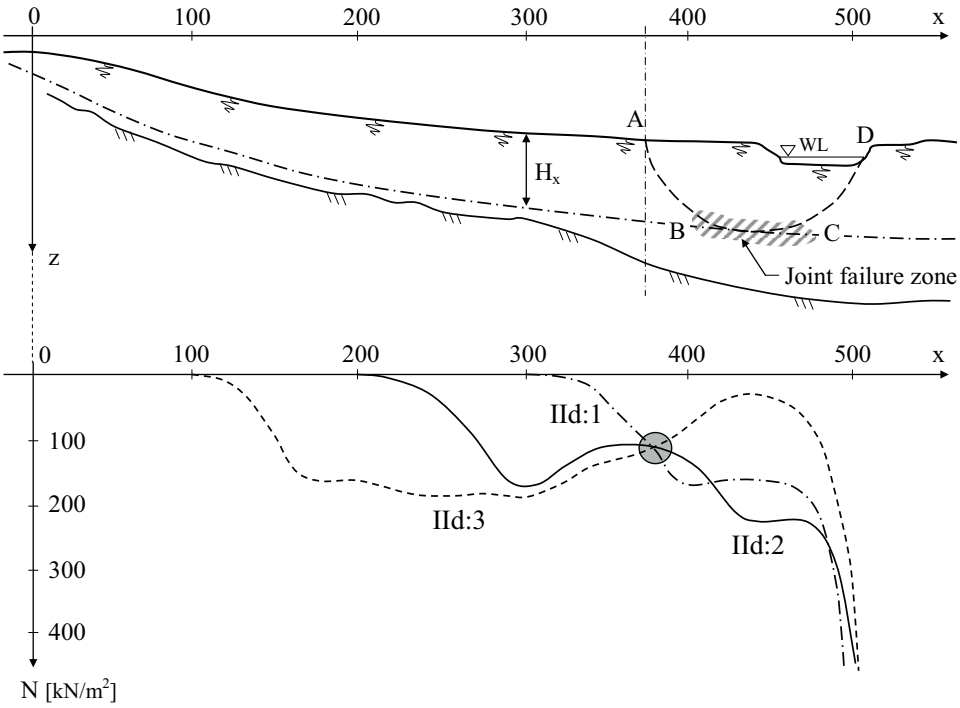

Figure 6:3.2 Results of retrogressive analysis of a non-uniform slope showing the maximum additional tensile forces $N_{x=380} = N_{cr}$ that can be applied at the foot of the slope lest uphill progressive (retrogressive) failure develops. (Scale: Vert. scale = 2 times hor. scale). Three different starting points x = 300, x = 200 and x = 100 m are used to analyse Case II in Figure 6:3.1.

However, although it may be coincidental, the critical value of N is remarkably equal for x ≈ 380 m, where $N_x = N_{cr} \approx 120$ kN/m for all of the curves starting at $x \geq 100$ m.

If, in the current case, N_{cr} is deemed to be 120 kN/m it may be of interest to estimate what kind of destabilizing agent that would be liable to trigger retrogressive failure in the slope. (Cf Figure 6:3.3.)

Two versions of this issue are treated below, namely:
1) Local slope failure at the river bank and
2) Failure due to pile driving activity near the river canyon.

1) *Disturbance due to local slope failure near the riverbank*
The slide may be due to ongoing erosion, excavation or a local fill on the riverbank. Assuming that the value of K_o does not change, the scarp ΔH shown in Figure 6:3.3 represents a loss (ΔE_R) of passive resistance:

$\Delta E_R = K_o[(\rho \cdot g \cdot H^2/2 - 2c \cdot H) - (\rho \cdot g \cdot (H - \Delta H)^2/2 - 2(c - \Delta c) \cdot (H - \Delta H))]$

$= K_o[(\rho \cdot g \cdot (H \cdot \Delta H - \Delta H^2/2) - 2c \cdot \Delta H - 2\Delta c \cdot H + 2\Delta c \cdot \Delta H)]$ ……Eq. 6.3

Provided ΔH is small compared to H and Δc small compared to c, the terms $\Delta H^2/2$ and $\Delta c \cdot \Delta H$ can be disregarded and taken to be ≈ 0.

$\Delta E_R \approx K_o \cdot [\rho \cdot g \cdot H \cdot \Delta H - 2c \cdot \Delta H - 2\Delta c \cdot H)]$ ……Eq. 6.3a

$\Delta H \approx (\Delta E_R/K_o + 2\Delta c \cdot H)/(\rho \cdot g \cdot H - 2c)$

i.e. retrogressive slope failure is triggered if $\mathbf{\Delta E_R > N_{cr}}$

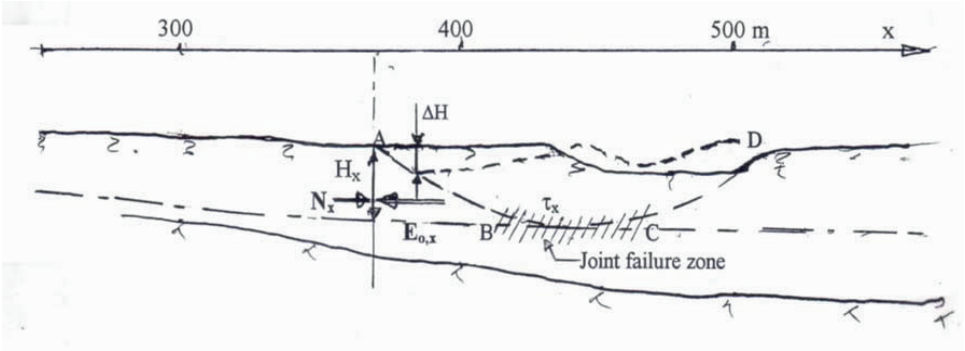

Figure 6:3.3 Detail of the slope shown in Figure 6:3.2 illustrating the effect of agents capable of initiating retrogressive failure. Scale: Height/Length ratio = 1:1.
ΔH denotes height of scarp caused by an initial riverbank slide along the slip surface ABC
Δc_u denotes the deterioration of shear strength over a length BC = L (m), generated for instance by pile driving activity or by disturbance in zone BC in connection with a slide along ABC.

Hence $\mathbf{\Delta H \approx (N_{cr}/k_o + 2\Delta c \cdot H)/(\rho \cdot g \cdot H - 2c)}$

For H =22 m, $K_o \approx 1.0$, $\rho \cdot g = 16.5$ kN/m^3, c = 27.5 kN/m^2, $\Delta c = 0.4 \cdot 27.5$ kN/m^2 and $N_{cr} = 120$ kN/m

$\Delta H \approx (120/1 + 2 \cdot 0.4 \cdot 27.5 \cdot 22)/(16.5 \cdot 22 - 2 \cdot 27.5) =$

$= (120 + 484)/(363 - 55) = 1.96$ m ≈ 2.0 m

The computation indicates that a local slide forming a scarp ΔH of about 2 meter would suffice to set off a slide involving the entire slope.

2) *Disturbance caused by pile driving*
Assume that pore water pressure rise and/or laterally induced displacement of the soil mass, due to piling activity near the riverbank, reduce the shear resistance in part BC of the failure zone of the 'potential' long slip surface by a factor (f) over a length BC = L = 20 m. The residual shear strength is then $c_R = f \cdot c_u$ and the loss of shear resistance is $\Delta c = (1\text{-}f) \cdot c$.

The corresponding loss of horizontal support in the portion BC of the failure zone of a potentially possible retrogressive slide then amounts to:
$\Delta E_o = \Delta c \cdot L = (1\text{-}f) \cdot c \cdot L = (1\text{-}f) \cdot 27.5 \cdot 20 = 550 \cdot (1\text{-}f)$ kN/m
Hence, a retrogressive slide is triggered if $\mathbf{\Delta E_o = 550 \cdot (1\text{-}f) \geq N_{cr}}$, i.e. for
$550 \cdot (1\text{-}f) = 120$ kN/m → $(1\text{-}f) = 120/550 = 0.218 \approx \mathbf{0.2}$
Thus, a loss of shear strength of about 20 % (i.e. $c_R = 0.8c$) would, according to the analysis, be sufficient to destabilize the entire slope by triggering a major retrogressive landslide.

6.34 Disturbance Condition **2b** – Long term stability conditions
As explained in more detail in Section 10.2 under the heading *'History of a slope'*, strength properties, earth pressures and shear stresses in the slope have in the past adapted to the prevailing geometric and hydrological conditions on the site. Every existing natural slope is in principle stable by some undefined factor of safety in excess of 1.0.
However, the long-term stability of an inherently stable slope of this kind may, in the way described in Condition 2a, also be jeopardized by permanent loading or lasting change, if the load effect is applied all at once or at too high a rate.

By contrast, slowly and gradually applied permanent loads will in principle generate slope failure only if the *drained* shear resistance is exceeded.
In the basically stable example shown in Case I (Figure 6:3.1), the long term shear strength is mobilized over almost the entire length of the slope indicating a global safety factor of about 1.0 when applying Ideal-Plastic Failure Analysis (I-PlFA) based on the long-term shear strength ($c^{t=\infty}$). It should be observed that this condition does not apply at all to Case II.

Intrinsic deformation-induced failure
Yet, when estimating the effects of a *gradually* applied *permanent* man-made or natural disturbance at the foot of a slope, the 'long-term' shear strength and stress-deformation characteristics of the clay should be applied, and the effects of the deformations within the soil mass duly be accounted for.
Therefore, as the in situ conditions in the study of retrogressive slides are to be established by progressive creep analysis, it is recommended that also the effects of long-time additional loads should be checked in this way. This is of particular importance in highly over-consolidated clays, as even long-time deformations per se generate loss of shear resistance that in turn may lead to further deformation.… and so on.
This failure condition is dealt with in more detail in Section 7.52.

It may be argued that conventional I-PlFA analysis would apply well enough when studying the impact of long-time disturbance agents of permanent nature. However, when considering such disturbance of local character in hundreds of meter long natural slopes, retrogressive failure analysis (ReFA) considering differing deformations within the potentially sliding soil mass is strongly advocated. Cf Section 7, Figure 7:4.1.)

The use of Finite Element Analysis (FEM) represents another approach to establishing the long term in situ conditions. This may in particular be recommendable in highly over-consolidated clays as the gradual effects of hydrological change over time can readily be studied. (Cf A. Locat, 2007, Section 8.3)

6.35 Conclusions
a) Major retrogressive failure in natural slopes may result from the loss of support or instability in the vicinity of the foot of the slope.

b) When studying the effect of such disturbance, it is imperative to establish the prevailing in-situ long-time stress conditions along the slope, especially in the area subject to disturbance. The in-situ shear stresses and the earth pressure distribution along the slope can be estimated by applying the stress/deformation relationships considered valid for long-time creep deformation.

c) Furthermore, it is imperative to differentiate between the long-term (drained response) and the immediate short-term (un-drained) response of the soil material.
The effect of additional disturbance agents, acting (or applied) during short periods of time, must be studied on the basis of stress/strain relationships that are compatible with the deformation-softening behaviour of the soil at the current rate of loading and under prevailing drainage conditions in the potential failure zone.
This has the crucial implication for long natural slopes that, although being stable under drained conditions, they may well fail in un-drained response to deformations caused by some local disturbance agent. If the residual shear strength then falls below the in situ stress over some length, the possibility of retrogressive failure formation is at stake, and must be taken into consideration.

d) The different phases to be studied when analyzing the stability of a natural slope in respect of retrogressive failure development are thus discerned as:

Phase 1) *The long-time in situ state of stress.*

Phase 2) *The disturbance conditions*
Disturbance condition 2a concerns the effects of additional loading or disturbance of any kind on short term stability, considering in particular deformation induced temporary loss of shear resistance. This reduction may be related to un-drained or partially un-drained conditions or to rapid forced displacements of a transient nature.
Disturbance condition 2b deals with the effects on long-term slope stability of *gradually* applied additional permanent load, erosion, slowly developing hydrological change and of chemically induced degeneration of shear strength.
In slopes of highly over-consolidated clay, where reduction of effective stresses caused by erosion has taken place, the gradual deformation-induced loss of shear resistance is a likely result of disturbance of this category (Cf Sections 7.52 and 8.3)

Phase 3) *The dynamic disintegration phase.* (Cf Section 6,4)

6.4 *Final disintegration of the soil mass*

There are several different ways, in which the soil mass may finally collapse, depending essentially on the geometry of slope and firm bottom, soil structure, as well as on the strength and stress/deformation properties of the soil layers involved.
Various possible disintegration scenarios exist, and the final outcome of potential instability has to be evaluated in each individual case.
However, in order to illustrate the issue in question, a few likely scenarios will be discussed.

6.41 Serial retrogressive slides.
A classic type of ground disintegration in up-slope progressive landslides is the formation of consecutive circular slip surface failures – here defined as 'serial retrogressive slides'.
This phenomenon is likely to occur whenever a steep scarp is formed in highly deformation-softening homogeneous clay. Serial retrogressive slides were for instance recorded in the

aftermaths of the main slides in Surte, (1950) and Tuve, (1977). In both of these cases smaller slides spread backwards from the steep scarps formed by the major initial slides.
(Cf Figure 2:4.2d and Sections 5.1 & 5.2.)

In the Rissa slide in Norway, the whole sequence of slide events began – and ended – with slides of serial retrogressive character, (Gregersen, 1981).

An important prerequisite for serial retrogressive slides is that the disintegrated soil mass, involved in the immediately preceding slide, moves away further downhill in a virtually liquid state owing to extreme sensitivity and/or to specific slope geometry.

6.42 Collapse of parts of the soil mass in brittle active failure – 'column failure'
Uphill progressive failure involves by its very nature significant reduction of the horizontal earth pressure in large portions of a slope.
Janbu (1979) described a failure mechanism in quick clays, by which the practically total loss of horizontal normal stress, characterized by a dramatic reduction of the ratio $\sigma_{hor}/\sigma_{vert}$ ($\approx \sigma_3/\sigma_1$), leads to vertical collapse of large sections of the soil mass in what was denoted as 'column failure'.
Insufficient or lacking horizontal (normal) stress aggravates the brittleness of the inherently sensitive soil mass to the extent that it disintegrates in a process of virtual liquefaction – i.e. leaving the site as a mudflow. The final phases of the Rissa slide, which were shown on film at various international geotechnical conferences, exemplify soil break-down of the kind.

6.43 Simultaneous collapse of the entire slope in active failure – 'spreads'
As mentioned above the characteristics of the soil structure is an important factor in the disintegration process. For example, the soil in a slope may consist entirely of non-sensitive clay, except for a significantly deformation-softening layer in the soil profile. In such a case, failure can progress from the disturbance at the foot of the slope right up to the crest of the slope before ultimate disintegration in active failure.
In other words, the soil mass remains temporarily as an integral block until down-slope displacements reach a point, where the related de-loading of horizontal earth pressure ends in general active failure as illustrated in Figure 2:4.2c.

In slides of this kind, the jagged ground surface of so called 'horsts' and 'grabens' (i.e. ridges and depressions) extend all over the ground involved in the earth movement. Slides with final configuration of this kind are often denoted 'spreads'. A recent example of spread failure was the Saint-Barnabé-Nord Slide (2005) in Quebec, Canada. (Cf A. Locat, 2007, Section 8.3).

Case records in Sweden exhibiting this mode of disintegration are the slides at Sköttorp (1946) and at Nor (1969). These slides are briefly described in Sections 8.4 and 8.5 of this document.

7. Analytical FDM-model for uphill progressive (retrogressive) slides - theory

7.1 *General*

The Finite Difference Model (FDM) for studying retrogressive landslides, accounted for in the following, is mathematically practically identical to the FDM-model outlined in Section 4. It is therefore convenient to follow the same presentation of the model as in that section.
The application of the FDM-model to retrogressive failure analysis will in the following be referred to as ReF-analysis (or ReFA). (1)
However, there are notable differences in material behaviour in retrogressive and progressive landslides, and – particularly in the final phases – there are important dissimilarities as regards slide development and the final configuration of the disintegrated soil mass. (Cf Section 6.2.)

(1) In geotechnical literature retrogressive landslides are often denoted as 'spreads'.

The said differences originate primarily from different development of the states of principal stress in uphill progressive failures as compared to downhill progressive failures. In the former case, the ratio of horizontal stress σ_x to vertical stress σ_z, (i.e. σ_x/σ_z) is significantly reduced in the evolution of a slide, whereas in downhill progressive slides the very opposite is true.
This circumstance has a decisive impact not only on peak and residual shear strengths but also on the deformation and brittleness characteristics of clays. (Cf e.g. Janbu (1979).

As stated in Section 4, slope stability analysis should ideally define the critical conditions in a slope directly on the basis of the input data. But apart from being rather complicated, such analysis may also be unnecessarily laborious, considering that critical failure planes can mostly be identified by the morphology of firm bottom and the stratification of the soil structure.
Hence, the approach to slope stability analysis presented in this document does not imply an integral 'closed' analysis with the critical failure planes emerging directly from the input data and the ensuing computations. Instead, the methodology resembles conventional limit plastic equilibrium modelling in so far as the potential failure planes are presumed to be known. The most critical situation may therefore – as in conventional stability calculations – have to be found by 'trial and error' procedures.

Nevertheless, as explained in Section 4, the proposed analysis differs from ideal-plastic limit equilibrium methods in the following ways:

a Whereas, in the ideal-plastic failure approach (I-PlFA), the equilibrium of the *entire* sliding body of soil is investigated, ReFA-analysis focuses on the equilibrium of each individual element into which the body of soil is subdivided.

b Furthermore, the main relevant deformations within and outside the potentially sliding soil mass are considered. Hence, the axial displacements in the slide direction due to earth pressure changes in the slope are at all times maintained compatible with the shear deformations of the discrete vertical elements. In doing so, it is possible to model the shear stress distribution, and the extent to which the shear capacity can be mobilized along the potential failure zone and the associated failure plane. The differential equations are integrated and solved numerically.

c The shearing properties of the soil are defined by a full non-linear stress-strain deformation relationship and not only by a discrete shear strength parameter, as in traditional limit equilibrium calculations. This constitutive relationship is separated into two stages (I and II), simulating the conditions before and after the formation of a discrete failure surface like in the specific type of direct ring-shear tests reported by Bernander & Svensk (1985). (2)
(Cf Figures 7:1.1 and 7:2.2.)
The stress/deformation relationships may be chosen so that they correspond to the actual rates of loading and to other inherent conditions, such as drainage, in different parts of the slope.

(2) In these tests, the soil sample was confined by a set of freely movable steel rings instead of by the normally used rubber or plastic membrane.

d By using different stress/deformation relationships, relating to different rates of stress (or load) application, the time factor can in principle be included in the analysis.
However, when dealing with slope failure in significantly deformation-softening soils, considering the time factor necessitates studying slide development in distinctly separate phases. This follows from the fact that the residual shear resistance of sensitive clays may vary substantially from one phase of a landslide to another, depending mainly on the different rates of stress change and on permeability conditions for excess pore water pressure dissipation.
This constitutes a feature of paramount importance as the different stages of a major slide can be identified and analyzed. Among other, it makes it possible to model the in situ earth pressure conditions in the slope prior to the incident generating the currently studied disturbance condition.

e Local horizontal or vertical loads, as well as local features in the geometry of a slope that may be conducive to the initiation and propagation of retrogressive failure can be taken into account.

f Although the location of the potential failure plane is assumed to be known, the length of the active zone as well as the final extension of a slide emerge explicitly from the computations.

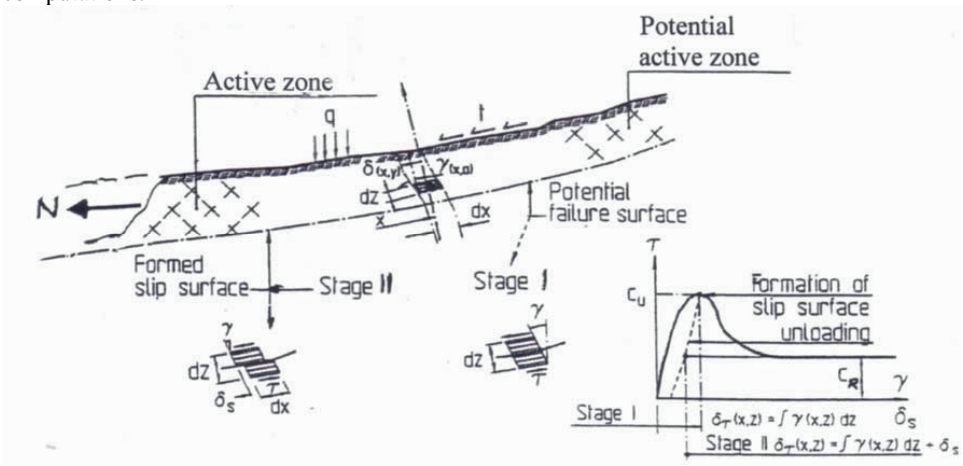

Figure 7:1.1 Structure and development of an uphill progressive (retrogressive) landslide – notations and principles.

7.2 *Soil model – derivation of formulae*

7.21 Basic assumptions – drainage conditions

An uphill progressive (or retrogressive) landslide may begin as a drained, partially un-drained or fully un-drained local failure depending on the rate, at which the agents causing the local zone of instability intervene. The soil strength parameters applied for defining the critical conditions conducive to the initiation of retrogressive slope failure must therefore be compatible with the nature of the additional loading effect being investigated.

Importantly, the following may be noted:

a) In soft sensitive normally (or slightly over-consolidated) clays, the deformation-induced loss of residual shear strength ($c– c_R$) is primarily caused by the pore water pressure increase related to collapsible soil. Hence, even when a potential local failure is initially of a drained nature, locally increasing load may induce large' peak resistance' strains, gradually generating un-drained or partially un-drained response in a developing failure zone.

b) In highly over-consolidated clays a corresponding deformation-induced loss of residual shear strength ($c– c_R$) can arise from inherent reduction of vertical effective stresses over time related to geological processes. Such evolutionary change may result from over-all soil erosion, local fluvial soil erosion and rising ground water levels. ([3]) Over-consolidation may also be due to the weight of glacial ice sheets that have melted away in the past.

([3]) Regarding the impact of loss of effective stress on shear resistance, Cf Ladd & Foot, 1974.

Therefore, although total stress parameters are to some extent used in the structure-mechanical analysis of the slide events, the strength parameters (including the constitutive stress-deformation relationships) may be based on un-drained, partially un-drained or drained soil behaviour, whichever condition that is valid in the case investigated.

Ground water conditions and possible artesian conditions may enter into the analysis by considering the OCR-ratio.

Furthermore, the soils of the entire slope profile are taken to be saturated. This means that seepage pressures due to percolation of ground water down the slope are accounted for, even in cases with permeable soil strata.

If the slope is partially submerged, the stabilizing effect of horizontal hydraulic pressure can be considered in the model.

7.22 Basic assumptions in the analytical model

Some of the general principles and notations applied in the adopted model for slope failure are shown in Figures 7:1.1, 7:2.1 and 7:2.2.

The basic mathematical approach used is a two-dimensional finite difference model. Nevertheless any desired three-dimensional shape of the sliding body can be accommodated by varying the width b(x). As shown in Figure 7:2.1, the potentially sliding soil volume is subdivided into discrete vertical elements of length Δx. However, contrary to the assumptions made in Section 4, the coordinate (x) is now taken positive in the down-slope direction.

The x-axis is, in the derivations below, oriented along the slip surface, which is justified as long as $\cos \beta \approx 1$. Cf specific comments in Section 3.6.

Each vertical slice is subdivided into a number of elements of height Δz in the z – direction permitting modelling of the shear deformations within and outside the soil profile. In particular, the deformations of the intensely sheared zone in the vicinity of the potential (or if applicable the established) slip surface are accounted for. (Cf e.g. Figure 4:6.2)

Hence, the incipient failure zone contributes to a major part of the total shear displacement of a vertical soil element, and that to a significant extent before local failure and the formation of a regular slip surface or narrow shear band.
This is therefore a crucial feature in the current context, as the resilience of the shear failure zone actually constitutes the prerequisite condition for an effective and calculable resistance to slope failure by concentrated loading. (Cf Equation 7:1b.)
Or to phrase the issue somewhat differently, the critical parameters N_{cr}, L_{cr} and δ_{cr}, related to the triggering of retrogressive failure, depend directly on the total resilience of the entire zone subject to shear deformation. In fact, if the resilience of the failure zone were negligible, any minor load concentration could release slope failure.

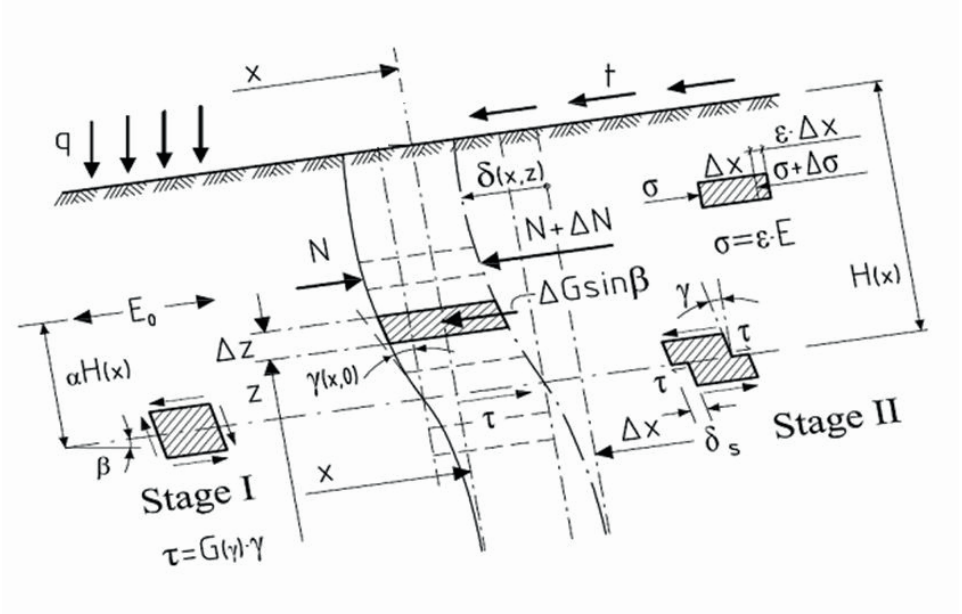

Figure 7:2.1 FDM - model for uphill progressive (retrogressive) failure – denotations. E_o indicates the in-situ earth pressure condition.

The denotations used in the subsequent derivation of Equations 7:1, 4:1 to 4:5 are identical to those defined in Section 4.22 as follows: (Cf also Figure 7:2.1.)

δ_x Average down-slope displacement of the soil above the potential slip surface
αH_x Level, at which the mean down-slope displacement is considered to be valid
$E_o(x)$ In situ earth pressure at point x
N (x) Earth pressure increment due to additional load or to retrogressive failure formation
E(x) $= E_o(x) + N(x)$
τ (x,z) Total shear stress in section x at elevation z
τ (x,o) Total shear stress at failure plane (z = 0)
$\tau_o(x,z)$ In situ shear stress in section x at elevation z,
$\tau_o(x,o)$ In situ shear stress at failure plane (z = 0)
γ (x,z) Shear strain in point (x,z)
$\sigma(x)$ Mean incremental down-slope axial stress
q(x) Additional vertical load
t(x) Additional load in the down-slope direction

$H(x)$ Height of element
$b(x)$ Width of element
E_{el} Secant elastic modulus in down-slope compression
G Secant modulus in shear in the range $\tau(x,z) \rightarrow \tau(x,z) + \Delta\tau(x,z)$
$\beta(x)$ Slope gradient at coordinate x
$\delta_S(x)$ Off-set (slip) in the failure surface in relation to the sub-ground
L_{cr} Limit length of mobilization of shear stress at N_{cr}
N_{cr} Critical tensile load effect initiating local slope failure
δ_{cr} Critical displacement in terms of axial deformation at N_{cr}
(For denotations not given here, see 'Notations'.)

7.23 Basic differential equations

Derivation of formulae valid in stage I, i.e. for values of $\gamma(x) < \gamma_f$

Figure 7:2.1 is almost identical to Figure 4:2.2 in Section 4, the main difference being that the x- coordinate is now assumed positive in the downhill direction for computational convenience. This implies in principle that the differential ΔN is positive in the direction of the x-axis, where positive N now signifies a tensile force. In the current context $\delta(x)$ denotes displacement generated by tensile strain.

The time dependent stress/deformation relationships used, are in principle the same as those shown in Figure 4:4.2 in Section 4.
Applying the denotations given above and Figure 7:2.1, the equilibrium of an element $[H(x)\cdot b(x)\cdot\Delta x]$ requires that

$$\mathbf{\Delta N - \tau(x,o)\cdot b(x)\cdot\Delta x + \tau_o(x,o)\cdot b(x)\cdot\Delta x + q(x)\cdot b(x)\cdot\sin\beta(x)\cdot\Delta x + t(x)\cdot b(x)\cdot\Delta x = 0}$$

or

Change of shear stress *Vertical load* *Down-slope load*

$$\mathbf{\Delta N = \tau(x,o)\cdot b(x)\cdot\Delta x - \tau_o(x,o)\cdot b(x)\cdot\Delta x - q(x)\cdot b(x)\cdot\sin\beta(x)\cdot\Delta x - t(x)\cdot b(x)\cdot\Delta x}$$

$$\mathbf{= [\tau(x,o) - \tau_o(x,o)]\cdot b(x)\cdot\Delta x - q(x)\cdot b(x)\cdot\sin\beta(x)\cdot\Delta x - t(x)\cdot b(x)\cdot\Delta x} \quad \text{..…... Eq. 7:1}$$

Hence:

$$\mathbf{N_x = \Sigma_o^x \Delta N} \quad \text{and} \qquad \text{…..…... Eq. 7:1a}$$

$$\mathbf{N_{cr} = \Sigma_o^{Lcr} \Delta N} \qquad \text{…..…... Eq. 7:1b}$$

Equations 7:1, 7:1a and 7:1b are identical to Equations 4:1, 4:1a and 4:1b valid for downhill progressive failure in Section 4, i.e.

Change of shear stress *Vertical load* *Down-slope load*

$$\mathbf{\Delta N = [\tau(x,o) - \tau_o(x,o)]\cdot b(x)\cdot\Delta x - q(x)\cdot b(x)\cdot\sin\beta(x)\cdot\Delta x - t(x)\cdot b(x)\cdot\Delta x} \quad \text{.....…… Eq. 4:1}$$

Hence, Equation 4:1 may be applied also to retrogressive landslides provided the x-coordinate is taken to be positive in the down-slope direction and that **N** and **ΔN** are conceived as tensile forces instead of compressive forces.

Also, as in Section 4, the in situ shear stress at the potential slip surface level is: (4)

Gravitational load *Change of in situ stress*

$$\mathbf{\tau_o(x,o) = \Sigma_o^{H(x)} g\cdot\rho(z)\cdot\Delta z\cdot\sin\beta(x) - \Delta E_o(x)/(b(x)\cdot\Delta x)} \quad \text{..…… Eq.4:2}$$

(4) As x is positive in the down-slope direction, ΔE_o is positive for increasing in situ earth pressure in the direction of x, thus counteracting the down-slope gravitational load.

The axial *tensile deformation* of an element in the x direction is defined as

$\Delta\delta_N = (N+\Delta N/2) \cdot \Delta x / [E_{el} \cdot H(x) \cdot b(x)]$ …… Eq.4:3

where $\Delta\delta_N$ is the incremental mean down-slope displacement due to the tension of an element.

However, the accumulated mean down-slope displacement (δ_N), to which a vertical element is subjected must, as in the case of downhill progressive failure, be compatible with the shear deformation of the same element relative to the ground below the slip surface. This condition may, as in Section 4, be expressed as:

$\delta_\tau(x) = \Sigma_o^{\alpha H(x)}[(\tau(x,z) / G(x,z,\tau) - \tau_o(x,z) / G(x,z,\tau)] \cdot \Delta z + \delta_S(x,o)$ …..… Eq..4:4

$= \Sigma_o^{\alpha H(x)}[(\gamma(x,z,\tau) - \gamma_o(x,z,\tau_o)] \cdot \Delta z + \delta_S(x,o)$ ……. Eq.4:4a

The compatibility criterion with regard to downhill displacement demands that

$\delta_N(x) = \Sigma_o^x(\Delta\delta_N) = \delta_\tau(x)$ For $\gamma(x,z) < \gamma_f$, $\delta_S(x,o) = 0$ ...……. Eq.4:5

The known constitutive relationship defined by the shear stress/deformation curve is expressed as

$\tau(x,z) = \phi(\gamma(x,z), \delta_S, d\delta_S/dt)$ or inversely, …… Eq.4:6

$\gamma(x,z, \delta_S, d\delta_S/dt) = \phi_I(\tau(x,z))$ …… Eq.4:6 a

Conclusion:

In the analysis of stress and deformation for uphill progressive slope failure, the basic FDM-equations for downhill progressive failure can be applied, provided the direction of the x-coordinate is reversed and that the sign of the incremental force **N** is changed. Hence, positive N signifies tension instead of compression.

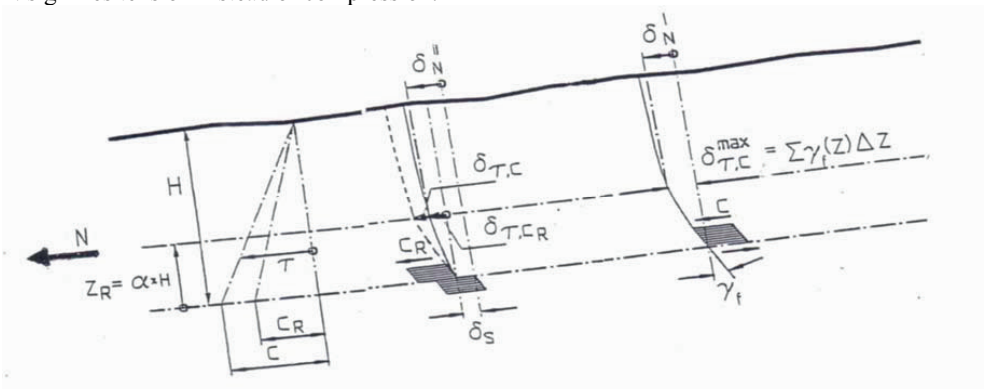

Stage II: $\delta_N = \delta_\tau = \delta_{\tau,cR} + \delta_S = \delta_{\tau,c} - \delta^{el}{}_{\tau,c \rightarrow,cR} + \delta_S$ Stage I: $\delta_N = \delta_\tau$

Figure 7:2.2 The down-slope displacement of a soil element (δ_N) must be compatible with the shear deformation (δ_τ) of the same element in relation to the sub-ground. In the figure, only deformations above the failure surface are defined, implying that the failure surface follows firm bottom in the case illustrated.

Thus, the shear stress $\tau(x,z)$ is a function of the shear strain $\gamma(x,z)$ and the displacement δ_S in the slip surface. If this function is known, the differential Equations 4:1 to 4:6 can be integrated numerically yielding the states of stress and the displacements for any chosen mode of mobilizing the resistance to failure propagation – and that in any chosen portion of the slope. (Cf Figures 6:3.2 and 7:4.1).

Equation valid in stage II, i.e. for values of $\delta_{S(x)} > \delta_{S(cR)}$
When the residual shear strength is attained in the slip surface, Equation 4:1c is substituted for Equation 4:1.

$$\mathbf{\Delta N = [c_R(x,o)-\tau_o(x,o)]\cdot b(x)\cdot \Delta x - q(x)\cdot b(x)\cdot \sin\beta(x)\cdot \Delta x - t(x)\cdot b(x)\cdot \Delta x} \quad \text{…….. Eq.4:1c}$$

where τ_o is defined as before

$\tau_o(x,o) = [\Sigma_o^{H(x)} \cdot g\cdot \rho(z)\cdot \Delta z]\cdot \sin\beta\,(x) - g\cdot \rho_W \cdot D_W(x)\cdot \sin\beta(x) - \Delta E_o(x)/\, b(x)\cdot \Delta x$…… (Eq.4:2) and

$c_R(x,o)$ = the residual large deformation strength – and/or if applicable the high deformation rate resistance – of the soil at z = 0.

Modulus of elasticity
The modulus of elasticity (E_{el}) enters into the analysis (Equation 4:3) when evaluating the displacement of a vertical section in the down-slope direction. Referring to the constitutive relationship shown in Figure 4:4.2, the initial shear modulus, which is valid below the elastic limit defined by (τ_{el}) and (γ_{el}), can be expressed as:

$G_{el} = \tau_{el}/\gamma_{el}$ and the corresponding E-modulus is then according to basic theory

$E_{el} = 2(1+\nu)\cdot G_{el} = \Omega\cdot c$

where Ω is a coefficient relating the E-modulus to the current peak shear strength (c).

In the analysis of uphill progressive failure, the incremental effect N_x constitutes a tensile force resulting in de-loading of the in situ earth pressures along the slope. As the E-modulus under de-loading conditions is normally higher than at loading, this effect should be taken into account. For further comments and exemplification confer Section 4.22 in Section 4.

Regarding the value of 'α' in Equations 4:4 and 4:4a and the shear stress distribution, confer Sections 4.25 and 4.26.

7.3 *Computation procedure*

The computational procedure in uphill progressive failure analysis is identical to that of downhill progressive failures, provided the following items are kept in mind:
- The x-coordinate is positive in the down-slope direction;
- The earth pressure increments N_x and ΔN are tensile forces reducing in situ earth pressures;
- The displacement in the down-slope direction is generated by tensile strain.

As demonstrated in Sections 4.3 and 4.4, the aim of the FDM-analysis is to determine the effects of the additional loads (N_i, q, and t) in terms of stresses and deformations all the way to a chosen location (x=0), which in the current case is situated somewhere up-slope. This is achieved by taking relevant stress/deformation relationships into account. Additional critical load may typically be located in a steep part at the foot of the slope, for instance in the vicinity of the scarp of a river-bank. The objective of the computations is to identify the critical conditions in respect of retrogressive failure. The additional tensile force, in terms of loss of support at the foot of the slope, capable of triggering such a failure is denoted N_{cr}. The step by step integration of the Equations 7:1 (4:1) and 4:2 to 4:6 can be made according to the procedure presented in Section 4.4 and will not be fully repeated in this context. **([5])**

([5]) Reference is also made to the Excel spread sheet demonstrated in Bernander, (2008), LTU 2008:11, Appendix C. The spread sheet was originally designed for the analysis of retrogressive slope failures. Cf also Appendix I of this document, where the method of procedure is exemplified for downhill progressive failure.

Yet, the method of procedure is briefly described again as follows:

Step 1:
Step 1a Beginning at some up-slope point x = 0 – where the in situ conditions are considered to be unaffected by the additional load being investigated – the shear stress is increased by $\Delta\tau$ kN/m^2, so that $\tau_1 = \tau_o + \Delta\tau_1$. The value of τ_o is defined by Equation 4:2. The abscissa of the studied section is then $x_1 = 0 + \Delta x_1$

The choice of the location for the coordinate x = 0 constitutes the uphill boundary condition – being a point, where the sought parameters N_x, δ_N, δ_τ, $E_{o,x}$ and $(\tau_x - \tau_{x,o})$ are taken to be known, or where they can be defined by ordinary soil mechanical procedures.
The analysis yields the additional force N_x, corresponding to zero displacement ($\delta \approx 0$) at the coordinate x = 0. **([6])**

The down-slope boundary condition demands that N_x is equal to the additional force (or load effect) N at the lower limit of the presumptive slide, i.e. where $N_x = N$ and $x = L_{cr}$.
The iterative process involved may require 'trial and error' choices of the location of the coordinate x = 0. (Cf Figure 7:4.1).

The in situ distribution of shear stress ($\tau_{x,o}$) can be determined by analyzing the shear stress redistribution generated by long-term creep effects, as they can be defined by appropriate long-term stress/strain relationships.

([6]) As stated in Section 4, it should be observed that the line defined by the in-situ stress $\tau_o(x)$ actually constitutes an asymptote to the curve $\tau(x)$ – the point x defined by the differential $(\tau_x - \tau_{o,x}) = 0$ being theoretically located at an infinite distance from A. This difficulty may be overcome by placing the point x = 0 where $(\tau_x - \tau_{ox})$ has a defined, but negligible value.

Step 1b Equation 7:1 or 4:1 gives the value of $\Delta N_1 = N_1$ in terms of Δx_1.
Step 1c Equation 4:3 yields the corresponding value of the displacement δ_{N1}, while $\delta_{\tau 1}$ is computed from Equation 4:4a.
Step 1d The value of Δx_1 is then obtained by the compatibility criterion (Equation 4:5), which is solved with respect to Δx_1.
Step 1e ΔN_1 may then be computed from Equation 7:1 and δ_N from Equation 4:3.
Step 1f The analyzed section is then advanced a distance of Δx_2, i.e. $x_2 = x_1 + \Delta x_2$.

Step 2 From this point and on, the calculation proceeds by repeating steps 1a) to 1f) for each vertical element and by advancing in steps of suitably chosen values of $\Delta\tau$ and Δx. The values of δ_N and δ_τ can then be expressed in terms of the assumed values of $\Delta\tau$ and Δx, and the correlating values of Δx and $\Delta\tau$ in each iterative step cycle have to be found by iteration so that the compatibility equation 4:5 is satisfied, i.e.
$\delta_N = \Sigma_o^x(\Delta\delta_N) = \delta_\tau$

The computational procedure is exemplified in more detail as an Excel spread sheet in Bernander (2008), Appendix C. Although being used there for studying downhill progressive failure, this spread sheet is also applicable to the analysis of retrogressive landslides.
The procedure is in principle the same as the one exemplified in Appendix I of this document applying to downhill progressive failure analysis

7.4 *Objectives and procedures for investigation of uphill progressive landslides*

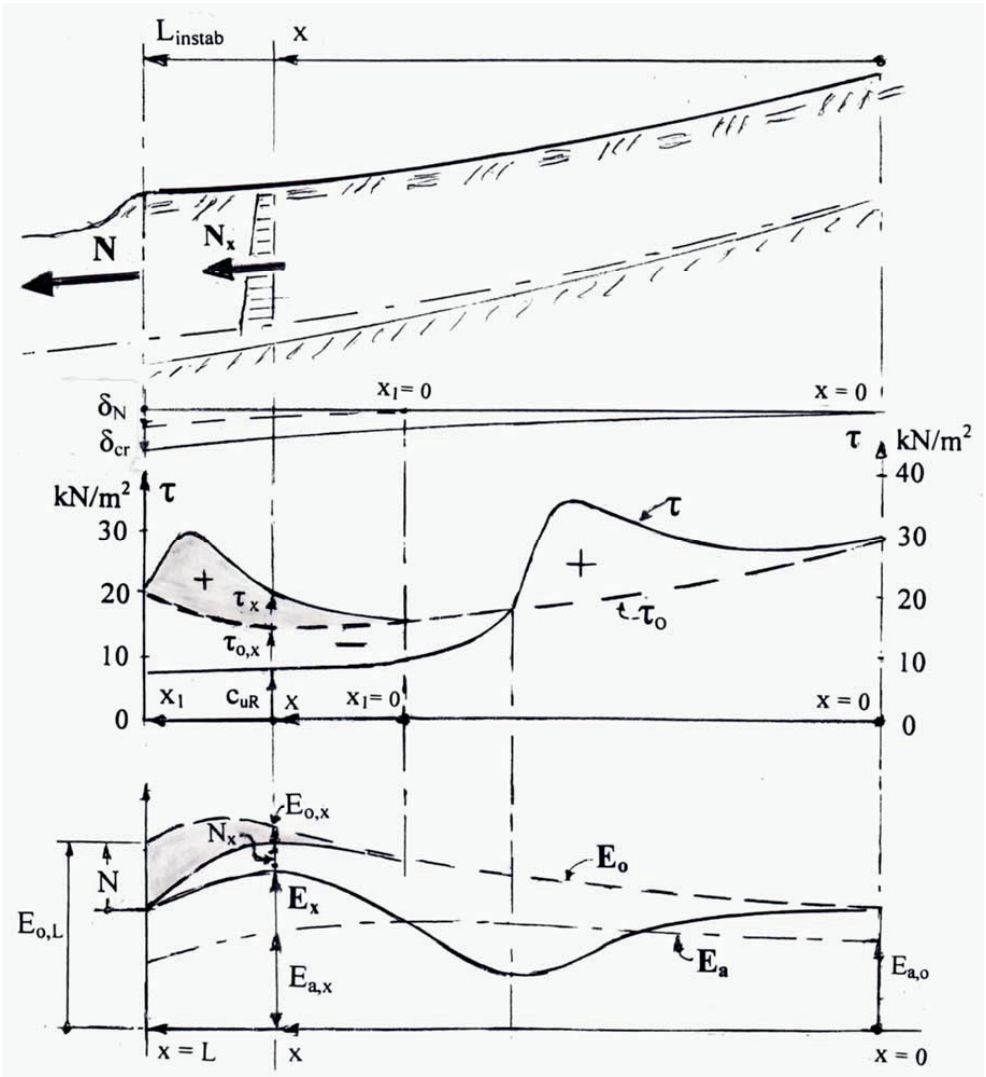

Figure 7:4.1 Principal results from uphill progressive failure analysis according Equations 7:1 and 4:2 to 4:6. Compare with Figure 8:3.3a and b.
The figure indicates three possible critical conditions of equilibrium in retrogressive slope failure:
Condition 2a) The disturbing load N having attained the limiting critical value $N = N_{cr}$, followed by active failure.
Condition 2b) Provided active failure does not occur, a critical condition may develop if the critical displacement ($\delta_{cr} = \delta_{instab}$) is exceeded, in which case the slope will fail even if the additional external load N were (hypothetically) removed – i.e. global failure takes place when $\delta \geq \delta_{cr}$.
Condition 2c) In the specific case shown in Figure 7:4.1, the slope will disintegrate in active failure before arriving at the critical displacement $\delta_{cr} = \delta_{instab}$ as $E_x = E_{o,x} - N_x$ falls below $E_{a,x}$, in part of the slope, which may disintegrate as described in Sections 6.42 or 6.43.

In Figure 7:4.1, the principal parameters derived from the computations are shown. The force N_x acting in a down-slope location denotes, as already mentioned, the earth pressure change that must not be exceeded at the section defined by the coordinate x, lest the displacements induced by N_x propagate beyond the starting point ($x \approx 0$) of the calculations.
N_x will, therefore, assume different values depending on the extent to which, as defined by the point of reference $x = 0$, the resistance up-slope of N_x is mobilized. Hence, any chosen portion of the slope may be analyzed for any selected failure plane.

The different stages and stability conditions of a retrogressive landslide have been discussed in Section 6, according to which the analysis shall focus on the conditions prior to possible global failure, i.e. the disturbance Phase 2. As opposed to Phases 4 and 5 in downhill progressive landslides, there is in a retrogressive slide no predictable final state of equilibrium once active failure and due disintegration of the sliding soil mass have been initiated.

In uphill progressive landslides – as in downhill progressive ones – the dynamic (or 'quasi dynamic') phase of the slide is triggered when the value of N for some reason exceeds the critical value N_{cr}. The term 'quasi dynamic' refers to the possibility of gradual progressive failure propagation in terms of an extremely slow creep movement over time, as defined in failure Conditions 2b) and 2c) below. (Cf Figure 7:4.1).

A cardinal precondition to be considered is the in-situ 'creep state', which as suggested in Section 6, can be defined as a slow uphill progressive failure, in principle according to Section 4. The in-situ state may of course also be determined by other computational methods. In the current context FEM-analysis is likely to be a suitable approach.
(Cf Section 8.3)

The in-situ state is referred to as stability ***Condition 1*** (or Phase 1) as in Section 6.3,

7.41 Safety criteria – ***Condition 2***, The disturbance condition, (Phase 2)

*Condition **2a** – Critical load due to local failure*
The disturbance condition, in which local failure is initiated by lacking support in terms of a tensile force N, is illustrated in Figure 7:4.1. The critical value of $N = N_{cr}$, potentially triggering total slope failure (Phase 2), is defined by the location of the reference point ($x = x_1$) for which $\tau_x = c_{Rx} = \tau_{ox}$ at the coordinate $x = x_1$.
Finding the most critical situation usually necessitates a procedure of combined 'trial and error' and interpolation. Also, as in conventional slope stability analysis, different failure planes may have to be investigated. **([7])**
Once the value of $N = N_{cr}$ at the location $x = x_1 = L_{cr}$ has been established, the safety factor against retrogressive slope failure may be expressed as
$\mathbf{F_s = N_{cr} / N}$ …… (Equation 3:7)
or, if additional loads (q and t) shown in Figures 4:2.1 and 4:2.2 also have to be considered,
$\mathbf{F_s = (N,q,t)_{cr}/(N,q,t)}$ …… (Equation 3:7a)
where $(N, q, t)_{cr}$ denote a critical combination of additional loading acting in the slope.

([7]) For more detail regarding computational procedures, confer Bernander, (2008), LuTU 2008:11, where Appendix C is applicable also to retrogressive failure analysis.

*Condition **2b** – Critical deformation (cf Figure 7:4.1)*
As in downhill progressive landslides, there exists also in retrogressive slides a certain condition defined by the critical displacement ($\delta_{cr} = \delta_{instab}$), in which case a slope will fail even if the triggering external load N at this point ceases to be active for some reason. As discussed below, ongoing long-term de-loading due to erosion may generate considerable displacements.

$$\boldsymbol{\delta_L \leq \delta_{cr}} \qquad \text{..... Eq. 7:4}$$

where δ_{cr} corresponds to δ_{instab} in Figure 4:2.4a.

Intrinsic deformation-induced retrogressive failure condition
The loss of down-slope support as well as locally reduced effective stress conditions because of erosion, inexorably imply deformations including related creep.
Failure Condition 2b) may therefore be at stake if the shear resistance in potentially critical parts of a slope is subject to gradual deformation-induced deterioration over time.

This applies in particular in slopes of highly *over-consolidated* clay, where deformation inevitably entails loss of shear resistance that in turn generates more deformation, causing again further loss of shear resistance …. and so on – possibly forming a 'self-generating' or intrinsic long-time failure process. (Cf Section 6.34.)
Importantly, the gradual extension of the zone subject to deformation-softening generates, per se, increasing downhill displacement.

Hence, 'Intrinsic retrogressive failure' related to the critical displacement (δ_{cr}) can occur in slopes of highly over-consolidated clay subject to erosion, provided active failure does not occur before the critical value of δ_{cr} is reached.

Chemical change of cat-ions caused by ground water seepage is another conceivable instability factor in this context.

*Condition **2c** – Intrinsic deformation-induced active failure condition (as per Figure 7:4.1)*
In the long-time transitory stage between failure Condition 2a) and Condition 2b), the earth pressure may locally, or in part of the slope fall below the active earth pressure, i.e. $E_x = E_{o,x} - N_x \leq E_{a,x}$).

This failure condition is illustrated in the case shown in Figure 7:4.1. As indicated there, the slope will in this particular case disintegrate in active failure before reaching the critical displacement δ_{cr} – possibly in the mode depicted in Figure 2:4.2d.
(Cf Sections 6.42 and 6.43.)

7.5 Synopsis

7.51 Short-term retrogressive failures – Condition 2a
In uphill progressive landslides, there is normally no predictable structure in the ultimate slide configuration due to lacking down-slope support.
As exemplified in Figures 2:4.2c and 2:4.2d, disintegration in active failure may take place in different modes, which are basically of a random character. This applies in particular to slides in soft and mildly over-consolidated clays, when the incidence of the additional disturbance

agent is of a decisive and short-term nature. Figure 6:3.2 shows an example of this type of retrogressive failure.

7.52 Long-time retrogressive intrinsic deformation-induced failure – Conditions 2b and 2c
By contrast, if the loss of shear resistance from a peak value (c) to the residual value (c_R) takes place as an extended time-dependent process in parts of a slope, a condition eventuating in global retrogressive slope failure (or spread) may slowly evolve. (Cf Section 6.34.)
Many retrogressive landslides (or spreads) occur as a result of long-time erosion in massive deposits of highly over-consolidated clays. The time scale of such processes may be a matter of centuries or millennia.
The following phenomena have to be considered in this context:
- The active disturbing agent – *erosion* – may result in massive loss of 'horizontal' support in the lower parts of a slope (or in the vicinity of a steep scarp) as well as significant overall reduction of vertical effective stresses. This is, for instance the case in Figure 8:3.2 featuring the Saint-Barnabé-Nord slide. (Cf Section 8).
- The loss of down-slope support inevitably generates ***uphill progressive tensile strains resulting in displacements*** in the downhill direction, inexorably entailing deformation-softening in the now highly over-consolidated down-slope clay layers. (Cf Bjerrum, 1967.)
- Deterioration of shear resistance, as well as growing extension of the zone subject to change, entail additional deformation and due deformation-softening in highly over- consolidated clay layers…. and so on.
- Gradual propagation further uphill of displacement and deformation-softening contribute over time to undermining the stability of the entire slope.

These phenomena are gradual, extremely slow processes in the potentially un-stable soil mass, essentially changing the states of internal stress without the presence of any active (short term) additional external load. Hence, a condition may develop that eventually leads to global retrogressive slope failure or spread. (Cf e.g. Skempton, 1964.)

'Instrinsic deformation-induced slope failure' implies that the determining geotechnical preconditions, from a 'slide hazard' point of view, may have been established already hundreds, may be even thousands of years before the incidence of the actual slide event.

Impact of FDM- progressive failure analysis considering deformations in the soil mass.
It may be pointed out that, for reasons given above, uphill progressive failure FDM-analysis renders 'additional edge' to the assessment of the impact of time-related deterioration of shear resistance.
The FDM-analysis highlights and defines important phases of the failure process. Furthermore, it underlines the fact that the degeneration of shear resistance over gradually *increasing* distance contributes, per se, to significant additional displacement that in turn leads to further degradation of c_R …… and so on.

The important conclusion of the reasoning above is that a retrogressive failure or 'spread' may actually be a very slow long-time phenomenon. The 'progressive transition' between failure Conditions 2a) and 2b), as defined above, may last over an extremely extended period of time, possibly a matter of hundreds or even thousands of years.

In other words, the current type of slope failure is – owing to preconditions established far back in the past – predestined to take place at some *undefined* point of time, more or less at

random. In fact, a retrogressive slide or spread of this type may very well occur without any identifiable disturbance agent that can be linked with on-going human activity or with some extreme climatic condition.
Or, to phrase the issue differently: Even if a slide has occurred during a spell of continuous heavy precipitation, raining may still only constitute 'the droplet that made the cup flow over'.

Many slides in the highly over-consolidated clays of eastern Canada are likely to belong to this category of random and time-wise unpredictable landslide hazards.

The thorough and highly instructive study of the Saint-Barnabé-Nord slide (Canada) by A. Locat, (2007) corroborates, in the opinion of the author of this document, the presence of precarious stability features of the kind discussed above.
Locat applied the uphill progressive FDM-analysis (ReFA) presented in this document. (Cf Section 8.3.)

Concluding remarks
Because of 'intrinsic deformation-induced' instability, slopes of the current kind may conceal potential disaster, the sudden occurrence of which is extremely difficult to predict, especially in the absence of some major relevant externally active triggering agent.

Yet, uphill progressive FDM-analysis of the kind demonstrated in this section provides at least a ***means of identifying potentially hazardous slope features*** so that remedial measures to preventing impending disaster can be implemented.

8. Numerical studies of retrogressive landslides using the Finite Difference Model

8.1 General

Retrogressive slides of the kind dealt with in Sections 6 and 7 are rather uncommon in Sweden, mainly due to the fact that areas with highly over-consolidated clays are sparse. (Cf Section 6.2.)
Yet, investigations of uphill progressive failures occurred have indicated a certain similarity to downhill progressive slides from structure-mechanical points of view although – as pointed out in Section 6.2 – there are important differences as regards preconditions and slide development.
Subsequent work by the author focused on retrogressive slides (or spreads) – to some extent in co-operation and communication with the geotechnical section of Département de Génie Civil at Université Laval, (Québec), (1) – has indicated that the Finite Difference FDM-approach proposed in this document is applicable also to slides in highly over-consolidated clays such as, for instance, the Champlain clays of eastern Canada. Research targeting this field of geotechnical engineering has a long history in this country.

Hence, the scope of this section is limited and will, apart from comments on the investigation of the Saint-Barnabé-Nord landslide by A. Locat, (2007), only briefly deal with results from two studies of uphill progressive slope failure performed in 2005 using the FDM-approach to retrogressive analysis (ReFA).

(1) The division is headed by professor Serge Leroueil.

8.2 Regarding existing software for FDM analysis

8.21 FDM computer program in Window's C++
In Section 4.5 available computer software in C++ is briefly described, by which each iterative computation step is a matter of seconds, once input slope data have been inserted. (Cf Figures 4:5.1 & 4:5.2.)
This program was originally designed solely for downhill progressive failure analysis but should in principle be applicable also to retrogressive failure analysis – the equations being virtually identical.

However, details in the present software structure appear to preclude the use of the program when the signs of main parameters, and the direction of the x-coordinate in relation to slope geometry, are reversed. Yet, adaptation of this software to retrogressive slide formation would actually not be a difficult task.
In the example presented in Figures 6:3.1 to 6:3.3 and the results of which are discussed in Section 6, the in-situ stress condition has been established using the Windows C++ program in the same way as for a downhill creep failure condition.

Yet, using this particular software for determining the in-situ condition is feasible only as long as the potential failure surface is located at sufficient depth below the ground surface, and is therefore not applicable when the failure surface emerges near the foot of a steep down-slope scarp.
.

8.22 Spread sheet in Window's Excel (2005) – FDM-approach
For want of suitable computer software for the study of two cases of uphill progressive slope failure, a program in the form of an Excel spread sheet was designed for this purpose early in 2005. The program, which is applicable to the analysis of both uphill and downhill progressive landslides is exemplified in Bernander, (2008), Appendix C, (LuTU 2008:11) where it is used, among other, for investigating the spread of downhill progressive slides over virtually horizontal ground.

As explained in detail in Appendices A and B of the same report, the Excel spread sheet is easy to use for uniformly inclining slopes, where the depth of the failure surface is taken to be constant. Applied in this way, the spread sheet is well suited for educational purposes, promoting the understanding of the complicated mechanisms operating in progressive landslides.
However, although applicable also to arbitrary slope geometry within the chosen framework, the spread sheet is too laborious for every day use related to more accurate analysis of downhill or uphill progressive failure in slopes with complex geometry.

8.3 The Saint-Barnabé-Nord landslide in Québec, Canada

On December 10 (2005), a large landslide (or spread) took place 25 km northwest of the town Trois-Rivières in Saint-Barnabé-Nord Municipality, Québec, Canada. The length of the ground area involved in the slide was almost 200 m and the mean width being about 160 m. Hence, the area involved amounted roughly to 3 hectares. The thickness of the over-consolidated varved silty clay deposit varied from 22 m to 55 m between the lower and the upper slide limits. The depth below the ground surface to the failure plane was about 25 m over a distance of 70 m.
The silty clay, deposited in the glacial Champlain Sea, was highly over-consolidated the peak shear strength in direct shear tests near the slip surface being typically in the order of 80 kN/m^2.

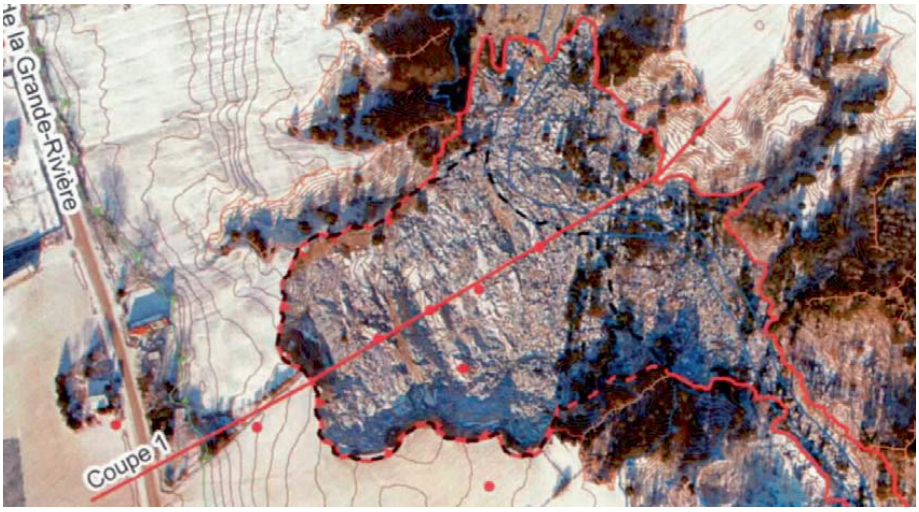

Figure 8:3.1 Aerial photo of the Saint-Barnabé-Nord slide. Map of elevation contours in the slide area. According to A. Locat (2007)

A comprehensive study of the Saint-Barnabé-Nord slide, (2005) was performed by Ariane Locat at Laval University, Québec. (Cf A. Locat, 2007.) Those dedicated to issues related to retrogressive 'spreads' are recommended studying this thorough post-slide investigation.

Of primary interest in this context is the ambition, in an important part of the study, to explain the cause of the slope failure by applying the FDM-approach proposed in this document – especially as this analysis relates to a retrogressive landslide that has actually occurred.
In the current case, the modified FDM-adaptation to retrogressive slide formation described in Sections 7.2 and 8.22 was used.

8.31 The in-situ condition – *Condition 1 (or Phase 1)*
A crucial issue in this context was defining the in-situ state of stress and the earth pressure distribution before the slide. In Locat's study the assessment of the in-situ condition was done by FEM-analysis, duly considering the way the effective stresses in the clay deposit had been affected by massive erosion in past eras, as well as by the associated change of pore water pressures related to the evolution of ground water seepage over time.

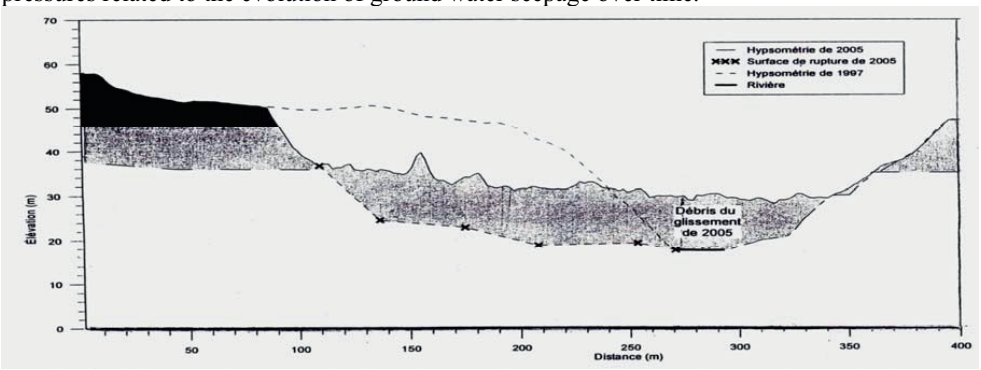

Figure 8:3.2 Section through the Saint-Barnabé-Nord slide. (According to A. Locat (2007). Note the difference between vertical and horizontal scales. (The positions of the co-ordinate axes are in this figure somewhat modified and different from those shown in Figures 8:3.3a and 8:3.3b).

8.32 Results from the FDM-analysis made
As regards the retrogressive FDM-analysis, Locat (2007) concludes that it did not identify the *precise* cause of the Saint-Barnabé-Nord slide. Nevertheless, the following important findings from the study were presented:
1) The slide *cannot* be explained in terms of analysis based on plastic limit equilibrium.

2) The critical tensile force ($N_i = N_{cr}$) at the foot of the slope, capable of triggering a slide, was according to the analysis found to be 181.8 ≈ 182 kN/m for a value of c_R = 20 kN/ m^2.
The associated critical displacement was δ_{Ncr} = 0,041 m. (Cf Figure 8:3.3a.)
At this stage, the earth pressure $E(x) = E_o(x)-N(x)$ proved to be higher than the active earth pressure ($E_{a,Rankine}$) for all values of x.

3) For values of c_R = 20 kN/ m^2, the critical deformation $\delta_{cr} = \delta_{instab}$ and the instability length (L_{instab}) were determined to be 0.28 m and 165.5 m respectively. **([2])** (Cf Figure 8:3.3b.)

([2]) This situation corresponds to Condition 2b in Section 7.4. The critical deformation ($\delta_{cr} = \delta_{instab}$) and the length parameter L_{instab}, being of major interest also in the analysis of *downhill* progressive slides, have been defined in Bernander (2000). Cf Figures 4:2.4a, 4:7.2 or 7:4.1 in the present document.)

4) As the uphill progressive failure in the current study develops from the initiating phase – i.e. when $\delta = 0.041$ m – towards the condition when $\delta_{cr} = 0.28$ m and $x = L_{instab} \approx 165$ m, the computed earth pressure $E(x) = E_o(x) - N(x)$ happens to fall below $E_{a,Rankine}$ between x = 288 m and x = 324 m (i.e. over distance of 36 m). (Cf Figure 8:3.3b.)
Figure 7:4.1 in Section 7 exemplifies a similar case).

Hence, this specific active earth pressure condition will in the current case lead to the disintegration of the soil mass forming the typical pattern of 'horsts' and 'grabens' (i.e. ridges and depressions) that may be seen on the aerial view in Figure 8:2.1.

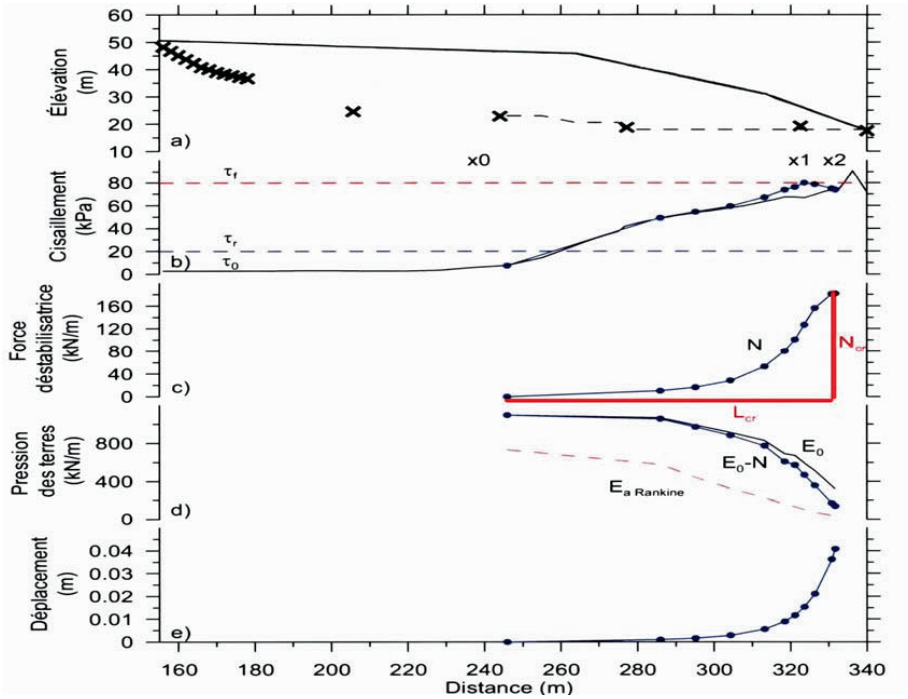

Legend applying to Figures 8:3.3a & 8:3.3b

- Ground surface
- Failure surface as measured by 'piezocone'
- Failure surface in computer model
- Curve line prior to disturbance
- Curve line after disturbance

Figure 8:3.3a Results from Finite difference (FDM) analysis of the Saint-Barnabé-Nord landslide showing the critical tensile force N_{cr} with a capacity to initiate uphill progressive slope failure. The associated critical length (L_{cr}) and displacement are also indicated. (From **A. Locat, (2007)**. The situation shown in the figure corresponds in principle to Condition 2a in Figure 7:4.1 in Section 7.

As mentioned, Locat does not claim having established the *precise* cause of the landslide, and this is of course true in an absolute sense.

Yet, the results of the FDM-analysis made present a good understanding of the inherent preconditions of instability that finally led to the Saint-Barnabé-Nord landslide. This may be explained as follows in Sections 8.33 to 8.36.

8.33 About the triggering phase - disturbance ***Condition 2a***
Admittedly, there did not really exist any identified *external* tension force $N_i = N_{cr} \approx 182$ kN/m acting at the canyon scarp. Yet, merely a moderate displacement in the potentially developing (or existing) failure zone – causing for instance a loss of shear resistance due to deformation-softening of say $\Delta c = 9$ kN/m^2, over a length of 20 m – would bring about a destabilizing effect corresponding to a value of $N_i = 9 \cdot 20 = 180$ kN/m. (Cf Figure 8:3.3a.)

Local *gradual* long-term degeneration of shear resistance of this magnitude in the most critical portion of a slope is actually a very likely scenario in a highly over-consolidated clay deposit of the current kind. The residual resistance c_R ($= c - \Delta c = 80 - 9 = 71$ kN/m^2) would in this case correspond to about 89 % of the *original* peak strength (80 kN/m^2) of the over-consolidated clay.

Referring e.g. to the findings of Ladd & Foot (1974), the reduction of the effective stress by erosion in the steeply inclining ground towards the river, can readily explain a deformation-induced loss of shear resistance of this magnitude.

Considering, the specific features of the site of the Saint-Barnabé-Nord slide shown in Figure 8:3.2, the total loss of vertical effective stress because of long-time erosion – at a distance of 20 m up-slope from the foot of the scarp – can be estimated to have been about 75 %.
The corresponding loss of shear resistance would then amount to $\Delta c \approx 60$ kN/m^2, i.e. a condition strongly indicating that a failure plane, extending far from the foot of the slope, had very likely developed already long ago in past times. (Cf Figure 8:3.2.)

Furthermore, the computed associated displacement near the canyon is in the order 40 mm. Movements of this size would hardly be noticeable at visual inspection, and monitoring such deformations over time would require accurate instrumentation.

However, as the computed earth pressures at this stage still exceed active Rankine pressure, the soil mass could still retain its monolithic structure in the current state.

Synopsis as regards the disturbance condition.
From the results of Locat's analysis it may be concluded that retrogressive failure could readily have developed because of inherent, gradually changing conditions at the foot of the slope – i.e. without major interference from any external agent in connection with the slide event.
Nevertheless, a likely triggering factor in this context may consist of 'jacking' forces due to hydraulic pressure in tension cracks extending from the ground surface down to the ground water level, or deeper. **([3])** During long spells of rainy weather, forces of this transitory nature may – as illustrated in Figure 10:3.1 in Section 10 – last long enough to form the apparent triggering agent of a slide.
However, such a condition would relate the failure event to intense and continuous rainfall and thus to a certain point in time – thereby falsely indicating that raining was the main cause of the landslide.

In a case like this, heavy rain is most likely just '*the droplet that made the cup flow over'.*

([3]) In over-consolidated clays cracks in a potentially active zone may extend below the mean ground water level in the formation.

8.34 About the critical deformation phase - ***Condition 2b***

Critical deformation (δ_{cr}) in uphill, as well as in downhill progressive slope failure (δ_{instab}), is defined as a condition, in which the progressive failure process will continue even if the triggering external load ceases to be active for some reason. A condition of this nature may actually develop in highly over-consolidated clays due to long-time *deformation-induced* loss of shear resistance. The deformations (or the displacements in the failure plane) may then gradually increase to a point, where the critical value ($\delta_{cr} = \delta_{instab}$) related to global retrogressive failure (or spread) is reached. (Cf e.g. Figure 7:4.1.) **([4])**

([4]) As explained in Section 7.52, dealing with the 'Intrinsic deformation-induced failure condition', long-term retrogressive failure due to erosion and related hydrological change may also apply in this context. The critical deformation is then attained as a result of slow progressive time dependent deterioration of the stability conditions that is mainly related to deformation-induced loss of shear resistance and associated movement and creep effects.

In Locat's analysis, the critical deformation condition is shown in Figure 8:3.3b.

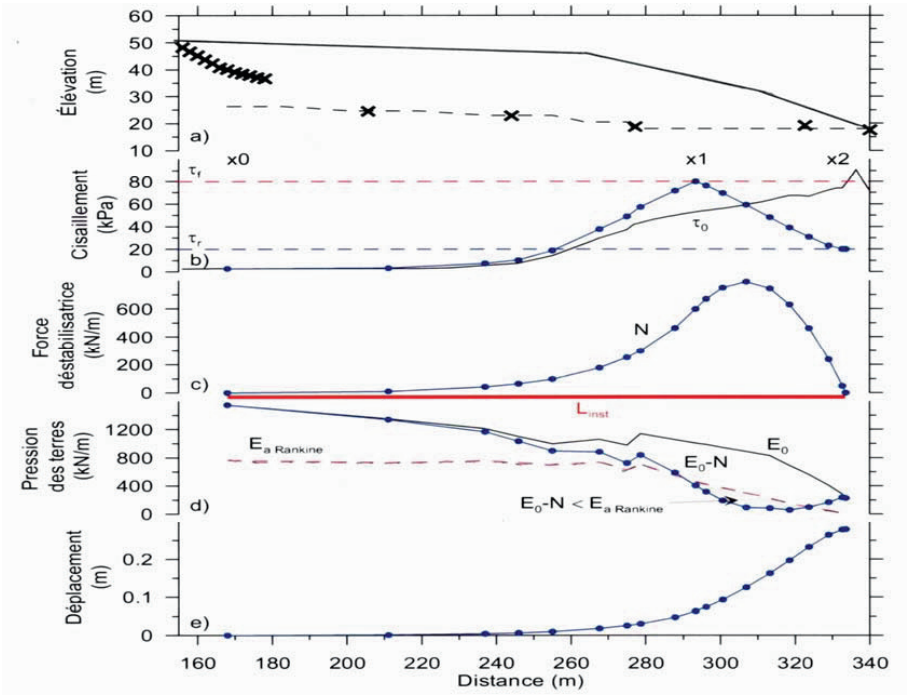

Figure 8:3.3b Results from Finite Difference retrogressive failure analysis of the Saint-Barnabé-Nord landslide showing the critical deformation condition, in this case resulting in active disintegration failure. Associated spread length ($L_{instab} \approx$ 165 m) and displacements are also indicated. (According to A. Locat, (2007). The situation shown in the figure corresponds in principle to Condition 2b in Figure 7:4.1 in Section 7. Regarding legend, see Figure 8:3.3.a

Once, the critical force exceeds the value of N_{cr} ($\approx$ 182 kN/m), progressive failure development is inevitable. Yet, the *gradual* displacement-induced deterioration of shear resistance may still only result in slow time-dependent increase of deformations and associated effects of creep. This means that the *transition* from the previous triggering phase

(defined by N_{cr}) to the current critical phase (defined by δ_{cr}) can, as emphasized in Section 7.52, be a lengthy process that, provided the soil structure remains monolithic, merely evolves into an intermediate 'temporary' but long lasting state of equilibrium.

The critical deformation ($\delta_{cr} = \delta_{instab}$) in the stage depicted in Figure 8:3.3b is 0.28 m when the residual shear resistance c_R is assumed to be 20 kN/m^2. However, interestingly δ_{cr} is found to be remarkably insensitive to the value of c_R – i.e. $\delta_{cr} = 0.24$ m even for a value of c_R that is as low as 5 kN/m^2. **([5])**
The fact that δ_{cr} is in the order of 0.3 m at this stage, indicates that a slip surface is actually already developed – notably prior to the subsequent phase of disintegration. **([6])**

([5]) This agrees well with similar studies of downhill progressive slides.
([6]) Confer the corresponding phenomenon in downhill progressive slides before the final disintegration in passive failure shown in Figure 3:3.5. (Cf also Bernander, (2008), where this issue is dealt with in detail as regards downhill slides in Section 5 of LuTU 2008:11.)

8.35 About the final disintegration phase – ***Condition 2c***
According to Locat's analysis the earth pressure E_x (= $E_o - N_x$) in the soil mass falls in this case below active Rankine pressure over a distance from x = 228 m to x = 334 m already before reaching Condition 2b, where $\delta = \delta_{cr}$ (= δ_{instab}). This implies that the process of disintegration of the soil mass begins to take place.
In over-consolidated clays, the active failure normally ends up as the configuration of 'horsts and grabens' seen on Figure 8:3.1. (Cf also Figure 2:4.2c in this document.)

8.36 ***Conclusions*** from the FDM-study of the Saint-Barnabé-Nord landslid***e***
The retrogressive analysis of the Saint-Barnabé-Nord landslide renders a valid structure-mechanical account of the mechanisms relevant to the studied kind of slope hazard, identifying the magnitude of the load capable of generating local instability, as well as the limiting conditions leading to final disintegration of the slope in active failure.

In the opinion of the author of this document, any existing slope exhibiting similar geotechnical features should be regarded as an impending potential hazard of a random nature.
Yet, slope failure can nevertheless be prevented by proper analysis considering deformations and deformation-softening, and by subsequent implementation of pertinent remedial measures.

8.4 *The Landslide at Sköttorp along the Lidan River, Southwest Sweden*

In February, 1946, a slide with a length (in the slide direction) to width relationship of about 200 to 360 m took place in moderately over-consolidated clay along the Lidan River at Sköttorp. An interesting and in many respects detailed investigation of the slide by Odenstad (1951) was published as Proceedings No 4 of the 'Royal Swedish Geotechnical Institute'. (The former name of Swedish Geotechnical Institute.)

Already in this report, Odenstad characterized the Sköttorp slide as having been generated by instability at the foot of the slope, featured by the scarp of the Lidan River canyon. It was concluded that failure had developed retrogressively up-slope in a step by step disintegration process – this being a way of explaining the 'horsts and grabens' configuration of the finished slide.

It is not within scope of present report to deal in detail with case records of retrogressive slides in Sweden. Yet, it may be of interest in the current context to mention that analyses of the Sköttorp slide by the author (2005) – based on the uphill progressive approach featured in Section 7 – essentially corroborate Odenstad's comprehension of the retrogressive character of the slide.
The analysis according to the uphill progressive failure FDM-approach indicated expressively that the slip surface tended to develop in the uphill direction far away from the unstable scarp. This condition evolved *prior to* the final disintegration in active failure in the way evidenced by the study of the Saint-Barnabé-Nord slide. (Cf Conditions 2b and 2c in Section 8.3. and Figure 2:4.2c in Section 2.)

The studies by the author of the Sköttorp slide (not published) were of a preliminary nature of the sort exemplified in Figures 6:3.1 and 6:3.2 in Section 6.

8.5 *The Landslide along the Nor River, Southwest Sweden*

On April 12, 1969, another large landslide occurred in moderately over-consolidated glacial clay along the bank of the Nor River not far north of Lake Vänern in south-western Sweden. The length to width ratio was about 140 m to 350m.

As may be concluded directly from Figure 8:5.1, the The Nor River slide clearly features active failure development. The slide was described in a task report from SGI, dated November 3, 1970 by Lindskog and Wager, who also claimed its retrogressive character, referring among other to Odenstad's uphill failure evolution in distinct steps.

As in the case of the Sköttorp slide, preliminary FDM-analyses (2005) confirmed the uphill progressive nature also of this slide.

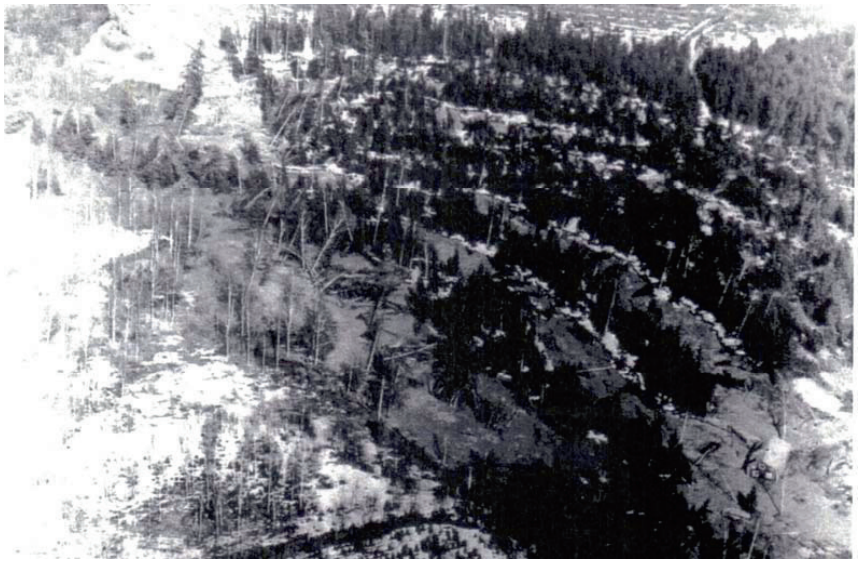

Figure 8:5.1 Aerial photo of the retrogressive landslide along the eastern bank of the Nor River, Sweden.

9. Factors conducive to the brittle nature of slope failure

9.1 *Brittleness due to inherent properties of the soil*

9.11 Importance of brittleness for the determination of slope stability
Brittleness in clay material implies high deformation modulus and energy accumulation at loading, leading to sudden failure and breakdown when the stress state becomes critical. Hence, brittleness affects both the initiation of progressive failure and the final ground configuration of a landslide.

9.12 Inherent sensitivity of soft clays
Although the current report focuses on the effects on slope stability of strain-softening in soils, the topic of sensitivity as such will not be dealt with in great detail here. Elaborating on this issue is not within the scope of the report. The interested reader is referred to literature on the subject.
Valuable contributions to the knowledge of the properties of soft Scandinavian clays have, for instance, been made by R Larsson (1977) in the SGI Report No 4, named "Basic Behaviour of Scandinavian Soft Clays" and by Karlsrud, Aas & Gregersen in their State-of-the-art Report to the Toronto Symposium on Land-slides (1984).

However, some important points that will be considered in the current context are:

1) When studying brittle slope failure, it is necessary to know not only the peak shear strength of the soil but its entire stress/strain/displacement behaviour, especially the residual shear strength at large deformations (c_R). Hence, the constitutive relationship should include modelling of the post peak conditions subsequent to the formation of a slip surface or shear band – the residual shear resistance at slip being strongly dependent on displacement and, in particular, the rate of displacement.

As emphasized in Section 3.1 the residual shear strength (c_{ur}), as determined in the laboratory on completely remoulded (stirred) clay samples, has little relevance as regards the real residual shear resistance in an incipient failure zone. In the present report, this lack of proven compatibility is dealt with by differentiating between the completely remoulded laboratory shear strength (c_{ur}) and the un-drained resistance (c_{uR}) – or the partially drained resistance (c_R) – that can actually be mobilized in an incipient failure zone.

The sensitivity of normally consolidated clays is largely indicated by the ratio of natural water content to liquid limit (w/w_L), or more specifically by the liquidity index:
$I_L=(w- w_P)/(w_L-w_P)$, where w_P is the plasticity limit.

The time of applying additional load and the concurrent drainage conditions in the potential failure zone are of paramount importance in this context. These vital strength and deformation properties are not adequately revealed by present soil testing procedures, and new methods for laboratory testing and/or testing in the field will have to be developed.
For instance, according to a current laboratory procedure in Sweden, clay samples are sheared in DSS-tests at a standard rate of 0.15 radians/24 hours. This corresponds to a rate of displacement of about 0.125 mm/hour on a 20 mm thick sample and 1.25 mm/hour on a 200 mm high specimen. The question is in what way such test results are compatible – especially as regards post peak residual resistance – with the conditions actually prevailing in the various phases of progressive slope failure. The rates of displacement in the different

phases of development in an ongoing slide may vary from millimetres per day to meters per minute.

2) As regards the formation of failure planes in small test samples of clay, it may be observed that the use of rubber membranes in DSS tests is prone to distort the stress/deformation relationship of soft clays. This is because membranes contribute in particular to the residual shear strength of soft clays by delaying and controlling slip-surface formation. One way of avoiding this problem is to confine specimens in DSS tests by means of horizontal rings, which can move freely relative to one another. (Bernander & Svensk, 1985). In respect of the effects of time, see Section 9.6 below.

9.13 Brittleness related to over-consolidation

Strain- and displacement-softening is not limited to sensitive normally consolidated clays. Over-consolidated clays under ongoing deformation tend to attain values of residual shear resistance that are related to the current vertical effective stress in the formation. (Ladd & Foot, 1974).

The effects of deformation-softening in highly over-consolidated clays are dealt with in Sections 6, 7 and 8. Such clays are known to show brittle behaviour, a condition frequently leading to retrogressive landslides, often denoted as 'spreads'. Retrogressive slides in e.g. London clay (Skempton, 1964) and Champlain clays (Canada) are well known occurrences of this type.

Brittleness of the kind is even more pronounced in highly over-consolidated cemented clays. Fissures in such clay, which are oriented along a potential failure surface may be, or evolve to be, slicken-sided, thus forming planes of acute weakness. Bjerrum (1967) studied numerically the possibility of brittle retrogressive failure in slopes of cemented tertiary clays.

Even for moderate values of the over-consolidation ratio (OCR), clays may exhibit significant strain softening. For instance, excess pore water pressures generating reduced effective stress conditions are conducive to brittle soil behaviour.

9.14 Slide development as a function of brittleness index

The brittleness index was defined by Bishop, (1967) as $B_I = 1 - c_R/c_u$. The higher the value of B_I, the more potential energy is released in the failure process, (Cf. Section 2.4). The effects of varying brittleness are illustrated in Figure 9:1.1, where a slope has been analyzed assuming five different values of the c_R/c_u- ratio.

Table 9.1.1 *Results of the sensitivity study*

	Disturbance condition		Global failure condition				
c_R/c_u	N_{cr} kN/m	L_{cr} m	E_{max} kN/m	$E_{Rankine}$ kN/m	$L_{E>E(Rankine)}$ m	q_{cr}^{PrF} * kN/m^2	$q_{cr}^{I\text{-}PlFA}$* kN/m^2
0.7	120	117	904	1250	0 #	12.0	110
0.6	105	108	1180	1250	60 #	10.5	110
0.5	100	107	1600	1250	210 #	10.0	110
0.4	97	105	2130	1250	290 #	9.7	110
0.3	95	103	2800	1250	410 #	9.5	110

* These parameters denote the magnitude of the evenly distributed load on the ground surface that would initiate failure according to PrF and I-PlF analyses respectively.

As the ratio of c_R/c_u ranges from 0.3 to 0.7, the force required to initiate a slide varies from 95 to 120 kN/m. The value of N_{cr} is thus not extremely sensitive to the ratio of c_R to c_u. This applies even more to the corresponding critical lengths (L_{cr}). The results of varying the c_R/c_u-ratio are shown in Table 9.1.1. (Confer also Appendix B in LuTU 2008:11, where the issue has been studied more comprehensively.)

By contrast, as demonstrated in Table 9.1.1 and Figure 9:1.1, the risk and the extent of global slope failure are radically affected by this parameter.
Considering that the corresponding ratios between $q_{cr}^{\text{I-PlFA}}$ and q_{cr}^{PrFA} in Table 9:1 range from about 11 to 9, it is clear that computations based on the plastic equilibrium concept may greatly underestimate the ultimate consequences and degree of disaster related to landslides in deformation-softening soils.

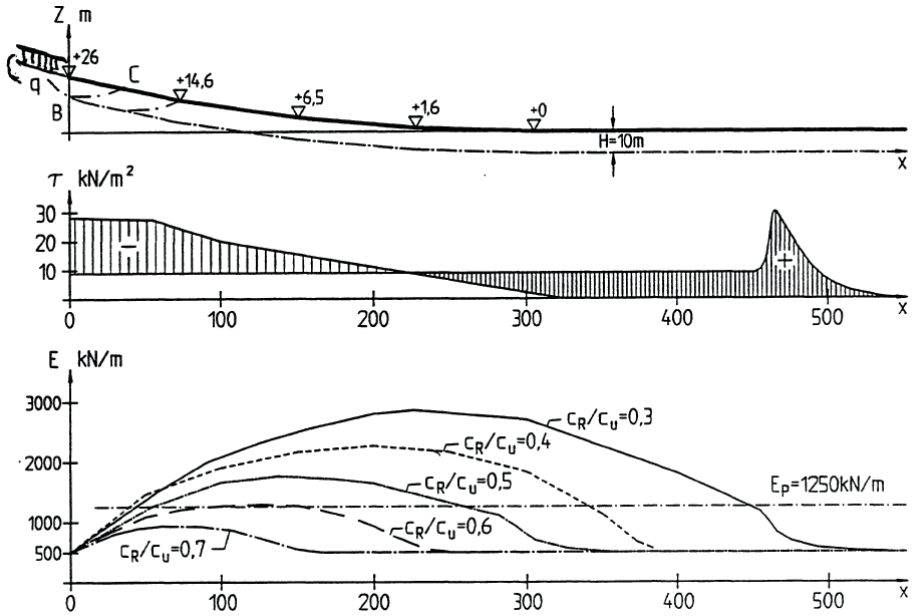

c_R/c_u = 0.30 – 0.70 γ_{el} = 2 % γ_f = 6 % δ_{cr} = 0.3 m $G_o = \tau_{el}/\gamma_{el}$ = 750 kN/m^2
c_u =30 kN/m^2 τ_{el} = 15 kN/m^2 $E_{el,o} = 3G_o$ = 100·c_u = 2250 kN/m^2
$\rho \cdot g$ = 15,5 kN/m^3 k_o^{max} = 0,594 (computed) E_{mean} = 100·$c_{u,mean}$ = 2250 kN/m^2

Figure 9:1.1 Diagram illustrating the static build-up of down-slope earth pressures (Phase 4) for five different scenarios based on the c_R/c_u ratios of 0.3, 0.4, 0.5, 0.6 and 0.7. Note that already for c_R/c_u = 0.5, the length of the potential passive zone amounts to some 270 m, whereas for c_R/c_u = 0.7 no veritable landslide is likely to occur. (Cf similar study by Bernander & Gustås, NGM 1984.)
The slope shape is defined (in 2-D) by the expression $z = 26 \cdot (x/300)^2$ m.

Figure 9:1.1 indicates that a local up-slope failure at c_R/c_u- ratios greater than 0.7 will in general not generate static earth pressures sufficient to provoke disintegration and excessive heave of the ground further down the slope. Progressive failure would in such cases only result in limited displacement, settlement and crack formation in the upper parts of the slope. (Cf Section 5.5, dealing with the earth movement at Rävekärr.)

By contrast, in the scenarios based on c_R/c_u - ratios less than 0.6, passive resistance is exceeded already by *static* earth pressure build-up, entailing massive heave and associated ground movement over long distances, as evidenced in most of the slides listed in Chapter 5, 'Case records'.
The high rates of deformation in the final dynamic phase of the slides (Phase 5 according to Section 3.3) tend to further reduce the un-drained residual shear strength c_{uR}, thus boosting the static and dynamic forces determining the features of the finished landslide.

9.15 Sensitivity due to layers of cohesion-less soils
Loosely compacted silts and sands, with relative densities well below the critical relative density (D_{cr}), are generally prone to deformation-softening or even to liquefaction. However, in natural slopes with creep deformations going on for centuries or more under constant shear, layers of cohesion-less material are likely to have been pre-sheared to the effect that a state of critical density prevails – i.e. a condition, which is not very conducive to strain-softening from additional shear.
Yet, even soils in states of critical density tend to develop excess pore water pressure (or to liquefy) when subjected to pressure wave radiation associated with blows from pile driving, heavy soil compaction or rock blasting. To some extent this may also apply to clays.

9.16 Conclusions
Considering the results shown in Table 9.1.1 and Figure 9:1.1, it is evident that if we aspire to predict the possible outcome of local disturbance in a slope, it will be imperative to devise methods and procedures designed to document the true soil behaviour under the conditions that actually prevail during earth movements of this kind.
The figure also indicates that progressive failure is conceivable also in soft normally consolidated clays of moderate sensitivity, as postulated by Kjellman, (1954).

9.2 *Brittleness related to slope geometry*

The risk of brittle failure in natural slopes is by no means restricted to the degree of strain softening in the soil. Geometry and morphology of the soil profile greatly contribute to brittle behaviour in the formation of slides.

9.21 Exemplification
Figures 9:2.1 a and b show two slopes with different profiles, whereas all other relevant parameters are taken to be identical, including the elevations of the points A and B and the distance between them. **Slope a)** inclines linearly, while **Slope b)** follows a curve defined by the expression $z = 26 \cdot (x/300)^{1.7}$ m.
The strength parameters being identical, the computed safety factors against slope failure based on ideal-plastic failure analysis (I-PlFA) are practically the same. Notably, this is valid despite the fact that the ground surface gradients, and the profiles of the assumed failure planes, vary in different ways between points A and B in the two cases.

In contrast to the results of I-PlF-computations, progressive failure analyses (PrFA) according to Sections 3 and 4 reveal that the potential slide hazard is radically different in Slope a) and Slope b). The critical loads (N_{cr}), defining the risk of initial local failure, are presented in Table 9.2.1 for a c_R/c-ratio of 0.4. Notably, the safety factor against slide initiation as per Equation 3:8 ($F_s^I = N_{cr}/N_i$) is about **90 %** higher for Slope a), than for Slope b).

Table 9.2.1 *Impact of slope geometry - Exemplification*

	Slope shape	c_R/c	F_s^I	L_{cr}	δ_{cr}
In the case of Slope **a)**	Linear	0.4	**286/**N_i	88 m	0.093 m
In the case of Slope **b)**	$z = 26\cdot(x/300)^{1.7}$ m	0.4	**151**/N_i	84 m	0.096 m
($\rho\cdot g$ = 16 kN/m^3 c = 25 kN/m^2 $E_{el} = 75\ c_{u,mean}$)					

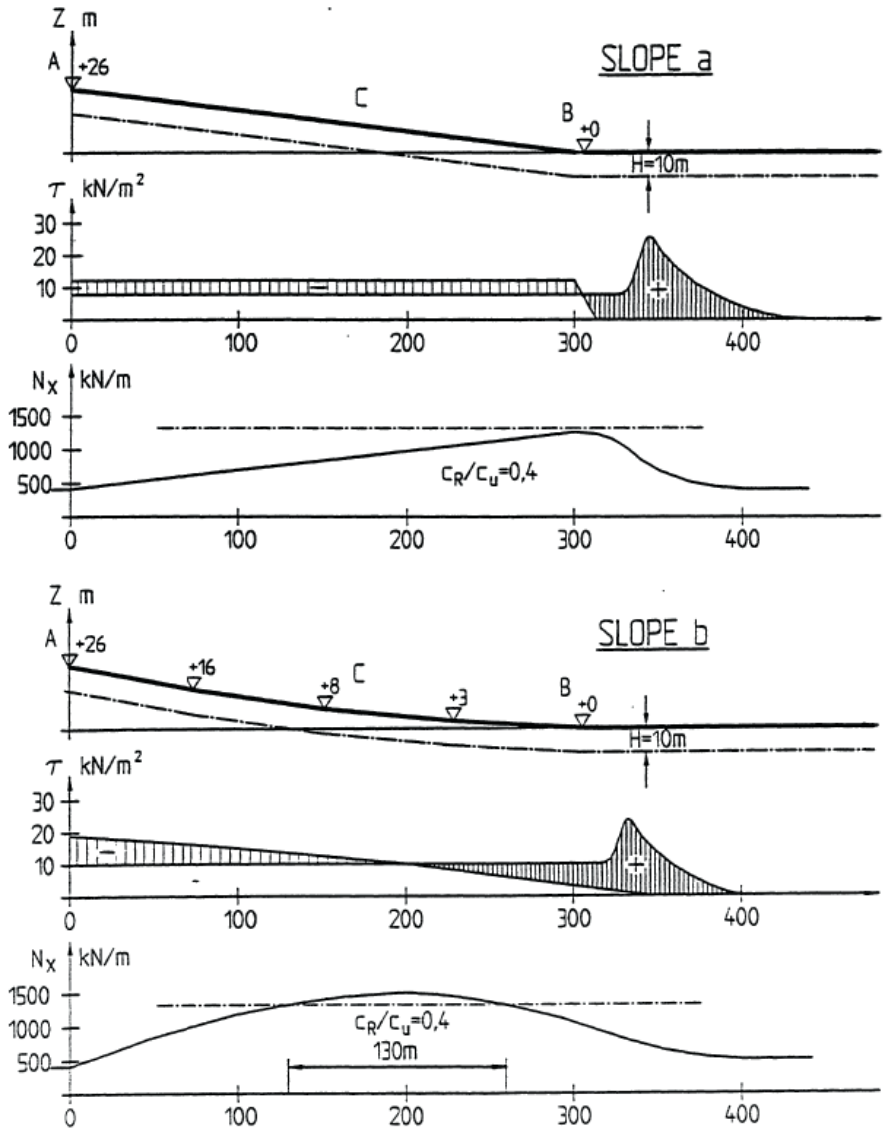

Figure 9:2.1 **Slope a)**: The ground surface and the assumed failure plane slope ***linearly*** from point A to point B. **Slope b)**: The ground and the assumed failure plane follow a curve defined by the expression $z = 26\cdot(x/300)^{1.7}$ from point A to point B. (In principle from Bernander & Svensk, 1982)

Moreover, as may be concluded from Figure 9:2.1 and Table 9.2.2, the degree of disaster that would ensue if local failure were to be triggered by some disturbance, is far more serious for Slope b) – i.e. the risk of an extensive passive zone being formed is much greater in Slope b) than in Slope a).
The criterion with regard to possible disintegration of the ground in passive Rankine failure at the foot of the slope is according to Equation 3:9: $F_s^{II} = E_p^{Rankine}/E_x^{max}$.
For the values of F_s^{II} confer Table 9.2.2.

Table 9.2.2 *Global effects related to slope geometry*

	Shape	c_R/c_u	$E_p^{Rankine}/E_x^{max}$	F_s^{II}	Minimum extension of potential passive zone
Slope **a)**	Linear slope	0.4	1300/1287	**1.01**	**0** m
Slope **b)**	$z = 26\cdot(x/300)^{1.7}$	0.4	1300/1476	**0.88**	**145** m

Hence, according to the analysis, Slope a) may only experience minor ground movements, while a major a massive landslide will take place in Slope b).

9.22 Impact of inclining seams of cohesion-less soil
The geometry of soil strata formed in the sedimentary process may also have a decisive impact on landslide initiation.
A specific situation arises when, as a result of out-wash from adjacent moraine or sandy beds, inclusions of coarser sediments have been deposited during the evolution of a clay formation. (Cf Figure 9.2.2.)

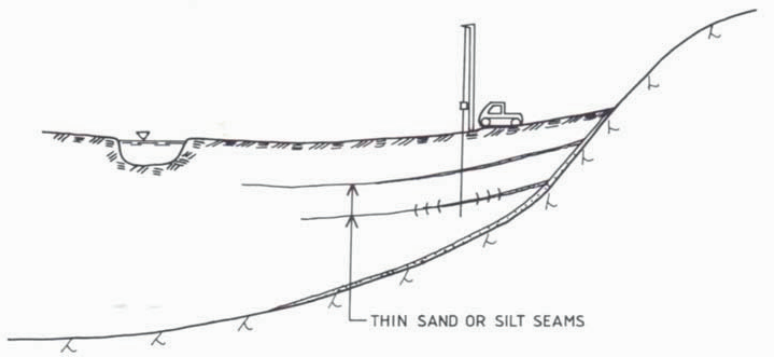

Figure 9:2.2 Layers of silty or sandy out-wash in a soft clay deposit conducive to progressive failure formation. (According to Broms, 1982)

Discrete coarse layers of this kind often tend to occur in parts of a slope that, at some epoch in the past, have constituted a shoreline environment of the regressing glacial sea. The presence of such layers of possibly collapsible material may, located as they often are in the upper part of a slope, be highly conducive to progressive failure formation due to liquefaction or partial loss of shear resistance – i.e. likely consequences of soil compaction (vibration), pile driving and rock blasting.

Confer in this context the great Surte slide, the ground movement at Rävekärr and the slide at Trestyckevattnet in Sections 5.2, 5.5 and 5.6, which were all triggered by impacts related to construction activities.

Conclusions: Slope geometry and the morphology of sedimentary layers have a decisive impact on the formation of progressive failure in slopes of strain softening soils.
The safety factors as regards global failure in the two slopes shown in Figure 9:2.1 are virtually identical according to computations based on the conventional plastic equilibrium concept.
Yet, progressive FDM-analysis clearly shows that the inherent risk in terms of human life, social economy and property are dramatically different in the slopes investigated.
It seems evident therefore that analysis of slope stability on the basis of 'ideal-plastic' behaviour of clays should not be applied, unless the residual shear strength at large deformation is actually documented to be sufficiently high.

9.3 *Effect of slope geometry on creep deformations*

The geometry of a slope and the structure of the sub-ground significantly influence the effect of creep deformations on the values of $K_0 = E_0/E_{\varphi=0}$. The following conclusions were made by the author of this report in a study of the effect of creep deformations in slopes.
(Cf Bernander (1981), Active Earth Pressure Build-up, a trigger mechanism…etc',.)

a) Creep deformations in uniform slopes with uniform depth to the slip surface do not affect the distribution of strain and earth pressures or the distribution of the related K_o-values.

b) By contrast, creep deformations in non-uniform slopes can be shown to influence the accumulation of strain according to the law:
$\varepsilon_x = \text{const} \cdot \beta_x^{n-1} \cdot d\beta_x/dx$, where
β_x is the slope gradient of firm bottom and $d\beta_x/dx$ is the curvature.
(n) is a value defining creep rate as a function of shear stress level, i.e. in principle as derived from Singh & Mitchell, (1968).

This implies for instance that with a value of n = 2, the impact of creep on K_0-values and earth pressures is most important in those parts of a slope, where the product of gradient and curvature has a maximum. Thus, increase of K_0 due to creep is typically most significant on the up-slope side of the toe of a slope.
A way of understanding this phenomenon in a qualitative sense is to note that, as creep deformations in steep portions of a slope are faster and greater than those in gently sloping ground, tension or compression tends to occur in the transition zones between areas with significantly differing slope inclination.

c) The downhill strains are associated with vertical strains causing either settlement or heave in the zones where strains accumulate.

As indicated by Equation 3:5b$_1$ (or 3:9a) in Section 3.3, the magnitude and distribution of K_0 has an important impact on the risk of landslide formation.

Conclusions: Creep phenomena significantly affect the propensity for slope failure.
(Cf. Section 11:22, Assessment of K_0-values).
Slow creep movements often tend to attenuate the effect of slope geometry on slope stability, whereas rapid creep in the active zone may be conducive to failure formation.

Another implication of the significant build-up of in situ earth pressures, and related higher values of K_0, near the toe of a slope is the consequential over-consolidation, related to the

increase of horizontal effective stresses in relation to prevailing vertical effective stress conditions. The outcome of this earth pressure build-up tends to even out normal growth of shear strength with depth in the soil profile. The slope at Surte (Section 5.2, Case records) exemplifies this type of over-consolidation due to horizontal stress increase.

Importantly, assessment of the effects of long time creep in slopes is used in the current FDM-approach as a way, by which the in-situ stress conditions can be established.

9.4 *Brittleness related to state of stress*

The effects on shear strength and brittleness of clays, linked with the state of principal stresses have long been recognized in soil mechanics literature. The shear stress/strain behaviour may vary widely with the ratio of horizontal normal stress to vertical stress, i.e. σ_h/σ_v. The fact that this ratio tends to adopt low values in the active zone, usually located in the upper and steeper parts of a slope, means that brittleness is often concurrent with high mobilization of shear strength. This setting is an important factor promoting the formation of downhill progressive failures. (Cf Janbu, (1979*)* and Bernander, (1981), Active Earth Pressure Build-up ….).

9.5 *Brittleness related to distribution and location of incremental loading*

In the study of large translational landslides using the I-PlFA approach, the distribution of additional loading has little or no impact on the safety factor resulting from the calculations. This is, of course, only valid provided that the plasticity of the soil is actually unlimited – i.e. a condition that is rarely fulfilled even in the moderately sensitive normally consolidated clays of Scandinavia.

By contrast, the effect of concentrated loading on slope stability in deformation-softening soils is largely what progressive failure in slopes is all about – i.e. a 'Fracture Mechanics' phenomenon. Structures of strain-softening material simply react in a more brittle way to concentrated load than to evenly distributed loading.
For instance, if the force N_i – induced by the local fill in the example given in Section 3.32 – had instead been evenly distributed over a major portion of the slope, the outcome of the analysis would clearly have been radically different. The difference can readily be defined and quantified using the analytical model demonstrated in Section 4.

Conclusion – Load distribution is a cardinal issue in the analysis of slope stability in sensitive soils. Addressing this issue is a mandatory requirement for reliable prediction of potential slope failure.

9.6 *Brittleness related to the rate of load application*

Another crucially important factor in landslide mechanisms is the time span, in which the incremental load – potentially triggering a slope failure – is applied.
Time-related effects on slide initiation can be accommodated in the FDM-approach presented in Section 4 by selecting the constitutive relationship (defined in Equation 4:6) in such a way that it is consistent with the actual rate of load application.
For instance, pile-driving operations would normally require the use of un-drained response in the soil, while drained or 'partially drained' soil parameters would be applicable in cases of slowly constructed earth fills or refuse dumps.

In general, long-time stress/deformation relationships tend to increase the critical force (N_{cr}) as well as the critical length (L_{cr}). Slopes in normally consolidated clays generally adapt themselves to slowly changing conditions. (Cf Section 10.1)

.

9.7 *Brittleness related to hydrological conditions*

Although it is not within the scope of this report to engage in this topic, it may in the current context be important to remind of the fact that it is just as essential to consider the hydrological conditions in progressive failure analysis as it is in conventional approaches to assessing slope stability.

Reference may also be made to the influence of climatic history and seasonal variations. Long spells of dry weather and extended periods of extreme precipitation tend to modify the in situ earth pressures in a slope, subject to the manner in which the hydrological conditions act on long term creep movements. Ground water conditions may, for instance, substantially affect the drained shear strength parameters in different parts of a slope, thus modifying the distribution of K_0 values over time.

According to Equation 3:9a the values of K_0 affect the risk of global failure significantly. The climatic history of the slope may therefore be a condition well worth studying in this context. Also this phenomenon can be investigated by applying the proposed model for progressive failure analysis of slope stability.
Theoretical analyses performed on slopes gradually emerging out of the glacial sea indicate that large downhill displacements must have taken place over time.

10. Agents prone to triggering progressive slope failure

10.1 *General - history of a slope in the Göta River valley*

The stability conditions in natural slopes are closely related to their geological and hydrological history. Slopes of clay in western Sweden are made up of glacial and post-glacial deposits that emerged from the regressing sea after the last glacial period. Hence, the sediments deposited at the end of this period in sea and fjords, which later were to become western Sweden, are now found in valleys and plains considerably above present sea level, forming deep layers of soft clays and silty clays.

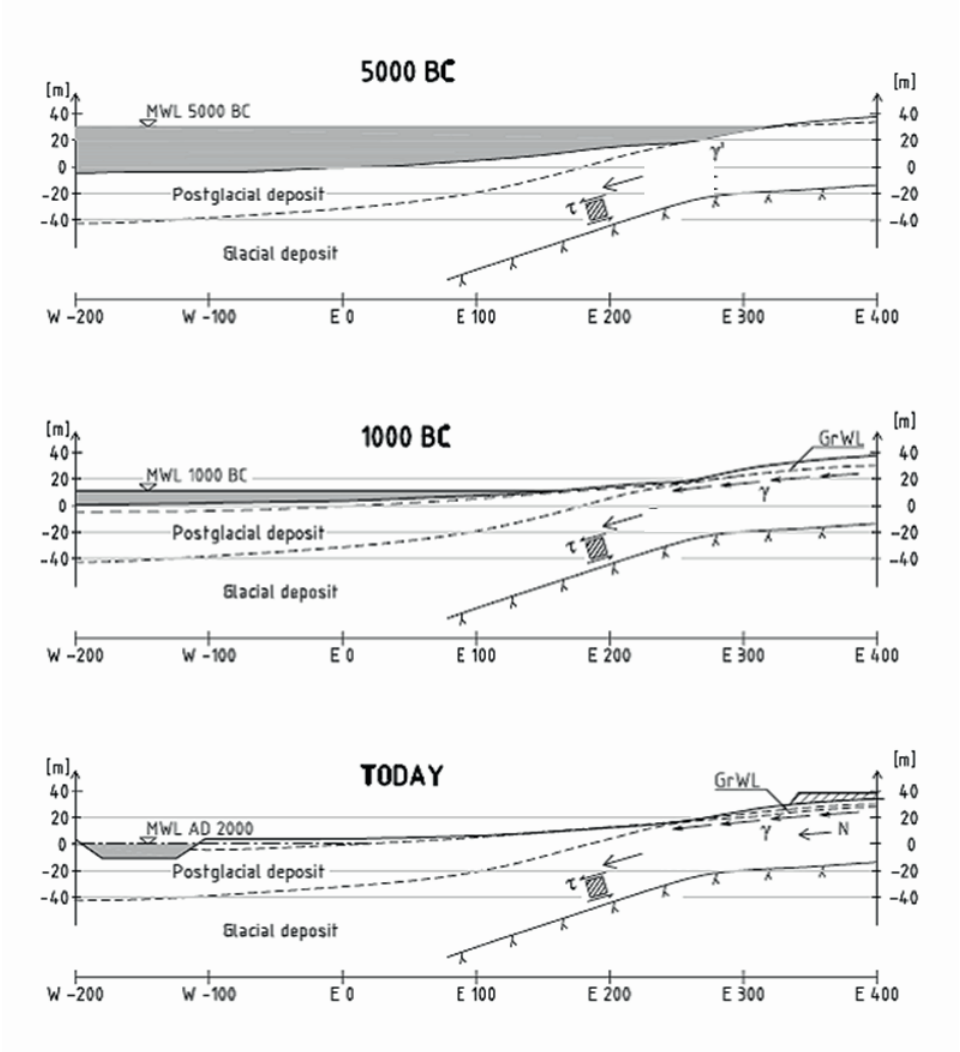

Figure 10:1.1 History of a slope in the Göta River valley, Southwest Sweden. Significant settlement and down-slope displacement have developed during past millennia because of retreating water level, changing hydrology (GWL and ground water flow) and due increase of effective stress conditions.

As the ground gradually rose above the sea level, the strength properties of the soils and the earth pressures in the slope have, by consolidation and ongoing creep movement, slowly accommodated over time to increasing loads due to changing hydrological conditions. Apart from the retreating free water level, this metamorphosis consists of dry crust formation, increased downhill seepage pressures, falling ground water table and the due increase of effective stresses in the soil mass. Chemical deterioration may have affected soil strength and sensitivity.

The progressive FDM-analysis used in this report indicates that the soil mass in the mentioned course of events has undergone large downhill displacements, often in the order of many meters. (Evidence of this phenomenon has been observed by the author in several cases.)

In consequence, existing slopes are basically stable, as long as they remain undisturbed by human activity and unaffected by significant intrinsic deterioration phenomena. Considering the likelihood of extreme excess pore water pressure events during past centuries and millennia, the nominal safety factor should – provided hydrology has remained unaffected by human interference – at least be assumed to exceed the value of 1.0 by some indefinable measure.

However, deterioration of shear strength and especially increasing sensitivity in the uphill portion of a long clay slope – e.g. because of long-time upward ground water seepage – is prone to make the entire slope acutely vulnerable to progressive failure. This is frequently a precondition in Scandinavian landslides, many of which have been triggered by documented – yet seemingly trivial – human interference.

Hence, in long natural slopes of soft sensitive clays, the real slide hazard cannot be defined in the conventional way by the principle of plastic equilibrium. Results of analyses considering deformation and deformation- softening clearly indicate that the true degree of safety can only be correctly assessed by investigating the response – in terms of progressive failure – of clearly defined disturbance conditions. This means that the *nature*, the *impact* and the *precise location* in the slope of the disturbing agent have to be taken into account in the analysis.

In other words, landslide hazard cannot be defined solely by the inherent properties of the slope and the magnitude of total load applied. The nature and distribution of the additional loading, as well as the rate of applying the same, are decisive factors in this context.

Conclusion
A long natural slope may remain stable during millennia and yet be liable to fail in progressive failure because of some additional load to which it has not been exposed previously. Critical issues in this context, besides geometry, are then how sensitive soils will respond to concentrated additional short term loading (or other disturbance such as pile driving, vibration, or blasting) in terms of increased stress and deformation, due strain softening and temporary rise of pore water pressures.

Expressing the crucial question somewhat differently:
" How is prevailing stability affected by locally applied load effects, for which the '*time horizon'* is measured in days, weeks or months instead of the long-time changes that have developed gradually during hundreds or thousands of years?"

10.2 *Failure initiation by natural causes*

Natural phenomena susceptible of triggering landslides are:
- High pore water pressure build-up due to long spells of extreme precipitation;
- Reduced effective shear strength because of high pore water pressures in discrete more *permeable* layers in the formation – in extreme cases liquefaction of collapsible soils;
- Down-slope undercutting by erosion (Cf Section 6);
- Intrinsic change of soil properties such as strength and sensitivity due to leaching or other chemical action affecting cat-ions in clayey soils – quick clay formation;
- Seismic tremor and earthquakes;

The factors listed above have a common feature. Their impact is acutely aggravated if deformations and strain softening are considered in the analysis – a fact that is clearly revealed when applying the current progressive FDM-approach. For instance, the accumulated effect of long-time quick clay formation over centuries may finally lead to a situation, where only minor disturbance from other agents may trigger a progressive slide.

Many landslides have actually occurred during, or subsequently to, spells of heavy rainfall. The problem with this particular disturbing agent is that it can in most cases be argued that the excess piezometric regime presumed to have caused the slide has most probably been exceeded over and over again in the past.
It is therefore reasonable to assume that, when landslides happen during markedly rainy periods, there has most likely been *at least one other* contributing triggering factor. This factor may of course be of man-made origin but can also be an effect produced by one of the other agents listed above.

Bernander (1981) proposed a self-generated process named 'Active Pressure Build-up - a Triggering Mechanism in Landslides in Sensitive Clays', by which the additional forces emanate from the effects of accelerated creep on horizontal principal stress in the active uphill transition zone between moving and firm ground. But even this failure mechanism requires an additional factor to explain why failure has not occurred already in the past.

10.21 Downhill or uphill progressive slope failure?– Basic preconditions

The issue, as to whether a long natural slope is likely to disintegrate in downhill or uphill progressive failure, is determined by the basic geological and geotechnical pre-conditions – and that most importantly by the prevailing degree of consolidation, as defined by the value of the *over-consolidation ratio* (OCR).
In this context, the effects of *downhill creep movement* caused by additional load and inherently changing conditions within the soil mass along the slope, have to be considered.

Downhill progressive landslides
In slopes of *normally consolidated* clays, *long-term* change of loading, increase of sensitivity and due creep-induced strain softening will normally only result in stress and earth pressure redistribution while equilibrium is still maintained.
This is simply due to the fact that the deleterious effects of gradual disturbance on shear resistance in part of the slope are compensated over time by reconsolidation – as long as the effective stress conditions remain unchanged.

Downhill progressive landslides are therefore prone to occur in *soft sensitive* clays, usually being triggered by some *short-term* external *additiona*l load – usually related to identifiable human activity. (Cf e.g. Table 5.7.1 and Section 10.3 below.)

Uphill progressive (retrogressive) landslides
Deposits of *highly over-consolidated* clays are often exposed to extremely slow river-bed erosion and the formation of steep canyons. In this case, the effects of shear strength deterioration generated by gradually failing horizontal support, as well as by due creep and strain softening over time, are *not recoverable*. This is why consequent long-term creep movement may eventually lead to random *intrinsic slope failure* without any directly identifiable cause of failure. The issue is dealt with in more detail in Sections 7.4 and 7.5.

Conclusion: The occurrence of downhill respectively uphill progressive landslides depends largely on the geologic history of the site, and is in particular related to the over-consolidation ratio (OCR) of the clay formation. In both instances, the critical condition may have developed over time due to intrinsic change of properties within the soil mass.
However for reasons given, the triggering agent in downhill progressive landslides is usually more readily identifiable than in uphill progressive slides (or spreads). (Cf Sections 7.52 and 8.3.)

10.3 *Failure initiation by man-made intervention*

In most landslides in soft sensitive clays, even those having occurred during intensely wet periods, it has in effect been possible to identify the presence of other contributing agents. As indicated in Table 5.7.1, these agents are often related to construction activities of the following kind:

- Stockpiling of heavy materials, earth fills, construction of road embankment supports;
- Excavation work, straining the initiation zone in *lateral* direction;
- Driving of soil displacing steel pipes, prefabricated concrete piles or soil displacing sand drains;
- Soil compaction using heavy vibratory equipment;
- Rock blasting;
- Man-made interference with hydrological conditions changing the existing ground water regime.

All of the downhill progressive slides treated in Chapter 5 ‘Case records’, except the Tuve slide, occurred while construction work within the slide area was actually going on in the upper part of the slope.
Yet, in SGI Report No 18 regarding the Tuve slide, the triggering mechanism is also ascribed to the possible joint effect of a road embankment constructed some years before, conceivable man-made modification of the hydraulic regime, and exceptionally high pore water pressures at the upper limit of the main slide - i.e. basically results of human interference.

The remaining 13 landslides listed in Table 5.7.1 were undoubtedly caused directly by either earth construction work or by pile driving. However, this does not imply that, in some of the cases, exceptionally high pore water pressures may not have contributed to some extent, which in the nature of things can rarely be determined after the slide event. However, extreme rainfall conditions were actually not documented in any of the listed landslides.

It may be noted in this context that the slope in Surte had remained stable ever since it emerged from the sea some thousands of years ago. Yet, only driving of a few pre-cast piles for the foundation of a family house in a steep part of the slope was sufficient to trigger this catastrophic event. A slope of this kind may be regarded as a ´a *time-set bomb* ticking through the millennia.'
Pile driving has been recorded as an effective triggering agent in many other slides and ground movements in Sweden. (Cf. Section 5.1 and Section 10:2 above, *History of a slope*.)

It is not the author's intention to elaborate here on all the specific effects of the various kinds man-made disturbance such as those listed in Table 5.7.1.
Nevertheless, it must be emphasized that stockpiling of heavy materials, earth fills, construction of road embankments are particularly *common* features in connection with landslides of the current kind.

Yet, even so it is clear that many of these slides have actually taken place during periods of intense raining. Figure 10:1.2 offers an explanation of the tendency of slides, with documented impact of human activity, to occur during wet spells. The figure illustrates how water saturation in the fill mound as well as in cracks in the active zone (above GWL) can give rise to formidable destabilizing down-slope forces.
A numerical exemplification of this phenomenon, with reference to the landslide at Småröd, is given in Section 5.7.

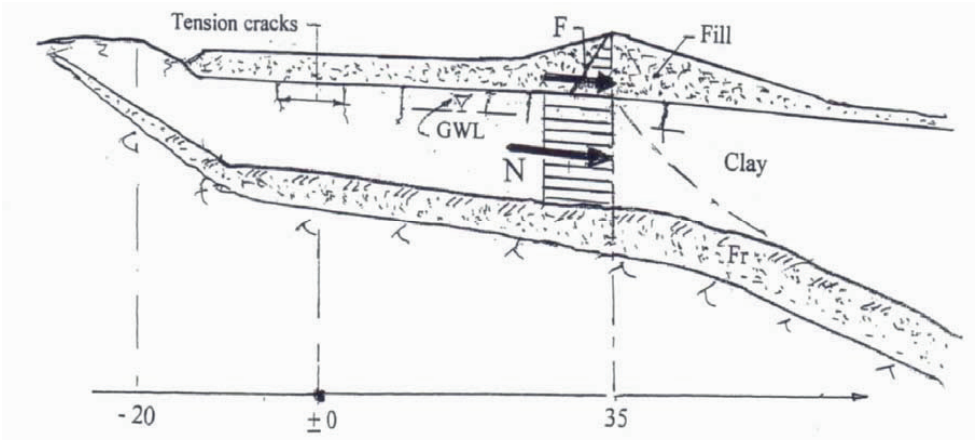

Figure 10:1.2 Formidable downhill forces may arise due to drawn-out rainfall in stockpiled earth fills and/or in cracks above GWL. Cracking in the potentially active zone inevitably follows from the deformations generated by the applied additional load. (Cf numerical example in Section 5.7. The figure was earlier presented as Figure 5:7.2.)

Pile driving
Pile driving should also be regarded as a particularly risky operation in the current context. Its effect is threefold:
Firstly, piles actually displace the soil in the down-slope direction by amounts varying from a few centimetres to several decimetres, thus initiating strain softening and possibly slip surface formation. This phenomenon alone is a powerful triggering mechanism.
(See comments on this subject in Section 3.35).

Secondly, high pore water pressures are generated in clayey material. Several tenths of meters of excess pore water head have been recorded in connection with large piling jobs.

Thirdly, pressure wave radiation from hammer-blows or vibrating hammers tend to promote deformation-softening or tendency to liquefaction even in soil layers that, owing to deformation over time, have attained a state of 'critical relative density'.
The possible effect on strata of loose, collapsible cohesion-less soils may of course be devastating.

11. Principles and procedures for investigating landslide formation in slopes prone to fail progressively

11.1 *General comments*

Many a geotechnical engineer may ask himself why he should abandon the simple method of analysis offered by the concept of ideal-plastic limit equilibrium in favour of a significantly more complicated procedure, such as the one outlined in this section and in Sections 3 and 4? Deliberating this issue, the following aspects should be considered:

11.11 Valid failure mode in sensitive soil
Analyses in soil mechanics based on full plasticity of the soil have limited validity in many practical applications, especially in long slopes of soft sensitive clay. It is then of vital importance to apply analytical methods, by which shear deformations and strain softening in the potentially sliding soil mass are accounted for. In the current document, this is achieved by using appropriate constitutive stress/strain relationships.
It is also mandatory to establish in what way these deformations may be linked with corresponding deformations in the sub-base.
The current approach, based on the FDM-analyses proposed in Sections 4 and 7, enables the determination of the distribution along the slope of shear stresses, earth pressures and displacements, generated by any additional load applied.

11. 2 *Critical conditions in long slopes of sensitive clay*

11.21 Failure modes
Critical parameters
A crucial circumstance emerging from this kind of analysis is that, contrary to the implications of the plastic equilibrium approach (I-PlFA), shear stresses due to concentrated loading are only mobilized over a limited length (L_{cr}) prior to the initiation of slip surface formation and the subsequent development of progressive failure. The limited length of stress mobilization implies a corresponding limit (N_{cr}) for the triggering load.

Critical failure planes
Another important general condition, revealed by using the FDM-model, is the tendency of failures in sloping ground to propagate along planes roughly parallel to firm bottom (or to firmer sedimentary layers) rather than along shorter failure planes *surfacing* in the slope. Thus, slip circles emerging in sloping ground seldom turn out to represent the most critical failure condition in soft clays, and particularly not in markedly sensitive clays – i.e. provided the condition defined b y Equation 3:3 is fulfilled. (Cf Section 4.6, Figures 4:6.1 and 4:6.2.)

Global failure
If the critical load (N_{cr}) is exceeded, progressive failure may result in global slope failure, provided that the build-up of down-slope earth pressures surpass passive resistance.

11.22 Different phases in progressive landslide development
A vital feature in analyses of progressive failure formation is that landslides cannot, as a rule, be studied as a *singular* case (or event) of static loading, because slides of this kind develop in different consecutive phases with very distinctive conditions as regards rates of loading and stress change, drainage, geometry etc. (Cf Sections 3.31 and 3.32.)

The FDM-analyses also indicate that the slip surface in the progressive phase has a tendency to develop far *beyond* the toe of a slope (i.e. often hundreds of meters), and that notably *prior to* the possible final break-down in passive failure. (Cf Figure 3:3.5.)
This specific phenomenon is demonstrated at length in Bernander, (2008), Section 5 of Report LuTU 2008:111.

11.23 Examples of slides explained by the FDM-approach
As mentioned in the Abstract, SGI Report No 10 contained nine diverging explanations of the great Tuve slide by various experts. If SGI:s own version in Report No 18 is included, it adds up to ten different approaches to defining the causes and the development of this slide. Similarly, the Surte slide was treated in two comprehensive reports, and in the aftermath also in terms of contentious discussion in technical journals. Yet all these accounts remained, as indicated in Sections 5.1 and 5.2, contradictory or inconclusive on essential issues.

By contrast, analyses of the Surte and the Tuve slides in line with Sections 3 and 4 provide straightforward explanations of the widespread passive zones in almost horizontal ground. This is a feature that cannot be explained on the basis of ideal-plastic soil properties but emerges directly as a *compelling* result from analyses based on strain softening.

Conclusion
In the determination of slope stability, consideration of deformations in the soil mass is mandatory, whenever the soil does not meet the plasticity requirement for the current application. This can e.g. be achieved by applying the analytical approach highlighted in Section 4.
In practical engineering, this means that progressive failure analysis should be performed in all investigations of long slopes with strain softening clay layers – in particular when additional load is applied in up-slope locations, where the ground surface and/or underlying firm bottom layers incline steeply.

11.3 *Investigation procedure*

The procedure advocated below is exemplified in the studies performed in Section 5 regarding the landslides in Surte, in Tuve and at Trestyckevattnet.

11.31 General
When investigating landslide hazard, the geological history of the area concerned is a subject of primary interest. The issue has been treated to some extent in Section 10.1.

A vital question when investigating the stability of a slope in sensitive soft clay is then the way critical portions of the slope will respond to additional loading or disturbance, for which the ‘time horizon’ is expressed in terms of *days*, *weeks* or *months* instead of hundreds or thousands of years?
If then, local failure is deemed to be conceivable, what degree of disaster is likely to ensue? Will local instability just result in minor cracking in the up-slope ‘active zone’ or will it terminate in a disastrous landslide displacing vast areas of horizontal ground over great distances?

The proposed analysis according to Section 4 provides a means of finding the answer to such questions. The recommendations below apply primarily to soft strain softening clays.

11.32 In-situ condition – Assessment of in situ K_0 - values (Phase 1)

As indicated in Section 9.3, the propensity to progressive slope failure and subsequent disintegration of the potential passive zone largely depend on the prevailing in-situ distribution of earth pressures. Hence, an estimate of the values of K_0 - i.e. σ_h/σ_v in Equation 3:9a - should be made.

The K_0-values may be chosen empirically on the basis of past experience. However, they may also be calculated according to Section 4, in which case a reasonable long term stress/deformation relationship is applied – the basic idea being that creep in a slope can be regarded as an extremely slow progressive failure process. In the absence of specific tests related to a creep situation, long term shear strength and perfect plastic properties in the soil can be presumed in this context. (Cf. Section 9.3, 'Effects of slope geometry on creep deformations'.)

The input value of K_0 may, in this phase of the analysis, be taken as the K_0 -values considered to be valid in the currently studied case, i.e. typically varying from say 0.5 to 1.0 in different parts of the slope. Using FDM-analysis, based on long-time stress/strain relationships, possible inaccuracy in the first assessment of the input K_0-values can then be adjusted.

The boundary condition in this calculation is that the force N_i has to be consistent with the conditions in situ at the upper limit of the potentially sliding soil volume. (Cf e.g. Figures 4:5.1, 5:1.7 and 5:2.8, regarding computed curves for the in situ earth pressures $E_{o,(x)}$).

11.33 Preliminary assessment of Critical Length (L_{cr})

The distance in the downhill direction from a local load, along which the additional shear stresses in the potential failure zone can be mobilized, is limited. (Cf Section 3.3).

This fact has a *crucial* implication because, at a distance of L_{cr} from the point of load application, the effect of the additional load can no longer be registered in terms of earth pressure or displacement. This circumstance rules out, or radically reduces, the possibility of utilizing earth pressure resistance in less sloping ground further downhill for the stabilization of up-slope additional loads.

Referring to Sections 3.4 and 4.6 concerning the significance of the ratio between the critical length L_{cr}, and the total length of the prospective slide (L_{tot}), it is recommended that slope stability investigations in long natural slopes of soft clay should begin with, at least, a rough estimate of the critical length $L_{cr.}$ This applies particularly in cases of highly concentrated additional loading.

Low values of the ratio L_{cr}/L_{tot} – i.e. significantly lower than about 2.0 – signal risk of progressive failure formation from the impact of local up-slope loads. Thus, the value of L_{cr}/ L_{tot} can be regarded as a vital measure of the applicability of the conventional plastic equilibrium approach to the current investigation.

The implication of a low L_{cr}/L_{tot}-ratio is of great significance also in another way. It means that the failure resistance along slip surfaces – more or less in line with the sloping ground surface and /or firm bottom layers – is normally much lower than resistance based on failure planes surfacing in the slope closer to the additional load. (Cf. Section 4.6). The value of L_{tot} should include a relevant portion of level ground ahead of the foot of the slope.

11.34 Disturbance condition – assessment of the critical load susceptible of initiating progressive failure (Phase 2)

As already dealt with in previous sections, slope failure in deformation softening soils is of a different character depending on how the in situ stresses (τ_o) relate to the residual shear strength (c_R). Progressive failure, as defined in this document, is conceivable only if in part of

the slope, at some point in time, the residual shear strength falls below the prevailing in situ shear stress because of some additional loading effect or disturbance i.e.

Case 1 $\mathbf{c_R(x) - \tau_o(x) \leq 0}$ (Eq. 3:2)

Departing from the previously established in situ condition, the critical additional load (N_{cr}) can now be calculated using the procedure outlined Section 4.3. This is done by determining how far from the additional load shear stresses can be mobilized along the potential failure zone – i.e. before the prevailing in situ stress τ_o exceeds the available post-peak shear strength, $c_R(x)$. The boundary criteria at the lower limit of the investigated load effect are therefore in this phase that $N_i = N_{cr}$ and that $\tau_o = c_R$. (Cf Figure 3:3.3).

Another critical condition is the 'forced' deformation δ_{instab} for which the slope fails even if there is no sustained active force following up the incipient failure. Driving of soil displacing piles constitutes a case when this criterion may be applicable.
$\mathbf{\delta_N < \delta_{instab}}$ (Cf Section 3.34 and Figure 4:2.4a).

The constitutive relationship to be used in this study must be compatible with the nature of the additional load and the rate of applying the same. Pile driving may for instance produce *un-drained* response in the imminent failure zone, whereas for a slowly built up embankment or stockpile, drained or *partially* drained parameters may be appropriate.

The main results from this phase of the stability investigation are
- The critical additional load, N_{cr}
- The shear stress distribution and the critical lengths, L_{cr} and L_{instab}
- The critical displacements at the upper slide limit, δ_{cr} and δ_{instab}.
  (Cf Section 3.3, Stability conditions prior to local failure).

If the current combination of the loads N_i, q and t, as defined in Figures 4:2.1and 4:2.2 exceed the corresponding critical combination of these loads, then a progressive failure is triggered. The safety factor against such a failure is

$$\mathbf{F_s^I = N_{cr} / N_i > 1} \qquad \text{……..Eq.3:8}$$

or, if the additional loads (q,t) shown in Figure 4:2.1 are also considered,

$$\mathbf{F_s^I = (N_i,q,t)_{cr} / (N_i,q,t) > 1} \qquad \text{……. Eq.3:8a}$$

where $(N_i,q,t)_{cr}$ denotes a critical combination of the additional loads

The calculation procedure is exemplified in Appendix I of this document, as well as in Appendix B of LuTU 2008:11.

At this point further checking may be made with regard to the possibility of failure along a plane surfacing immediately down-slope of the area subjected to the additional loading:

$$E_{cr} = E_o + N_{cr} < K_0 \cdot \gamma \cdot H^2/2 + 2 \cdot \sqrt{(1 + c_R/c)} \cdot {}_o\int^H c_u \cdot dz \qquad \text{……..Eq. 3:3}$$

Equation 3:3 defines one of the prerequisite conditions for progressive failure development. If the resistance along a failure plane following sloping firm bottom (or firmer sedimentary

strata) is lower than the local passive resistance, possible failure will propagate along that plane. As mentioned previously, this condition is normally fulfilled in sloping ground with sensitive soils, provided the slip surface is located at sufficient depth below the ground surface.
Thus, *importantly*, shorter failure planes and slip circles, i.e. failure modes for which ideal plastic analysis may still be valid as such, do not in general constitute the most critical failure condition in long slopes of deformations-softening soil. This invalidates in many applications the use of the conventional ideal-plastic equilibrium approach. (Cf Section 4.6, Figure 4:6.1.)
It may be noted that this condition tends to become even more pronounced for failure planes along sedimentary layers, considering that sensitivity properties and excess pore water pressures are more likely to correlate with the sedimentary soil structure than across (or at an angle to) the same.

Hence, when the condition $c_R(x) \leq \tau_o(x)$ applies, the permissible load effect computed on the basis of progressive failure formation is generally *significantly* smaller than the corresponding load based on plastic equilibrium analysis, and that even for failure planes of moderate length. Frequently, in very sensitive (quick) clays, the results of the two types of analysis are not even in the same order of magnitude. (Cf. Sections 3.32 b, 3.4, 5.1 and 5.2 'Case records')
The issue is comprehensively dealt with in Appendix B of LuTU 2008:11).

Choice of c_R/c-value
The values of N_{cr} and L_{cr} relate to the c_R/c- ratio but, as indicated in Sections 5.1, 5.2 and Table 9.1.1, they are not particularly sensitive even to considerable variation of this brittleness ratio.
When investigating a long slope with significantly sensitive soil, it may therefore be wise to adopt (at least tentatively) reasonably low values for c_R/c. It is essential to recognize that, although high values closer to 1.0 (i.e. the ideal-plastic condition) can very well be valid in a stable long term situation, short term disturbance agents causing accelerated creep deformations may readily entail *temporary* but drastic reduction of the c_R/c - ratio.

The choice of input values of c_R/c in the disturbance situation should therefore be of a conservative nature but as always, it will be up to the investigating engineer to determine the conditions applicable to the current situation.

Case 2 $\mathbf{c_R - \tau_o \geq 0}$
By contrast, if the residual shear strength (c_R) remains in excess of the in situ stress (τ_o) throughout the duration of additional loading, the redistribution of earth pressures resulting from the deformation-softening will, instead of entering a dynamic phase, merely entail growing downhill displacement as the additional load is increased. This failure process is of a static and ductile character, the ultimate load no longer being limited to the critical value (N_{cr}) as per Case 1.

In Case 2, the proposed FDM-analysis will be in agreement with conventional plastic equilibrium analysis (I-PlFA) in the limit case when the ratio of $\mathbf{c_R/c = 1}$. (Cf Section 3.4).

Unless relevant data are well documented, Case 2 stands out as a rather uncertain state of stability. Yet, it is very likely that it actually represents a common scenario.

Interestingly, the state when $\mathbf{c_R}$ is close to $\boldsymbol{\tau_o}$ represents a situation, where an impending (or beginning) landslide movement may come to a stop owing to ceasing precipitation or to some other random favourable change of the prevailing load conditions.

The number of landslides that *'just almost happened'* is a story untold.

11.35 Global failure condition (Phase 4) – assessment of possible equilibrium subsequent to dynamic earth pressure redistribution

The objective in this part of the study is to ascertain if there is a possible state of *static* equilibrium subsequent to the dynamic redistribution of unbalanced up-slope earth pressures in the development of progressive failure.
At this stage, it is for good reason assumed that the potentially sliding soil mass, at least transiently, retains its geometrical shape before possible disintegration in passive failure.

Observe that at this point the failure surface has already propagated far beyond the toe of the slope – often hundreds of meters. Confer in this context the detailed explanation of the said condition in Section 3.32 **'**Assessment of passive resistance in Phase 4.'

The significance of this state of static equilibrium is that it constitutes a measure of what may happen if the critical load (N_{cr}) according to the forgoing section is exceeded – i.e. will the initiated progressive failure result in a veritable landslide or not?

$$\mathbf{F_s^{II} = E_p / (E_o + N_{cr})} \qquad \text{…….……(Eq. 3:8)}$$

For instance, if the passive resistance is not exceeded at the foot of the slope, the incipient landslide will come to an end resulting only in limited displacements at the upper end of the slope studied. (Confer e.g. the slide at Rävekärr, Section 5.5).

On the other hand, if the computed static earth pressures exceed passive resistance, the current state of equilibrium will be of a transient nature – and will gradually merge into the truly *dynamic phase* of the slide. At this point, the heave of the ground in the passive zone provides the prerequisite for the soil mass further up-slope to move downhill at an accelerated pace. The *landslide proper* is set in motion – i.e. Phase 5.

It may be recommended that investigations regarding Phase 4 be carried out irrespective of the degree of risk as defined by the safety factor $F_s^I = N_{cr}/N_i$ in respect of the initiating up-slope failure. In many instances, it can be of vital interest to estimate the consequences of global failure being set off because of some unknown circumstance.
A detailed exemplification of the specific phenomena related to Phase 4 is presented in Bernander, (2008), Section 5 of LuTU 2008:11.
(Cf also Section 3.31 and Figures 3:3.4 & 3:3.5 in this document.)

Note: If additional, more accurate predictions of the final slide event (i.e. Phase 6) are considered necessary, they will have to be made on the basis of Newtons laws of motion as exemplified in Section 5.1.

11.4 Final comments

Slope stability analysis in long slopes of sensitive clays, as outlined in this report, has among other, the following merits:

- The study pinpoints the precise instability features in the slope structure, making it possible to assess the distribution of shear stresses and displacements due to additional load;

- Appropriate safety factors may be defined;

- Remedial measures addressing local weak points in the slope may be undertaken;

- The relationship between the critical length (L_{cr}) and the total length (L_{total}) of the investigated part of the slope – e.g. the ratio L_{cr} /L_{total} – provides a quick indication as to whether conventional plastic equilibrium analysis is reasonably applicable in a current case or not;

- The FDM-analysis reveals information about the risk and the consequences associated with local instability features, enabling estimation of the degree of potential disaster involved. Such information is by *definition* not accessible in the plastic limit equilibrium approach when applied to slopes with strain softening clay layers.

As mentioned in Section 5.2, FDM-analyses as per Section 4 demonstrate conclusively that the slope in Surte harboured a primordial weakness, allowing a disturbance caused by a minor piling job to trigger a 600 x 400 m^2 landslide in a residential area. Notably, the effect of the piling job was at the time considered to be of little consequence by most of the experts who subsequently investigated the causes of the slide disaster.

The hazardous slope stability condition in Surte may be thought of as a ***'time-set' bomb ticking over millennia.***

12. References

This chapter presents references to literature dealing with progressive and retrogressive landslides, slope stability and, in some instances, also to fracture mechanics of structures trying to bridge the gap between traditional soil mechanics and more stringent structural analysis. All of the following references are not cited in the report.

Aas, G. (1966). Special Field Vane Tests for the Investigation of Shear Strength of Marine Clays (In Norwegian). *Report, Publication 68, Norwegian Geotechnical Institute, Oslo.*

Aas, G. (1981). Stability of Natural Slopes in Quick Clays. *Proc. 10th ICSMFE, Stockholm, 1981*, *Vol. 3, pp 333-338. Also in NGI Publ. No 135, 1981.*

Aas, G. (1983). A Method of Stability Analysis applicable to Natural Slopes in Sensitive and Quick Clays. *Proc. Symposium on Landslides. Linköping 1982, Swedish Geotechnical Inst. Report No 17, pp 7-25.*

Alén, Claes (1998). On probability in Geotechnics. Random Calculation Models Exemplified on Slope Stability Analysis and Ground - Superstructure Interaction. *Doctoral Thesis, Chalmers University of Technology, Gothenburg.*

Andreasson, L. (1978). Tuveskredet, *Väg- & Vattenbyggaren*, Nr 1, 1978.

Andresen, L & Jostad H. P. (2002). A constitutive model for anisotropic and strain-softening clay. Proc. Numerical Modelling in Geomechanics – NUMOG VIII, Rome, pp. 79-84.

Andresen, L & Jostad H. P. (2004). Analyses of progressive failure in long naturals slopes. *Proc. Num. Mod. Geomech. – NUMOG IX, Ottawa, Canada, pp 603-608.*

Andresen, L & Jostad H. P. (2007). Numerical modelling of failure mechanisms in sensitive soft clay – applicati0n to offshore geohazards. *OTC 18640, Offshore Technology Conference 2007, Houston, Texas, 7p.*

Bazant, Zdenek P and Planas, Jaimes (1988): Fracture and Size Effect in Concrete and Other Quasi-brittle Materials. 616 pp. CRC, Boca Raton, Fl, ISBN 0-8493-8284-X.

De Beer, E. & van Impe, W. (1984). Landvallen in Loop-kleien. *Tijdschrift der Openbare Werken van Belgie, Nr 1.(In Flemish)*

Berg, G. (1981). Tuveskredet 1977-11-30, Inlägg om skredets orsaker. (Comments on the Causes of the Tuve Slide). *SGI Rapport nr 10. 1981. (In Swedish.)*

Bergfelt A. (1981) Tuveskredet 1977-11-30, Inlägg om skredets orsaker. (Comments on the Causes of the Tuve Slide). *SGI Rapport nr 10. 1981. (In Swedish)*

Bernander, S. (1975 -). Many of Stig Bernanders papers can be downloaded from http://www.ltu.se/staff/s/stiber-1.57743

Bernander, S. (1975). Lerors hållfasthet och deformationsegenskaper i konstruktioner där leran icke utgör den enda stabiliserande komponenten (Strength and deformation capacity of clays in structures where the clay is not the only stabilizing component. In Swedish) *Nordic Geotechnical Meeting, Copenhagen, May 22-24, 1975. Copenhagen: Polyteknisk Forlag*, pp 155-172.

Bernander, S. (1978). Brittle Failures in Normally Consolidated Soils. *Väg- & Vattenbyggaren, No 8- 9, pp 49-53.* Also available as a reprint 8 pp.

Bernander, S. (1981a). Active Pressure Build-up – A Trigger Mechanism in Large Landslides in Sensitive (Quick) Clays. *Technical Report 1981:49T, Luleå University of Technology, Sweden.*

Bernander, S. (1981b). 'Icke-lineär' deformationsanalys vid beräkning av släntstabilitet – Är det en nödvändighet eller en onödig komplikation? (Non-linear deformation analysis – Is it a necessity or a just a redundant complication? In Swedish). *Teknisk Rapport 1981:68T, Luleå University of Technology, Sweden,* 18 pp.

Bernander, S. & Olofsson, Ingvar (1981a). Tuveskredet 1977-11-30, Inlägg om skredets orsaker. (Comments on the Causes of the Tuve Slide. In Swedish). *SGI Rapport nr 10. 1981.*

Bernander, S. & Olofsson, Ingvar (1981b). On Formation of Progressive Failures in Slopes. *Proc. 10th ICSMFE, Stockholm1981, Vol 3, 11/6*, pp 357-362.

Bernander, S. & Olofsson, I H. (1981c). The Landslide at Tuve, Nov. 1977 (In Swedish). *Technical Report 1981:48T, Luleå University of Technology, Sweden.* Revised version of Bernander & Olofsson (1981a).

Bernander, S. (1982). Active Pressure Build-up – a Trigger Mechanism i Large Landslides in Sensitive (quick) Clays, *Symposium on Slopes on Soft Clays, Linköping, Sweden, SGI Report No 17, 1983.*

Bernander, S. & Svensk, I. (1982). On the Brittleness of soft Clays and its Effect on Slope Stability. *Väg- och Vattenbyggaren No 7 – 8, 1982.* (In English).

Bernander, S. (1983). Angående Statens Geotekniska Instituts Rapport Nr 18 om Tuveskredet 30 nov. 1977. *Geotekniknytt, Institutionen för Geoteknik, Chalmers tekniska Högskola. (In Swedish)*. No 1, Appendix.

Bernander, S. (1984). Relationship between the Appearence of a Finished Slide and the Mechanisms Acting during the Slide. *Proc. Nordic Geotechn. Meeting, Linköping, pp 409-416.*

Bernander, S. & Gustås, H. K. G. (1984a). A Dynamic Study of Downward Progressive Failure in a Natural Slope. *Proc. Nordic Geotechn. Meeting Linköping, pp 431-442.*

Bernander, S. & Gustås, H. K. G. (1984b) Consideration of in situ Stresses in Clay Slopes with Special Reference to Progressive Failure Analysis. *Proc. IVth Internat. Symposium on Landslides, Toronto, 6 pp.*

Bernander, S. (1985). On Limit Criteria for Plastic Failure in Strain-rate Softening Soils. *Proc. 11th ICSMFE, San Fransisco, Balkema, Vol. 1/A/2, pp 397 – 400.*

Bernander, S. & Svensk, I. et al. (1985). Shear strength and deformation properties of clays in direct shear tests at high strain rates. *Proc. 11th ICSMFE, San Fransisco, Balkema, Vol. 2/B/5, pp 987 – 990.*

Bernander, S., Gustås, H. & Olofsson, Jan (1988). Improved Model for Progressive Failure Analysis of Slope Stability. *Proc. Nordic Geotechn. Meeting (NGM), Oslo 1988, 4 pp.*

Bernander, S., Gustås, H. & Olofsson, Jan (1989). Improved Model for Progressive Failure Analysis of Slope Stability. *Proc. 12th ICSMFE, Rio de Janeir, Balkema, Vol 21/3, pp 1539-1542.*

Bernander, S. (1993): Dynamic Response of Buildings on Breakwater in Monaco. *International Association of Bridges and Structural Engineering, Colloquium (Göteborg) Structural Serviceability of Buildings, IABSE Reports, Vol. 69, Zürich 1993*, pp 291-295.

Bernander, S (1998): Prevention of thermal cracking in concrete at early ages. *State of the art report prepared by RILEM Technical Committee 119, Avoidance of Thermal Cracking in Concrete at Early Ages. Ed by R Springenschmid, London, Taylor and Francis,* pp 255-314. ISBN 0-419-22310-X.

Bernander, S. (2000). Progressive Landslides in Long Natural Slopes. Formation, potential extension and configuration of finished slides in strain-softening soils. *Licentiate Thesis 2000:16, Luleå University of Technology*, ISSN: 1402 – 1757. 16+104+17 pp. Available at http://epubl.ltu.se/1402-1757/2000/16/index.html.

Bernander, S (2004): Grouting in Sedimentary and Igneous Rock with Special reference to Pressure Induced Deformations. *Technical Report 2004:12,* Luleå University of Technology, Dept. of Civil and Mining Engineering, Div. of Structural Engineering and Foundation, 118 pp.

Bernander, S (2007): Analys av progressive skred utförda av Con-Geo. Bilaga till Rapport 1 - Skredorsak. Skredet i Småröd., (Landslide in Småröd.. Progressive failure analysis. In Swedish), *IIG-SNRA (2007), Vägverket, Borlänge*, 7 pp.

Bernander, S. (2008). Downhill Progressive Landslides in Soft Clays. Triggering Disturbance Agents, Slide Propagation over Horizontal or Gently Sloping Ground, Sensitivity Related to Geometry. *Research report 2008:11, Division of Structural Engineering, Division of Soil Mechanics and Foundation Engineering. Department of Civil, Mining and Environmental Engineering, Luleå University of Technology*, 16+101 pp. Available at http://pure.ltu.se/portal/files/3030557/RR-2008-11.pdf

Berndtsson, J & Lind, G.B. (1981). Tuveskredet 1977-11-30. Inlägg om skredets orsaker. (Comments on the Causes of the Tuve Slide. In Swedish). *SGI Rapport nr 10.1981.*

Berre T. & Bjerrum, L. (1973). Shear Strength of Normally Consolidated Clays. *Proceedings, 8th ICSMFE, Moscow.*

Bishop, A.W. & Bjerrum, L. (1960). The Relevance of the Triaxial Test to the Solution of Stability Problems. *Proc. of the ASCE research conference on shear strength of cohesive soils, Boulder, pp 437 -501.*

Bishop, A.W. Webb, D.L. & Lewin, P.I. (1965). Undisturbed Samples of London Clay from the Ashford Common shaft; Strength-effective stress relationships. *Geotechnique 15, No 1, 1-13.*

Bishop, A.W. (1967). Progressive Failure with Special Reference to the Mechanism Causing It. *Proc. Geotechnical Conference, Oslo. Vol. 2, pp 142-150.*

Bishop, A.W. & Lovenbury, H.T. (1969). Creep Characteristics of two Undisturbed Clays. *Proc. of the 7th Int. Conf. on Soil Mech.& Found. Engineering, Mexico City, I, 29-37.*

Bishop, A.W. (1971). The influence of progressive failure on the choice of the method of stability analysis. *Technical Notes , Géotechnique, Vol. 21 pp 168-172.*

Bjerrum, L. (1954). Stability of Natural Slopes in quick Clay. *European Conf. on Stability of Earth Slopes, Stockholm. Also publ. in Geotechnique No 2, 1954, pp 16-40.*

Bjerrum, L. and Eide, O. (1956). Stability of Strutted Excavations in Clay. *Geotechnique*, Vol 6, no 1, p 32-47.

Bjerrum, L. (1961). The Effective Shear Strength Parameters of Sensitive Clays. *Proceed. Vth ICSMFE. Paris.*

Bjerrum, L. (1967). Progressive failure in slopes of over-consolidated plastic clay and shales. 3rd Terzaghi Lecture presented in Miami Florida 1966. *American Soc. of Civil Eng., ASCE,* Journal of the Soil Mech. & Foundations Division, Vol 93, 1967, SM5, pp 3-49.

Bjurström, G. & Broms, B. (1982). The Landslide at Frö-Land, June 5, 1973. *Proc. Symposium on Land-Slides, Swedish Geotechnical Institute Report No 17. Linköping* 1973.

Broms, B. (1969). Undergrundens bärförmåga och deformation. (Carrying Capacity and Deformation of Soils. In Swedish) *Chapter 322 in BYGG, Huvuddel 3, Konstruktionsteknik, Stockholm,AB Byggmästarens Förlag, pp 73-86.*

Broms, B. & Stål, T. (1980). Landslides in Sensitive Clays. *Proceedings International Symposium on Landslides, New Delhi, Vol. 2 pp 39-66.*

Broms, B. & Fagerström, H. (1981). Tuveskredet. Comments on the Causes of the Tuve Slide *SGI-Rapport nr 10. 1981. (In Swedish)*

Broms, B. (1982). Progressive Translatory Landslides. *Symposium on Slopes on Soft Clays, Linköping, Sweden, SGI Report No 17, 1983.*

Broms, B. (1982). Stability of Slopes with Respect to Liquefaction. *Symposium on Slopes on Soft Clays, Linköping, Sweden, SGI Report No 17, 1983.*

Burland, J. B., Longworth and Moore, J. F. A. 1977. A study of ground movement and progressive failure caused by a deep excavation in Oxford clay, *Géotechnique, Vol. 27, No 4, pp 557-591.*

Bygg (1972).”Stabilitet och brottproblem” *Handboken Bygg. Del 1b. Kap 174 av Hans Fagerström*. (Handbook on Building, Part 1b, Chapter 174. In Swedish) Stockholm, Byggmästarens Förlag 1972. 603 pp.

Caldenius, C. & Lundström, R. (1956). The Landslide at Surte on the Göta River. *Geological Survey of Sweden, SGU Report No 27, Publ. Stockholm.*

Carson, M. A. (1977). On the retrogression of landslides in sensitive muddy sediments. *Canadian Geotechnical Journal, Vol. 14, pp 582-602*

Carson, M. A. (1979). Le glissement de Rigaud (Québec) du Mai 1978. Une interpretation du mode de rupture d’aprésla morphologie de la cicatrice. *Géographie physique et Quaternaire, Vol. XXXIII,No. 1, pp 63-92.*

Carson, M. A. (1979). On the retrogression of landslides in sensitive muddy sediments – Reply. *Canadian Geotechnical Journal, Vol. 16, pp 431-444*

Chen, S Y., Zhang, X.s., Tang, W., S. (1997). A Numerical Method for Analyzing Progressive Process of Landslide in Soil Slope. *Proc. of the 9th International Conference on Computer Methods in Geomechanics. Wuhan, China.*

Choudhury, R N. (1980). A Reassessment of Limit Equilibrium Concepts in Geotechnique. *ASCE- Proc. Symposium on Limit Equilibrium Plasticity and Generalized Stress Strain Applications in Geotechnical Engineering. Florida.*

Choudhury, R N. (1984). Recent Developments in Land-slide studies: Probabilistic Methods. *State-of-the-Art Report, Session VII(a).*

Christian, J. T. & Whitman, R. (1969). One-dimensional Model for Progressive Failures. *Proc. 7th ICSMFE, Mexico City, Vol. 2, pp 541-545.*

Cruden, D M. (1976) Major Rock Slide in the Rockies. *Canadian Geotechnical Journal. Vol. 13, pp 8-20.*

Cruden, D M. (1985) Rock Slope Movement in the Canadian Cordillera. *Canadian Geotechnical Journal. Vol. 23, pp 528-540.*

Demers, D., Leroueil, S. & D'Astous, J. (1999).Investigation of a landslide in Maskinongé, Québec. *Canadian Geotechnical Journal. Vol. 36, pp 1001-1014.*

Eide, O. & Bjerrum, L. (1954). The slide at Bekkelaget. *Proc. European Conf. on Stability of Earth Slopes, Vol. 2, pp 1-1. Stockholm.*

Eide, O. & Bjerrum, L. (1955). The slide at Brekkelaget. *Geotechnique*, Vol 5, No 1, March 1955, pp 88-100.

Ekelöf, Stig, Ed. (1979): *Teknik i 150 år. Chalmers tekniska högskola, Göteborg 1829 - 1979.* (Technology during 200 years. Chalmers University of Technology, Göteborg 1829-1979. In Swedish). 250 sid. ISBN 91-7032-000-4.

Elfgren, L., Editor (1989). Fracture Mechanics of Concrete Structures. From theory to applications. *Report of the Technical Committee 90 FMA, Fracture Mechanics to Concrete – Applications. RILEM (The International Union of Testing and Research Laboratories for Materials and Structures.) Chapman & Hall Ltd, London, New York, 407 pp.*

Emborg, M. and Bernander, S. (1984): Temperature stresses in early age concrete due to hydration. *Nordic Concrete Research*, Vol 3, 1984, pp 28-48.

Emborg, M. and Bernander, S. (1994): Assessment of the risk of thermal cracking in hardening concrete. *Journal of Structural Engineering (ASCE), Vol 120, No 10*, pp 2893-2914.

Fang , Y S. (1984). Preliminary Study on the Kinematic Mechanism of Catastrophic Landslides and on Prediction of their Velocities and Travel Distances. *Unpublished M.A. thesis, Chengdu College of Geology. China.*

Fellenius, Wolmar (1918). Kaj- och jordraset I Göteborg. *Teknisk Tidskrift V.V.*, Vol 2, pp 17-19.

Fredlund, D. G. (1984). Analytical Methods for Slope Stability Analysis. *Proceedings of the IVth International Symposium on Landslides, State-of-the-Art, Sept 16-21, Toronto, Canada, pp 229-250.*

Gould, J. P. (1960). A study on the shear failure in certain tertiary marine sediments. *Proc. ASCE, Research Conference ob Shear Strength of Cohesive Soils, Boulder, Colorado, 1960*, pp 615-641

Gregersen, O. (1981) The Quick Clay Slide at Rissa, Norway. *10th ICSMFE , Proc.Vol. 3, pp 421-426. Stockholm. Also in NGI Publication No 135, Oslo.*

Grimstad, G. (2004). Project task: Shear band and progressive failure in slopes of quick clay. *Geotechn. Group, Civil Engineering Department, NTNU, (Norwegian University for Technical and Natural Sciences), Trondheim.*

Grimstad, G. Thakur, V. & Nordal, S. (2005). Experimental Observation on Formation and Propagation of Shear Zone in Norwegian Quick Clay. *Landslides and Avalanches. 11th ICFL, Trondheim, Norway.*

Grimstad, G. Degago, S. A., Nordal, S. & Karstunen, M. (2010). Modelling of creep and rate effects in structured anisotropic soft clays. *Acta Geotechnica Journal, Vol.5, No 1, pp 69-81.* Available at: http//www.springerlink.com/content/0415473702752105/ (21 April 2011)

Grondin, D and Demers, D. (1996). The Saint-Liguori flakeslide: Characterization and remedial works. *Proc. of the 7th International Symposium on Landslides, Trondheim, Vol. 2 pp 743-748.*

Groth, P. (2000). Fiber Reinforced Concrete – Fracture Mechanics Methods Applied to Self-compacting Concrete and Energetically Modified Binders. *Doctoral Thesis, 2000:04*, Luleå University of Technology, Sweden.

Gylland, A., Sayd, M., Jostad, H. & Bernander, S. (2010). Investigation of Soil Property Sensitivity in Progressive Failure. *In T. Benz and S. Nordal (Eds.), Proc. of the 7th European Conference on Numerical Methods in Geotechnical Engineering, (NUMGE), Trondheim, Norway, 2-4 June, 2010, pp 515-520.*

Gylland, A. S., Nordal, S., Jostad, H. P., & Mehli, M. (2011). Pragmatic Approach for Estimation of Slope Capacity in Soft Sensitive Clay. *Electronic Journal of Geotechnical Engineering,(EJGE), Vol. 16, Bundle F, pp 575-590.* Available at: http//www.ejge.com/2011/Ppr11.041/Ppr11.041ar.pdf/ (21 April 2011)

Haefeli, R. (1965). Creep and Progressive Failuere in Snow, Soil, Rock and Ice. *Proc. 6th ICSMFE,* Vol. 3, pp 134-148. Montreal.

Hansbo, S. (1957). A New Approach to the Determination of the Shear Strength of Clay by the Fall Cone Test. *Proc. No 14, Swedish Geotechnical Institute. Stockholm.*

Hansbo, S. & Torstensson, B-A. (1978). Tuveskredet. *Delrapport, AB Jacobsson & Widmark, Lidingö.*

Hansbo, S. (1984). Soil Mechanics. (Jordmekanik). *Chapter G05 in BYGG - Geoteknik, Liber Förlag, Stockholm. (In Swedish)*

Hansbo, P., Runesson, K., Wiberg, N-E (1984). Stability and Progressive Failure of natural Slopes – A simple approach. *Publ 84:8 Structural Mechanics, Chalmers University of Technology, Göteborg ,ISSN 0347-9226.* Also in *Int. Conf. on Numerical Methods in Geomechanics*, Nagoya 1985, 7 pp.

Hill, R. (1958). A general theory of uniqueness and stability in elastic plastic solids. *Journ. of Mech. Phys. Solids*, No 6, pp 236 – 249.

Hillerborg, A., Modéer, M. & Pettersson, P-E. (1976). Crack Formation and Crack Growth by Means of Fracture Mechanics and Finite Elements. *Cement & Concrete Research. Vol. 6, pp 773-782.*

Hutchinson, J.N. (1961). A landslide on a thin layer of quick clay at Furre, Central Norway. *Géotechnique (11) , 2, pp 69-94.*

Höeg, K. (1972). Finite element analysis of strain softening clay. *Journal of Soil Mech. & Foundation Engineering. Div. 98 (SM1), pp. 43-59.*

I IG - SNRA (2007). Skredet i Småröd December 2006. (The Slide at Småröd, Cause of the Slide. In Swedish) *Independent Investigatory Group of the Swedish National Road Administration, Borlänge Sweden.*

Jakobson, B. (1952a). The Landslide at Surte on the Göta River. *Proc. No 5, Royal Swedish Geotechnical Insitute, Stockholm*

Jakobson, B. (1952b). Surteskredet. *Teknisk Tidskrift No:s* 43 *& 47 in 1952 and No 6 in 1953.*

Janbu, N. (1973). Shear Strength and Stability of Soils; the Applicability of the Coulombian Material 200 years after the 'ESSAY'. *Norwegian Geotechnical Institute. 47 p. Norwegian Geotechnical Society. NGF- foredraget 1973.*

Janbu, N. (1977). State-of-the-Art Report: Slopes and Excavations. *Proc. 9th ICSMFE, Tokyo.*

Janbu, N., Kjekstad, O. & Senneset, K. (1977). Slide in Overconsolidated Clay below Embankment. *Proc. 9th ICSMFE, Vol. 2 PP 95-102, Tokyo.*

Janbu, N. (1979). Failure Mechanism in Quick Clays. *NGM-79, Nord. Geotekniker mötet, Helsinki.*

Janbu, N. (1979). Mechanisms of Failure in Natural and Artificial Soil Structures. *Intern. Symposium, Oaxaca, Mexico. Proc. Vol. 1.*

Jansson, M. & Stål, T. (1981). The Landslide at Tuve on November 1977. *Swedish Geotechnical Institute, SGI-varia No 56.*

Jostad, H.P. & Andresen, L. (2002). Capacity analysis of anisotropic and strain softening clays. Submitted to *NUMOG VIII*; Rome, Italy.

Jostad, H.P. & Andresen, L. (2004). Modelling of Shear band propagation in clays using interface elements with finite thickness. *Submitted to. Num. Mod. Geomech. – NUMOG IX, Ottawa, Canada.*

Karlsrud, K. (1982). Analysis of a Small Slide in Sensitive Clay in Fredriksstad, Norway. *Proc. Nordic Geotechn. Meeting NGM-1984, Linköping, Sweden.*

Karlsrud, K., Aas, G & Gregersen, O. (1984). Can We Predict Geotechnical Hazards in Soft Sensitive Clays? Summary of Norwegian Practices and Experience. *Proc. IVth Internat. Symposium on Landslides, Toronto, Vol. 1, pp 107-130.*

Kjellman, W. (1954). Mechanism of Large Swedish Landslides. *Proc. European Conf. on Stability of Earth Slopes. Stockholm.* Also published as "Mechanics of Large Swedish Landslides" in *Géotechnique*, Vol 5, No 1, 1955, pp 74-78.

Kovacevic, N., Hight, D. W. & Potts, D. M. (2004). Temporary Slope Stability in London Clay – Back analyses of two case histories. Advances in geotechnical engineering. *The Skempton Conference, Vol.2 pp 842-855.*

Kvalstad T. J. & Andresen L. et al. (2005). The Storegga slide: evaluation of triggering sources and slide mechanisms. *Marine and Petroleum Geology 22, pp 245-256.*

Ladd, C. & Foot, R. (1974). New Design Procedure for Stability of Soft Clays. *JGED, ASCE, Vol. 100, No GT 7.*

La Rochelle, P. (1981). Causes and Mechanisms of Landslides in Sensitive Clays with Special Reference to Clays in the Québec Area. *Proc. 4th Guelp Symposium on Geomorphology, Ontario.*

La Rochelle, P. (1981). General Report. Session 11*, 10 th ICSMFE, Stockholm.*

Larsson, R. (1977). Basic Behaviour of Scandinavian Soft Clays. *Swedish Geotechnical Institute, Report No 4*, 108 +21 pp.

Larsson, R. (1981). Drained Behaviour of Swedish Clays. *Swedish Geotechnical Institute, report No 12,* 157 pp.

Larsson, R. & Jansson M. (1982). SGI 1981. Tuveskredet November 30, 1977. *Report No 18. Statens Geotekniska Institut, Sweden. (In English).*

Lefebvre, G. & La Rochelle, P. (1973). The Analysis of Two Slope Failures in Cemented Champlain Clays. *Canadian Geotechnical Journal, No 11, 1974, pp 89-108.*

Lefebvre, G. (1981). *Failure due to natural processes 'comme fluage ou fatigue'*

Lefebvre, G. (1982). Use of Post Peak Strength in Slope Stability Analysis. *Proc. Symposium on Land- slides. Linköping, Swedish Geotechnical Institute Report No 17.*

Leonards, G A. (1979). Stability of Slopes in Soft Clays. *Special Lecture , 6th Panamerican Conference on Soil Mechanics and Foundation Engineering. Lima, Peru.*

Leonards, G A. (1980). The Sixteenth Terzaghi Lecture, *Annual Convention, Hollywood Beach, Florida.*

Leroueil, S., Collins, G. & Tavenas, F. (1982). Total and Effective Stress Analysis of Slopes in Champlain Sea Clays. *Proc. Symposium on Landslides in Linköping, Swedish Geotechnical Institute Report No 17.*

Leroueil, S., Tavenas, F. & Le Bihan, J-P. (1983). Propriètés charactéristiques des argiles de l'est du Canada. *Revue Canadienne de Géotechnique*, Vol. 20, No 4 pp 681-705.

Leroueil, S. (1997). Geotechnical characteristics of eastern Canada clays. *Workshop on soft clays. Yokosuka, Japan*, 30 pp.

Leroueil, S. (2001). 39th Rankine Lecture: Natural slopes and cuts - Movement and failure mechanisms. *Géotechnique 51, No 3, pp 197-243.*

Leroueil, S. & Hight, D W. (2003). Behaviour and properties of natural soils and soft rocks. *Workshop on Characterization and engineering Properties of natural soils.* Balkema, Singapore pp 29 - 254

Leroueil, S. (2004). Key Note Lecture: Geotechnics of slopes before failure. *9th International Symposium on Landslides, Rio de Janeiro, Proceedings. Vol. 2, pp 863 – 884.*

Lindskog, G/Wager, O. (1970). Skred i Norsälven vid Trossnäs, Wärmlands län, den 12 april 1969. *SGI Report, Task K9590, 1970. (In Swedish.)*

Lo, K. Y. & Lee, C. F. (1973) Analysis of progressiv failure in clay slopes. *Proc. of the 8th ICSMFE, Moscow , Vol. 1, pp 251 – 258.*

Locat, A. (2007). Ètude d'un étalement latéral dans les argiles de l'est du Canada et de la rupture progressive. Le cas du glissement de Saint-Barnabé-Nord. *M.Sc. Thesis, Departement de Génie Civil, Faculté de Sciences et de Genie, Univ. Laval, Québec, 280 pp.*

Locat, A., Leroueil, S., Bernander, S., Demers, D., Locat, J., Ouehb, L. (2008). Study of a lateral spread failure in an eastern Canada clay deposit in relation with progressive failure: The Saint-Baranabé-Nord Slide. In : J. Locat, D.Perret, D. Turmel, D.Demers et S.Leroueil. *Proc. of the 4th Canadian Conference on Geohazards. From Causes to Management Vol. 1. Presses de l'Université Laval, Québec, pp 89 – 96.*

Lundström, R. (1981). Synpunkter på Tuveskredets utveckling inom den passive zonen. *SGI Report No 10. (In Swedish.)*

Lundström, R. (1997). Kinetic Energy and Dynamic Forces in Landslide Development. *Article in a book titled "Göteborgs Tekniska Historia" (In Swedish.). Media Print Uddevalla AB.*

Löfquist, B. (1952). Surterasets orsaker. *Teknisk Tidskrift No 6, Stockholm. (In Swedish)*

Löfquist, B. (1973). Lerskred genom vattenupptryck. *Väg- och Vattenbyggaren Nr 2. (Slides in Clay by Hydraulic Uplift) - (in Swedish)*

Löfquist, B. (1981). Tuveskredets orsaker. (The causes of the Tuve Slide.) *SGI Rapport Nr 10. (In Swedish)*

Massarch, R. (1976). Soil Movements Caused by Pile Driving in Clay. *Dept. of Soil and Rock Mechanics, Report, Job No 6 Royal Institute of Technology, Stockholm.*

Massarch, R. & Broms, B. (1981). Pile Driving in Clay Slopes. *Proceedings 10th ICSMFE, Stockholm.*

Meyerhof, C G. (1957). The Mechanism of Flow Slides in Cohesive Soils. *Géotechnique, Vol. 7, no 1.*

Miao Tiande., Ma Chongwu & Wu Shengzhi (1999). Evolution Model of Progressive Landslides. *Journal of Geotechnical and Environmental Engin., Vol. 125, No 10, Oct. 1999. pp 827-831*. The same reference as Tiande et al (1999).

Mitchell, J K. & Singh, A. (1968). General Stress-strain-time Function for Soils. *Journal. of Soil Mech. & Found. Div. ASCE, 93, SM1, pp 21-46.*

Mollard, J. D. & Hughes, G. T. (1973). Earthflows in the Grondines and Trois-Rivières Areas, Québec. *Dicussion – Canadian Journal of Earth and Sciences, Vol. 10, pp 324-326.*

Moore, I. D. & Rowe, R. K. (1988). Numerical Models for Evaluating Progressive Failure in Earth Structures – A review. *Computers and Geotechnics. Volume 6, Issue 3, 1988, Pages 217-239*

Nordal, S (1983). Elasto-plastic behavior of soils analyzed by the finite element method. *Dissertation*, Geoteknikk, NTH, Trondheim.

Nordal, S., Bostrøm, B & Fredriksen, F.J. (1988). An effective stress-soil model applied to an undrained finite element analysis of a gravity platform. *Proceedings of the International Conference on Behavior of Offshore Structures*, Tapir, 1:227-241.

Nordal, S., Jostad, H.P., Kavli, A., & Grande, L. (1989). A Coulombian soil model applied to an offshore platform. *Proceedings of the 12th ICSMFE*, Balkema 1:471-474

Nordal, S., Sällfors, G., Jendeby, L., Hartlén, J., Alén, C, and Högsta, U. (2008): Skredet i Småröd i december 2006 (The Landslide in Småröd in December 2006. In Swedish). *Väg- och Vattenbyggaren, Nr 1, 2008*, pp 8-16. Discussion by Ulf Ekdal in *Samhällsbyggaren, No 4, 2009,* pp 32-37, and answer by the authors in No 6, pp 30-34. Further discussions by Ekdal, 4 pp and by Stig Bernander, 11 pp on www.samhällsbyggaren.se, Debatt.

Nordal, S. (2008). Can We Trust Numerical Collapse Load Simulations Using Non-associated Flow Rules? *12th Internat. Conf. of the International Association for Computer Methods and Advances in Geomechanics, (IACMAG). Goa, India, pp 755-762.*

Odenstad, S. (1951). The Landslide at Sköttorp on the Lidan River. *Royal Swedish Geotechnical Institute, Proceedings no 4, 40 p.(Stockholm 1951).*

Olsson, C. (1981). Tuveskredet – kan det förklaras genom en konventionell stabilitetsbetraktelse. *SGI Report No 10. (In Swedish.)*

Ohlsson, U. (1995). Fracture Mechanics Analysis of Concrete Structures. *Doctoral Thesis, 1995:179 Div. of Structural Engineering, Luleå University of Technology, Luleå.*

Ouehb, L. (2007). Analyse du glissement de Saint-Liguori (1989) dnas l'optique d'une rupture progressive. M.Sc. Thesis, *M.Sc. Thesis, Université. Laval, Québec 284 p.*

Palmer, A C. & Rice, J R. (1973). The Growth of Slip Surface in the Progressive Failure of Over-consolidated Clay. *Proceedings of the Royal Society of London Series A, Mathematical and physical Sciences, (April 3, 1973), Vol 332, pp 527-548.*

Peck, R B. (1967). Stability of Natural Slopes. *Journal of Soil Mechanics & Foundations, Div. ASCE 93, SM4, pp 403-417.*

Picarelli, L, Urciuoli, G. & Russo, C. (2000.). Mechanisms of slope deformation in stiff clays and clay shales as a consequence of pore pressure fluctuations. *8th International Symposium on Landslides, Cardiff. On CD-Rom.*

Picarelli, L. (2000). Mechanisms and rates of slope movements in fine grained soils. *Intern. Conf. Geotech. & Geol. Engineering, Melbourne. Proc. GeoEng. 2000, Vol 1, pp 1618-1670.*

Puzrin, A. M., Germanovich, L N. & Kim, S. (2004). Catastrophic Failure of Submerged Slopes in Normally Consolidated Sediments. *Geotechnique, 54 (10), 631- 643. doi:10.1680/geot.54.10.631.56348*

Puzrin, A. M., Germanovich, L N. (2005). The Growth of Shear Bands in the Catastrophic Failure of Soils. *Proc.of the Royal Society of London A: Mathematical, Physical and Engineering Sciences, 461(2056),1199-1228. doi:10.1098/rspa.2004.1378* Available at*:* http://www.jstor.org/pss/30046963 (21 April 2011)

Puzrin, A. M. & Sterba, I. (2006). Inverse long-term stability analysis of a constrained landslide. Geotechnique, Vol. 56, No 7*, pp 483-489*

Puzrin, A. M., Saurer, E. & Germanovich, L N. (2010). A dynamic solution to the shear band propagation in submerged landslides. *Granular Matter (Springer), 12:253-265*. Available at: http//www.springerlink.com/content/4529573843x77971/ (21 April 2011)

Quinn, P., Diederichs, M. S., Hutchinson, D. J. and Rowe, R. K. (2007). An Exploration of the Mechanics of Retrogressive Landslides in Sensitive Clay. *Proc. of the 60th Canadian Conference, Ottawa, 721-727.*

Quinn, P. (2009). Large Landslides in Sensitive Clay in Eastern Canada and the Associated Hazard Risk to Linear Infrastructure. *Ph D Thesis, Department of Geological Sciences and Geological Engineering, Queen's University, Kingston, Ontario, Canada. April 2009, 465 pp.* Available at: http//qspace.library.queensu.ca/handle/1974/1781 (21 April 2011)

Rosenquist, I Th. (1977). A General Theory for Quick Clay Properties. *Proceedings 3rd European Clay Conference, Oslo*.

Saurer, E. & Puzrin, A. M. (2007). On simulation of shear band propagation in trapdoor-tests*. Proc. of the 10th Internat. Symposium on Numerical Models in Geomechanics, Rhodes, April 25-27, pp 119-123.*

Saurer, E. & Puzrin, A. M. (2008). Energy balance approach to shear band propagation in shear-blade tests. *Proc. of the 12th Internat. Conf. of the International Association for Computer Methods and Advances in Geomechanics, (IACMAG). Goa, India, pp 1024-103.* Available at: http//www.civil.iitb.ac.in/~dns/IACMAG08/pdfs/C03.pdf (21 April 2011)

Saurer, E. (2009) Shear band propagation in soil and dynamics of tsunamigenic landslides. *Ph D Thesis,ETH, Zürich, 188 pp. doi:10.3929/ethz-a-005951122.* Available at: http//www.civil.iitb.ac.in/e.library.queensu

Saurer, E. and Puzrin, A. M. (2010): Validation of the energy-balance approach to curve-shaped shear-band propagation in soil. Proceedings *of the Royal Society of London A: Mathematical, Physical and Engineering Sciences, 467, pp 627- 652. doi:10.1098/rspa.2010.0285.*

SGI Report No 10. (1981). Tuveskredet 1977-11-30, Inlägg om skredets orsaker. *Statens Geotekniska Institut, Linköping, Sweden. (In Swedish).150 pp.*

SGI Report No 17 (1983). Symposium on slopes of soft clays, Linköping, March 8-10, 1982. . *Statens Geotekniska Institut, Linköping, Sweden,* 461 pp.

SGI Report No 18. (1982). Tuveskredet, November 30, 1977. *Statens Geotekniska Institut, Linköping, Sweden. (In English).154 pp.*

SGI Report No 11 a. (1984). Tuveskredet , Slutrapport, Februari 1984. *Statens Geotekniska Institut, Linköping, Sweden. (In Swedish).85 pp.*

Skempton A.W. (1964). 4th Rankine Lecture: Long Term Stability of Clay Slopes. *Géotechnique, Vol. 14, No 2, pp 77-102.*

Skempton, A W & Hutchinson, J. (1969). Stability of Natural Slopes and Embankment Foundations. *Proc. 7th ICSMFE, Mexico City.*

Skempton, A. W. (1977). Slope stability of cuttings in brown London clay. *Proc., 9th Int. Conf. Soil Mechanics and Foundation Engineering*, Japanese Society of Soil Mechanics and Foundation Engineering, Tokyo, Japan, Vol. 3, pp 261-270.

Singh, A. & Mitchell, J K. (1968). General Stress-strain-time Function for Soils. *Journal. of Soil Mech. & Found. Div. ASCE, 93, SM1, pp 21-46.*

Suklje, L (1969): Rheological aspects of soil mechanics. *London: Wiley*, 571 pp, ISBN 0471835501

Sällfors, G. (1979). Långsträckta slänters stabilitet – en förenklad beräkningsmetod. *NGM 1979. (Helsingfors), pp 495-507.*

Sällfors, G. (1981). Skred ger besked - Tuveskredet. *(Comments on the causes of the Tuve Slide). SGI Rapport nr 10. (In Swedish)*

Sällfors, G. (1984a). State-of- the-Art Report: Soft Clays in Sweden. *IVth International Symposium on Landslides, Toronto.*

Sällfors, G. (1984b). Handbok för beräkning av slänters stabilitet (Handbook on Slope Stability Calculations. In Swedish). *Swedish Council for Building Research, Report R53:1984*, Stockholm, 70 pp.

Söderblom, R. (1974). Salt in Swedish Clays and its Importance for Quick Clay Formation. *Proc. No 22 Swedish Geotechnical Institute.*

Tavenas, F, Trak, B. & Lerouil, S. (1980). Remarks on the Validity of Stability Analyses. *Canadian Geotechnical Journal, Vol. 17, No 4.*

Tavenas, F. & Lerouil, S. (1981). Creep Failure of Slopes in Clays. *Canadian Geotechnical Journal, Vol.18.*

Tavenas, F. (1984). State-of-the-Art Report: Landslides in Canadian Sensitive Clays. *Proc. of the IVth International Symposium on Landslides. Toronto, Vol. 1. pp 141-153.*

Taylor, T W. (1948). Fundamentals of Soil mechanics. *New York, 1948, pp 392-345.*

Terzaghi, K. & Peck, R B. (1948). Soil Mechanics in Engineering Practice. *New York, John Wiley & Sons, Inc.*

Terzaghi, K. (1950). Mechanism of Landslides. From Theory to Practice in Soil Mechanics, *New York, John Wiley & Sons, 2nd Edition 1960, pp 202-245.*

Thakur, V. Nordal, S. & Grimstad, G. (2006). Phenomenological issues related to strain softening in sensitive clays. *Geotechnical and Geological Engineering, Vol. 24, No 6, pp. 1729-1747.*

Thakur, V. (2007). Strain Localization in Sensitive Soft Clays. *Ph D Thesis, Geotechnical Division, Department of Civil and Transport Engineering, Norwegian Institute of Science and Technology, NTNU. Trondheim and Norwegian Centre of Excellence: International Centre for Geohazards, ISBN 9788247139097*, *188 pp.*

Thun, Håkan (2006): Assessment of Fatigue Resistance and Strength in Existing Concrete Structures. *Doctoral Thesis 2006:65,* Div. of Structural Engineering, Luleå University of Technology, 169 pp. ISBN 978-91-85685-03-5.

Tiande, M., Chongwu, M., and Shengzhi, W. (1999). Evolution model of progressive failure of landslides. *ASCE Journal of Geotechnical and Geoenvironmental Engineering*, Vol 125(10), pp. 827-831

Torstensson, B-A. (1979). The Landslide at Tuve. *Proceedings Nordic Geotechnical Meeting (NGM), Esbo, Helsinki, pp 557-572*

Trak, B., La Rochelle, P., Tavenas, F., Leroueil, S. & Roy, M. (1980). A new Approach to the Stability Analysis of Embankments on Sensitive Clays. *Canadian Geotechnical Journal. Volume 17, No 4.*

Turnbull, W J. & Hvorslev, M J. (1967). Special Problems in Slope Stability. *Journal of Soil Mechanics & Foundation, Div. ASCE, 93, SM4, pp 499-528.*

Uchida, I. & Hirata, T. (1977). Failure of Embankment, Slope of silty sand "Masa". *Proc. 9th ICSMFE, Tokyo*.

Urciuoli G. (2002) Strains preceding failure in infinite Slopes. *Inter. Journ. of Geomech. 2(1), pp 93 -112.*

Urciuoli G., Picarelli, L. & Leroueil, S. (2007). Local Soil Failure before General Soil Failure. *Geotechnical and Geological Engineering, Volume 25, Number 1, pp 103-122.*

Vermeer, P A. & De Borst, R. (1984). Non-associated Plasticity for Soils, Concrete and Rock. *Heron, Vol. 29 (Special No).*

Wiberg, N-E., Koponen, M. & Runesson, K. (1990). Finite Element Analysis of Progressive Failure in Long Slopes. *International Journal for Numerical and Analytical Methods in Geo-mechanics, Vol. 14, pp 599-612.*

Zhang, Z., Zhan, S., Liu, H C., Xu, J. & Fang, Y S. (1987). The Formation and Kinematic Mechanism of the Landslides in Pleistocene Lacustrine Clay Beds near Longyang Gorge Damsite on the Yellow River. *Proceed. 1st International Symposium on Engineering Geomorphology, England.*

Appendix I - Exemplification of calculation procedure – downhill progressive failure

I. General

The Finite Difference Method of analysis (FDM) used in this appendix was presented in theory and principle at the Nordic Geotechnical Meeting in Oslo (1988), and later at the 12th ICSMFE in Rio de Janeiro (1989). Already at this time, a computer program for the analysis of downhill progressive slope failure, based on these principles, had been applied by the author in engineering practice from the end of 1984.
Yet, the approach to progressive slope failure in question was presented in more detail considerably later (i.e. May 2000) in a licentiate report LTU 2000:16. The existing computer software in HP-Basic was in this context transformed – essentially unchanged – into Windows C++ software. (Cf Section 4.53.)

Exemplification of progressive failure analysis, based on the equations given in the conference papers from 1988 and 1989, has among other been presented in the form of an Excel spread-sheet in Bernander, (2008), Report No LuTU 2008:11. The spread-sheet, which can be used for the analysis of both downhill and uphill progressive slope failures, is applicable to arbitrary slope geometry within the chosen framework.

As explained in detail in Appendices A and B of the LuTU 2008:11 report, the Excel spread sheet is convenient for the analysis of uniformly inclining slope sections, where the depth to the failure surface is virtually constant. The spread sheet is well suited for educational purposes, promoting the understanding of the complicated mechanisms related to progressive landslide development. (Cf Figure I:2.1.)

Although all spread sheet calculations are automatically performed by computer, every cognitive step in this analysis is controlled by the operator enabling continuous insight in the computation process. A deft user is able to perform a complete study of the critical triggering load condition in the upper part of a slope in about 15 minutes.
However, in slopes with *complex geometry*, the soft-ware in C++ referred to in Section 4.53 is recommended. A complete iterative integration, defining the critical triggering load, may then be a matter of just a few minutes.

I:11 Aim of the current exercise
The objective of this exercise is to show in principle and detail how the computations according to the proposed FDM-model are actually carried out.
Hence, the example presented in Section I.2 only serves to demonstrate the calculation procedure and does not claim or recommend any generally applicable laws of soil behaviour. In fact, an advantage of the FDM-approach described is that it can accommodate any defined shear stress/deformation property of the soil that the investigating engineer may wish to apply to the situation studied.

For the purpose of demonstration, parts of the exemplification in Sections I.2 to I.3 have been computed manually. Yet, because of limited space, all of the iterative computations performed in the computer spread sheet are not shown. Thus, many of the repetitive steps and iterations are only presented as input data and results.
Nevertheless, the interested reader should readily be able to follow the computation procedure of and how calculations according to the progressive failure FDM-approach are performed.

I.12 Integral calculation procedure

Figure I:1.1 illustrates the principles and the integration procedure for the proposed Finite Difference Method of analysis. In the current context, the aim is to determine the maximum load q_{cr} kN/m that can be placed in a certain up-slope location.

The integral computation begins at a point (x= 0) further down the slope, where the conditions of stress and deformation are un-affected by the applied additional load (q). Hence, the parameters $E_{0,x=0}$, $\tau_{0,x=0}$, , $N_{x=0}$ and $\delta_{x=0}$ constitute the down-slope boundary condition for the subsequent integral analysis. Correspondingly, the force $N_{x1} = q \cdot H$ at $x = x_1$ is the up-slope boundary condition that, when satisfied, determines the associated values of $\tau_{x=x1}$ and $\delta_{x=x1}$. In Figure I:1.1, the boundary condition at x = 0 is defined as:
$E_x = E_{0,x=0}$, $\tau_x = \tau_{0,x=0}$, $N_x = 0$, and $\delta_x = 0$

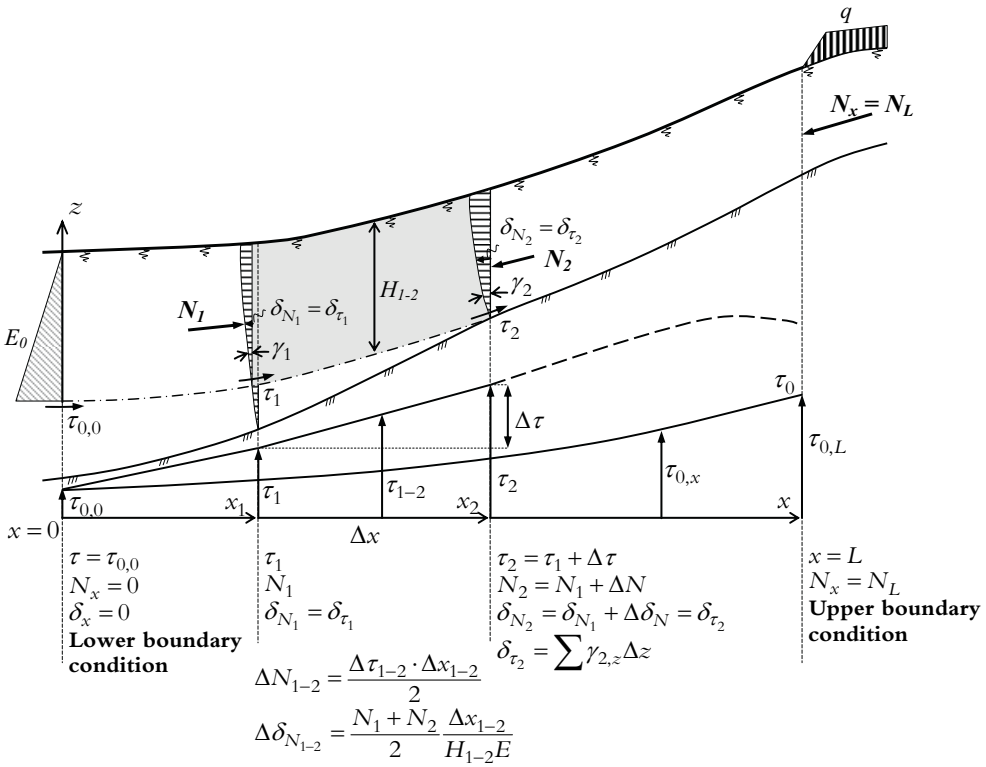

Figure I:1.1 Section illustrating the calculation procedure. Width b = 1.

As indicated in Figure I:1.1, the calculation proceeds by advancing in steps of suitably chosen values of $\Delta\tau$ and Δx. As the values of δ_N and δ_τ can then be expressed in terms of the assumed values of the increments $\Delta\tau$ and Δx, the correlating values of Δx and $\Delta\tau$ in each step cycle have to be found by iteration so that the compatibility equation is satisfied, i.e.:

$$\delta_{N,x} = \Sigma_0^x (\Delta\delta_N) = \delta_{\tau,x} \qquad \text{……Eq. 4:5}$$

For uniform slopes with constant depth to the failure surface, working in steps of $\Delta\tau$ and finding the corresponding compatible value of Δx is most convenient. In slopes with arbitrary geometry, working in steps of Δx and determining the compatible value of $\Delta\tau$ is preferable.

I.13 Shear deformation relationships

The constitutive relationships, represented in general terms by Equations 4:6 and 4:6a in Section 4, are in his context defined by the curves in Figure I:1.2. As may be concluded, different relationships apply to different ranges of shear stress and deviatory strain.

Stage I a: Elastic range

In the range $0 < \gamma_{x,z} < \gamma_{el}$ (i.e. for $0 < \tau_{xz} < \tau_{el}$), the relationship between shear stress and shear strain is taken to be linear. (Cf Figure I:1.2.)

$$\tau_x = G \cdot \gamma_x \text{ or } \gamma_x = \tau_x / G \qquad \text{……Eq. I:1}$$

$$\Delta\gamma_{x,z} = \Delta\tau_{x,z} / G \qquad \text{..…… Eq. I:1a}$$

where $G = \tau_{el} / \gamma_{el}$ (as defined in Figure I:1.2)

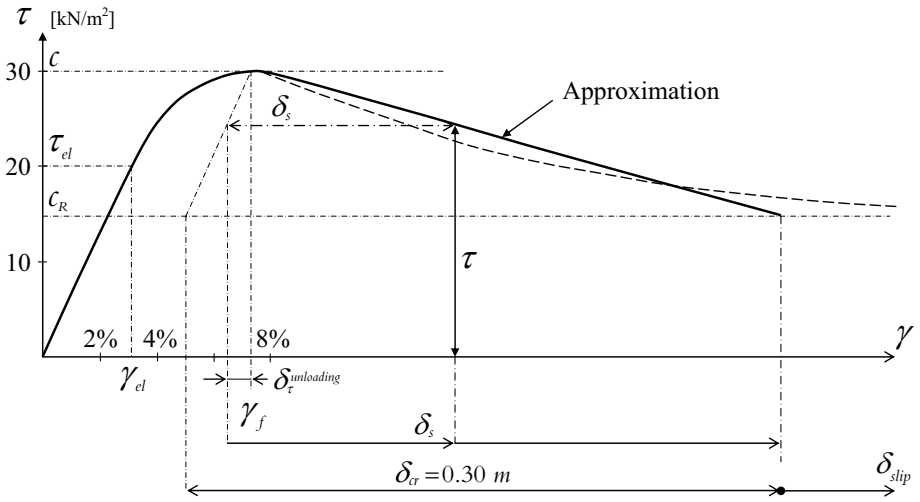

Figure I:1.2 Constitutive shear stress/deformation relationships. It may be noted that the ratio of τ_{el}/c is here assumed to be constant as c varies with the coordinate (z). Data from Section I.21.

Stage I b: Non-linear range from τ_{el} to peak strength c

In the non-linear range, where $\gamma_{el} < \gamma_{x,z} < \gamma_f$ (i.e. for $\tau_{el} < \tau_{xz} < c$), the relationship between shear stress and deviatory strain is taken to follow a 2 nd power parabolic law with its vertex at point (γ_f, c), as indicated in Figure I:1.2. Tangential continuity in Point (τ_{el},γ_{el}) demands the following relationship between γ_{el}, and γ_f : (**[1]**)

$$G_{el} = \tau_{el} / \gamma_{el} = 2(c - \tau_{el})/(\gamma_f - \gamma_{el}) \text{ i.e. } \gamma_{el} = \gamma_f \cdot \tau_{el} / (2c - \tau_{el}) \qquad \text{..……Eq. I:3}$$

(E.g. in the current case treated in Section 1.2, $\gamma_{el} = 0{,}075 \cdot 20/(2 \cdot 30\text{-}20) = 0.0375 = 3.75$ %)

(**[1]**) The parabolic relationship to the power of 2, which is used here for practical reasons, may of course be replaced by any other relationship considered appropriate by the investigating engineer. However, the issue as such has little impact on the accuracy of the results of the analysis.
Integrating Eq. I:2d with respect to the z- coordinate gives the total shear deformation in an element of length Δx.

Hence, the following expression can be derived:
$\tau_{xz} - \tau_{el} = 2\,(c-\tau_{el})\cdot[(\gamma_{x,z}-\gamma_{el})/(\gamma_f-\gamma_{el})] - (c-\tau_{el})\cdot[(\gamma_{x,z}-\gamma_{el})/(\gamma_f-\gamma_{el})]^2$ ……Eq. I:2
or $[(\gamma_{x,z}-\gamma_{el})/(\gamma_f-\gamma_{el})]^2 - 2\cdot[(\gamma_{x,z}-\gamma_{el})/(\gamma_f-\gamma_{el})] + (\tau_{xz}-\tau_{el})/(c-\tau_{el}) = 0$ ……Eq. I:2a
The solution of Equation I:2a is:
$[(\gamma_{x,z}-\gamma_{el})/(\gamma_f-\gamma_{el})] = 1 - [1-(\tau_{xz}-\tau_{el})/(c-\tau_{el})]^{1/2}$ …… Eq. I:2b

Equation I:2b may be transformed to:
$\boldsymbol{\gamma_{x,z} = \gamma_f - (\gamma_f-\gamma_{el})\cdot[1-(\tau_{xz}-\tau_{el})/(c-\tau_{el})]^{1/2}}$ …… Eq. I:2c
Check: For $\tau_{xz} = \tau_{el} \rightarrow \gamma_{x,z} = \gamma_{el}$ and for $\tau_{xz} = c \rightarrow \gamma_{x,z} = \gamma_f$ …… Q.E.D.

The difference in shear strain ($\Delta\gamma_{x,z}$) when increasing $\tau_{x(n),z}$ to $\tau_{x(n+1)z}$ is:
$\Delta\gamma_{x,z} = (\gamma_f-\gamma_{el})\cdot[[1-(\tau_{x(n),z}-\tau_{el})/(c-\tau_{el})]^{1/2} - [1-(\tau_{x(n+1)z}-\tau_{el})/(c-\tau_{el})]^{1/2}\,]$ ….Eq. I:2d

$\boldsymbol{\Delta\gamma_{x,z} = (\gamma_f-\gamma_{el})\cdot([1-(\tau_{x,z(0)}-\tau_{el})/(c_{x,z}-\tau_{el})]^{1/2} - [1-(\tau_{x,z}-\tau_{el})/(c_{x,z}-\tau_{el})]^{1/2})}$ .....Eq. I:4
where $\tau_{x(n),z}$ and $\tau_{x(n+1)z}$ denote the shear stresses in elements (n) and (n+1)

Stage I c*: *Combined elastic and non-linear range *– i.e. from* $\tau_z < \tau_{el} \rightarrow \tau_z < c$
When the current stress range spans across the transition point between elastic and non-linear behaviour, the following expression derived from Equations I:1a and I:4, is used:
$\boldsymbol{\Delta\gamma_{x,z} = (\tau_{el}-\tau_{x,z(0)})/G + (\gamma_f-\gamma_{el})\cdot(1-[1-(\tau_{x,z}-\tau_{el})/(c-\tau_{el})]^{1/2})}$ ……...Eq. I:4a

Stage II: Post peak range *(in the current case assumed to be linear)*
Stage II a – i.e. for $c > \tau_z > c_R$ $(0 < \delta_{S,z} < \delta_{cR})$
The post peak shear strength (= mobilized shear stress) c_{Rx} is now set as a function of $\delta_{S,z}$ according to Figure I:1.2.

Hence for $0 < \delta_{S,z} < \delta_{cR}$, the following integral relationships apply:
- *Deformation from* $\boldsymbol{\tau_{x,z(0)} \rightarrow \tau_{x,z(max)}}$ (at max. shear stress) when $\boldsymbol{\tau_o > \tau_{el}}$
$\boldsymbol{\Delta\gamma_{x,z}} = (\gamma_f-\gamma_{el})\cdot([1-(\tau_{o(x,z)}-\tau_{el})/(c_{x,z}-\tau_{el})]^{1/2} - [1-(\tau_{x,z,max}-\tau_{el})/(c_{x,z}-\tau_{el})]^{1/2})$ ..Eq.I.4($\tau_{x,z,max}$)
- *Deformation from* $\boldsymbol{\tau_{x,z(0)} \rightarrow \tau_{x,z(max)}}$ (at max. shear stress) when $\boldsymbol{\tau_o < \tau_{el}}$
$\boldsymbol{\Delta\gamma_{x,z}} = [(\tau_{el}-\tau_{x,z(0))})/G + (\gamma_f-\gamma_{el})\cdot(1-[1-(\tau_{x,z(max)}-\tau_{el})/(c_{x,z}-\tau_{el})]^{1/2})]$ .....Eq.I:4a($\tau_{x,z,max}$)
Elastic rebound – Range: $\tau_{x,z(max)} > \tau_{x,z} > c_R$
The elastic rebound due to de-loading from $\tau_{x,z(max)}$ to $\tau_{x,z}$ in an element ($\Delta x\cdot\Delta z$) is:
$\boldsymbol{\Delta\gamma_{x,z}} = -(\tau_{(x,z(max)}-\tau_{x,z})/G\cdot\Delta z$ (Cf Figure I.1.2.)
Hence, the total elastic rebound at failure plane
$\delta_{el}(x,z) = -\,{}_o\Sigma^{\alpha H}(\tau_{(x,z(max)}-\tau_{x,z})/G\cdot\Delta z$ …… Eq.I:1b
where αH denotes the thickness of the zone mainly contributing to shear deformation.

- *Slip in failure plane*
The post peak shear strength (= mobilized shear stress). $\tau_{x,o} = c_{Rx}$ is now set as a function of δ_S according to Figure I.1.2. Hence for the interval $0 < \delta_{S(x)} < \delta_{CR}$ we can derive the slip in the failure plane (i.e. where z =0) as being:
$\delta_S(\tau_x)/\delta_{cR} = (c-\tau_x)/(c-c_R)$ or $\delta_{S,}(\tau_x) = \delta_{cR}\cdot(c-\tau_x)/(c-c_R)$ ..…… Eq.I:6
where δ_{cR} = The slip at which minimum residual shear strength c_R is attained;
$\delta_S(\tau_x)$ = Slip in the failure plane at un-loading in the stress range $c > \tau_x > c_R$;
Check: For $\tau_x = c_R \rightarrow \delta_{S,}(\tau_x) = \delta_{cR}$ and for $\tau_x = c \rightarrow \delta_{S,}(\tau_x) = 0$

- *Total post peak deformation in Stage II a*
Hence, when $\boldsymbol{\tau_o > \tau_{el}}$ the *total* shear deformation of a vertical element Δx in Stage IIa,

including elastic rebound and slip, is derived by adding Equations I.4($\tau_{x,z,max}$), I:3 and I:6:

Displacement $\tau_o \rightarrow \tau_{x,z(max)}$ *when* $\tau_o > \tau_{el}$

$$\boldsymbol{\delta_\tau = {}_0\Sigma^{\alpha H}\,[(\gamma_f - \gamma_{el})\cdot([1-(\tau_{x,z\,(0)} - \tau_{el})/(c - \tau_{el})]^{1/2} - [1-(\tau_{x,z(max)} - \tau_{el})/(c - \tau_{el})]^{1/2}) -}$$

Rebound $\tau_{x,z(,max)} \rightarrow \tau_{x,z}$ *Slip deformation* $c \rightarrow \tau_{x,z} > c_R$

$$\boldsymbol{- (\tau_{x,z(max)} - \tau_{x,z})/G]\cdot\Delta z \; + \delta_{CR}\cdot(c - \tau_{x,o})/(c - c_R)} \quad (^{2a}) \qquad \text{…….……} \text{ Eq. I: 5}$$

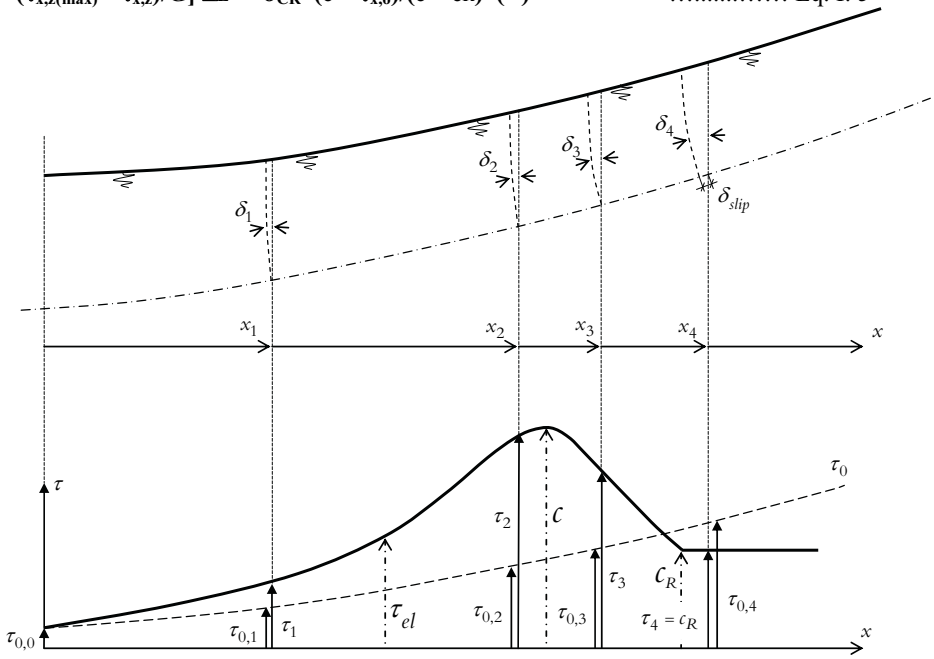

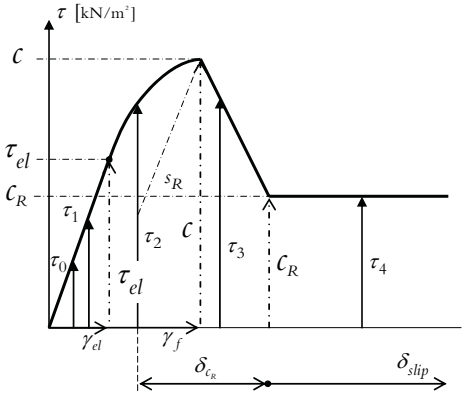

Shear deformation $\delta(x_1)$ is based on the shear stress range from $\tau_{o,1} \rightarrow \tau_1 < \boldsymbol{\tau_{el}}$

" " " $\delta(x_2)$ is based on the shear stress range from $\tau_{o,2} \rightarrow \tau_2 \leq \boldsymbol{c}$

" " " $\delta(x_3)$ is based on the shear stress range from $\tau_{o,3} \rightarrow \boldsymbol{c} \rightarrow \tau_3 > \boldsymbol{c_R}$

" " " $\delta(x_4)$ is based on the shear stress range from $\tau_{o,4} \rightarrow \boldsymbol{c} \rightarrow \boldsymbol{c_R} = \tau_4$

Figure I:1.3 Diagram indicating the different sections of the shear stress/deformation relationship, on which the analyses of downhill shear deformations $\delta_\tau(x)$ in different parts of a slope are based.

By contrast, when $\boldsymbol{\tau_o < \tau_{el}}$, the *total* shear deformation in terms of shear and slip in Stage IIa, using Eq. I.4a($\tau_{x,z,max}$), is:

Displacement $\tau_o \rightarrow \tau_{x,z(max)}$ *when* $\tau_o < \tau_{el}$

$$\boldsymbol{\delta_\tau = {}_o\Sigma^{\alpha H}\,[(\tau_{el} - \tau_{x,z\,(0)})/G + (g_f - g_{el})\cdot(1 - [1 - (\tau_{x,z(max)} - \tau_{el})/(c - \tau_{el})]^{1/2}) -}$$

Rebound $\tau_{x,z(max)} \rightarrow \tau_{x,z}$ *Slip deformation* $c \rightarrow \tau_{x,z} > c_R$

$$\boldsymbol{-(\tau_{x,z(max)} - \tau_{x,z})/G]\cdot\Delta z + \delta_{CR}\cdot(c - \tau_{x,o})/(c - c_R)} \quad (^{2a}) \qquad \text{…….……. Eq. I: 5a}$$

(^{2a}) Equations 1:5 and 1:5a apply at the failure plane. For elements above this plane, the expression representing 'slip' $\delta_{CR}\cdot(c - \tau_{x,o})/(c - c_R)$ is not applicable. For instance, Eq. 1:5 becomes:
$\delta_\tau = {}_o\Sigma^{\alpha H}\,[(\gamma_f - \gamma_{el})\cdot([1 - (\tau_{x,z\,(0)} - \tau_{el})/(c - \tau_{el})]^{1/2} - [1 - (\tau_{x,z(max)} - \tau_{el})/(c - \tau_{el})]^{1/2}) - (\tau_{x,z(max)} - \tau_{x,z})/G]\cdot\Delta z.$

Stage IIb - Post residual shear stress stage - i.e. when $\tau_{x,z} = c_R$ (residual) resistance and corresponding slip > δ_{cr} (Cf Figure I.1.2.)

The shear deformation at this stage is exclusively governed by the axial down-slope displacement (δ_N), and thus independent of the values of $\tau_{x,z}$ as indicated by Equation I:5b. For $\boldsymbol{\tau_o > \tau_{el}}$ and $\tau_{x,o} = c_R$ Equation I:5 changes to:

Displacement $\tau_o \rightarrow \tau_{x,z(max)}$

$$\boldsymbol{\delta_\tau = {}_o\Sigma^{\alpha H}\,[\gamma_f - \gamma_{el})\cdot([1 - (\tau_{o(x,z)} - \tau_{el})/(c - \tau_{el})]^{1/2} - [1 - (\tau_{x,z(max)} - \tau_{el})/(c - \tau_{el})]^{1/2}) -}$$

Rebound $\tau_{x,z(max)} \rightarrow c_R$ *Slip deformation when* $\tau_{x,z} = c_R$

$$\boldsymbol{-(\tau_{x,z(max)} - \tau_{x,z}))/G]\cdot\Delta z + \delta_{CR} + \delta_{slip} = \delta_N} \qquad \text{…….. Eq. I: 5b } (^{2b})$$

Again if $\boldsymbol{\tau_o < \tau_{el}}$ and $\tau_{x,o} = c_R$, Equation I:5a changes to:

Displacement $\tau_o \rightarrow \tau_{x,z(max)}$

$$\boldsymbol{\delta_\tau = {}_o\Sigma^{\alpha H}\,[(\tau_{el} - \tau_{o(x,z)})/G + (\gamma_f - \gamma_{el})\cdot(1 - [1 - (\tau_{x,z(max)} - \tau_{el})/(c - \tau_{el})]^{1/2})}$$

Rebound $\tau_{x,z(max)} \rightarrow c_R$ *Slip deformation when* $\tau_{x,z} = c_R$

$$\boldsymbol{-(\tau_{x,z(max)} - \tau_{x,z})/G]\cdot\Delta z + \delta_{CR} + \delta_{slip} = \delta_N} \qquad \text{..... Eq. I:5c } (^{2b})$$

(^{2b}) Equations 1:5b and 1:5c apply at the failure plane. For elements above this plane, the expressions $\delta_{CR} + \delta_{slip}$ representing 'slip' are not applicable.

Synopsis: The shear resistance is mobilized to a widely varying extent ahead of the additional load. This implies that entirely different sections of the constitutive relationship are valid for different parts of the slope. Figure I:1.3 demonstrates how this issue is dealt with in the current FDM- approach.

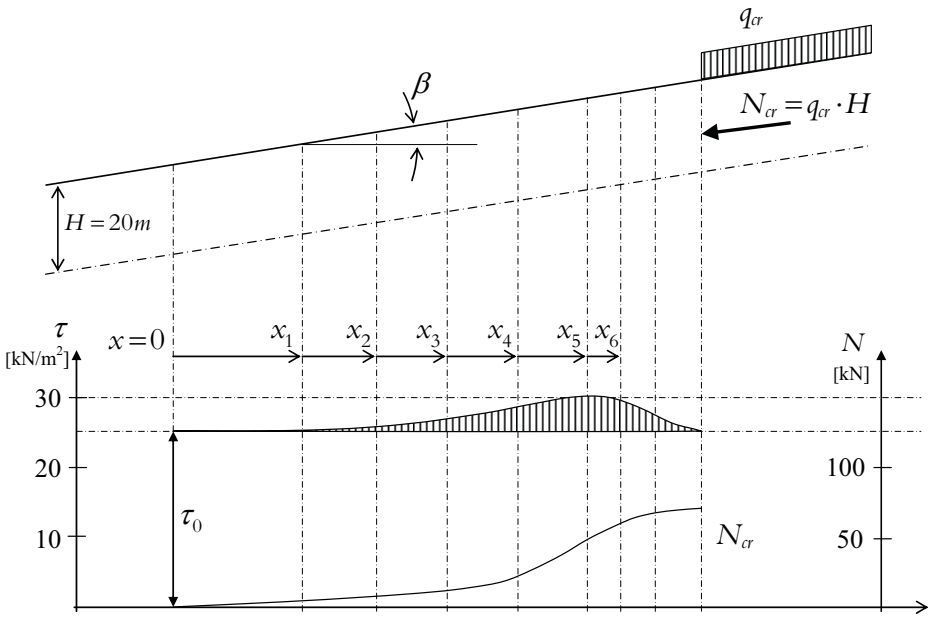

Figure I: 2.1 The part of the slope being analyzed in the example. The co-ordinates x_1 to x_n symbolize different steps in the integration procedure.

I.2 Calculation of local stability – *Triggering failure condition*

Determination of N_{cr}, L_{cr} and associated stresses and deformations

I.21 Slope data

The current calculation procedure is exemplified in detail in the form of an Excel Spread sheet in Bernander, (2008), Appendix C of Report LuTU 2008:11 together with numerous applications related to critical triggering load (N_{cr}) and to landslide spread over level ground.

Slope data, see Figure I:1.2, assumed in the current example, see Figure I:1.2: **([3])**

$\rho \cdot g = 16$ kN/m^3 $\quad K_o = E_0/E_{\varphi',=0} \approx$ constant $\quad \therefore \Delta E_o/\Delta x \approx 0$

$H = 20$ m $\quad b = 1$ m $\quad \beta = 3{,}727°$

Clay properties assumed: **([3])**

$c = 30$ kN/m^2 $\quad c_R/c = 0.50$ $\quad \tau_{el} = 20$ kN/m^2 $\quad E_{el} = 53.3 \cdot c_{mean} = 1200$ kN/m^2

$c_R = 15$ kN/m^2 $\quad \gamma_f = 7.5$ % $\quad \gamma_{el} = 3.75$ % $\quad G_{el} = \tau_{el}/\gamma_{el} = 533$ kN/m^2

$c_{mean} = 22.5$ kN/m^2 $\quad c_{surface} = 15$ kN/m^2 $\quad \delta_{cR} = 0.30$ m

([3]) In the example, fixed values are applied to many of the parameters that may in reality be variable with respect to x, such as β, H, E_o, c, γ_f, γ_{el}, c_R, τ_{el} etc. It is therefore important to note that these simplifications are made here solely in order to make the analysis of the calculations procedure and the results more transparent to the reader.
In fact, varying these parameters arbitrarily is accommodated by the equations used, and does not complicate the computations significantly when computers are used.
Hence, any desired configuration of ground surface and failure planes, as well as varying width, soil properties and in-situ earth pressures can be treated in an analysis.

As the computations in the subsequent exercise may appear to be of a laborious nature, it should be kept in mind that – once slope data have been inserted into the mentioned Excel spread sheet – the entire calculation procedure, demonstrated in the following Sections I.2 and I.3, is matter of some 15 to 20 minutes for an engineer acquainted with the soft-ware.

I.22 Calculation of the load N (or q) corresponding to peak shear strength

Applying Equation 4:2 (as per Section 4), the value of τ_{ox} is determined (b = 1 m)

$\tau_o(x,o) = [\Sigma_o^{H(x)} \cdot g \cdot \rho(z) \cdot 1 \cdot \Delta z] \cdot \sin\beta(x) - \Delta E_o(x)/(b(x) \cdot \Delta x)$

$= H \cdot g \cdot \rho \cdot \sin\beta(x) - \Delta E_o(x)/\Delta x$

$= 20 \cdot 16 \cdot \sin(3.727\,°) + 0$ $\approx$ **20.8** kN/m^2

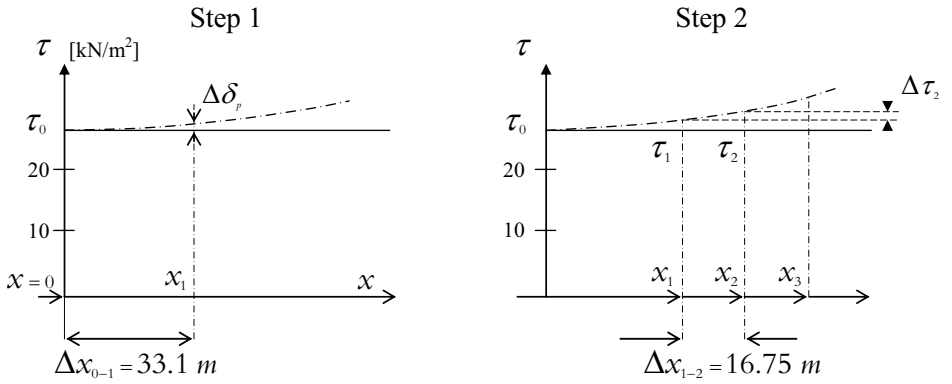

Figure I:2.2 Illustration of the first two calculation steps.

Step 1: **x = 0,** Set $\Delta\tau_1$ = **0.5** kN/m^2 at x_1 $\tau_o(x,o)$= 20.8 kN/m^2 $\tau(x_1,o)$= 20.8 kN/m^2

Applying Equations 4:1 and 4:2 from Section 4:

$\Delta N = [(\tau(x,o) - \tau(o,o))/2 - \tau_o(x,o)] \cdot b(x) \cdot \Delta x - q(x) \cdot b(x) \cdot \sin\beta(x) \cdot \Delta x - t(x) \cdot b(x) \cdot \Delta x$

$= 0.5 \cdot 1/2 \cdot \Delta x - 0 - 0$ = **0.25·Δx** kN/m

According to Equation 4:3,

$\Delta\delta_N = (N + \Delta N/2) \cdot \Delta x/[E_{el} \cdot H(x) \cdot b(x)]$

$= (0 + 0.25 \cdot \Delta x_1/2) \cdot \Delta x_1/[1200 \cdot 20]$ = **0.1042·Δx$_1^2$/20000** (m)

Equations: The following equations given in Section I.1 are applied:

The integral Equation 4:5 in Section 4 is generally applicable:

$\boldsymbol{\delta_\tau} = \Sigma_o^{\alpha H} [\boldsymbol{\Delta\gamma_{x,z}}] \cdot \Delta z + \delta_S(x,o) = \boldsymbol{\delta_N}$, …… Eq. 4:5

where:

a) In the elastic range (i.e. $\tau_{x,z} < \tau_{el} =$ 20 kN/m^2) Equation I:1a applies:

$\boldsymbol{\delta_\tau} = \Sigma_o^{\alpha H} [\Delta\gamma_{x,z}] \cdot \Delta z = {}_o\Sigma^{\alpha H} (\tau_{xz} - \tau_{xo})/G \cdot \Delta z$, …… Eq. I:1a

where in this case $G = 2(c - \tau_{el})/(\gamma_f - \gamma_{el}) = 2 \cdot 10/0.0375 = 533.3$ kN/m^2

b) In the plastic range, i.e. for $\boldsymbol{\tau_o > \tau_{el}}$ and $\tau_{el} < \tau_{x,z} <$ c kN/m^2, Equation I:4 applies:

$\boldsymbol{\delta_\tau} = {}_o\Sigma^{\alpha H} (\gamma_f - \gamma_{el}) \cdot ([1 - (\tau_{x,z(0)} - \tau_{el})/(c_{x,z} - \tau_{el})]^{1/2} - [1 - (\tau_{x,z} - \tau_{el})/(c_{x,z} - \tau_{el})]^{1/2}) \cdot \Delta z$ …... Eq. I:4

c) In the transition zone, i.e. for $\boldsymbol{\tau_o < \tau_{el}}$ and $\tau_{o,x,z} < \tau_{x,z} <$ c kN/m^2, Equation I:4a applies:

$\boldsymbol{\delta_\tau} = {}_o\Sigma^{\alpha H} (\tau_{el} - \tau_{x,z(0)})/G + (\gamma_f - \gamma_{el}) \cdot (1 - [1 - (\tau_{x,z} - \tau_{el})/(c - \tau_{el})]^{1/2}) \cdot \Delta z$ …..... Eq. I:4a

Table I:1 $\mathbf{x_0 \rightarrow x_1}$ Integration of Equations I:4, I:4a and I:1a. $\mathbf{\Delta\tau = 0.5}$ kN/m^2.

z (m)	τ_o(x,z)	$\Delta\tau$(x,z)	τ (x_1,z)	$\Delta\gamma_{x,z}\cdot$**100** (Eq. I:4)	$\Delta\gamma_{x,z}\cdot$**100**	Δ**z**	$\Delta\gamma_{x,z}\cdot\Delta$**z** m
0	20.80	0.500	21.30	0.099			
0.5					0.096	1.0	0.00096
1	19.76	0.475	20.24	0.094			
1.5				(Eq. I:4a)	0.091	1.0	0.00091
2	18.72	0.450	19.17	0.089			
2.5				(Eq. I:1a)	0.088	1.0	0.00088
3	17.68.	0.425	18.11	0.086			
3.5					0.085	1.0	0.00085
4	16.64	0.400	17.04	0.083			
4.5					0.082	1.0	0.00082
5	15.60	0.375	15.98	0.080			
5,5					0.079	1.0	0.00079
6	14.56	0.350	14.91	0.077			
6.3					0.051	0.6	0.00051
6.6	13.87	0.333	14.20	0.075			

$\delta_\tau = \Sigma_o^{1/3H}\Delta\gamma_{x,z}\cdot\Delta z =$ **0.00572 m**

In this initial step (Step 1), $\Delta\delta_N = \delta_\tau$. By equating the results (Equ.4:5)

$\Sigma\Delta\delta_N = 0.125\cdot\Delta x^2/20000$ = $\mathbf{\delta_\tau = 0.00572}$ m

$\Delta x^2 = 20000\cdot 0.00572/0.104 \rightarrow \mathbf{\Delta x = 33.13}$ m $N_x = 0 + (0.5\cdot 33.13\cdot 1)/2 =$ **8.28** kN/m

Results from Step 1: $x_o = 0$ m, $x_1 = 33.1$ m, $N_x = 0{,}00$ kN/m, $\delta(x_o) = 0.00000$ m, $\tau_o(x_1) = 20.8$ kN/m^2, $\tau_x(x_1) = 21.3$ kN/m^2, $N_{x1} = 8.28$ kN/m, $\delta(x_1) = 0.00572$ m

Step 2 From Step 1: $\tau_o(x_o,o) = 20.8$ kN/m^2, $\tau_x(x_1,o) = 21.3$ kN/m^2, $N_{x1} = 8.28$ kN/ m^2
Advance $\Delta\tau$ by **1.0** kN/m^2 $\tau_x(x_2,o) = 22.3$ kN/m^2
The results of computations using Equations I:4, I:4a and I:1a are presented in Table I:2.

Table I:2 Integration of δ_τ using Equations I:4, I:4a and I:1a. $\mathbf{\Delta\tau = 1.0}$ kN/m^2.

z (m)	τ_o(x,z)	$\tau(x_1,z)$	$\Delta\tau$	$\tau(x_2,z)$	$\tau(\Delta x_{1\text{-}2},z)$ mean	$\Delta\gamma_{x,z}$ x100	Δ**z**	$\Delta\gamma_{x,z}\cdot\Delta$**z** x100 m
0	20.80	21.30	1.00	22.30	21.84	0.306		
0.5						(Eq. I:4)	1.0	0.298
1	19.76	20.24	0.95	21.19	20.71	0.289		
1.5							1.0	0.281
2	18.72	19.17	0.90	20.07	19.62	0.272		
2.5						(Eq. I:4a)	1.0	0.266
3	17.68	18.11	0.85	18.96	18.53	0.260		
3.5						(Eq. I:1a)	1.0	0.255
4	16,64	17.04	0.80	17.84	17.44	0.250		
4.5							1.0	0.246
5	15.60	15.98	0.75	16.73	16.35	0.241		
5,5							1.0	0.236
6	14,56	14.91	0.70	15.61	15.26	0.232		
6.3							0.6	0.153
6.6	13.83	14.20	0.67	14.89	14.53	0.225		

$\delta_\tau = \Sigma_o^{1/3H}\Delta\gamma_{x,z}\,x\,\Delta z =$ **0.001734 m**

Iteration No 1:
Try $\Delta x_{1\text{-}2} = 20$ m → $x_2 = 33.13 + 20 =$ 53.13 m
ΔN = [(22.3+21.3)/2–20.8]·20 = 20 kN/m …….. (Eq. 4:1)
$\tau_o(x_1,o) = 21.3$ kN/m^2, $\tau_x(x_2,o) = 21.3+1.0 = 22.3$ kN/m^2,
$N_{x2} = (8.28 + 20)$ = 28.28 kN/m
$\Delta\delta_N$ = (8.28+20/2)·20/1200/20 = 0.01523 m …….. (Eq. 4:3)
$\delta_N = \sum\Delta\delta_N = 0.00572 + 0.01523 = 0.02095$ m
Results from Iteration No 1:
$\boldsymbol{\delta_N}$ = 0.2095 m ≠ $\boldsymbol{\delta_\tau}$ = **0**.01734 m. Equation 4:5 *is* ***not*** *satisfied.* Try another value of $\boldsymbol{\Delta x_{1,2}}$.

Iteration No 2 The procedure in Iteration 1 is repeated in respect of ΔN and δ_N
Try $\Delta x_{1\text{-}2} = 14$ m → $x_2 = 33.13 + 14 = 47{,}13$ m
ΔN = [(22.3+ 21.3)/2– 20.8]·14 = 14.00 kN/m ……. (Eq. 4:1)
N_{x2} = (8.28 + 14) = 22.28 kN/m
$\Delta\delta_N$ = (8.28 + 14/2)·14/1200/20 = 0.00891 m ……. (Eq. 4:3)
$\delta_N = \sum\Delta\delta_N = 0.00572 + 0.00891 = 0.01463$ m

Again, Equation 4:5 is still ***not*** satisfied, as $\delta_N = 0.01463$ m ≠ $\delta_\tau = 0.001734$ m .
However, interpolation from the results of the previous iterations indicates a correct value of $\Delta x_{1,2} = 16.75$ m.

Iteration No 3 The procedure in Iteration 1 is repeated in respect of ΔN and δ_N
Check the value of $x_{1\text{-}2} = 16.75$ m → $x_2 = 33.13 + 16.75 = 49.88$ m.
ΔN = [(22.3+ 21.3)/2– 20.8]·16.75 = 16.75 kN/m ……. (Eq. 4:1)
N_{x2} = (8.28 + 16.75) = 25.03 kN/m
$\Delta\delta_N$ =(8.28 + 16.75/2)·16.75/1200/20 = 0.01162 m ……. (Eq. 4:3)
$\delta_N = \sum\Delta\delta_N = 0.00572 + 0.01162 = 0.01734$ m
Result from Iteration No 3:
$\boldsymbol{\delta_N} = \sum\Delta\delta_N = 0.00572+0.01162 = 0.01734$ m = $\boldsymbol{\delta_\tau}$ = 0.01734 m, i.e. Equation 4:5 is satisfied.

Results from integration ***Step 2****:*
$x_1 = 33.13$ m τ_o = 20.8 kN/m^2
$x_2 = 49.88$ m $\tau_x(x_1)$ = 21.3 kN/m^2 $N(x_1)$ = 8.28 kN/m $\delta(x_1) = 0.00572$ m
$\tau_x(x_2)$ = 22.3 kN/m^2 $N(x_2)$ = 25.03 kN/m $\delta(x_2) = 0.01734$ m

Step No 3 From Step 2: $\tau_o(x_o,o) = 20.8$ kN/m^2, $\tau_x(x_2,o) = 22.3$ kN/m^2
Advance $\Delta\tau$ by 2.0 kN/m^2 $\tau_x(x_3,o) = 24.3$ kN/m^2.
Proceed to calculate δ_τ as done in Table I:3 below.

Iteration No 1:
Try $\Delta x_{2\text{-}3} = 10$ m → $x_3 = 49.88 + 10 =$ 59.88 m
$\tau_o(x_2,o) = 21.3$ kN/m^2, $\tau_x(x_3,o) = 21.3+1.0 = 22.3$ kN/m^2,
ΔN = [(24.3+22.3)/2–20.8]·10 = 25.0 kN/m ……. (Eq. 4:1)
$\Delta\delta_N$ = (25.03+25/2)·10/1200/20 = 0.01564 m ……. (Eq. 4:3)
$\delta_N = \sum\Delta\delta_N = 0.01734 + 0.01564 = 0.03298$ m
Results from Iteration No 1:
$\delta_N = 0.03298$ m ≠ $\delta_\tau = 0.04195$ m. Eq. 4:5 is ***not*** satisfied. Try another value of $\Delta x_{2,3}$.

Table I:3 Integration of Equations I:4, I:4a and I:1a. $\Delta\tau$ **= 2.0** kN/m^2.

z (m)	τ_o**(x,z)**	τ**(x$_2$,z)**	$\Delta\tau$	τ**(x$_3$,z)**	τ**(Δx$_{2\text{-}3}$,z)** mean	$\Delta\gamma_{x,z}$ **x100** (Eq. I:4)	Δ**z**	$\Delta\gamma_{x,z}\cdot\Delta$**z**
0	20.80	21.30	2.00	24.30	23.30	0.766		m
0.5							1.0	0.00742
1	19.76	20.24	1.90	23.09	22.14	0.718		
1.5						(Eq. I:4a)	1.0	0.00695
2	18.72	19.17	1.80	21.87	20.97	0.673		
2.5							1.0	0.00652
3	17.68	18.11	1.70	20.66	19.81	0.632		
3.5							1.0	0.00614
4	16,64	17.04	1.60	19.44	18.64	0.596		
4.5							1.0	0.00581
5	15.60	15.98	1.50	18.23	17.48	0.566		
5,5							1.0	0.00553
6	14,56	14.91	1.40	17.01	16.31	0.540		
6.3						(Eq. I:1a)	0.6	0.00357
6.6	13.87	14.20	1.33	16.20	15.53	0.525		

$\delta_\tau = \Sigma_o^{1/3H}\Delta\gamma_{x,z} \times \Delta z =$ **0.04195 m**

Iteration No 2:
Try $\Delta x_{2\text{-}3} = 18$ m → $x_3 = 49.88 + 18 =$ 67.88 m
ΔN = [(24.3+22.3)/2–20.8]·18 = 45.0 kN/m ……. (Eq. 4:1)
$\Delta\delta_N$ = (25.03+45/2)·18/1200/20 = 0.03565 m ……. (Eq. 4:3)
$\delta_N = \sum\Delta\delta_N = 0.01734 + 0.03565 =$ 0.05299 m
Results from Iteration No 2:
$\delta_N = 0.05299$ m ≠ δ_τ= 0.04195m. Eq. 4:5 is ***not*** satisfied. Try another value of $\Delta x_{2,3}$.
Interpolation between the results of the previous iterations indicates that the correct value of $\Delta x_{1,2}$ can be = 13.92 m.

Iteration No 3:
Try $\Delta x_{2\text{-}3} = 13.92$ m → $x_3 = 49.88 + 13.92 = 63.80$ m
ΔN = [(24,3+22,3)/2–20,8]·13.92 = 34.80 kN/m ……. (Eq. 4:1)
N_3 = 25.03 + 34.8 = 59.83 kN/m
$\Delta\delta_N$ = (25.03+34.8/2)·13.92/1200/20 = 0.02461 m ……. (Eq. 4:3)
$\delta_N = \sum\Delta\delta_N = 0.01734 + 0.02461 = 0.04195$ m
Result from iteration No 3:
$\delta_\tau = 0.04195$ m = $\delta_N = 0.04195$ m, i.e. Equation 4:5 is satisfied.

Results from integration Step 3:
$x_2 = 49.88$ m $\tau_o = 20.8$ kN/m^2
$x_3 = 63.80$ m $\tau_x(x_2) = 22.3$ kN/m^2, N (x_2) = 25.03 kN/m, $\delta(x_2) = 0.01734$ m
$\tau_x(x_3) = 24.3$ kN/m^2 N (x_3) = 59.83 kN/m $\delta(x_3) = 0.04195$ m

Step 4:
The calculation is continued using the Excel program, based on the expressions derived in Section I. following the procedure applied in Steps 2 and 3 of this section. The spread sheet given in Appendix C in LTU 2008:11 is well suited for this purpose. (Cf Bernander, 2008.)

Increasing τ_3 by $\Delta\tau_{3\text{-}4} = 3.5$ kN/m^2, and x_3 by $\Delta x_{3\text{-}4} = 13.15$ m gives (subsequent to iteration):
$\tau_o(x_4,o) = 20.8$ kN/m^2 $\tau_x(x_3,o) = 24.3$ kN/m^2
$\Delta\tau_{o,3\text{-}4} = 3.5$ kN/m^2 $\tau_x(x_4,o) = 24.3 + 3.5 = 27.8$ kN/m^2,

Hence:

$\Delta N = [(278 + 24.3)/2 - 20.8]\cdot 13.15 = 69.04$ kN/m …….(Eq. 4:1)

$N_{x4} = (59.83 + 69.04) = 128.87$ kN/m

$\Delta\delta_N = (59.83 + 69.04/2)\cdot 13.15/1200/20 = 0.05170$ m ……..(Eq. 4:3)

$\boldsymbol{\delta_{N4}} = 0.04195 + 0.05170 = 0.09365$ m $= \boldsymbol{\delta_\tau}$ ……..(Eq. 4:5)

Equation 4:5 is satisfied.

Results from Step 4:

$x_3 = 63.80$ m $\tau_o = 25$ kN/m^2

$x_4 = 76.95$ m $\tau_x(x_3) = 24.3$ kN/m^2, $N(x_3) = 59.83$ kN/m, $\delta(x_3) = 0.04195$ m

$\tau_x(x_4) = 27.8$ kN/m^2 $N(x_4) = 128.87$ kN/m $\delta(x_4) = 0.09365$ m

Step 5:

Repeating the procedures in Step 4 gives:

Advance τ by $\Delta\tau = 2.2$ kN/m^2, and (subsequent to iteration) x_4 by $\Delta x_{4\text{-}5} = 7.315$ m

$\tau_o(x_4,o) = 20.8$ kN/m^2 $\tau_x(x_4,o) = 27.8$ kN/m^2

$\Delta\tau_{o,4\text{-}5} = 3.5$ kN/m^2 $\tau_x(x_5,o) = 27.8 + 2.2 = 30.0$ kN/m^2,

$\Delta N_{4\text{-}5} = [(30.0 + 27.8)/2 - 20.8]\cdot 7.315 = 59.24$ kN/m …….(Eq. 4:1)

$N_{x5} = (128.87 + 59.24) = 188.11$ kN/m

$\Delta\delta_{N,4\text{-}5} = (188.12 + 59.24/2)\cdot 7.315/1200/20 = 0.04831$ m ……..(Eq. 4:3)

$\boldsymbol{\delta_{N5}} = 0.09365 + 0.04831 = 0.14196$ m $= \boldsymbol{\delta_\tau} = 0.14196$ m …..(Eq. 4:5)

Equation 4:5 is satisfied.

Results from Step 5: Corresponding to mobilizing peak the shear strength, c = **30.0** kN/m^2

$x_4 = 76.95$ m $\tau_o = 20.8$ kN/m^2

$x_5 = 84.27$ m $\tau_x(x_4) = 27.8$ kN/m^2, $N(x_4) = 126.87$ kN/m, $\delta(x_4) = 0.09365$ m

$\tau_x(x_5) = \mathbf{30.0}$ kN/m^2 $N(x_5) = 188.11$ kN/m $\delta(x_5) = 0.14196$ m

I.23 Post-peak analysis – Determination of the Critical load (N_{cr})

At this point of the computation procedure, the shear strength c = 30 kN/m^2 is fully mobilized and a slip surface begins to form. The shear/deformation relationship is now on expressed according to Equations I:5b or I:5c considering the slip δ_S and the effects of rebound due to de-loading. In other respects, the calculation proceeds in principle as before. For increasing x-values, shear stress will decline and eventually attain the value of the residual shear strength, which in the current case is $c_R = 15$ kN/m^2.

Step 6:

When $\boldsymbol{\tau_o > \tau_{el}}$, the constitutive law in the post-peak range according to Equation I:5 applies:

$\delta_\tau = {}_o\Sigma^{\alpha H}[(\gamma_f - \gamma_{el})\cdot([1 - (\tau_{x,z(0)} - \tau_{el})/(c - \tau_{el})]^{1/2} - [1 - (\tau_{x,z,max} - \tau_{el})/(c - \tau_{el})]^{1/2}) -$

Rebound $\tau_{x,z(,max)} \rightarrow \tau_{x,z}$ *Slip deformation* $c \rightarrow \tau_{x,z} > c_R$

$- (\tau_{x,z(max)} - \tau_{x,z})/G]\cdot\Delta z + \delta_{CR}\cdot(c - \tau_{x,o})/(c - c_R)$ ……(Eq. I: 5) **(4)**

By contrast, when $\boldsymbol{\tau_o < \tau_{el}}$ Equation I:5a applies:

$\delta_\tau = {}_o\Sigma^{\alpha H}[(\tau_{el} - \tau_{x,z(0)})/G + (\gamma_f - \gamma_{el})\cdot(1 - [1 - (\tau_{x,z\,(max)} - \tau_{el})/(c - \tau_{el})]^{1/2}) -$

Rebound $\tau_{x,z(max)} \rightarrow \tau_{x,z}$ *Slip deformation* $c \rightarrow \tau_{x,z} \rightarrow c_R$

$- (\tau_{x,z(max)} - \tau_{x,z})/G]\cdot\Delta z + \delta_{CR}\cdot(c - \tau_{x,o})/(c - c_R)$ ……. (Eq. I: 5a) **(4)**

(4) Equations 1:5 and 1:5a apply at the failure plane. For elements above this plane, the expression $\delta_{CR}\cdot(c - \tau_{x,o})/(c - cR)$, representing 'slip' is not applicable.

The analysis is in principle performed as demonstrated in Steps 2 and 3. The shear deformations are thus integrated in Table I:4 for $\Delta\tau_{5\text{-}6} = \mathbf{-\ 5.0}$ kN/m^2

Table I:4 Integration of Equations I:5 and I:5a. $\Delta\tau_{5\text{-}6} = \mathbf{-\ 5.0}$ kN/m^2, $\tau_6 = 25.0$ kN/m^2

z (m)	$\tau_o(x,z)$	$\tau(x_5,z)$	$\Delta\tau$	$\tau(x_6,z)$	$\tau(\Delta x_{5\text{-}6},z)$ mean	$\Delta\gamma_{x,z}$ x10 (Eq. I:5)	Δz	$\Delta\gamma_{x,z}\cdot\Delta z$
0	20.80	30.00	-5.00	25.00	27.50	0.2646		m
0.5							1.0	0.02124
1	19.76	28.50	-4.75	23.75	26.13	0.1600		
1.5						(Eq. I:5a)	1.0	0.01420
2	18.72	27.00	-4.50	22.50	24.75	0.1239		
2.5							1.0	0.01120
3	17.68	25.50	-4.25	21.25	23.38	0.1000		
3.5							1.0	0.00914
4	16.64	24.00	-4.00	20.00	22.00	0.0828		
4.5							1.0	0.00764
5	15.60	22.50	-3.75	18.75	20.63	0.0701		
5,5							1.0	0.00656
6	14.56	21.00	-3.50	17.50	19.25	0.0611		
6.3							0.6	0.00355
6.6	13.87	20.10	-3.35	16.75	18.43	0.0571		

. $\mathbf{\delta_\tau =\ 0.07353}$ m ([5])

([5]) According to Eq. I:5 and I:5a and excepting slip in failure surface

The slip at the failure surface
$\Delta\delta_{5\text{-}6} = \delta_{CR}\cdot(c - \tau_{x,o})/(c - c_R) = 0.3\cdot(30 - 25)/(30 - 15) = 0.10$ m
$\mathbf{\delta_\tau}$ = 0.07353 + 0.100 = **0.17353** m

Iteration No 1: Try $\Delta x_{5\text{-}6} = 2.5$ m → $x_6 = 84.27$ m + 2.5 = 86.77 m
$\tau_x(x_5)$ = 30.0 kN/m^2, $\tau_x(x_6)$ = 25.0 kN/m^2
$N(x_5)$ = 188.11 kN/m $\delta(x_5)$ = 0.14196 m
$\Delta N_{5\text{-}6}$ = [(30.0+25.0)/2–20,8]·2.5 = 16.75 kN/m .....(Eq. 4:1)
$\Delta\delta_N$ = (188,11+16.75/2)·2.5/1200/20 = 0.02047 m .....(Eq. 4:3)
δ_N = $\sum\Delta\delta_N$ = 0.14196 + 0.02047 = 0.16243 m
Result from Iteration No 1:
$\mathbf{\delta_N}$ = 0.16243 m ≠ δ_τ = 0.17353 m. Eq. 4:5 is ***not*** satisfied. Try another value of $\Delta x_{5,6}$.

Iteration No 2: Try $\Delta x_{5\text{-}6} = 5.0$ m → x_6 = 84.27+ 5.0 = 89.27 m
$\Delta N_{5\text{-}6}$ = [(30.0+25.0)/2–20.8]·5.0 = 33.5 kN/m ..... (Eq. 4:1)
$\Delta\delta_N$ = (188.11+33.5/2)·5/1200/20 = 0.04268 m ..... (Eq. 4:3)
δ_N = $\sum\Delta\delta_N$ = 0.14196 + 0.04268 = 0.18464 m
Result from Iteration No 2:
$\mathbf{\delta_N}$ = 0.18464 m ≠ δ_τ = 0.17353 m. Eq. 4:5 is ***not*** satisfied. Try another value of $\Delta x_{5,6}$.
Interpolation between the results of the previous iterations indicates that the correct value of $\Delta x_{5\text{-}6}$ can be = 3.775 m.

Iteration No 3: Try $\Delta x_{5\text{-}6} = 3.775$ m → x_6 = 84.27+3.775 = 88.05 m
$\Delta N_{5\text{-}6}$ = [(30.0+25.0)/2–20,8]·3.775 = 25.29 kN/m .....(Eq. 4:1)
N_6 = 188.11+25.29 = 213.39 kN/m
$\Delta\delta_N$ = (188.11+25.29/2)·3.775/1200/20 = 0.003157 m ..... (Eq. 4:3)
δ_N = $\sum\Delta\delta_N$ = 0.14196 + 0.03157 = 0.17353 m

Result from iteration No 3:
$\boldsymbol{\delta_N}$ = 0.17353 m = $\boldsymbol{\delta_\tau}$ = 0.17353 m**,** i.e. Equation 4:5 is satisfied.
Results from integration Step 6:
x_5 = 84.27 m τ_o = 20.8 kN/m^2
x_6 = 88.05 m $\tau_x(x_5)$ = 30.0 kN/m^2, N (x_5) = 188.1 kN/m, $\delta(x_5)$ = 0.14196 m
$\tau_x(x_6)$ = 25.0 kN/m^2, N (x_6) = 213.4 kN/m $\delta(x_6)$ = 0.17353 m

Step 7: The value of τ_6 is reduced by $\boldsymbol{\Delta\tau_{6\text{-}7} = -2.5}$ kN/m^2 , i.e. $\boldsymbol{\tau_7}$ = 22.5 kN/m^2.
The integration of Equations I:5 and I:5a is carried out as in Step 6 but using the Excel spread sheet in Bernander (2008), Appendix C. This gives $\boldsymbol{\delta_\tau}$ = **0.19547** m
The subsequent iterations are carried out as in Step 6. The relevant value of $\Delta x_{6\text{-}7}$ is found to be 2.427 m.
$\Delta x_{6\text{-}7}$ = 2.42 m → x_7 = 88.05+2.42 = 90.47 m
$\Delta N_{6\text{-}7}$ = [(25.0+22.5)/2–20.8]·2.427 = 7.15 kN/m …….(Eq. 4:1)
N_7 =213.4+7.14 = 220.5 kN/m
$\Delta\delta_{N,6\text{-}7}$ = (213.4+7.15/2)·2.427/1200/20 = 0.02194 m ……. (Eq. 4:3)
δ_{N7} = $\sum\Delta\delta_N$ = 0.17353 + 0.02194 = 0.19547 m
Result from iterations in Step 7:
$\boldsymbol{\delta_N}$ = 0.19547 m = $\boldsymbol{\delta_\tau}$ = 0.19547 m**,** i.e. Equation 4:5 ***is satisfied***.

*Results from integration **Step 7:***
x_6 = 88.05 m τ_o = 20.8 kN/m^2
x_7 = 90.47 m $\tau_x(x_6)$ = 25.0 kN/m^2, N (x_6) = 213.4 kN/m, $\delta(x_6)$ = 0.1735 m
$\tau_x(x_7)$ = 22.5 kN/m^2, N (x_7) = 220.5 kN/m $\delta(x_7)$ = 0.1955 m

Step 8: The value of τ_7 is reduced by $\boldsymbol{\Delta\tau_{7\text{-}8} = -1.70}$ kN/m^2**,** i.e. $\boldsymbol{\tau_8}$ = 20.8 kN/m^2
The integration and subsequent iterations are carried out as in Step 7. The relevant value of $\Delta x_{7\text{-}8}$ is found to be 4.934 m and the corresponding value of $\boldsymbol{\delta_\tau}$ = 0. 2104 m.
$\Delta x_{7\text{-}8}$ = 1.618 m → x_8 = 90.48+ 1.618 = 92.10 m
$\tau_x(x_7)$ = 22.5 kN/m^2, $\tau_x(x_8)$ = 22.5–1.70 = 20.8 kN/m^2
$\Delta N_{7\text{-}8}$ = [(22.5+20.8)/2–20,8]·1.618 = 1.37 kN/m …….(Eq. 4:1)
N_8 =220.5 + 1.37 = 221.87 kN/m
$\Delta\delta_{N,7\text{-}8}$ = (221.87+1.37/2)·1.618/1200/20 = 0.01491 m ……. (Eq. 4:3)
$\delta_{N,8}$ = $\sum\Delta\delta_N$ = 0.1955 + 0.01491 = 0.2104 m
Result from iterations:
$\boldsymbol{\delta_N}$ = 0.2104 m = $\boldsymbol{\delta_\tau}$ = 0.2104 m**,** i.e. Equation 4:5 is satisfied.

Results from integration Step 8:
x_7 = 90.48 m τ_o = 20.8 kN/m^2
x_8 = 92.10 m $\tau_x(x_7)$ = 22.5 kN/m^2 N (x_7) = 220.5 kN/m $\delta(x_7)$ = 0.1955 m
$\tau_x(x_8)$ = 20.8 kN/m^2 N (x_8) = 221.9 kN/m $\delta(x_8)$ = 0.2104 m

Key results: $\boldsymbol{N_{max} = N_{cr} \approx 221.9}$ kN/m, $\boldsymbol{L_{cr}}$ = **92.1** m, $\boldsymbol{\delta_{cr}}$ = **0.210** m
At this point, the shear stress $\tau_x(x_8)$ is equal to the in-situ stress τ_o (= 20.8 kN/m^2) implying that all *available* shear resistance in excess of the in-situ stress (τ_o) is mobilized.
Hence, the maximum resistance to the formation of progressive slope failure $N_{cr}(x) = N(x_8)$ = 221.9 kN/m is now attained. If, for instance, a load N_i = 140 kN/m is applied at this location the safety factor (F_s) against progressive failure formation would be:

$F_s = N_{cr}(x_8)/N_i = 221.9/140 = 1.585$

Conclusion: The **critical load** for downhill progressive slope failure is $\mathbf{N_{cr}}$ = **221.9** kN/m.
In the current case N_{cr} corresponds to a distributed load q_{cr} = 221.9/20 = **11.1** kN/m^2.
The associated critical displacement is $\boldsymbol{\delta_{cr}}$ = **0. 210** m and the maximum length of influence of the load N_{cr} is: $\mathbf{L_{cr}}$ = **92.1** m

I.24 Shear stress attaining residual resistance c_R

Step 9:

The value of τ_8 is reduced by $\boldsymbol{\Delta\tau_{8\text{-}9}}$ = –5.80 kN/m^2, i.e. $\boldsymbol{\tau_9}$ = 15.0 kN/m^2 = $\mathbf{c_R}$
The integration and subsequent iterations are carried out as in Step 9. The relevant value of $\Delta x_{8\text{-}9}$ is found to be 4.98 m and the corresponding value of $\boldsymbol{\delta_\tau}$ = 0. 2549 m.

$\Delta x_{8\text{-}9}$ = 4.98 m → x_9 = 92.10+ 4.98 = 97.08 m
$\tau_x(x_8)$ = 20.8 kN/m^2, $\tau_x(x_9)$ = 20.8–5.80 = 15.0 kN/m^2
$\Delta N_{8\text{-}9}$ = [(20.8+15.0)/2–20,8]·4.98 = –14.45 kN/m …….(Eq. 4:1)
N_9 = 221.9 – 14.45 = 207.45 kN/m
$\Delta\delta_{N,8\text{-}9}$ = (221.9 –14.45 /2)·4.98/1200/20 = 0.04454 m ……. (Eq. 4:3)
$\delta_{N,9}$ = $\sum\Delta\delta_N$ = 0.2104 + 0.04454 = 0.2549 m
Result from iterations:
$\boldsymbol{\delta_N}$ = 0.2549 m **=** $\boldsymbol{\delta_\tau}$ = 0.2549 m**,** i.e. Equation 4:5 is satisfied.

Results from integration Step 9:

x_8 = 92.10 m	τ_o = 20.8 kN/m^2			
x_9 = 97.08 m	$\tau_x(x_8)$ = 20.8 kN/m^2	N (x_8) = 221.9 kN/m	δ (x_8) = 0.2104 m
	$\tau_x(x_9)$ = 15.0 kN/m^2	N (x_9) = 207.5 kN/m	δ (x_9) = 0.2549 m

I.25 Calculation of $\boldsymbol{\delta_{instab}}$ and $\mathbf{L_{instab}}$ (cf Figures 4:2.4a and 7:4.1)

Having determined the value of the triggering load (N_{cr}), the analysis of progressive slope failure initiation was completed.
Nevertheless, for further information the iterative procedure in Steps 6 to 9 may be continued until the value of N is equal to zero. This means finding the situation, in which a forced deformation (δ_{instab}) would trigger slope failure, even if the agent causing the deformation would be removed instantly.

Step 10:

From this point and on Equations I:5b and I:5c apply.
However, the following data being known L_{instab} and δ_{instab} can, in the current case, be evaluated directly from the results of Step 9.
The values from Step 9 are:
x_9 = 97.08 m $\tau_x(x_9)$ = c_R = 15.0 kN/m^2 N(x_9) = 207.5 kN/m   δ (x_8) = 0.2549 m
Hence:
$\Delta x_{9\text{-}10}$ = $N_{cr}/(\tau_{0\,(x9)} - c_R)$ = 207.5/(20.8-15) = 35.77 m
$\boldsymbol{\delta_{instab}}$ = δ_9 +(N_9 – 0)·$\Delta x_{9\text{-}10}$/2/(E_{el}H) = 0.2549 + (207.5+ 0)/2·35.77/1200/20 =
= 0. 2549 + 0.1546 = **0.410** m
$\mathbf{L_{instab}}$ = $x_8 + \Delta x_{8\text{-}9}$ = 97.08 + 35.77 = **132.9** m

General comment:

As mentioned, the integration steps 1 to 10 can be carried out using the Excel spread sheet in Bernander, (2008). Once slope input data have been inserted into the software, the time

required to performing the calculations demonstrated in Sections I.2 and I.3 is a matter of 15 to 20 minutes for an experienced engineer.

It may be noted that also when the slope properties are of an *arbitrary* nature, the parameters $\mathbf{N_{cr}}$, $\mathbf{\delta_{cr}}$, $\mathbf{L_{cr}}$, $\mathbf{\delta_{instab}}$ and $\mathbf{L_{instab}}$ can be evaluated by the Excel spread sheet.

Yet, for slopes with complex geometry, the much faster to use computer software in Windows C++, referred to in Section 4.53, is recommended.

I.3 Calculation of the configuration and final spread of a landslide

The Excel spread sheet, partly applied in Appendix I, is well suited for evaluating the configuration and final spread of progressive landslides over level ground.

Estimating the conceivable *degree* of ultimate comprehensive failure that may result from an up-slope failure – due to a locally applied additional load – is then a matter of about half an hour.

A detailed exemplification of the interesting characteristics of progressive landslide spread over level ground in sensitive clays is given in Bernander (2008), Section 5, (pp 31 → 36) and Appendix A, pp (53 → 63). A few pages exemplifying the spreadsheet procedure is given at the end of this Appendix.

Downhill progressive slide - triggering load

Case, Appendix I - Slope 1:15,337, arctan 0,0652 = 3,73 dgr

C_R = 15 kN/m2 t_0 = 20.8 kN/m2

Author: Stig Bernander

11 05 15 Page 9

Step	x	tel	t	N	S:a dn		x	y	H+y	Gradient		
	m	kN/m2	kN/m2	kN/m	m		m			Gr		
0	0,00	**16,00**	**20,80**	0	0,000	**$t = t_0$**	0,00	0,00000	20,000	0,01	**Equ. I:4a**	**Stage I**
1	33,13		21,30	8,3	0,006		33,13	0,33130	20,331	0,01	"	
2	49,88		22,30	25,0	0,017		49,88	0,49880	20,499	0,01	"	
3	63,80		24,30	59,8	0,042		63,80	0,63800	20,638	0,01	"	
4	76,95		27,80	128,9	0,094		76,95	0,76950	20,770	0,01	"	
5	84,27		30,00	188,1	0,142		84,27	0,84265	20,843	0,01	"	
6	84,27		30,00	188,1	0,142		84,27	0,84265	20,843	0,01	"	
7	**84,27**		**30,00**	**188,1**	0,142	**$t = c_{peak}$**	84,27	0,84265	20,843	0,01	**$t < c_{peak}$**	"
8	88,04		25,00	213,4	0,174		88,04	0,88040	20,880	0,01	**Equ. I:5a**	**Stage IIa**
9	90,47		22,50	220,5	0,195		90,47	0,90467	20,905	0,01	"	
11	**92,08 L_{cr}**		**20,80**	**221,9**	**0,210**	**N_{cr}**	92,08	0,92085	20,921	0,01	"	
12	97,06		15,00	207,4	0,255	$t_0 = C_{R(x)}$	97,06	0,97065	20,971	0,01	"	
13	**132,80 L_{instab}**		**15,00**	**0,0**	**0,409**	**L_{instab}**	132,80	1,32805	21,328	0,01	**Equ. I:5c**	**Stage IIb**
14	143,20		15,00	-60,4	0,396		143,20	1,43205	21,432	0,01	"	
15	148,54		15,00	-91,3	0,379		148,54	1,48545	21,485	0,01	"	
16	188,54		15,00	-323,5	0,034		188,54	1,88545	21,885	0,01	"	
17	276,59		15,00	-834,6	-2,091		276,59	2,76595	22,766	0,01	"	
18	447,18		15,00	-1824,7	-11,541		447,18	4,47185	24,472	0,01	"	

q_{crit} 11,10 kN/m2

Figure I:2.3 Results of the analysis

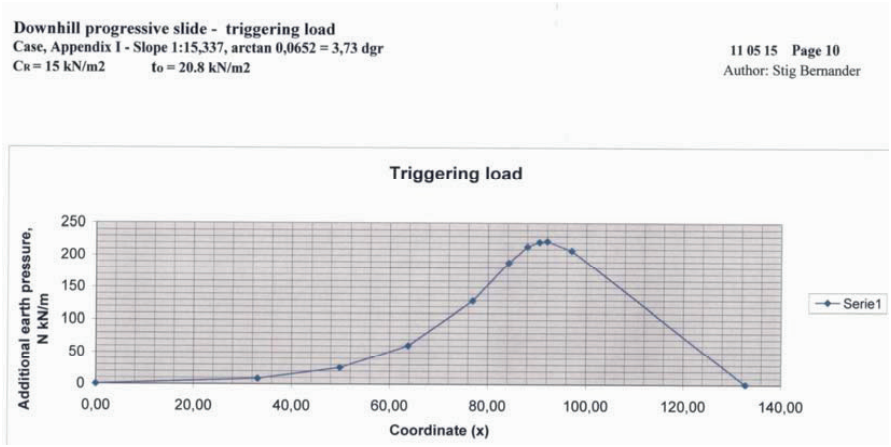

Figure I:2.4 Additional load N(x)

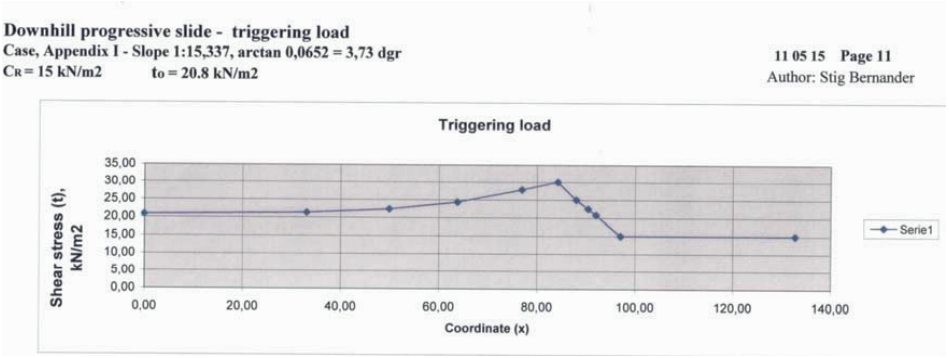

Figure I:2.5 Shear stresses t(x) or τ(x)

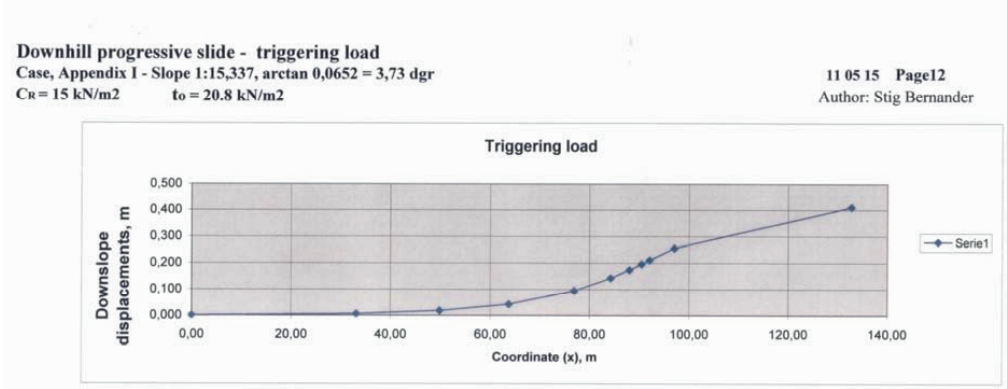

Figure I:2.6 Displacements

Downhill progressive slide - triggering load, basic ex. **Author: Stig Bernander** **OK** **Page 1**

Case, Appendix I - Slope 1:15,337, arctan 0,0652 = 3,73 dgr **11 05 15** Arketyp

C_R = 15 kN/m2

Input data:

H = 20 m **Gradient = tan Gr = 1:15,337** , **Gr** = arc tan 0,0652 = 3,73 Dgr

Density = 16,0 kN/m3 **(Residual shear strength)** **(Surface strength)** **(Mean shear strength)**

C_{peak} = 30 kN/m2 C_{lab} = 25 kN/m2 C_R = 15 kN/m2 C_R/C_{lab} = 0,60 C_s = 15 kN/m2 C_{mean} = 22,5 kN/m2

Shear deformation at failure (g_f) = 3 % C_R/C_{peak} = 0,50 τ_{el} = 20 kN/m2

Post-peak deformation at C_R = 0,30 m Shear deform. at elastic limit (g_{el}) = 3.75 %

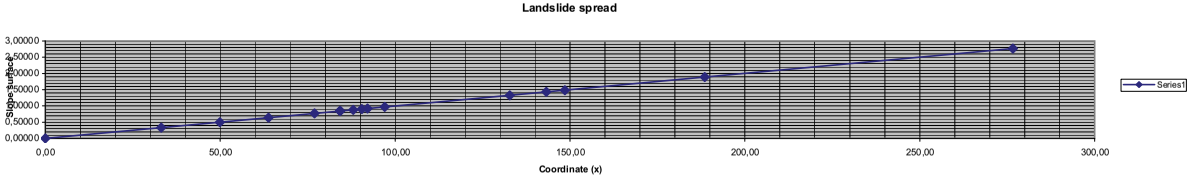

$\tau_{x,z} < \tau_{el}$			
$g_{x,z(1)} = \tau_x/G$, $g_{el} = g_f{*}\tau_{el}/(2c - \tau_{el})$ and $G = \tau_{el}/g_{el}$	**Stage I**	**Equ. I:1a**	**S:a $d_{(x,z),t}$ = Integral ($g_{x,z,(1)}$)dz**
$\tau_o < \tau_{xz} < c$, $\tau_o > \tau_{el}$	$\tau_o < \tau_{xz} < c$	$\tau_o > \tau_{el}$	
$g_{x,z(4)} = (g_f\text{-}g_{el}){*}(1 - ROT(1 - (\tau_{o(x,z)} - \tau_{el})/(c - \tau_{el}))$	**Stage I**	**Equ. I:4**	**S:a $d_{(x,z),t}$ = Integral ($g_{x,z,(4)}$)dz**
$\tau_o < \tau_{el}$ $- ROT(1 - (\tau_{(x,z)} - \tau_{el})/(c - \tau_{el})))$		$\tau_o < \tau_{el}$	
$g_{x,z(4a)} = (\tau_{el} - \tau_{o,(x,z)})/G + (g_f\text{-}g_{el}){*}(1 - ROT(1 - (\tau_{(x,z)} - \tau_{el})/(c - \tau_{el})))$		**Equ. I:4a**	**S:a $d_{(x,z),t}$ = Integral ($g_{x,z,(4a)}$)dz**
$c < \tau_{xz} < c_R$, $\tau_o > \tau_{el}$	$c < \tau_{xz} < c_R$	$\tau_o > \tau_{el}$	$\tau_{xz} > c_R$
$g_{x,z(5)} = (g_f\text{-}g_{el}){*}(ROT(1 - (\tau_{o(x,z)} - \tau_{el})/(c - \tau_{el})) -$	**Stage II**	**Equ. I:5**	**S:a $d_{(x,z),t}$ = Integral ($g_{x,z,(5)}$)dz +**
$\tau_o < \tau_{el}$ $- ROT(1 - (\tau_{(x,z,max)} - \tau_{el})/(c - \tau_{el}))) - (\tau_{(x,z,max)} - \tau_{(x,z)})/G$		$\tau_o < \tau_{el}$	$\tau_{xz} < c_R$ **$+S_{cR}(c - \tau_{x,z})/(c - c_R)$**
$g_{x,z(5a)} = (\tau_{el} - \tau_{o,(x,z)})/G + (g_f\text{-}g_{el})(1 - ROT(1 - (\tau_{(x,z,max)} - \tau_{el})/(c - \tau_{el})))$ -	**Stage IIa**	**Equ. I:5a**	**S:a $d_{(x,z),t}$ = Integral ($g_{x,z,(5a)}$)dz +**
$\tau_{x,o} = c_R$ $- (\tau_{(x,z,max)} - \tau_{(x,z)})/G$	$\tau_{x,o} = c_R$		**$+S_{cR}(c - \tau_{x,z})/(c - c_R)$**
$g_{x,z(5b)} = g_{x,z(5)}$ (or $g_{x,z(5a)}$) $- (\tau_{(x,z,max)} - c_R)/G$	**Stage IIb**	**Equ. I:5c**	**S:a $d_{(x,z),t}$ = Integral ($g_{x,z,(5c)}$)dz+S_{cR}+Sslip**

Downhill progressive slide - triggering load **Stage I** (1) **11 05 15** **Page 2**

				Density	c(s)=	g el =	Gradient	G mod.	c (peak)	E-mean	t el =	H =	Width, b	2
Iter.		g f =	0,075	16,000	**15**	0,0375	0,0652	533	**30,00**	1200	**20,00**	20,0	dx (m)	**33,130**
step	**No 1**	**xo**	x1	**0,00**	**Stress**	**x1**	**Mean**		kN/m2		kN/m2		**x1**	**33,13**
n	**z (n)**	**In situ***	**In situ***	**Shear**	**incre-**	**Shear**	**shear**	**gf - gel**	cu-t el	t el	**d(g)**	**d(g)*dz**	**cu**	**G**
	(m)	**shear**	**shear**	**stress**	**ment**	**stress**	**stress**	kN/m2	kN/m2	kN/m2	1	m	kN/m2	
20			to(x,z)	t(x,z)	dt(x,z)	t(x,z)+dt		0,0375	10,00		**Equ.I:4**			
0	0,00	20,80	**20,80**	**20,80**	**0,500**	**21,304**	21,054	0,0375	10,00	**20,00**	0,00099		30,00	533
								0,0375				0,00096		
1	1,00	19,76	**19,76**	19,76	0,475	20,239	20,001	0,0375	9,75	**19,50**	0,00094		29,25	520
								0,0375			**Equ.I:4a**	0,00091		
2	2,00	18,72	**18,72**	18,72	0,450	19,174	18,949	0,0375	9,50	**19,00**	0,00089		28,50	507
								0,0375			**Equ.I:1a**	0,00088		
3	3,00	17,68	**17,68**	17,68	0,425	18,108	17,896	0,0375	9,25	**18,50**	0,00086		27,75	493
								0,0375				0,00085		
4	4,00	16,64	**16,64**	16,64	0,400	17,043	16,843	0,0375	9,00	**18,00**	0,00083		27,00	480
								0,0375				0,00082		
5	5,00	15,60	**15,60**	15,60	0,375	15,978	15,790	0,0375	8,75	**17,50**	0,00080		26,25	467
								0,0375				0,00079		
6	6,00	14,56	**14,56**	14,56	0,350	14,913	14,738	0,0375	8,50	**17,00**	0,00077		25,50	453
								0,0375				0,00051		
6,67	6,67	13,87	**13,87**	13,87	0,333	14,199	14,032	0,0375	8,33	**16,67**	0,00075		25,00	444
	20,00								5,00	10			15,00	

Author: Stig Bernander		Scr	0,30	cR=	15,000
	Calc.	S(x)		cR/c(peak)	0,50
				dN	8,28
	Calc.			d(xn,n+1),N	0,00572
				dx,N-dx(t)	**0,00000**

S:a N x(n)	0,00		S:a d(xn),t	0,00572	
S:a d(xn),N	0,0000		S(x)=		m
S:a Nx(n+1)	**8,28**	Slip	d(slip) =	0,00000	m
S:a dx(n+1),N	**0,00572**		S:a dx(n+1),t	**0,00572**	m

* In situ shear stress to be modified by the expression dt =(E(n+1) -E(n))/dx (E(n+1) and E(n) are in situ earth pressures)

Downhill progressive slide - triggering load **Stage I** (7) **11 05 15** **Page 8**

				Density	c(s)=	g el =	Gradient	G mod.	c (peak)	E-mean	t el =	H =	Width, b	1,0
Iter.		g f =	0,075	16,000	**15**	0,0375	0,0652	533	**30,00**	1200	**20,00**	20,0	dx (m)	**0,000**
step	**No 7**	**x6**	x7	**84,27**	**Stress**	**x7**	**Mean**		kN/m2		kN/m2		**x7**	**84,27**
n	**z (n)**	**In situ**	**In situ**	**Shear**	**incre-**	**Shear**	**shear**	**gf - gel**	**cu-t el**	**t el**	**d(g)**	**d(g)*dz**	**c**	**G**
	(m)	**shear**	**shear**	**stress**	**ment**	**stress**	**stress**	kN/m2	kN/m2	kN/m2	1	m	kN/m2	
20		$\tau_{o(x,z)}$	$\tau_{o(x,z)+dt}$	$\tau_{(x,z)}$	$d\tau_{(x,z)}$	$\tau_{(x,z)+dt}$		0,0375			**Equ.I:4a**			
0	0,00	20,80	**20,80**	**30,00**	**0,000**	**30,000**	30,000	0,0375	10,00	**20,00**	0,03587		30,00	533
								0,0375				0,03123		
1	1,00	19,76	19,76	28,50	0,000	**28,500**	28,500	0,0375	9,75	**19,50**	0,02659		29,25	520
								0,0375				0,02487		
2	2,00	18,72	18,72	27,00	0,000	**27,000**	27,000	0,0375	9,50	**19,00**	0,02314		28,50	507
								0,0375				0,02190		
3	3,00	17,68	17,68	25,50	0,000	**25,500**	25,500	0,0375	9,25	**18,50**	0,02066		27,75	493
								0,0375				0,01967		
4	4,00	16,64	16,64	24,00	0,000	**24,000**	24,000	0,0375	9,00	**18,00**	0,01868		27,00	480
								0,0375				0,01785		
5	5,00	15,60	15,60	22,50	0,000	**22,500**	22,500	0,0375	8,75	**17,50**	0,01702		26,25	467
								0,0375				0,01630		
6	6,00	14,56	14,56	21,00	0,000	**21,000**	21,000	0,0375	8,50	**17,00**	0,01559		25,50	453
								0,0375				0,01016		
6,67	6,67	13,87	13,87	19,99	0,000	**19,995**	19,995	0,0375	8,33	**16,67**	0,01474		25,00	444

Author: Stig Bernander	S_{CR}	0,30	c_R=	15,000	m
Calc.	S(x)		$c_{R/C(peak)}$	0,50	
			dN	0,00	
Calc.			$d_{(xn,n+1),N}$	0,00000	
			dx,N-dx(t)	**-0,00002**	

S:a N x(n)	188,11		S:a d(xn),t	**0,14198**	
S:a d(xn),N	0,14196		S(x)=		m
S:a Nx(n+1)	**188,11**	Slip	d(slip) =		m
S:a dx(n+1),N	**0,14196**		S:a dx(n+1),t	**0,14198**	m

Progressive failure - Triggering load **Stage II** **11 05 15** **Page 1**

				Density	c(s)=	g el =	Gradient	G mod.	c(peak)	E-mean	t el =	H =	Width, b	1,0	
Iter.		g f =	0,075	16,000	**15,00**	0,0375	0,0652	533	**30,00**	1200	**20,00**	20,0	dx (m)	3,775	3,775
step	**No 8**	**x7**	x8	**84,27**	**Stress**		**Mean**		kN/m2		kN/m2		**x8**	**88,04**	
n	**z (n)**	**In situ**	**In situ**	**Shear**	**incre-**	**Shear**	**shear**	**gf - gel**	**cu-t el**	**t el**	**d(g)**	**d(g)*dz**	**c**		**G**
	(m)	**shear**	**shear**	**stress**	**ment**	**stress**	**stress**	kN/m2	kN/m2	kN/m2	**Equ.I:5**	m	kN/m2		
		to(x,z)	to(x,z)+dt	t(x,z)	dt(x,z)	t(x,z)+dt		0,0375	10,00					t(x,z),peak	
0	0,00	20,80	20,80	**30,00**	**-5,000**	**25,000**	27,500	0,0375	10,00	20,00	0,02646		30	30,00	533
								0,0375	10,00			0,02124			
1	1,00	19,76	19,76	28,50	-4,750	23,750	26,125	0,0375	10,00	19,50	0,01601		29,25	28,50	520
								0,0375	10,00		**Equ.I:5a**	0,01420			
2	2,00	18,72	18,72	27,00	-4,500	22,500	24,750	0,0375	10,00	19,00	0,01239		28,50	27,00	507
								0,0375	10,00			0,01120			
3	3,00	17,68	17,68	25,50	-4,250	21,250	23,375	0,0375	10,00	18,50	0,01000		27,75	25,50	493
								0,0375	10,00			0,00914			
4	4,00	16,64	16,64	24,00	-4,000	20,000	22,000	0,0375	10,00	18,00	0,00828		27,00	24,00	480
								0,0375	10,00			0,00764			
5	5,00	15,60	15,60	22,50	-3,750	18,750	20,625	0,0375	10,00	17,50	0,00701		26,25	22,50	467
								0,0375	10,00			0,00656			
6	6,00	14,56	14,56	21,00	-3,500	17,500	19,250	0,0375	10,00	17,00	0,00611		25,50	21,00	453
								0,0375	10,00			0,00355			
7	6,60	13,52	13,94	20,10	-3,350	16,750	18,425	0,0375	10,00	16,70	0,00571		25,05	20,10	445

Author: Stig Bernander	S(cR)	0,30	cR	**15,00**	m
Calc.	S(x)	**0,1000**	cR/C(peak)	0,500	
			dN	25,28	
Calc.			d(xn,n+1),N	0,03158	
			dx,N-dx(t)	**0,00001**	

S:a N x(n)	188,11		S:a d(xn),t	**0,07352**	
S:a d(xn),N	0,14196		S(x)=	**0,10000**	m
S:a Nx(n+1)	**213,39**	Slip	d(slip) =		m
S:a dx(n+1),N	**0,17353**		S:a dx(n+1),t	**0,17353**	m

Progressive failure - Triggering load **Stage II** **11 05 15** **Page 2** Author: Stig B

				Density	c(s)=	g el =	Gradient	G mod.	c(peak)	E-mean	t el =	H =	Width, b	1,0	
Iter.		g f =	0,075	16,000	**15,00**	0,0375	0,0652	533	**30,00**	1200	**20,00**	20,0	dx (m)	2,427	
step	**No 9**	**x8**	x9	**88,04**	**Stress**		**Mean**		kN/m2		kN/m2		**x9**	**90,47**	
n	**z (n)**	**In situ**	**In situ**	**Shear**	**incre-**	**Shear**	**shear**	**gf - gel**	**cu-t el**	**t el**	**d(g)**	**d(g)*dz**	**c**		**G**
	(m)	**shear**	**shear**	**stress**	**ment**	**stress**	**stress**	kN/m2	kN/m2	kN/m2	**Equ.I:5**	m	kN/m2		
		to(x,z)	to(x,z)+dt	t(x,z)	dt(x,z)	t(x,z)+dt		0,0375	10,00					t(x,z),peak	
0	0,00	20,80	20,80	**25,00**	**-2,500**	**22,500**	23,750	0,0375	10,00	20,00	0,02178		30	30,00	533
								0,0375	10,00			0,01661			
1	1,00	19,76	19,76	23,75	-2,375	21,375	22,562	0,0375	10,00	19,50	0,01144		29,25	28,50	520
								0,0375	10,00		**Equ.I:5a**	0,00970			
2	2,00	18,72	18,72	22,50	-2,250	20,250	21,375	0,0375	10,00	19,00	0,00795		28,50	27,00	507
								0,0375	10,00			0,00682			
3	3,00	17,68	17,68	21,25	-2,125	19,125	20,187	0,0375	10,00	18,50	0,00569		27,75	25,50	493
								0,0375	10,00			0,00490			
4	4,00	16,64	16,64	20,00	-2,000	18,000	19,000	0,0375	10,00	18,00	0,00411		27,00	24,00	480
								0,0375	10,00			0,00355			
5	5,00	15,60	15,60	18,75	-1,875	16,875	17,812	0,0375	10,00	17,50	0,00299		26,25	22,50	467
								0,0375	10,00			0,00262			
6	6,00	14,56	14,56	17,50	-1,750	15,750	16,625	0,0375	10,00	17,00	0,00225		25,50	21,00	453
								0,0375	10,00			0,00126			
7	6,60	13,52	13,94	16,75	-1,675	15,075	15,912	0,0375	10,00	16,70	0,00195		25,05	20,10	445

Author: Stig Bernander	S(cR)	0,30	cR	**15,00**
Calc.	S(x)	**0,1500**	cR/c(peak)	0,500
			dN	7,15
Calc.			d(xn,n+1),N	0,02194
			dx,N-dx(t)	**0,00000**

S:a N x(n)	213,39		S:a d(xn),t	**0,04546**	
S:a d(xn),N	0,17353		S(x)=	**0,15000**	m
S:a Nx(n+1)	**220,53**	Slip	d(slip) =		m
S:a dx(n+1),N	**0,19547**		S:a dx(n+1),t	**0,19547**	m

Progressive failure - Triggering load **Stage II** **11 05 15** **Page 3** Author: Stig B

				Density	c(s)=	g el =	Gradient	G mod.	c(peak)	E-mean	t el =	H =	Width, b	1,0
Iter.		g f =	0,075	16,000	**15,00**	0,0375	0,0652	533	**30,00**	1200	**20,00**	20,0	dx (m)	1,618
step	**No 10**	**x9**	x10	**90,47**	**Stress**		**Mean**		kN/m2		kN/m2		**x10**	**92,08**

n	**z (n)**	**In situ**	**In situ**	**Shear**	**incre-**	**Shear**	**shear**	**gf - gel**	**cu-t el**	**t el**	**d(g)**	**d(g)*dz**	**c**		**G**
	(m)	**shear**	**shear**	**stress**	**ment**	**stress**	**stress**	kN/m2	kN/m2	kN/m2	**Equ.I:5**	m	kN/m2		
		$\tau_{o(x,z)}$	$\tau_{o(x,z)+dt}$	$\tau_{(x,z)}$	$d\tau_{(x,z)}$	$\tau_{(x,z)+dt}$		0,0375	10,00					$\tau_{(x,z),peak}$	
0	0,00	20,80	20,80	**22,50**	**-1,700**	**20,800**	21,650	0,0375	10,00	20,00	0,01859		30	30,00	533
								0,0375	10,00			0,01346			
1	1,00	19,76	19,76	21,37	-1,615	19,760	20,567	0,0375	10,00	19,50	0,00834		29,25	28,50	520
								0,0375	10,00		**Equ.I:5a**	0,00663			
2	2,00	18,72	18,72	20,25	-1,530	18,720	19,485	0,0375	10,00	19,00	0,00493		28,50	27,00	507
								0,0375	10,00			0,00385			
3	3,00	17,68	17,68	19,12	-1,445	17,680	18,402	0,0375	10,00	18,50	0,00276		27,75	25,50	493
								0,0375	10,00			0,00202			
4	4,00	16,64	16,64	18,00	-1,360	16,640	17,320	0,0375	10,00	18,00	0,00128		27,00	24,00	480
								0,0375	10,00			0,00077			
5	5,00	15,60	15,60	16,87	-1,275	15,600	16,237	0,0375	10,00	17,50	0,00026		26,25	22,50	467
								0,0375	10,00			-0,00006			
6	6,00	14,56	14,56	15,75	-1,190	14,560	15,155	0,0375	10,00	17,00	-0,00038		25,50	21,00	453
								0,0375	10,00			-0,00029			
7	6,60	13,52	13,94	15,07	-1,139	13,936	14,505	0,0375	10,00	16,70	-0,00061		25,05	20,10	445

Author: Stig Bernander	S(cR)	0,30	cR	**15,00**
Calc.	S(x)	**0,1840**	cR/c(peak)	0,500
			dN	1,37
Calc.			$d_{(xn,n+1),N}$	0,01491
			dx,N-dx(t)	**0,0000**

	N crit				
S:a N x(n)	220,53		S:a d(xn),t	**0,02638**	m
S:a d(xn),N	0,1955		S(x)=	**0,18400**	m
S:a Nx(n+1)	**221,90**	Slip	d(slip) =		m
S:a dx(n+1),N	**0,21038**		S:a dx(n+1),t	**0,21038**	m

Progressive failure - Triggering load **Stage II** **11 05 15** **Page 4** Author: Stig B

				Density	c(s)=	g el =	Gradient	G mod.	c(peak)	E-mean	t el =	H =	Width, b	1,0
Iter.		g f =	0,075	16,000	**15,00**	0,0375	0,0652	533	**30,00**	1200	**20,00**	20,0	dx (m)	4,980
step	**No 11**	**x10**	x11	**92,08**	**Stress**		**Mean**		kN/m2		kN/m2		**x11**	**97,06**

n	**z (n)**	**In situ**	**In situ**	**Shear**	**incre-**	**Shear**	**shear**	**gf - gel**	**cu-t el**	**t el**	**d(g)**	**d(g)*dz**	**cu**		**G**
	(m)	**shear**	**shear**	**stress**	**ment**	**stress**	**stress**	kN/m2	kN/m2	kN/m2	**Equ.I:5**	m	kN/m2		
		$\tau_{o(x,z)}$	$\tau_{o(x,z)+dt}$	$\tau_{(x,z)}$	$d\tau_{(x,z)}$	$\tau_{(x,z)+dt}$		0,0375	10,00					$\tau_{(x,z),peak}$	
0	0,00	20,80	20,80	**20,80**	**-5,800**	**15,000**	17,900	0,0375	10,00	20,00	0,00771		30	30,00	533
								0,0375	10,00			0,00273			
1	1,00	19,76	19,76	19,76	-5,510	14,250	17,005	0,0375	10,00	19,50	-0,00226		29,25	28,50	520
								0,0375	10,00		**Equ.I:5a**	-0,00382			
2	2,00	18,72	18,72	18,72	-5,220	13,500	16,110	0,0375	10,00	19,00	-0,00537		28,50	27,00	507
								0,0375	10,00			-0,00630			
3	3,00	17,68	17,68	17,68	-4,930	12,750	15,215	0,0375	10,00	18,50	-0,00723		27,75	25,50	493
								0,0375	10,00			-0,00781			
4	4,00	16,64	16,64	16,64	-4,640	12,000	14,320	0,0375	10,00	18,00	-0,00839		27,00	24,00	480
								0,0375	10,00			-0,00872			
5	5,00	15,60	15,60	15,60	-4,350	11,250	13,425	0,0375	10,00	17,50	-0,00906		26,25	22,50	467
								0,0375	10,00			-0,00920			
6	6,00	14,56	14,56	14,56	-4,060	10,500	12,530	0,0375	10,00	17,00	-0,00933		25,50	21,00	453
								0,0375	10,00			-0,00560			
7	6,60	13,52	13,94	13,94	-3,886	10,050	11,993	0,0375	10,00	16,70	-0,00933		25,05	20,10	445

Author: Stig Bernander		$S(c_R)$	0,30	c_R	**15,00**
	Calc.	S(x)	**0,3000**	$c_R/c_{(peak)}$	0,500
				dN	-14,46
	Calc.			$d_{(x_n,n+1),N}$	0,04454
				dN-d(tau)	**0,0000**

$t = c_R$

S:a N $x_{(n)}$	221,90		S:a $d_{(x_n),t}$	**-0,03872**	m	**q_{crit}**
S:a $d_{(x_n),N}$	0,2104		S(x)=	**0,3000**	m	kN/m
S:a $N_{x(n+1)}$	**207,44**	Slip	d(slip) =	**-0,0064**	m	**10,37**
S:a $dx_{(n+1),N}$	**0,2549**		S:a $dx_{(n+1),t}$	**0,2549**	m	

Progressive failure - Triggering load

Stage II | **11 05 15** | **Page 5** | Author: Stig E

				Density	c(s)=	g el =	Gradient	G mod.	c(peak)	E-mean	t el =	H =	Width, b	1,0	
Iter.		g f =	0,075	16,000	**15,00**	0,0375	0,0652	533	**30,00**	1200	**20,00**	20,0	dx (m)	35,740	
step	**No 12**	x11	x12	**97,06**	**Stress**		**Mean**		kN/m2		kN/m2		**x12**	**132,80**	
n	**z (n)**	**In situ**	**In situ**	**Shear**	**incre-**	**Shear**	**shear**	**gf - gel**	**cu-t el**	**t el**	**d(g)**	**d(g)*dz**	**c**	**g (x=n)**	**G**
	(m)	**shear**	**shear**	**stress**	**ment**	**stress**	**stress**	kN/m2	kN/m2	kN/m2	**Equ.I:5**	m	kN/m2		
		to(x,z)	to(x,z)+dt	t(x,z)	dt(x,z)	t(x,z)+dt		0,0375	10,00					t(x,z),peak	
0	0,00	20,80	**20,80**	**15,00**	**0,000**	**15,000**	15,000	0,0375	10,00	20,00	0,00771		30	30,00	533
								0,0375	10,00			0,00273			
1	1,00	19,76	19,76	14,25	0,000	14,250	14,250	0,0375	10,00	19,50	-0,00226		29,25	28,50	520
								0,0375	10,00		**Equ.I:5a**	-0,00382			
2	2,00	18,72	18,72	13,50	0,000	13,500	13,500	0,0375	10,00	19,00	-0,00537		28,50	27,00	507
								0,0375	10,00			-0,00630			
3	3,00	17,68	17,68	12,75	0,000	12,750	12,750	0,0375	10,00	18,50	-0,00723		27,75	25,50	493
								0,0375	10,00			-0,00781			
4	4,00	16,64	16,64	12,00	0,000	12,000	12,000	0,0375	10,00	18,00	-0,00839		27,00	24,00	480
								0,0375	10,00			-0,00872			
5	5,00	15,60	15,60	11,25	0,000	11,250	11,250	0,0375	10,00	17,50	-0,00906		26,25	22,50	467
								0,0375	10,00			-0,00920			
6	6,00	14,56	14,56	10,50	0,000	10,500	10,500	0,0375	10,00	17,00	-0,00933		25,50	21,00	453
								0,0375	10,00			-0,00560			
7	6,60	13,52	13,94	10,05	0,000	10,050	10,050	0,0375	10,00	16,70	-0,00933		25,05	20,10	445

Author: Stig Bernander		S(cR)	0,30	cR	**15,00**
	Calc.	S(x)	**0,3000**	cR/c(peak)	0,500
				dN	-207,43
	Calc.			d(xn,n+1),N	0,15446
				dx,N-dx(t)	**0,0000**

		Instab				
S:a N x(n)	207,44		S:a d(xn),t	**-0,03872**	m
S:a d(xn),N	0,2549		S(x)=	**0,3000**	m
S:a Nx(n+1)	**0,0**	Slip	d(slip) =	**0,1481**	m
S:a dx(n+1),N	**0,4094**		S:a dx(n+1),t	**0,4094**	m

Progressive failure - Triggering load **Stage II** **11-04-01** **Page 6** Author: Stig B

				Density	c(s)=	g el =	Gradient	E-mod/cu	c(peak)	E-mean	t el =	H =	Width, b	1,0
Iter.		g f =	0,075	16,000	**15,00**	0,0375	0,0652	533	**30,00**	1200	**20,00**	20,0	dx (m)	10,400
step	**No 13**	**x12**	x13	**132,80**	**Stress**		**Mean**		kN/m2		kN/m2		**x13**	**143,20**

n	**z (n)**	**In situ**	**In situ**	**Shear**	**incre-**	**Shear**	**shear**	**gf - gel**	**cu-t el**	**t el**	**d(g)**	**d(g)*dz**	**c**	**g (x=n)**	**G**
	(m)	**shear**	**shear**	**stress**	**ment**	**stress**	**stress**	kN/m2	kN/m2	kN/m2	**Equ.I:5b**	m	kN/m2		
		$\tau_{o(x,z)}$	$\tau_{o(x,z)+dt}$	$\tau_{(x,z)}$	$d\tau_{(x,z)}$	$\tau_{(x,z)+dt}$		0,0375	10,00					$\tau_{(x,z),peak}$	
0	0,00	20,80	20,80	**15,00**	**0,000**	**15,000**	15,000	0,0375	10,00	20,00	0,00771		30	30,00	533
								0,0375	10,00			0,00273			
1	1,00	19,76	19,76	14,25	0,000	14,250	14,250	0,0375	10,00	19,50	-0,00226		29,25	28,50	520
								0,0375	10,00		**Equ.I:5a**	-0,00382			
2	2,00	18,72	18,72	13,50	0,000	13,500	13,500	0,0375	10,00	19,00	-0,00537		28,50	27,00	507
								0,0375	10,00			-0,00630			
3	3,00	17,68	17,68	12,75	0,000	12,750	12,750	0,0375	10,00	18,50	-0,00723		27,75	25,50	493
								0,0375	10,00			-0,00781			
4	4,00	16,64	16,64	12,00	0,000	12,000	12,000	0,0375	10,00	18,00	-0,00839		27,00	24,00	480
								0,0375	10,00			-0,00872			
5	5,00	15,60	15,60	11,25	0,000	11,250	11,250	0,0375	10,00	17,50	-0,00906		26,25	22,50	467
								0,0375	10,00			-0,00920			
6	6,00	14,56	14,56	10,50	0,000	10,500	10,500	0,0375	10,00	17,00	-0,00933		25,50	21,00	453
								0,0375	10,00			-0,00560			
7	6,60	13,52	13,94	10,05	0,000	10,050	10,050	0,0375	10,00	16,70	-0,00933		25,05	20,10	445

Author: Stig Bernander		S(cR)	0,30	cR	**15,00**
	Calc.	S(x)	**0,3000**	cR/c(peak)	0,500
				dN	-60,36
	Calc.			$d_{(xn,n+1),N}$	-0,01308
				dx,N-dx(t)	**0,0000**

t = cR

S:a N x(n)	0,01		S:a d(xn),t	**-0,03872**	
S:a d(xn),N	0,4094		S(x)=	**0,3000**	m
S:a Nx(n+1)	**-60,4**	Slip	d(slip) =	**0,1350**	m
S:a dx(n+1),N	**0,3963**		S:a dx(n+1),t	**0,3963**	m

Progressive failure - Triggering load

				Density	c(s)=	g el =	Gradient	E-mod/cu	c(peak)	E-mean	t el =	H =	Width, b	1,0
Iter.		g f =	0,075	16,000	**15,00**	0,0375	0,0652	533	**30,00**	1200	**20,00**	20,0	dx (m)	170,590
step	No 17	x16	x17	**276,59**	**Stress**		**Mean**		kN/m2		kN/m2		x17	**447,18**
n	**z (n)**	**In situ**	**In situ**	**Shear**	**incre-**	**Shear**	**shear**	**g_f - g_{el}**	**cu-t el**	**t el**	**d(g)**	**$d_{(g)}$*dz**	**c**	**g (x=n)**	**G**
	(m)	**shear**	**shear**	**stress**	**ment**	**stress**	**stress**	kN/m2	kN/m2	kN/m2	**Equ.I:5c**	m	kN/m2		
		$t_{o(x,z)}$	$t_{o(x,z)+dt}$	$t_{(x,z)}$	$dt_{(x,z)}$	$t_{(x,z)+dt}$		0,0375	10,00					$t_{(x,z),peak}$	
0	0,00	20,80	20,80	**15,00**	**0,000**	**15,000**	15,000	0,0375	10,00	20,00	0,00775		30	30,00	533
								0,0375	10,00			0,00274			
1	1,00	19,76	19,76	14,25	0,000	14,250	14,250	0,0375	10,00	19,50	-0,00227		29,25	28,50	520
								0,0375	10,00			-0,00382			
2	2,00	18,72	18,72	13,50	0,000	13,500	13,500	0,0375	10,00	19,00	-0,00537		28,50	27,00	507
								0,0375	10,00			-0,00630			
3	3,00	17,68	17,68	12,75	0,000	12,750	12,750	0,0375	10,00	18,50	-0,00723		27,75	25,50	493
								0,0375	10,00			-0,00781			
4	4,00	16,64	16,64	12,00	0,000	12,000	12,000	0,0375	10,00	18,00	-0,00839		27,00	24,00	480
								0,0375	10,00			-0,00872			
5	5,00	15,60	15,60	11,25	0,000	11,250	11,250	0,0375	10,00	17,50	-0,00906		26,25	22,50	467
								0,0375	10,00			-0,00920			
6	6,00	14,56	14,56	10,50	0,000	10,500	10,500	0,0375	10,00	17,00	-0,00933		25,50	21,00	453
								0,0375	10,00			-0,00560			
7	6,60	13,52	13,94	10,05	0,000	10,050	10,050	0,0375	10,00	16,70	-0,00933		25,05	20,10	445

		S(c_R)	0,30	c_R	15,00
	Calc.	S(x)	**0,3000**	c_R/c(peak)	0,500
				dN	-990,10
	Calc.			$d_{(xn,n+1),N}$	-9,45071

S:a N $x_{(n)}$	-834,55		S:a $d_{(xn),t}$	**-0,03871**	m
S:a $d_{(xn),N}$	-2,0906		S(x)=	**0,30000**	m
S:a $Nx_{(n+1)}$	**-1824,7**	Slip	d(slip) =	**-11,8026**	m
S:a $dx_{(n+1),N}$	**-11,5413**		S:a $dx_{(n+1),t}$	**-11,5413**	m

Doctoral and Licentiate Theses in Soil Mechanics and Foundation Engineering at Luleå University of Technology

Many of the theses can be downloaded from http://pure.ltu.se/portal/sv/publications/search.html

Doctoral Theses

Börgesson, Lennart (1981): *Mechanical properties of inorganic silt*. Doctoral Thesis 09D.

Carlsson, Torbjörn (1986*): Interactions in MX-80 bentonite/water/electrolyte systems.* Doctoral Thesis 55D.

Yu, Yao (1993): *Testing and modelling of silty and sulphide-rich soils.* Doctoral Thesis 121D.

Sheng, Daichao (1994): *Thermodynamics of freezing soils: theory and application.* Doctoral Thesis 141D.

Viklander, Peter (1997): *Compaction and thaw deformation of frozen soil: permeability and structural effects due to freezing and thawing.* Doctoral Thesis 1997:22.

Knutsson, Sven (1998): *Soil behavior at freezing and thawing.* Doctoral Thesis 1998:20.

Westerberg, Bo (1999): *Behaviour and modelling of a natural soft clay: triaxial testing, constitutive relations and finite element modelling.* Doctoral Thesis 1999:13.

Mattsson, Hans (1999): *On a mathematical basis for constitutive drivers in soil plasticity.* Doctoral Thesis 1999:02.

Mácsik, Josef (1999)*; Soil improvement based on environmental geotechnics: environmental and geotechnical aspects of drainage of redox-sensitive soils and stabilisation of soils with by-products*. Doctoral Thesis 1999:09.

Hermansson, Åke (2002): *Modeling of frost heave and surface temperatures in roads*. Doctoral Thesis 2002:13.

Edeskär, Tommy (2006): *Use of tyre shreds in civil engineering applications: technical and environmental properties.* Doctoral Thesis 2006:67.

Bernander, Stig (2011): *Progressive Landslides in Long Natural Slopes. Formation, Potential Extension and Configuration of Finished Slides in Strain-Softening Soils.* In collaboration with the Division of Structural Engineering. Doctoral Thesis. ISBN 978-91-7439-283-8

Licentiate Theses

Knutsson, Sven (1985): *Thermal properties of bentonite based barriers: theoretical considerations and laboratory tests with special reference to the Buffer Mass Test in Stripa mine,* Licentiate Thesis 1985:12.

Rydén, C. (1986): *Pore pressure in thawing soll,* Licentiate Thesis 1986:14.

Lindmark, P. (1989): *Jord- och vattenförorening vid avfallsupplag,* Licentiate Thesis 1989:03

Sheng, D. (1990): *Numerical modelling of frost and thaw penetration,* Licentiate Thesis 1990:03.

Johansson, L. (1990): *Geomechanical properties of tailings: a study of backfill materials for mines,* Licentiate Thesis 1990:16.

Eriksson, LG. (1992): *Sulfidjordars kompressionsegenskaper: inverkan av tid och temperatur : en laboratoriestudie,* Licentiate Thesis 1992:08.

Mácsik, J. (1994): *Risken för utfällning av ferriföreningar ur dräneringsvatten från anaeroba och aeroba sulfidjordar,* Licentiate Thesis 1994:10.iklander, P. (1994): *Frusen jords packnings- och deformationsegenskaper,* Licentiate Thesis 1994:25.

Westerberg, B. (1995): *Lerors mekaniska egenskaper: experimentell bestämning och kvalitativ modellering med tillämpning på lera från Norrköping,* Licentiate Thesis 1995:02.

Vikström, L. (1999): *Uppmätta och beräknade tjällyftningar och tjäldjup i jord: en analys av ingångsparametrarnas betydelse för beräkningsresultatet,* Licentiate Thesis 1999:63.

Bernander, S. (2000): Stig Bernander (2000): *Progressive Landslides in Long Natural Slopes. Formation, potential extension and configuration of finished slides in strain-softening soils*. Licentiate Thesis 2000:16. In collaboration with the Division of Structural Engineering

Hermansson, Å. (2000): *Frost modelling and pavement temperatures: summer pavement temperaures and frost modelling,* Licentiate Thesis 2000:18.

Pousette, K. (2001): *Stabilisering av torv: olika faktorers inverkan på stabiliseringseffekten,* Licentiate Thesis 2001:06.

Forsström, A. (2002): *Use of thermosyphons in a subarctic climate,* Licentiate Thesis 2002:24.

Svedberg, B. (2003): *Miljögeotekniskt bedömningssystem: applikation på väg- och järnvägsbyggnadsmaterial,* Licentiate Thesis 2003:46.

Edeskär, T. (2004): *Gummiklipp som konstruktionsmaterial i mark- och anläggningstekniska tillämpningar,* Licentiate Thesis 2004:39.

Rostmark, S. (2004): *Frysmuddringsteknik för sanering av förorenade sedimentområden,* Licentiate Thesis 2004:77.

Bjelkevik, A. (2005): *Stability of tailings dams: focus on water cover closure,* Licentiate Thesis 2005:85.

Johansson, K. (2005): *Planeringshjälpmedel för ökad tillgänglighet på grusvägnätet: en studie av datorverktyget HDM-4,* Licentiate Thesis 2005:42.

Åkerlund, H. (2005): *Dränerande sildammar för deponering av anrikningssand,* Licentiatsavhandling, Licentiate Thesis 2005:55.

Novikov, E. (2008): *The behaviour of mica-rich aggregates under the temperate climate conditions,* Licentiate Thesis 2008:25.

Kondelchuk, D. (2008): *Studies of the free mica properties and its influence on quality of road constructions,* Licentiate Thesis 2008:26.

Johansson, E. (2008): *Free mica in crushed rock aggregates,* Licentiate Thesis 2008:23.

Jantzer, I. (2009): *Critical hydraulic gradients in tailings dams: comparison to natural analogies,* Licentiate Thesis. ISBN 978-91-7439-055-1.

Berglund, A. (2010): *Prognos av vägars bärförmåga vid tjällossningen: användning av temperatur som nyckeltal,* Licentiatavhandling. ISBN 978-91-7439-187-9.

Zardari, M.A. (2011): *Stability of tailings dams: focus on numerical modelling,* Licentiate Thesis. ISBN 978-91-7439-245-6.

Jia, Q. (2011): *Dust from mining area and proposal of dust emission factors,* Licentiate Thesis. ISBN 978-91-7439-277-7.

Doctoral and Licentiate Theses in Structural Engineering at Luleå University of Technology

Many of the theses can be downloaded from http://pure.ltu.se/portal/sv/publications/search.html

Doctoral Theses

Ulf Arne Girhammar (1980): *Dynamic Fail-Safe Behaviour of Steel Structures.* Doctoral Thesis 06D.

Kent Gylltoft (1983): *Fracture Mechanics Models for Fatigue in concrete Structures*. Doctoral Thesis 25D.

Thomas Olofsson (1985): *Mathematical Modelling of Jointed Rock Masses*. In collaboration with the Division of Rock Mechanics. Doctoral Thesis 42D.

Lennart Fransson (1988): *Thermal ice pressure on structures in ice covers*. Doctoral Thesis 67D.

Mats Emborg (1989): *Thermal stresses in concrete structures at early ages*. Doctoral Thesis 73D.

Lars Stehn (1993): *Tensile fracture of ice. Test methods and fracture mechanics analysis*. Doctoral Thesis 129D.

Björn Täljsten (1994*): Plate Bonding. Strengthening of existing concrete structures with epoxy bonded plates of steel or fibre reinforced plastics*. Doctoral Thesis 152D.

Jan-Erik Jonasson (1994): *Modelling of temperature, moisture and stresses in young concrete*. Doctoral Thesis 153D.

Ulf Ohlsson (1995): *Fracture Mechanics Analysis of Concrete Structures*. Doctoral Thesis 179D.

Keivan Noghabai (1998): *Effect of Tension Softening on the Performance of Concrete Structures*. Doctoral Thesis 1998:21.

Gustaf Westman (1999): *Concrete Creep and Thermal Stresses. New creep models and their effects on stress development*. Doctoral Thesis 1999:10.

Henrik Gabrielsson (1999): *Ductility in High Performance Concrete Structures. An experimental investigation and a theoretical study of prestressed hollow core slabs and prestressed cylindrical pole elements*. Doctoral Thesis 1999:15.

Patrik Groth (2000): *Fibre Reinforced Concrete - Fracture Mechanics Methods Applied on Self-Compacting Concrete and Energetically Modified Binders*. Doctoral Thesis 2000:04.

Hans Hedlund (2000): *Hardening concrete. Measurements and evaluation of non-elastic deformation and associated restraint stresses*. Doctoral Thesis 2000:25.

Anders Carolin (2003): *Carbon Fibre Reinforced Polymers for Strengthening of Structural Members*. Doctoral Thesis 2003:18.

Martin Nilsson (2003): *Restraint Factors and Partial Coefficients for Crack Risk Analyses of Early Age Concrete Structures*. Doctoral Thesis 2003:19.

Mårten Larson (2003): *Thermal Crack Estimation in Early Age Concrete – Models and Methods for Practical Application*. Doctoral Thesis 2003:20.

Erik Nordström (2005): *Durability of Sprayed Concrete. Steel fibre corrosion in cracks*. Doctoral Thesis 2005:02.

Rogier Jongeling (2006): *A Process Model for Work-Flow Management in Construction. Combined use of Location-Based Scheduling and 4D CAD*. Doctoral Thesis 2006:47.

Jonas Carlswärd (2006): *Shrinkage cracking of steel fibre reinforced self compacting concrete overlays - Test methods and theoretical modelling*. Doctoral Thesis 2006:55.

Håkan Thun (2006): *Assessment of Fatigue Resistance and Strength in Existing Concrete Structures*. Doctoral thesis 2006:65.

Joakim Lundqvist (2007): *Numerical Analysis of Concrete Elements Strengthened with Carbon Fiber Reinforced Polymers*. Doctoral thesis 2007:07.

Arvid Hejll (2007): *Civil Structural Health Monitoring - Strategies, Methods and Applications*. Doctoral Thesis 2007:10.

Stefan Woksepp (2007): *Virtual reality in construction: tools, methods and processes.* Doctoral thesis 2007:49.

Romuald Rwamamara (2007): *Planning the Healty Construction Workplace through Risk assessment and Design Methods*. Doctoral thesis 2007:74.

Björnar Sand (2008): *Nonlinear finite element simulations of ice forces on offshore structures*. Doctoral Thesis 2008:39.

Bengt Toolanen (2008*)*: *Lean contracting : relational contracting influenced by lean thinking*. Doctoral Thesis 2008:41.

Sofia Utsi (2008): *Performance based concrete mix-design: aggregate and micro mortar optimization applied on self-compacting concrete containing fly ash*. Doctoral Thesis 2008:49.

Markus Bergström (2009): *Assessment of existing concrete bridges: bending stiffness as a performance indicator*. Doctoral Thesis. ISBN 978-91-86233-11-2

Tobias Larsson (2009): *Fatigue assessment of riveted bridges*. Doctoral Thesis.ISBN 978-91-86233-13-6

Thomas Blanksvärd (2009): *Strengthening of concrete structures by the use of mineral based composites: system and design models for flexure and shear*. Doctoral Thesis.

Anders Bennitz (2011): *Externally Unbonded Post-Tensioned CFRP Tendons – A System Solution.* Doctoral Thesis. ISBN 978-91-7439-206-7

Gabriel Sas (2011): *FRP Shear Strengthening of Reinforced Concrete Beams*. Doctoral Thesis. ISBN 978-91-7439-239-5

Peter Simonsson (2011): *Buildability of Concrete Structures – Processes, Methods and Material.* Doctoral Thesis. ISBN 978-91-7439-243-2

Licentiate theses

Lennart Fransson (1984): *Bärförmåga hos ett flytande istäcke. Beräkningsmodeller och experimentella studier av naturlig is och av is förstärkt med armering*. Licentiate Thesis 1984:012L.

Mats Emborg (1985): *Temperature stresses in massive concrete structures. Viscoelastic models and laboratory tests*. Licentiate Thesis 1985:011L.

Christer Hjalmarsson (1987): *Effektbehov i bostadshus. Experimentell bestämning av effektbehov i små- och flerbostadshus*. Licentiate Thesis 1987:009L.

Björn Täljsten (1990): *Förstärkning av betongkonstruktioner genom pålimning av stålplåtar*. Licentiate Thesis 1990:06L.

Ulf Ohlsson (1990): *Fracture Mechanics Studies of Concrete Structures*. Licentiate Thesis 1990:07L.

Lars Stehn (1990): *Fracture Toughness of sea ice. Development of a test system based on chevron notched specimens*. Licentiate Thesis 1990:11L.

Per Anders Daerga (1992): *Some experimental fracture mechanics studies in mode I of concrete and wood*. Licentiate Thesis 1992:12L.

Henrik Gabrielsson (1993): *Shear capacity of beams of reinforced high performance concrete*. Licentiate Thesis 1993:21L.

Keivan Noghabai (1995): *Splitting of concrete in the anchoring zone of deformed bars. A fracture mechanics approach to bond*. Licentiate Thesis 1995:26L.

Gustaf Westman (1995): *Thermal cracking in high performance concrete. Viscoelastic models and laboratory tests*. Licentiate Thesis 1995:27L.

Katarina Ekerfors (1995): *Mognadsutveckling i ung betong. Temperaturkänslighet, hållfasthet och värmeutveckling*. Licentiate Thesis 1995:34L.

Patrik Groth (1996): *Cracking in concrete. Crack prevention with air-cooling and crack distribution with steel fibre reinforcement*. Licentiate Thesis 1996:37L.

Hans Hedlund (1996): *Stresses in High Performance*

Mårten Larson (2000): *Estimation of Crack Risk in Early Age Concrete. Simplified methods for practical use*. Licentiate Thesis 2000:10.

Stig Bernander (2000): *Progressive Landslides in Long Natural Slopes. Formation, potential extension and configuration of finished slides in strain- softening soils*. Licentiate Thesis 2000:16. In collaboration with the Division of Soil Mechanics and Foundation Engineering

Martin Nilsson (2000): *Thermal Cracking of young concrete. Partial coefficients, restraint effects and influences of casting joints*. Licentiate Thesis 2000:27.

Erik Nordström (2000): *Steel Fibre Corrosion in Cracks. Durability of sprayed concrete*. Licentiate Thesis 2000:49.

Anders Carolin (2001): *Strengthening of concrete structures with CFRP – Shear strengthening and full-scale applications*. Licentiate thesis 2001:01.

Håkan Thun (2001): *Evaluation of concrete structures. Strength development and fatigue capacity*. Licentiate thesis 2001:25.

Patrice Godonue (2002): *Preliminary Design and Analysis of Pedestrian FRP Bridge Deck*. Licentiate thesis 2002:18.

Jonas Carlswärd (2002): *Steel fibre reinforced concrete toppings exposed to shrinkage and temperature deformations*. Licentiate thesis 2002:33.

Sofia Utsi (2003): *Self-Compacting Concrete - Properties of fresh and hardening concrete for civil engineering applications*. Licentiate thesis 2003:19.

Anders Rönneblad (2003*):* Product Models for Concrete Structures - Standards, Applications and Implementations*.* Licentiate thesis 2003:22.

Håkan Nordin (2003): *Strengthening of Concrete Structures with Pre-Stressed CFRP*. Licentiate Thesis 2003:25.

Arto Puurula (2004): *Assessment of Prestressed Concrete Bridges Loaded in Combined Shear, Torsion and Bending*. Licentiate Thesis 2004:43.

Arvid Hejll (2004): *Structural Health Monitoring of Bridges. Monitor, Assessand Retrofit*. Licentiate Thesis 2004:46.

Ola Enochsson (2005*):* CFRP Strengthening of Concrete Slabs, with and without Openings. Experiment, Analysis, Design and Field Application*.* Licentiate Thesis 2005:87.

Markus Bergström (2006): *Life Cycle Behaviour of Concrete Structures – Laboratory test and probabilistic evaluation*. Licentiate Thesis 2006:59.

Thomas Blanksvärd (2007): *Strengthening of Concrete Structures by Mineral Based Composites*. Licentiate Thesis 2007:15.

Alann André (2007): *Strengthening of Timber Structures with Flax Fibres*. Licentiate Thesis 2007:61.

Peter Simonsson (2008): *Industrial bridge construction with cast in place concrete: New production methods and lean construction philosophies*. Licentiate thesis 2008:17.

Anders Stenlund (2008*):* Load carrying capacity of bridges: three case studies of bridges in northern Sweden where probabilistic methods have been used to study effects of monitoring and strengthening. Licentiate thesis 2008:18.

Anders Bennitz (2008): *Mechanical Anchorage of Prestressed CFRP Tendons - Theory and Tests*. Licentiate thesis 2008:32.

Gabriel Sas (2008): *FRP shear strengthening of RC beams and walls*. Licentiate Thesis 2008:39.

Tomas Sandström (2010): *Durability of concrete hydropower structures when repaired with concrete overlays.* Licentiate Thesis. ISBN 978-91-7439-074-2.

The photo on the next page was taken just before the defense of the thesis on August 16, 2011. Seated from left: Ola Dahlblom, Thomas Olofsson, Steinar Nordal, Stig Bernander, Claes Alén, Staffan Larsson and Hans-Peter Jostad.

About the Author

Stig Bernander was born on February 5, 1928, in Mnene, Rhodesia, Africa. He attended primary and secondary schools in Mnene and Bulawayo, Rhodesia, and in Gothenburg, Sweden. He studied civil engineering at Chalmers University of Technology and obtained a M.Sc. in 1951.

Having worked for the Swedish Board of Roads in Stockholm 1951-53, he moved to Skanska Contracting Co, which in those days was named Skånska Cementgjuteriet AB. In 1972 he became Head of their Design Department in Gothenburg. He retired in 1991 and started a consulting company of his own, Congeo AB.

Stig Bernander has designed or been engaged in major civil engineering works such as bridges, dams, harbors, tunnels, dry docks, off-shore structures, buildings, underground storages and water supply structures in Sweden, Denmark, Norway, Poland, Monaco, Egypt, Saudi Arabia, India, Sri Lanka and Zimbabwe.

In the years 1980 – 98, Stig Bernander served as an Adjunct Professor at the Division of Structural Engineering at Luleå University of Technology, working primarily with crack prevention and modeling of temperature stresses in hardening concrete - taking various boundary conditions into account.

After the large landslide in Tuve (Gothenburg, 1977), Stig Bernander began developing a finite difference model for slope stability analysis taking the deformation-softening of soft sensitive clays into consideration. In the model, the mean down-slope deformation in each element caused by normal forces is maintained compatible with the deformation generated by shear stresses.

He developed software for the model and presented it at international soil mechanics conferences during the 1980-ies. In 2000 he summarized his findings in a Licentiate thesis. An easy-to-use spread-sheet has also been developed.

In this thesis the author conveys his experiences of slide modeling focusing on the nature of triggering agents and the different phases that a slope may undergo before its stability becomes truly critical.